The Involvement of Receptor Interacting Protein Kinase 1 (RIPK1) in the Pathogenesis of Acute Pancreatitis

Thesis submitted in accordance with the requirements of the University of Liverpool for the degree of Doctor of Philosophy

By

Yulin Ouyang

July 2017

Abstract

Acute pancreatitis (AP) is a severe and potentially fatal human disease characterized by parenchymal necrosis with associated inflammation. Necroptosis is a form of controlled necrosis which is mediated through receptor interacting protein kinase 1 (RIPK1), RIPK3 and mixed lineage kinase domain-like protein (MLKL) as a regulated cell death pathway. Accumulating studies have demonstrated that necroptosis plays an important role in the pathogenesis of AP related to RIPK3 and MLKL. However, the function of RIPK1 in the pancreas, especially under pathological conditions, has remained unclear. The aims of this study were to investigate the effects of RIPK1 kinase activity, using gene modification and pharmacological inhibition, on *in vitro* cell death, reactive oxygen species (ROS) production, and Ca^{2+} signalling and *in vivo* using three experimental AP models, to further understand the role of RIPK1 in AP.

Both genetic modification and pharmacological inhibition led to significant reductions of acinar cell necrosis. In addition, chemical inhibitors were also found to reduce TLCS-induced apoptosis, ROS production and CCK-induced sustained Ca^{2+} elevations. The severity of experimental pancreatitis in TLCS-, FAEE- and CER-AP was only partially protected in $Ripk1^{K45A}$ mice compared to strain-matched controls. Application of Nec-1 (56 mg/kg) through a mini pump as a treatment markedly reduced the severity of AP in all three experimental models. In addition, inhibition of indoleamine 2, 3-dioxygenase (IDO), another reported target of Nec-1, caused partial protection in TLCS-AP.

In conclusion, RIPK1 kinase activity may play a role in the pathogenesis of AP, however, the results indicated that it would not be an appropriate target for drug development. In contrast, Nec-1 significantly ameliorated AP in all experimental models tested, likely through multiple pathways, suggesting further elucidation of its effects might assist development of novel therapies.

Acknowledgements

Firstly, I wish to thank my supervisors Dr David Criddle, Professor Robert Sutton and Dr Rajarshi Mukherjee for their help, support, advice and enthusiasm. Without their excellent supervision, this PhD project would not have been possible. A special thanks to Dr David Criddle for his patience guidance, encouragement and trust in research and in life.

I would also like to thanks, Wen Li, who taught me *in vivo* experiment, Diane Latawiec, who undertaken scoring and cell death experiments with me; Dr Jane Armstrong who offer me crucial techniques, and Dr Awais who showed me confocal experiments. Also, thanks Professor Alexei Tepikin for the help and guidance during my time in the laboratory; thanks to Svetlana Voronina, Michael Chvanov, Helen Tanton and Francesca De Faveri in physiology for providing invaluable support in experiments and in life. A further thank you to all the members of in the PBRU especially Simon Win, Jack Morton, Xiaoying Zhang, Wei Huang, Peter Szatmary, Ajay Sud, Becky Taylor. All the help and efforts from you made my PhD colourful and enjoyable.

I would also like to thank Chinese Scholarship Council (CSC) for funding my study in the United Kingdom and thanks NIHR Liverpool Pancreas Biomedical Research Unit (PBRU) for funding all my research. Also, thanks our industrial collaborators Glaxo Smith Kline, especially the support from Peter Gough and John Bertin.

Last but not least thank you to my mum, family and friends for their faith, encouragement and love to help me throughout this PhD.

Without all the support above, none of this would be possible. I am full of gratitude for all the beautiful things happened in my life. And all of you constitute my amazing PhD life.

Table of Contents

Abbreviations

$[Ca^{2+}]_c$	Cytosolic Ca^{2+} concentration
1-MT	1-Methyl-l-tryptophan
AP	Acute pancreatitis
ATP	Adenosine triphosphate
BSA	Bovine serum albumin
CaMKII	Calcium-calmodulin kinase
CCK	Cholecystokinin
CER-AP	Caerulein-hyperstimulation acute pancreatitis model
cFLIP	Cellular FLICE-inhibitory protein
cIAP1/2	Cellular inhibitor of apoptosis proteins 1/2
CM-H_2DCFDA	Chloromethyl-2,7-dichlorodihydrofluorescein diacetate acetyl
CYLD	Cylindromatosis
DD	Death domain
DISC	TAK1-binding protein death-inducing signalling complex
DMSO	Dimethyl sulphoxide
DUB	Deubiquitination
ER	Endoplasmic reticulum
ERCP	Endoscopic retrograde cholangiopancreatography
EtOH	Ethanol
F/F_0	Fluorescence intensity normalized to the initial intensity
FADD	Fas-Associated protein with death domain
FAEE	Fatty acid ethyl ester
FAEE-AP	POA-stimulated alcoholic acute pancreatitis model
GSK	Glaxo Smith Kline
H&E	Hematoxylin and eosin
i.p.	Intraperitoneal
ID	Intermediate domain
IDO	Indoleamine 2,3-dioxygenase
IFN	Interferon

IκB	Inhibitor of κB
IKK	IκB kinase
IL	Interleukin
JNK	c-Jun N-terminal kinase
KD	Kinase domain
KMO	Kynurenine monooxygenase
KP	Kynurenine pathway
LPS	Lipopolysaccharide
LUBAC	Linear ubiquitin chain assembly complex
Lys	Lysine
MEFs	Mouse embryonic fibroblasts
Met	Methionine
MLKL	Mixed lineage kinase domain-like protein
MPO	Myeloperoxidase
MTH-trp	Methylthiohydantoin-dl-tryptophan
NADPH	Nicotinamide adenine dinucleotide phosphate
Nec	Necrostatin
NEMO	NF-κB essential modulator
NF-κB	Nuclear factor κ-light-chain-enhancer of activated B cells
Orai1	Calcium release-activated calcium channel protein 1
PAC	Pancreatic acinar cell
PBS	Phosphate-buffered saline
PEG	Poly ethylene glycol
PERK	protein kinase R (PKR)-like endoplasmic reticulum kinase
PI	Propidium iodide
PKC	Protein kinase C
POA	Palmitoleic acid
POAEE	Palmitoleic acid ethyl ester
RHIM	RIP homotypic interaction motif
RIPK	Receptor interacting protein kinase
ROS	Reactive oxygen species
s.c.	Subcutaneous
SEM	Standard error of the mean

SERCA	Sarcoplasmic/endoplasmic reticulum Ca^{2+}-ATPase
Smac	Second mitochondria-derived activator of apoptosis
SOCE	Store-operated Ca^{2+}-entry
STIM	Stromal interaction molecule
TAB	TAK1-binding protein
TAK	TGFβ-activated kinase 1
TLCS	Taurolithocholic acid -3-sulphate
TLCS-AP	TLCS- stimulated biliary acute pancreatitis model
TLR	Toll-like receptor
TNF	Tumor necrosis factor
TRADD	TNF-receptor-associated death domain
TRAF	TNF receptor-associated factor
TRAIL	Tumour necrosis factor-related apoptosis inducing ligand
XIAP	X-linked inhibitor of apoptosis protein
Ub	Ubiquitination
Wt	Wild-type
zVAD-FMK	Carbobenzoxy-valyl-alanyl-aspartyl-[O-methyl]-fluoromethylketone

Chapter 1: Introduction

1.1 The Pancreas

The pancreas, located in the upper cavity of the abdomen, has a dimension of 12~20 cm in length and weighs 80g in an adult. The pancreas is normally divided into four major regions including head, neck, body, and tail. The pancreas head is the largest part which is located to the right of the spine surrounded by the duodenum. The neck of the pancreas is 3~4 cm wide, joining the head and body. The body lies against the aorta and is in contact with the stomach, and the tail is connected to the spleen.

The pancreas has both endocrine (Islets of Langerhans) and exocrine portions (pancreatic acinar cells). In its endocrine capacity, the pancreas produces hormones including insulin, amylin, glucagon, somatostatin and pancreatic polypeptide through five types of endocrine cell subsets: alpha, beta, delta, gamma and epsilon. In its exocrine function, the pancreas secretes pancreatic juice which contains enzymes to help digest food. Its secretory function is controlled by a reflex mechanism including input from both the sympathetic and parasympathetic autonomic nervous system and gastrointestinal hormones secretin and cholecystokinin (CCK). Secretin acts on the pancreatic ducts to cause copious secretion of alkaline pancreatic HCO_3^- rich juice poor in enzymes. Acetylcholine produced by parasympathetic fibres of the vagus nerve stimulates pancreatic enzyme secretion with minimal effects on fluid and bicarbonate secretion. CCK stimulates acinar cells to release of zymogen granules and causes the production of pancreatic juice rich in enzymes but low in volume (Pandol 2010).

1.2 Acute pancreatitis and cell signalling

1.2.1 Acute pancreatitis

Acute pancreatitis (AP) is a potentially fatal human disease, and it is one of the most common gastrointestinal admission-related disease characterised by the onset of parenchymal and peripancreatic fat necrosis with associated inflammation. It is the second highest cause of hospital stay and the fifth leading cause of in-hospital deaths in the US (Lankisch, Apte et al. 2015). In the UK, around 20,000 people are admitted to hospital with AP. One in five of these cases are severe, resulting in ~1000 deaths annually. Research showed that 70~80% AP is induced by gallstones and alcohol abuse; diverse causes account for the other cases of AP with ~10-15% induced by hypercalcaemia, hypertriglyceridaemia, post-endoscopic retrograde cholangiopancreatography (ERCP), drugs, abdominal trauma, infection, tumours; idiopathic aetiology; with smoking as an independent risk factor. There is a genetic susceptibility to AP, including mutations of human cationic trypsinogen (PRSS1), chymotrypsin C (CTRC), serine protease inhibitor, Kazal type1 (SPINK) and cystic fibrosis transmembrane conductance regulator (CFTR) for recurrent AP (Mounzer and Whitcomb 2013). Furthermore, AP patients have a higher chance to develop chronic pancreatitis, which is a risk factor for pancreatic cancer (Frossard, Steer et al. 2008).

All the causes of AP mentioned above involve acinar cell injury. Calcium (Ca^{2+}) toxicity is considered an early event in AP that contributes to subsequent premature enzyme activation, vacuolization, apoptosis and necrosis (Petersen

and Sutton 2006). Cytosolic Ca^{2+} overload followed by mitochondrial Ca^{2+} overload results in mitochondrial membrane potential depolarization and impaired ATP production (Booth, Murphy et al. 2011, Criddle 2016). Mitochondrial dysfunction also causes an imbalance in ROS levels/antioxidant capabilities of the cell that leads to lipid peroxidation, DNA strand damage (Werner, Hartwig et al. 2012).

Patterns of cell death are the key determinants of disease severity in AP. Necrosis triggers acute inflammation and exacerbates pancreatitis, whereas apoptosis leads to very little or no inflammation in AP (Kaiser, Saluja et al. 1995, Petrov, Shanbhag et al. 2010, Wang, Han et al. 2013). In parallel with these events, the up-regulation of cytokines and chemokines amplifies the inflammatory reaction, the extent of the pancreas injury increasing the mortality in the different stages of the disease (Malmstrom, Hansen et al. 2012).

Current medical management of AP relies on traditional supportive care including fluid resuscitation, pain control, nutrition support and treatment of local or systemic complications which are palliative and nonspecific. Further understanding of physiology and pathophysiology molecular pathways involved in AP is therefore crucial for the development of potential pharmacological therapies.

1.2.2 The role of ROS in AP

Reactive oxygen species (ROS) are chemically active oxygen containing molecules generated under physiological conditions as a necessary part of the

ATP-producing machinery of the cell. The majority of primary cellular ROS is produced in the mitochondria under physiological conditions through the electron transport chain complexes (Turrens 2003, O'Malley, Fink et al. 2006, Davidson 2010). In physiological processes, ROS exert signalling roles (Hamanaka and Chandel 2010), however, excessive generation of ROS has been shown to promote damage in a variety of cell types (Forkink, Smeitink et al. 2010).

During the course of AP, increased superoxide, hydrogen peroxide and lipid peroxide levels and diminished antioxidant status were present in the blood of AP patients in comparison to healthy controls (Tsai, Wang et al. 1998). Multiple sources of ROS are likely to be relevant to AP pathogenesis. For example, ROS induced both activation and proliferation of immune cells to the organ during AP (Sundaresan, Yu et al. 1995, Suh, Arnold et al. 1999). ROS production is enhanced in neutrophils obtained from patients with AP (Tsuji, Watanabe et al. 1994), and ROS derived from neutrophil NADPH oxidase may be key to implementing damage in experimental AP (Gukovskaya, Vaquero et al. 2002). In the pancreas, NADPH oxidase was not detectable in primary PACs with immunohistochemistry (Gukovskaya, Gukovsky et al. 2002) and the increase in intracellular ROS induced by menadione largely occurred within mitochondria, and was unaffected by the enzyme inhibitor diphenyliodonium chloride (DPI) (Criddle, Gillies et al. 2006). Application of the oxidant menadione in PACs induced a rise of ROS that promoted apoptotic cell death (Criddle, Gillies et al. 2006), an effect that was independent of Ca^{2+} (Booth, Murphy et al. 2011) . In contrast, application of taurolithocholic acid - 3-sulphate (TLCS) in human and murine PACs produced a Ca^{2+}-dependent

elevation of ROS from the mitochondria (Booth, Murphy et al. 2011). Manipulations of this ROS production affected PAC cell death by either promoting or inhibiting apoptosis; a reduction of ROS decreased apoptosis but enhanced TLCS-induced necrosis, whereas increasing ROS caused the converse.

These observations suggested the importance of ROS in local pancreatic injury during AP, although their role in *in vivo* AP is unclear. For example, generation of ROS alone did not induce pathological changes characteristic of AP, suggesting ROS elevation is not the initiator of AP, but may be an accompanying phenomenon, and that factors other than ROS are involved in triggering AP damage *in vivo* (Rau, Poch et al. 2000). Furthermore, results from *in vitro* and *in vivo* studies are not clear. For example, the mitochondrial-targeted antioxidant MitoQ effectively reduced H_2O_2-induced ROS production in PACs, however, it did not improve severe TLCS-AP (Huang, Cash et al. 2015).

Importantly, antioxidant therapy in AP has produced different outcomes, that may be influenced by differeing conditions and experimental design (Armstrong, Cash et al. 2013). For example, initial promise was shown by a study in which micronutrient antioxidant therapy improved recurrent attacks and/or constant pancreatic pain, potentially offering an approach for the treatment of recurrent (non-gallstone) pancreatitis and pancreatic pain (Uden, Bilton et al. 1990). However, other studies showed that antioxidant treatment decreased oxidative stress but failed to improve hospital stay and complication rates in AP patients (Sateesh, Bhardwaj et al. 2009), and combined

antioxidant therapy did not reduce in-hospital mortality in patients with severe AP (Virlos, Mason et al. 2003, Siriwardena, Mason et al. 2007).

1.2.3 The role of Ca^{2+} in AP

Ca^{2+} signals are involved in many signalling pathways in cellular physiology, from fertilisation, through cell function, to cell death (Berridge, Lipp et al. 2000). Cytosolic Ca^{2+} signals are critical for fluid and enzyme secretion of the pancreas. Under normal conditions, the plasma membrane is impermeable to extracellular Ca^{2+}, and most of the intracellular Ca^{2+} is stored in the ER and other intracellular Ca^{2+} stores (Ashby and Tepikin 2001). In response to physiological stimulation with CCK, and Ach, PACs generate the second messengers, inositol triphospate (IP_3), cyclic ADP ribose (cADPR) and nicotinic acid adenine dinucleotide phosphate (NAADP) that cause Ca^{2+} release from internal Ca^{2+} stores through binding to IP_3 receptors (IP_3Rs) and ryanodine receptors (RyRs) on the ER and other intracellular Ca^{2+} stores that elicits cytosolic Ca^{2+} spikes (Petersen and Sutton 2006, Petersen 2009). The normal basal cytosolic Ca^{2+} concentration is restored through the sarco-endoplasmic reticulum Ca^{2+}-ATPase (SERCA) pump that refills the ER, and the plasma membrane Ca^{2+}-ATPase (PMCA) pump that extrudes Ca^{2+} out of the cell (Petersen and Tepikin 2008). Physiological Ca^{2+} signals are generally restricted to the apical pole and buffered by mitochondria which temporarily take up Ca^{2+} released from the ER, thereby up-regulating ATP production, and preventing global waves from reaching the basolateral area (Tinel, Cancela et al. 1999, Petersen 2002, Voronina, Longbottom et al. 2002).

Under certain pathological conditions, the depletion of ER Ca^{2+} and extracellular Ca^{2+} entry across the plasma membrane results in sustained global elevations of Ca^{2+}. Pancreatitis-associated toxins, including supramaximal CCK, bile acid and non-oxidative alcohol metabolites, induce Ca^{2+} release through IP_3Rs and RyRs, resulting in the depletion of internal Ca^{2+}stores including within the ER. Following ER store depletion, Ca^{2+} influx into the cell through store-operated Ca^{2+} entry (SOCE) occurs as a compensatory mechanism for Ca^{2+} loss from internal cellular stores (Raraty, Ward et al. 2000, Criddle, Sutton et al. 2006, Gerasimenko, Gerasimenko et al. 2014). Impaired PMCA activity and reduced PMCA expression also leads to cytotoxic Ca^{2+} overload (Bruce 2017). Sustained cytosolic Ca^{2+}overload leads to mitochondrial Ca^{2+} overload (Booth, Murphy et al. 2011), causing mitochondrial membrane potential depolarization, mitochondrial permeability transition pore induction, impaired ATP production, premature Ca^{2+}-dependent activation of zymogen granules and vacuole formation, and eventually results in cell death pathway activation and severe PAC injury (Raraty, Ward et al. 2000, Murphy, Criddle et al. 2008, Gerasimenko, Gerasimenko et al. 2014).

Researchers demonstrated transient release of Ca^{2+} from the ER and acidic stores, induced by mild stimuli, promotes apoptosis. This action may depend on a partial mitochondrial depolarisation and transient opening of the mitochondrial permeability transition pore (MPTP), which does not adversely influence ATP production (Halestrap 2006). An unbalanced Ca^{2+} signal causes mitochondrial dysfunction further promoting the release of apoptosis-inducing factor (AIF) from mitochondria increasing the apoptosis (Lemasters,

Theruvath et al. 2009). However, severe insults induced sustained global Ca^{2+}elevations that inhibit mitochondrial function with a consequent drastic fall of ATP production that leads to necrosis (McConkey and Orrenius 1996, Criddle, Gerasimenko et al. 2007). In necrotic cells, activation of Ca^{2+}-dependent proteases such as calpains (Croall and Ersfeld 2007) and Ca^{2+}/calmodulin-dependent protein kinases such as calcium-calmodulin kinase (CaMKII) were also reported to contributed to high Ca^{2+} entry induced necrosis (Nomura, Ueno et al. 2014, Zhang, Zhang et al. 2016).

1.2.4 Cell death in AP

Necrosis

Necrosis is an un-programmed cell death induced by infection, toxins, trauma which characterised by cell swelling, plasma membrane rupture, a loss of organelle structure without chromatin condensation, and release of cellular contents into the extracellular space initiates inflammation in the surrounding tissues (Laster, Wood et al. 1988). PAC necrosis is largely uncontrolled and can be initiated by a variety of toxins, including bile salts, fatty acid ethyl esters (FAEEs) and fatty acids, that induce cytosolic Ca^{2+} overload, depolarization of mitochondrial membrane potential and failure of ATP production (Raraty, Ward et al. 2000, Kim, Kim et al. 2002, Voronina, Longbottom et al. 2002, Voronina, Sukhomlin et al. 2002, Criddle, Gerasimenko et al. 2007).

Severe AP is usually accompanied by a large amount of PAC necrosis, which leads to the pancreatic inflammation, further causing a systemic inflammatory syndrome response (SIRS) and multiple organ failure (Wang, Han et al. 2013). Infected necrosis induced approximately 11% to 39% death of AP patients (Petrov, Shanbhag et al. 2010, Bugiantella, Rondelli et al. 2016). Parenchymal necrosis in pancreatitis has been used for diagnosis, indication of severity and treatment in the clinic. For example, the determinant-based classification of AP classified AP severity as mild, severe and critical based on the absence/presence of sterile/infected pancreatic necrosis (Dellinger, Forsmark et al. 2012). And the results from three different severities of the murine AP model showed that institute of cancer research (ICR) mice had the most severity of necrosis in CER- AP, BALB/c mice with modest severity had less

necrosis, and C57BL/6 mice with mild severity had the least necrosis, indicating that the degree of necrosis determines AP severity (Wu, Mulatibieke et al. 2017).

Necroptosis

Necroptosis is mediated by Receptor interacting protein 1 (RIPK1), RIPK3 and the downstream protein mixed lineage kinase domain-like protein (MLKL) as a regulated cell death in response to death receptors, Toll- and NOD-like receptors, T cell receptor, genotoxic stress and viruses (Vandenabeele, Galluzzi et al. 2010). Necroptosis has the same endpoint as necrosis but can be controlled, and this makes it an important target in the fields of inflammation and immune diseases (Linkermann and Green 2014, Zhao, Jaffer et al. 2015). Accumulating studies have demonstrated that necroptosis plays an important role in the process of AP. For example, in genotype modification experiments, $Ripk3^{-/-}$ was protective in CER-AP and TLCS-AP reported by different groups (He, Wang et al. 2009, Louhimo, Steer et al. 2016, Liu, Fan et al. 2017) and RIPK3 with siRNA partly alleviated CCK-induced PAC necrosis (Wu, Mulatibieke et al. 2017). Pancreatic Atg7 deletion caused severe AP with progressive cell death, fibrosis and inflammation, and additional removal of RIPK3 further accelerated pancreatic tissue damage and associated with premature mortality (Zhou, Xie et al. 2017). However, one study showed that loss of RIPK3 had no effect on CER-AP (Newton, Dugger et al. 2016). $MLKL^{-/-}$ mice also showed improvement in CER-AP (Wu, Huang et al. 2013), and knockdown of MLKL with siRNA partly reversed necrosis in CCK-stimulated PACs (Wu, Mulatibieke et al. 2017).

In pharmacological inhibitor studies, Necrostatin-1 (Nec-1) (a RIPK1 kinase inhibitor) was shown to reduce PAC injury and cell death in CER-AP, TLCS-AP and L-arginine-induced pancreatitis (Louhimo, Steer et al. 2016, Zou, Xiong et al. 2016). However, the area is controversial with studies showing that RIPK1 kinase modification and Nec-1 application did not improve CER-AP (Linkermann, Brasen et al. 2012, Newton, Dugger et al. 2016, Liu, Fan et al. 2017, Wu, Mulatibieke et al. 2017) (see Section 1.5 RIPK1 and AP for further details).

Because of the controversial studies of necroptosis on AP, whether AP mediated through necroptosis was argued, and other pathway such as ferroptosis, rather than necroptosis is responsible. Since ferroptosis critically depends on lipid peroxidation (Yang, Kim et al. 2016) and has been widely associated with pathologies in the organs like brain and pancreas (Tonnus and Linkermann 2017).

Apoptosis

Apoptosis is genetically controlled and occurs via caspase-dependent mechanisms (Orrenius, Gogvadze et al. 2007). It possesses distinct outcomes compared with necrosis (Melino, Knight et al. 2005) and occurs with minimal release of intracellular contents and inflammation (Kroemer and Zitvogel 2007, Orrenius, Gogvadze et al. 2007).

The role of apoptosis in AP may therefore be protective (Bhatia 2004, Criddle, Gerasimenko et al. 2007). In experimental AP models, the quantification of apoptotic PACs was inversely correlated with the severity of the disease, and some studies suggested that promotion of apoptosis may be beneficial,

whereas inhibition of apoptosis was harmful (Kaiser, Saluja et al. 1995, Mareninova, Sung et al. 2006). Thus, increased caspase activity was protective against pancreatic necrosis in CER-AP, whereas caspase inhibitors were found to increase pancreatic necrosis (Mareninova, Sung et al. 2006). Application of the oxidant menadione in PACs induced a rise of ROS that promoted apoptosis (Criddle, Gillies et al. 2006). Application of TLCS in PACs induced increases of cytosolic Ca^{2+} and mitochondrial Ca^{2+}, which led to dose-dependent increases in intracellular ROS and mitochondrial ROS, impaired production of ATP, apoptosis and necrosis. The potentiation of intracellular ROS correlated with increased apoptosis and reduced necrosis, whereas the antioxidant N-acetylcysteine reduced ROS and apoptosis but increased necrosis (Booth, Murphy et al. 2011). Protective actions of apoptosis been confirmed in several studies using both *in vitro* (Bhatia, Wallig et al. 1998, Baumgartner, Gerasimenko et al. 2007) and *in vivo* experimental approaches (Kaiser, Saluja et al. 1996, Bhatia, Wallig et al. 1998, Bhatia 2004, Mareninova, Sung et al. 2006).

Autophagy

Autophagy occurs at a basal rate in most cells to eliminate protein aggregates and damaged or unneeded organelles (Glick, Barth et al. 2010). In mouse exocrine pancreas, the basal autophagy level is higher than in liver, kidney, heart, or endocrine pancreas (Mizushima, Yamamoto et al. 2004). Starvation greatly stimulates autophagy in the pancreas resulting in a dramatic decrease of zymogen granules in PACs (Mizushima, Yamamoto et al. 2004, Mareninova, Hermann et al. 2009).

Studies showed that large vacuoles accumulate in PACs in experimental and human pancreatitis (Aho, Nevalainen et al. 1982, Brackett, Crocket et al. 1983, Niederau and Grendell 1988). In addition, autophagosome formation was stimulated in AP, with decreased efficiency of autophagic degradation and lysosomal hydrolytic activity (Mizushima, Yamamoto et al. 2004, Mareninova, Hermann et al. 2009, Gukovskaya and Gukovsky 2012). Pancreatitis-induced vacuole membrane protein 1 (VMP1) was activated in AP (Dusetti, Jiang et al. 2002) and VMP1 pancreas-specific transgenic expression in mice promoted autophagosome formation (Ropolo, Grasso et al. 2007, Vaccaro, Ropolo et al. 2008). The combination of alcohol and endotoxaemia resulted in the depletion of lysosomal-associated membrane protein-2 (Lamp-2), leading to accumulation of autophagosomes and switching from apoptosis to necrosis (Fortunato, Burgers et al. 2009). Mice deficient in Atg5 (a protein central to autophagy) caused deficient lysosomal degradation, decreased trypsin activity and improvement of AP (Mareninova, Hermann et al. 2009).

1.3 Experimental acute pancreatitis models

Different experiment AP models contributed tremendously to the understanding of AP. There are a range of animal species have been used to investigate AP including murine, opossums, guinea pig, rabbits, dogs, cats, pig, and primates (Johnson and Doppman 1967, Bawnik, Orda et al. 1974, Waterworth, Barbezat et al. 1974, Musa, Nelson et al. 1976, Chetty, Gilmour et al. 1980, Simpson, Toner et al. 1983, Senninger, Moody et al. 1986). Also, different approaches have been tried including diets, different substance injections, surgical methods and genetic modifications (Lombardi, Estes et al. 1975, Whitcomb 2001, Huang, Cash et al. 2015). Commonly used experimental AP models focus on the mouse/rat which is easier to access and is generally more reproducible. Therefore, these sections will discuss the murine models of AP. However, different models vary according to the mechanism and disease severity, so the actual choice of appropriate models depends on the strategy of the study.

More clinical relevant models in mouse include ductal ligation and bile acid-induced AP which are relevant to acute biliary pancreatitis, FAEE-AP which represents alcohol-induced AP, radiocontrast agent iohexol influx induced AP which is relevant to post-ERCP pancreatitis. Less clinically relevant models include caerulein-AP, L-Arginine-induced AP, choline-deficient enriched with ethionine (CDE) diet-induced AP.

1.3.1 Duct ligation and bile acid AP

Gallstones are the most common cause of AP which accounts for 30~50% of clinical AP, however, the exact mechanism is incompletely understood (Pandol, Saluja et al. 2007). The most accepted theory is that the obstruction of the major papilla by gallstones causes efflux of pancreatic zymogens, creates elevated pressure in the pancreas and leads to reflux of bile into pancreatic duct which then initiates a complex cascade to induce AP (Swaroop, Chari et al. 2004, Saluja, Lerch et al. 2007). There are two main models created from this theory, one is the surgical ligation AP model, and the other is the ductal infusion AP model.

Ligation induced AP models

The ligation-induced model to some extent mimics the early stage of gallstone-induced AP (Acosta and Ledesma 1974) and may be useful to clarify the early events underlying the development of AP (Ohshio, Saluja et al. 1991). This model has variability based on species and duration of obstruction. For example, in the opossum, ligation of the pancreatic duct or common bile duct induced 100% hemorrhagic AP mortality in 14 days (Senninger, Moody et al. 1986), while the ligation of the common biliopancreatic duct in rat induced multiple organ failure characteristised by pancreatic necrosis, infiltration and multiple microthrombi in the lung, stomach and kidney (Vasilescu and Tasca 1991). However, most other laboratory animals did not develop AP with necrosis or inflammation except chronic pancreatic atrophy induced by long term ligation (Ohshio, Saluja et al. 1991).

Closed duodenal loop (CDL)-induced AP model involves surgically closing the duodenal papilla while bile is diverted into the jejunum via an implanted cannula (Pfeffer, Stasior et al. 1957). Since permanent ligation of the duodenum caused the death of the animal within a short period, temporary ligation of the duodenum in rats was used to reduce the mortality (Orda, Hadas et al. 1980). After the loop had been formed, fluid volumes and amylase concentrations in the closed loop induced an earlier appearance of PAC damage, and elevated serum lipase, alkaline phosphatase, and lactic dehydrogenase (Schapiro, Britt et al. 1973).

Though ligation-induced AP models avoided agents that may produce unknown effects，compared with the bile acid infusion model，the relatively unstable outcome, variability among species, individuals and limited reproducibility make the ligation model less popular for AP investigation. The combination of ligation with other models such as bile acid infusion (Le, Eisses et al. 2015) and secretory hyperstimulation (Popper, Necheles et al. 1948) caused more severe AP and has received wider acceptance.

Bile acid infusion model

The initial ductal infusion AP model was performed by Bernard (1985). He injected bile and olive oil into a canine pancreas through the ampulla of Vater to induce pancreatitis. During the past few decades, various bile salts such as sodium CDC (Na-CDC), sodium taurocholate (Na-TC) (Laukkarinen, Van Acker et al. 2007, Jia, Yamamoto et al. 2015), sodium glycol deoxycholic acid (Na-GDC), TDC (Na-TDC) and TLCS (Ma, Wu et al. 2013, Huang, Cash et al. 2015, Huang, Cane et al. 2017) were reported to induce AP in different species

(Lampel and Kern 1977, Aho, Nevalainen et al. 1980, Renner and Wisner 1986, Perides, van Acker et al. 2010). Among these bile salts, TLCS was found to be the most effective one, which induced Ca^{2+} oscillations at low concentration (25 μM~200 μM) and induced long-lasting Ca^{2+} rises followed by the influx of extracellular Ca^{2+} at the concentration of 300~500 μM (Voronina, Longbottom et al. 2002). To date, the most commonly used retrograde ductal infusion protocols were described in the rat (Aho, Koskensalo et al. 1980) and in the mouse (Perides, van Acker et al. 2010).

These models enabled researchers to apply the bile components into the pancreas in a more controlled way. The severity of these models can be manipulated by altering the concentration, volume, infusion time and the pressure (Laukkarinen, Van Acker et al. 2007, Wittel, Wiech et al. 2008). Studies showed that TLCS-AP develops within 2~24 h after induction and is characterised by typical oedema, infiltration, necrosis and haemorrhage. It is worth mentioning that because of the characteristics of this procedure, infusion predominantly affects the pancreatic head (Wittel, Wiech et al. 2008, Perides, van Acker et al. 2010).

1.3.2 Alcoholic AP

Alcohol is the 2nd major cause of AP (Irving, Samokhvalov et al. 2009). Experiments showed that ethanol administration alone increased pancreatic duct permeability (Wedgwood, Adler et al. 1986), stimulated the release of CCK (Saluja, Lu et al. 1997), reduced pancreatic blood flow and microcirculation (Friedman, Lowery et al. 1983), decreased pancreatic oxygen consumption (Foitzik, Fernandez-del Castillo et al. 1995) and induced

oxidative stress (Weber, Merkord et al. 1995). However, ethanol application alone or ethanol feeding induced liver injury rather than pancreatitis (Siech, Heinrich et al. 1991, Andrzejewska, Dlugosz et al. 1998). Therefore, researchers combined ethanol with other toxins such as CCK (Pandol, Periskic et al. 1999)，caerulein (Lugea, Gong et al. 2010), infection with the avirulent strain (Jerrells, Chapman et al. 2003) to improve the sensitization of ethanol on the pancreas.

Later studies showed that the effects of alcohol on pancreas are likely to involve the of metabolism of alcohol. Rather than ethanol itself, the pancreas uses both oxidative and non-oxidative metabolism (OME and NOME) to degrade alcohol. NOME combines ethanol with fatty acids (e.g. palmitoleic acid POA) and metabolizes them to FAEEs, which then accumulate in the pancreas resulting in acute damage and inflammation (Werner, Laposata et al. 1997, Werner, Saghir et al. 2001, Gukovskaya, Mouria et al. 2002, Wilson and Apte 2003, Criddle, Raraty et al. 2004). A study by our group showed that the combination of ethanol and POA induced mouse pancreatic damages including extensive acinar cell oedema, neutrophil infiltration and necrosis. The pivotal role of FAEEs in inducing AP was demonstrated by inhibiting an FAEE synthase enzyme, carboxyl ester lipase, to reduce FAEE generation and markedly reduce pancreatic damage *in vivo* and *in vitro* (Huang, Booth et al. 2014).

1.3.3 Caerulein hyperstimulation AP

The caerulein model (CER-AP) is a secretagogue hyperstimulation model created by the administration of supramaximal doses of caerulein (an

analogue of CCK). The procedures of CER-AP are normally conducted by hourlyintraperitonial (i.p.) injections of caerulein at a certain concentration. Various degrees of severity can be achieved by adjusting either the dose or the number of injections. In the early phase of CER-AP, a significant amount of autophagic vacuoles appeared within the acinar cell accompanied by an increase in lysosomal enzyme activity and activation of trypsinogen (Willemer, Elsasser et al. 1992). Inflammation and acinar cell necrosis were prominent at 6 h after injections and reached a maximum after 12 h in mice and rat (Niederau, Ferrell et al. 1985, Wu, Mulatibieke et al. 2017). At each time point, the necrosis in the mouse model was more severe than that in the rat model. However, the apoptosis in rats was much greater than in mice. The extent of apoptosis in both mice and rats reached a maximum at 9 hours and decreased at 12 hours (Wu, Mulatibieke et al. 2017).

This model is simple, stable, highly reproducible, and shares similar histopathological changes with the early phase of clinical AP (Rifai, Elder et al. 2008). Also, the model is suitable for investigating pancreatitis related pulmonary pathology representative of the early stages of the human respiratory distress syndrome (Guice, Oldham et al. 1988, Feddersen, Willemer et al. 1991). In addition, this model allows pancreatic regenerate within 6 days after AP induction, so it is suitable for the investigation of healing and regeneration of damaged tissue (Willemer, Elsasser et al. 1992).

1.3.4 Other models

L-Arginine-induced AP model: L-Arginine is an amino acid which causes AP at high does, and carries a serious morbidity and mortality. Though it is unlikely

that human AP is induced by basic amino acid overdose, the L-Arginine AP model is characterised by a significant amount of PAC necrosis which makes it a useful tool for acute necrotizing pancreatitis research. For example, a single dose of 500 mg/100 g i.p. injection resulted in 70~80% of PAC necrosis within 3 days (Biczo, Hegyi et al. 2011) with no evidence of pathophysiological lesions in the lung, heart, intestine, testis, spleen and thymus (Hegyi, Rakonczay et al. 2004). Meanwhile, the dose and time dependency of the arginine model is suitable to study the different phases of pancreatitis (higher dose for pathological mechanism of AP, lower dose for regenerative processes of AP) (Hegyi, Rakonczay et al. 2004). However, caution is required since the dosage of L-arginine on AP is species dependent. For example, 2.5 g/kg L-arginine induced mild acute necrotizing pancreatitis in rats (Hegyi, Rakonczay et al. 2004), whereas lower than 4 g/kg L-arginine had no effect on pancreatic histology in mice (Biczo, Hegyi et al. 2011).

Radiocontrast agent iohexol influx induced-ERCP AP model: ERCP plays a vital role in the management of diseases involving the bile duct and the pancreatic duct. However, it is an invasive procedure which can cause AP by 1% to 30% (Freeman and Guda 2004). It can be induced by providers (Testoni, Mariani et al. 2010, Committee, Anderson et al. 2012), procedures (number of attempts or longer time needed to cannulate the bile duct successfully), radiocontrast agents (Jin, Orabi et al. 2015) and also varies among patients (2~4% in low-risk patients and up to 8~40% in high-risk patients). The radiocontrast iohexol influx-AP model has recently been developed to mimic the post-ERCP induced pancreatitis by retrograde infusion of radiocontrast agent iohexol into mice (Jin, Orabi et al. 2015). The mechanisms of Iohexol

infusion induced AP may occur through activation of NF-κB, calcium signalling and calcineurin pathways (Jin, Orabi et al. 2015, Orabi, Wen et al. 2017).

CDE diet-induced AP model: Studies showed that female mice with a choline-deficient diet enriched with 0.5% ethionine (a derivative of methionine (Met)) developed severe acute hemorrhagic pancreatitis and had a 100% mortality rate after 4 days (Lombardi, Estes et al. 1975). The CDE diet-induced AP usually takes 2~3 days to develop, and is characterised by massive fat necrosis in the exocrine parenchyma, intense haemorrhaging, and an inflammatory reaction of the stroma throughout the peritoneal cavity. The severity of CDE diet-induced AP in mice is affected by diet regimen, sex, and age (Dazai, Katoh et al. 1991, Niederau, Luthen et al. 1992). The mechanisms of CDE in AP, however, are still unclear. However, the obvious sex differences in this model suggest that oestrogen may play a role.

1.4 Receptor interacting protein kinase 1

Protein serine/threonine kinase receptor interacting protein 1 (RIP/RIP1/RIPK1) is the first member of RIP kinase family (Stanger, Leder et al. 1995). Studies showed that TNFR1 recruits RIPK1 to induce cell death, and different domains of RIPK1 are involved in transducing TNFR1 signals to programmed cell death or NF-κB activation (Hsu, Huang et al. 1996). In 1998, research showed that mice lacking RIPK1 died with widespread inflammation and cell death in several tissues highlighting the functions of RIPK1 *in vivo* (Kelliher, Grimm et al. 1998). The first paper that reported RIPK1-dependent cell death showed that Fas-triggered non-apoptotic cell death was independent of caspase activation but dependent on RIPK1 kinase activity (Holler, Zaru et al. 2000). Later, RIPK1 was demonstrated to be a key upstream molecule and a specific target in necroptosis. Since then RIPK1 has become a hotspot and a potential therapeutic target for regulating multiple pathways especially necroptosis.

1.4.1 Structure

RIPK1 is classified as serine/threonine kinase (Stanger, Leder et al. 1995) which contains 671 amino acids and exists in the cytoplasm, plasma membrane (Micheau and Tschopp 2003) and possibly mitochondria depending on the cell type (Ishida, Sekine et al. 2012, Wang, Jiang et al. 2012, Tait, Oberst et al. 2013).

RIPK1 contains three major domains (Figure 1.4.1). **The C-terminal (death domain, DD)** which is necessary for binding other death receptors such as

tumour necrosis factor (TNF)-R1, tumour necrosis factor-related apoptosis inducing ligand (TRAIL)-R1 and 2, TNF-receptor-associated death domain (TRADD) and Fas-Associated protein with death domain (FADD). Human RIPK1 is 68% identical to murine RIPK1 with the greatest similarity occurring in the death domain (Hsu, Huang et al. 1996). The central region of RIPK1 is **the intermediate domain (ID)** which contains a RIP homotypic interaction motif (RHIM). RHIM relates to protein-protein interaction and is responsible for recruiting other kinases such as RIPK3 (Sun, Yin et al. 2002). **The N-terminal domain (kinase domain, KD)** contains detectable autophosphorylation sites and regulates RIPK1 kinase activity.

Experiments showed that these three domains were linked to distinct activities. For example, overexpression of intact RIPK1 protein induced both NF-κB activation and apoptosis, however, the overexpression of RIPK1 DD induced apoptosis while it inhibited NF-κB activation. The kinase activity is dispensable for the induction of death receptor-mediated apoptosis but is required for activation of necroptosis under apoptosis-deficient conditions (Hsu, Huang et al. 1996). Knockout of RIPK1 KD and DD induced cytotoxicity even in the absence of any trigger (Duprez, Bertrand et al. 2012). Mutations of RHIM in the ID abolished the RIPK1-mediated rescue of necroptosis in Jurkat cells (Cho, Challa et al. 2009). Also, knockout of RIPK1 ID converted the cellular response to TNF from RIPK1 kinase-dependent necroptosis to RIPK1 kinase-dependent apoptosis (Duprez, Bertrand et al. 2012).

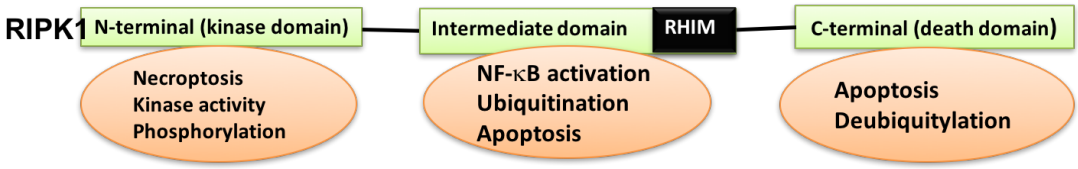

Figure 1.4.1: RIPK1 domains and their related functions. RIPK1 consists of a kinase domain, a RHIM containing intermediate domain and a death domain.

1.4.2 Post-translational modifications

Protein post-translational modification influences physiological and pathological functions by adding functional groups, cleaving regulatory subunits or degrading proteins. These modifications include phosphorylation, glycosylation, ubiquitination, nitrosylation, methylation, acetylation, lipidation and proteolysis (Sambataro and Pennuto 2017). RIPK1, as a serine/threonine kinase, is closely regulated by phosphorylation and ubiquitination.

Phosphorylation

Research showed that low levels of basal RIPK1 phosphorylation were detected in the absence of stimulation, and obvious RIPK1 phosphorylation was detected when programmed necrosis was induced (Cho, Challa et al. 2009). RIPK1 can be auto-phosphorylated or can be phosphorylated by other kinases. Ser14/15, Ser20, Ser161 and Ser166 represent autophosphorylation sites of RIPK1, and Ser89, Ser6, Ser25, Ser303, Ser320, Ser330/331 and Ser333 are likely to be the sites which can be phosphorylated by other kinases (Degterev, Hitomi et al. 2008). Phosphorylation of these sites can either inhibit or promote its kinase activity. For example, autophosphorylation of Ser161 in the activation loop (T-loop) decreased RIPK1 kinase activity and contributed to Nec-1 mediated kinase inhibition (Xie, Peng et al. 2013). One study showed that necroptosis was reduced by up to 40% via autophosphorylation (Degterev, Hitomi et al. 2008), while another showed that there was only ~20% reduction (McQuade, Cho et al. 2013). In addition, RIPK1 Ser161 autophosphorylation was enhanced by ROS and involved RIPK1 transducing the necroptotic signal through necrosome formation (Zhang, Su et al. 2017).

The Ser166A residue is another important phosphorylation site of RIPK1. Its mutation partially diminished necroptosis induced by RIPK1 overexpression and remarkably reduced the interaction of RIPK1 with caspase 8 and RIPK3 (Shen, Liu et al. 2017). Phosphorylation of other sites such as Ser25, Ser296, Ser331 and Ser416 also protected cells from RIPK1 kinase-dependent death. The protective effects may occur through modulation of IκB kinase (IKK) *α*/IKK*β*-mediated RIPK1 phosphorylation in the TNFR complex I and affect RIPK1 binding to TNFR complex II (Dondelinger, Jouan-Lanhouet et al. 2015). And the phosphorylation of Ser320 in RIPK1 suppressing its kinase activity after TNFα stimulation may association with Caspase8 and FADD proteins (Mohideen, Paulo et al. 2017).

On the contrary, Ser89 can be phosphorylated by protein kinases (PK) A, PKC or c-Jun N-terminal kinase (JNK) which caused hyper-activated RIPK1 kinase and increased TNFα-induced necroptosis (McQuade, Cho et al. 2013).

RIPK3 also plays a role in regulating RIPK1 phosphorylation, since RIPK1 phosphorylation was completely abrogated in RIPK3-knockout mouse embryonic fibroblasts (MEFs) (Cho, Challa et al. 2009). One study also showed that after RIP(K45A) eliminated interference from auto-phosphorylation in HEK293E cells, RIP(K45A) was phosphorylated in the presence of RIPK3, but not in the presence of a kinase-dead RIPK3. Mutation of the RIPK3 RHIM abrogated RIPK1 phosphorylation indicating that RIPK1 phosphorylation by RIPK3 is dependent on the formation of a RIPK1 and RIPK3 necrosome (Sun, Yin et al. 2002)

Ubiquitination and deubiquitination

Ubiquitin modifies substrates by covalent attachment through a three-step enzymatic reaction. This ubiquitin conjugation, called ubiquitination (Ub), typically occurs on lysine (Lys) residues of substrates. It is an ATP-dependent dynamic process catalyzed by the sequential action of a ubiquitin activating enzyme, E1, a ubiquitin conjugating enzyme, E2 and a ubiquitin ligase, E3 and are cleaved by deubiquitinase (DUB). Thus, a balance between the formation and removal of ubiquitin chains contributes to the regulation of cellular functions (Hershko and Ciechanover 1998).

Ubiquitination and deubiquitination are essential for RIPK1 mediated NF-κB activation (Li, Kobayashi et al. 2006) and programmed cell death (Gerlach, Cordier et al. 2011). Enzymes that can ubiquitinate RIPK1 include cellular inhibitor of apoptosis proteins (cIAP1/2), linear ubiquitin chain assembly complex (LUBAC), TNF receptor-associated factor 2 (TRAF2) and A20 (named after its cDNA clone number). Deubiquitination converts RIPK1 to a death signalling molecule engaging both apoptosis and necroptosis. Enzymes that can deubiquitinate RIPK1 include ubiquitin-specific proteases (USPs), cylindromatosis (CYLD), A20 and OTU domain-containing deubiquitinase with linear linkage specificity (OTULIN).

In the TNFR pathway, the stable formation of TNFR1 Complex I around ubiquitinated RIPK1 is crucial for providing survival signals through NF-κB activation. The ubiquitination of this complex related to Lys 63-, Met 1-, Lys 11- and Lys 48- ubiquitin chains. By adding Lys 63-, Met 1- can stabilize the complex and induce NF-κB activation. cIAP1/2 (Park, Yoon et al. 2004, Bertrand, Milutinovic et al. 2008, Mahoney, Cheung et al. 2008, Dynek,

Goncharov et al. 2010) and TRAF2/5 (Lee, Shank et al. 2004, Zhang, Blackwell et al. 2010) are able to add a Lys 63-linked ubiquitin chain, and LUBAC can add a Met 1-linked ubiquitinate chain (Lee, Shank et al. 2004, Tokunaga, Sakata et al. 2009, Zhang, Blackwell et al. 2010, Emmerich, Schmukle et al. 2011) to modulate RIPK1-mediated formation of a docking site for TGFβ-activated kinase 1 (TAK1)-TAK binding protein 2 (TAB2)-TAB3 and recruitment of NEMO then recruit IKK. Addition of Lys 11- and Lys 48-ubiquitinate chains caused RIPK1 degradation. Assembly of a K11-linked chain through cIAP1/2 caused degradation of RIPK1 (Dynek, Goncharov et al. 2010, Ikeda 2015). A20 attached a Lys 48-linked polyubiquitination chain onto its substrate RIPK1 downregulating NF-κB signalling (Heyninck, De Valck et al. 1999, Wertz, O'Rourke et al. 2004).

Deubiquitination inhibits RIPK1-mediated NF-κB activation and promotes TNFα-induced cell death. Deuniquitination of Lys 63 ubiquitin chain by CYLD (Moquin, McQuade et al. 2013), A20 (He and Ting 2002, Onizawa, Oshima et al. 2015) and USPs (Xu, Tan et al. 2010, Hou, Wang et al. 2013), and OTULIN regulated the Met1-ubiquitin chain preventing TNFα induced NEMO association with RIPK1 and subsequent NF-κB activation (Figure 1.4.2).

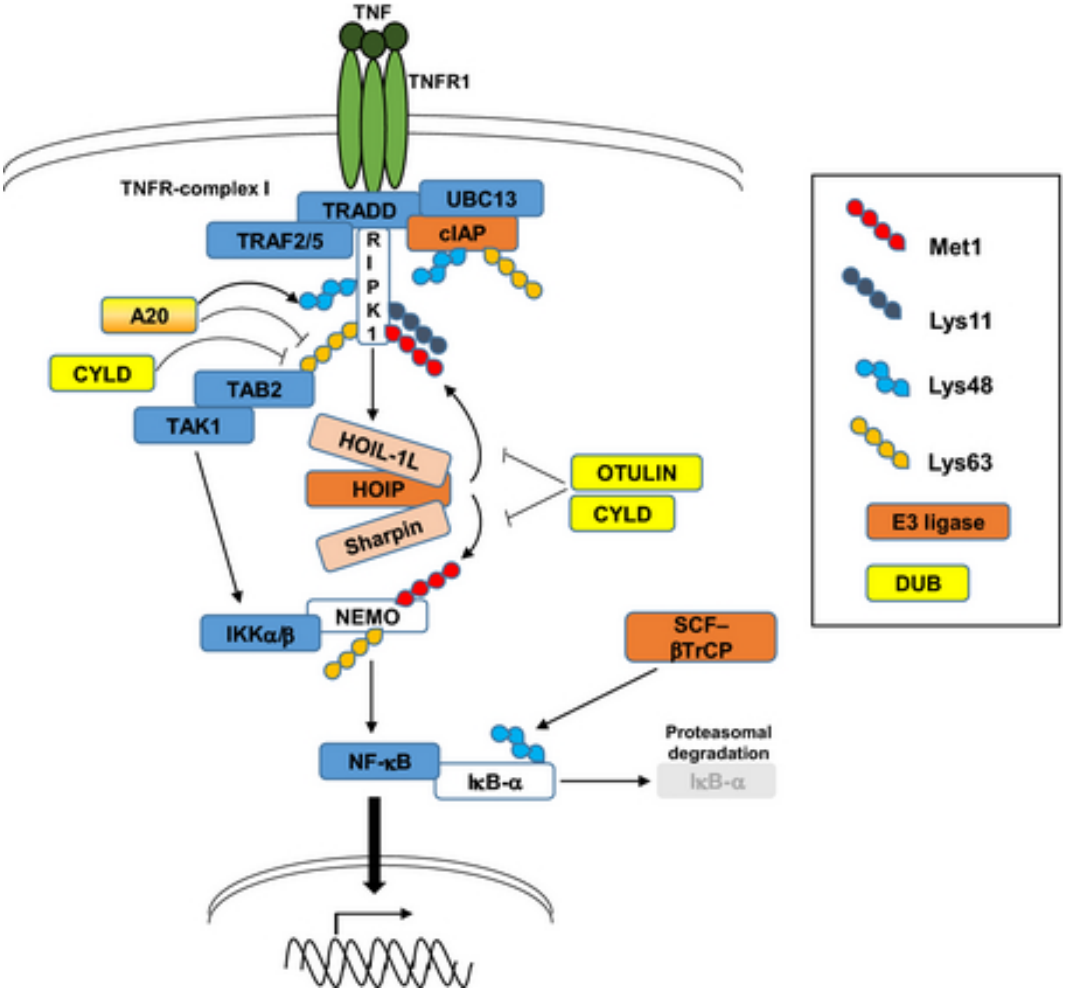

Figure 1.4.2 RIPK1 ubiquitination and deubiquitination in the TNF- induced NF-κB signalling. Different types of ubiquitin chains including Met 1-, Lys 11-, Lys 48-, and Lys 63- ubiquitin chains have roles in regulation of the downstream cascade. Ubiquitin chains are generated by E3 ligases (orange), such as cIAP, HOIP-containing LUBAC complex. These ubiquitin chains are hydrolyzed by DUBs (yellow) such as OTULIN and CYLD. A20 has a dual role as an E3 ligase as well as a DUB protine. Ubiquitination of RIPK1 has shown to be critical for the signaling pathway. SCF-bTrCP is responsible for proteasomal degradation of IκB-α. Adapted from (Ikeda 2015).

1.4.3 RIPK1 and cell fate

RIPK1 is emerging as an important determinant of cell fate in response to cellular stress. RIPK1 is believed to operate as a node driving NF-κB mediated cell survival, caspase-8 dependent apoptosis as well as RIPK3/MLKL-dependent necroptosis.

Cell survival-NF-κB pathway

RIPK1 was shown to be involved in TNFα, DNA damage (Hur, Lewis et al. 2003), Toll-like receptor (Shikama, Yamada et al. 2003, Kreuz, Siegmund et al. 2004, Dohrman, Kataoka et al. 2005, Cullen, Henry et al. 2013), Fas (APO-1/CD95) and TRAIL (Lin, Devin et al. 2000) induced NF-κB activation. RIPK1 was rapidly recruited to TNFR1 Complex I following TNF treatment and mediated NF-κB activation (Hsu, Huang et al. 1996). Overexpression of RIPK1 activated the NF-κB pathway (Dasgupta, Agarwal et al. 2008). Furthermore, a lack of RIPK1 in Jurkat T cells rendered them unable to activate NF-κB in response to TNFα stimulation (Ting, Pimentel-Muinos et al. 1996). $RIP^{-/-}$ embryonic stem cells failed to activate the NF-κB pathway and were sensitive to TNFα-mediated cell death (Kelliher, Grimm et al. 1998).

Using the TNFα-stimulated canonical NF-κB pathway as an example, RIPK1 was recruited by TRADD (Kischkel, Lawrence et al. 2000, Ishizawa, Tamura et al. 2006, Zhang, Zhou et al. 2011) and interacted with TNRAF 1 and 2 (Kataoka, Budd et al. 2000, Harper, Farrow et al. 2001), then bound to NF-κB essential modulator (NEMO) (Poyet, Srinivasula et al. 2000, Zhang, Kovalenko et al. 2000, Devin, Lin et al. 2001) stimulated IKK and activated the

NF-κB pathway (Inohara, Koseki et al. 2000, Lin, Devin et al. 2000, Poyet, Srinivasula et al. 2000).

When RIPK1 is cleaved, the NF-κB pathway is inhibited. For example, the C-terminal fragment of RIPK1, generated during apoptosis induced by caspase 8, acted as a negative inhibitor reducing TNFα-induced NF-κB activation by more than 70% (Lin, Devin et al. 1999, Martinon, Holler et al. 2000). This inhibition may be through the suppression of NF-κB inhibitor IKKβ (Kim, Choi et al. 2000) and enhanced the association between TNFR1, TRADD and FADD leading to a shift towards apoptosis (Kim, Choi et al. 2000). ABIN-2 (A20 binding inhibitor of NF-κB 2) (Liu, Yen et al. 2004) and OTULIN (Keusekotten, Elliott et al. 2013) blocked the interaction between RIPK1 and NEMO inhibiting NF-κB and potentiating apoptotic cell death. Also, the RHIM in RIPK1 ID mediated an interaction with RIPK3 to form the necrosome, inhibiting the ability of RIPK1 to further engage with the NF-κB pathway (Sun, Yin et al. 2002).

However, RIPK1 is not always necessary for NF-κB activation. For example, Epstein-Barr virus (EBV) transforming protein associated with TNFR1 and TRADD to mediate NF-κB activation but did not require RIPK1 (Izumi, Cahir McFarland et al. 1999). In primary human T cells and Jurkat cells, RIPK1 was essential for TNFR2 induced apoptosis but not for NF-κB activation. Also, in MEFs and E18 embryos, TNFα still activated NF-κB pathway when RIPK1 was knocked out (Wong, Gentle et al. 2010).

Cell Death-Apoptosis

RIPK1 has been shown to be important for the induction of apoptosis. For example, *in vitro* studies showed that RIPK1 knockout increased tongue squamous cancer cell apoptosis (Shan, Ma et al. 2015). RIPK1 was also a critical mediator of smac mimetic-mediated sensitization of glioblastoma cell apoptosis (Cristofanon, Abhari et al. 2015). *In vivo* studies showed that RIPK1 deficient mice displayed extensive apoptosis in lymphoid and adipose tissues (Kelliher, Grimm et al. 1998), and epithelium cell specific RIPK1$^{-/-}$ mice spontaneously developed intestinal epithelium cell apoptosis which leads to early death (Dannappel, Vlantis et al. 2014, Takahashi, Vereecke et al. 2014). In addition, knockdown of RIPK1 markedly exacerbated liver injury and induced lethality associated with massive hepatocyte apoptosis (Suda, Dara et al. 2016).

Further studies showed that RIPK1 associated apoptosis is dependent on the presence of caspase 8 (Barcia, Valle et al. 2003, Vanden Berghe, van Loo et al. 2004) and the formation of a RIPK1-FADD–Casp8–cFLIP-containing complex (ripoptosome) (cFLIP: cellular FLICE-inhibitory protein) (Kaiser, Daley-Bauer et al. 2014). If caspase 8 and cFLIPL were present, then RIPK1 was cleaved leading to apoptosis (Silke and Strasser 2013) at the site of D324 (Lin, Devin et al. 1999, Martinon, Holler et al. 2000, Silke and Strasser 2013). Caspase 8 also reduced necroptosis by preventing stable RIPK1-RIPK3 necrosome formation or through cleavage of CYLD to prevent RIPK1 deubiquitination (O'Donnell, Perez-Jimenez et al. 2011).

More specific studies showed that three domains of RIPK1 all affect apoptosis. Focal adhesion kinase suppressed RIPK1 and promoted pro-apoptotic signals through RIPK1 DD (Kurenova, Xu et al. 2004). Deletion of the RIPK1 DD eliminated the apoptotic response; one study showed that death domain itself was able to cause apoptosis (Stanger, Leder et al. 1995), while another revealed that an α-helical domain, was also needed for this activity (Grimm, Stanger et al. 1996). RIPK1 kinase activity relevant to the KD is controversial. Some researchers showed that RIPK1 kinase activity was not required for death receptor-mediated apoptosis (Wang, Du et al. 2008). However, emerging data suggested that RIPK1 kinase activity also driving the apoptotic response under certain conditions such as cIAP1/2 depletion or TAK1 kinase inhibition (Dondelinger, Aguileta et al. 2013). The RIPK1 kinase inhibitor Nec-1 or phosphorylation by IKKα/IKKβ both strongly reduced recruitment of RIPK1 and caspase 8 to FADD, indicating a role for RIPK1 kinase activity in apoptotic complex formation (Knox, Davies et al. 2011, Duprez, Bertrand et al. 2012). The RIPK1 ID is also thought to be involved in apoptosis. Mutation of RIPK1 ID enhanced recruitment of caspase 8 and FADD to form the complex IIa which allowed a cell death shift from TNFα-induced necroptosis to apoptosis in L929 cells (Duprez, Bertrand et al. 2012).

Cell death-Necroptosis

Necroptosis is a type of regulated cell death precisely controlled through RIPK1, RIPK3 and the downstream protein MLKL. It has the same outcome as necrosis. Necroptosis can be induced via death receptors, including CD95 (FAS) (Vercammen, Brouckaert et al. 1998), TNF receptors (Laster, Wood et al. 1988, Vercammen, Beyaert et al. 1998, Chan, Shisler et al. 2003), TRAIL-

R1/R2 (Jouan-Lanhouet, Arshad et al. 2012), and can also be initiated by the pathogen recognition receptor family including toll-like receptors, cytosolic NOD-like receptors and retinoic acid-inducible gene I-like receptors (Kalai, Van Loo et al. 2002). The necroptosis pathway has been most intensively studied with respect to death receptor stimulation (Vanlangenakker, Vanden Berghe et al. 2012).

The first step of this pathway through death receptors shares the same initiation complex as apoptosis and the NF-κB pathway, called the TNFR Complex I. The induction and the regulation of RIPK1 in the TNFR Complex I and ripoptosome has been discussed in the former sections. Here the focus will be on the specific steps of RIPK1 related necroptosis. After the ripoptosome is formed based on the existence and the activation of cFLIP and caspase 8, RIPK1 is activated and ready for the further steps involved in necroptosis (Dillon and Balachandran 2016). When cFLIPL and caspase 8 are both present, RIPK1 and RIPK3 in ripoptosome are cleaved, and apoptosis is inhibited, allowing necrosis to occur. The caspase-8-FLIPL-FADD platform is a gatekeeper preventing necroptosis under physiological conditions. Conversely, when caspase 8 is inhibited, RIPK1 kinase is activated and binds to RIPK3 (He, Wang et al. 2009, Zhang, Shao et al. 2009) and forms the necrosome through RHIM (Vandenabeele, Galluzzi et al. 2010, Wallach, Kovalenko et al. 2011). After necrosome formation RIPK3, activated by RIPK1 kinase, gains the ability to phosphorylate and activate MLKL to induce necroptosis (Zhao, Jitkaew et al. 2012, Murphy, Czabotar et al. 2013, Cai, Jitkaew et al. 2014). Conversely, when necroptosis is blocked, cells turn to caspase-dependent apoptosis (Melo-Lima, Celeste Lopes et al. 2014).

Besides RIPK3 and MLKL, there are other effectors downstream of RIPK1 that may relate to development of necroptosis. Research showed that RIPK1 was directly linked to adenine nucleotide translocase (ANT) which is an integral protein located in the inner mitochondrial membrane that exchanges mitochondrially synthesised ATP with cytosolic adenosine diphosphate (ADP) (Kroemer, Galluzzi et al. 2007). RIPK1 inhibited ANT and affected ATP synthase activity which induced ATP hydrolysis-driven extrusion of protons from mitochondrial matrix, leading to increasing of mitochondrial membrane potential (Vanden Berghe, Vanlangenakker et al. 2010). Protein kinase B (Akt) also engaged in the signalling cascade downstream of RIPK1 and provides a link connecting RIPK1 to JNK activation during necroptosis in L929 cells (McNamara, Ahuja et al. 2013).

However, recent research has indicated that RIPK1 does not constitute an absolute requirement for necroptosis induction. For example, murine cytomegalovirus infection induced RIPK3-dependent but RIPK1-independent necroptosis (Upton, Kaiser et al. 2010). In addition, RIPK1-deficient hematopoietic cells underwent RIPK3-mediated necroptosis (Roderick, Hermance et al. 2014) while TNFα activated RIPK3 in the absence of RIPK1 induced cell death by a caspase 8-dependent mechanism or a Bax/Bak- and caspase-independent mechanism (Moujalled, Cook et al. 2013). Furthermore, one study showed that RIPK1 was not only dispensable for necroptosis but may also act as an inhibitor, since silencing of the expression of RIPK1 failed to protect L929 cells from TNF-induced necroptosis and potentiated cell death, and Nec-1 enhanced the inhibitory effects of RIPK1 in this process (Kearney, Cullen et al. 2014).

Summary

RIPK1 recruits downstream kinases to the TNFR1 Complex I in the NF-κB, apoptosis and necroptosis pathway. In TNFR Complex I, RIPK1 is rapidly polyubiquitynated by Lys63-linked and linear Met1-linked ubiquitin chains act as adaptor proteins in IKK recruitment to form the Complex I including TNF-R1, TRADD, RIPK1, TRAF2, TRAF5 and cIAP1/2. The cIAPs ubiquitynate several components of this complex, and this is required to attract LUBAC. LUBAC subsequently consolidates this complex by promoting further ubiquitination through Lys63-linked ubiquitin chains to stabilise Complex I and recruits TAB and activates TAK1 in NF-κB pathway (Mihaly, Ninomiya-Tsuji et al. 2014). All these lead to recruitment of IKK and the activation of NF-κB. NF-κB-mediated upregulation of cFLIP suppresses cell death induced by Complex IIa including RIPK1, FADD and caspase 8. When ubiquitination of RIPK1 is prevented, TNFα-induced cell death was enhanced (Yu, Deng et al. 2015).

During apoptosis, RIPK1 needs to be phosphorylated and assembles the death effectors FADD and caspase 8 to form Complex IIa and create the pro-apoptotic signal (Dillon and Balachandran 2016). When cFLIPL and caspase 8 both present, RIPK1 and RIPK3 will be cleaved and necrosis ensues since apoptosis will be inhibited.

During necroptosis, when caspase 8 is inhibited, the RIPK1 kinase is activated and binds to RIPK3 to form the necrosome, which mediates the downstream events of necroptosis through MLKL. When necroptosis is blocked, cells turn to caspase-dependent apoptosis based on the existence of caspase8 and cFLIPL (Melo-Lima, Celeste Lopes et al. 2014) some research has designated

the ripoptosome as complex IIb and the necrosome as Complex IIc (Pasparakis and Vandenabeele 2015) (Figure 1.4.3).

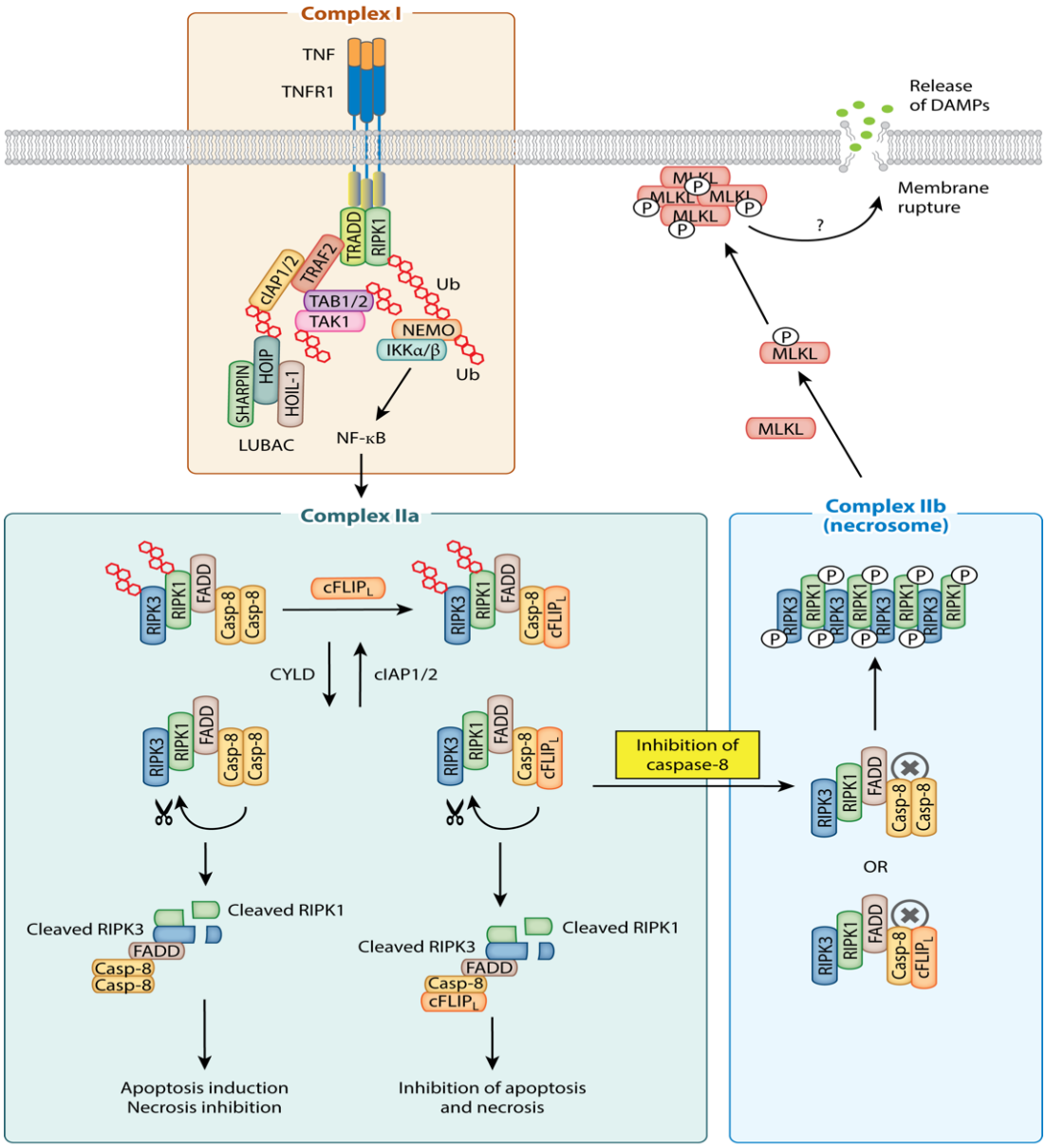

Figure 1.4.3 Schematic representation of TNFα induces NF-κB, apoptosis and necroptosis. Upon TNFα-binding to TNFR1, sequential formation of various complexes including Complex I, IIa and IIb takes place. Complex IIa or IIb may divert cell death to apoptosis when necrosome does not form. Formation of necrosome is essential for necroptosis that can be regulated by RIPK1 or RIPK3 and MLKL. Abrogation of NF-κB-mediated survival pathway also play important role in execution of necroptosis. Adapted from (Hong, Kim et al. 2016).

1.4.4 RIPK1 and ROS

Reactive oxygen species (ROS) have been proposed to exert a role in the execution of necroptosis. In the TNFα-induced necroptosis pathway, the cellular ROS level in MEFs was significantly elevated in Wt, but not in $RIP^{-/-}$, while a ROS scavenger butylated hydroxyanisole efficiently blocked cell death (Lin, Choksi et al. 2004, Shen, Lin et al. 2004). Knockdown of RIPK1 significantly reduced cell death and ROS generation in colon cancer cells (Yu, Hou et al. 2015) and human lung cancer cells (Wang, Chen et al. 2014). $Ripk1^{K45A}$ macrophages displayed a reduced level of ROS following reduced salmonella typhimurium infection-induced necroptosis *in vitro* (Shutinoski, Alturki et al. 2016).

Studies proved that this necroptosis-relevant ROS production was mediated through mitochondrial Complex I, since inhibition of cytoplasmic ROS generation by knockdown of NADPH oxidase components had no effect on TNFα-induced cell death, and suppression of mitochondrial Complex I attenuated TNFα mediated L929 cell death (Vanlangenakker et al., 2011) (Ardestani et al., 2013). In addition, mitochondrial Complex I inhibition triggered a mitophagy-dependent ROS increase leading to RIPK1 necroptosis in melanoma cells (Basit, van Oppen et al. 2017). However, studies have also suggested that depletion of mitochondria prevented ROS production but showed no effect on necroptotic cell death in NIH3T3 cells, suggesting that mitochondrial regulation of necroptosis may be dependent on cell type, and players other than mitochondrial ROS were likely to be involved in the execution of necroptosis (Tait, Oberst et al. 2013). Controversial evidence

showed that TNFα stimulation also regulated NADPH oxidase organiser 1 (NOXO1) subunit associated with RIPK1, TRADD, and Rho family of GTPases (Rac) then initiated ROS production and provoked prolonged JNK activation and necrosis in L929 cells (Kim, Morgan et al. 2007). When alkylating agent N-methyl-N′-nitro-N′-nitrosoguanidine induced necroptosis in MEFs, RIPK1$^{-/-}$ resulted in increased ROS production (Chiu, Ho et al. 2011)

Multiple studies in different cell types have shown that RIPK inhibitor Nec-1 affected ROS production. For example, Nec-1 significantly blocked TNFα-induced MEF cell death and ROS accumulation (Shindo, Kakehashi et al. 2013). Nec-1 protected against ROS-induced hepatotoxicity in acetaminophen-induced acute liver failure (Takemoto, Hatano et al. 2014). It was also found to reduce lesions, cytokines and ROS in the spinal cord trauma area (Wang, Wang et al. 2014). In ischemia-reperfusion injury, Nec-1 treatment attenuated ROS generation and increased expression of nitric oxide synthase 2 (NOS-2) and cyclooxygenases 2 (COX-2) (Zhang, Mao et al. 2014). Nec-1 and Nec-1s inhibition reduced ROS production induced by RIPK1-dependent necroptosis downstream of neutrophil death and neutrophil extracellular traps (NETs) formation (Desai, Kumar et al. 2016).

RIPK1 also modulates ROS production indirectly through other proteins. For example, RIPK1 affected RIPK3 and MLKL activity in the necroptosis pathway. RIPK3 interacted with the mitochondrial protein glutamate dehydrogenase 1 (GLUD1), and knockdown of GLUD1 could partially block TNFα-induced ROS production and necrosis in NIH3T3 cells (Zhang, Shao et al. 2009). RIP3- or

MLKL-deficient cells also showed ROS production was inhibited upon the induction of necroptosis (He, Wang et al. 2009).

RIPK1 may also indirectly affect JNK though the necroptosis pathway and then affect ROS levels. A previous study showed that Nec-1 and RIPK1$^{-/-}$ cells did not directly interfere with the generation of ROS associated with RIPK1/RIPK3-dependent necroptosis in peritoneal macrophages, however, an inhibitor of JNK abrogated necroptosis and induced a significant reduction of ROS (Fortes, Alves et al. 2012). Further, RIPK1 may be involved in the activation of caspase 2 (Ahmad, Srinivasula et al. 1997), mitogen-activated protein kinases (MAPK) (Devin, Lin et al. 2003), Akt-1 (Vivarelli, McDonald et al. 2004) the activities of which activity might be crucial for the modulation of mitochondrial function to affect ROS production (Lassus, Opitz-Araya et al. 2002, Majewski, Nogueira et al. 2004, Georgiadis and Knight 2012).

It is worth mentioning that the requirement of ROS for necroptosis seems to be dependent on cell type and toxins. For example, ROS scavengers did not inhibit necroptosis in HT-29 and Jurkat T cells (He, Wang et al. 2009). H_2O_2 caused cell death in L929 cells independently of RIPK1 or JNK (Vanden Berghe, Vanlangenakker et al. 2010). However, in MEFs, RIPK1 or JNK dependent pathways were shown to be essential for H_2O_2 induced necrosis (Shen, Lin et al. 2004).

1.4.5 RIPK1 and Ca^{2+}

In necroptosis studies, cytosolic Ca^{2+} elevations were observed in TNFα-induced mouse L929 cell necroptosis, and Ca^{2+} chelators exhibited a

protective effect upon necroptosis (Bianchi, Gerstbrein et al. 2004). The execution protein MLKL in necroptosis translocated to the plasma membrane and regulated Ca^{2+} influx through the TRPM7 (transient receptor potential melastatin related 7) as a downstream effector in TNFα-induced necroptosis in HT29 cells (Cai, Jitkaew et al. 2014). The development of Ca^{2+} leakage of the ER led to RIPK3- and CYLD-dependent necroptosis (Khan, Rizwan Alam et al. 2012). In addition, RIPK1 dependent hemagglutinating virus of Japan-envelope (HVJ-E)-induced cell death was linked to an increased concentration of cytoplasmic Ca^{2+} which triggered necroptosis by activating CaMK II and consequent RIPK1 phosphorylation (Nomura, Ueno et al. 2014). The ER stressor thapsigargin, which increases intracellular Ca^{2+} by inhibiting uptake into the ER by the SERCA pump, upregulated RIPK1 in Mel-RM, MM200 cells and four other melanoma cell lines (ME4405, SK-Mel-28, Mel-CV, and IgR3). Overexpression of RIPK1 enhanced melanocyte survival, and RIPK1 knockdown reduced viability of melanoma cells upon thapsigargin application (Jiang, Mao et al. 2009, Luan, Jin et al. 2015). The alkylating agent N-methyl-N′-nitro-N′-nitrosoguanidine induced RIPK1-dependent cell death that was associated with elevated Ca^{2+} at 6 h (Xu, Huang et al. 2006). This Ca^{2+} elevation was reduced by a deficiency of RIPK1 in MEFs (Chiu, Ho et al. 2011). In 2-methoxy-6-acetyl-7-methyljuglone (MAM)-induced HCT116 and HT29 cell death, MAM-induced necroptosis occurred through Ca^{2+} accumulation and sustained JNK activation. Both the calcium chelator (BAPTA-AM) and JNK inhibitor (SP600125) attenuated necroptosis (Sun, Wu et al. 2017).

However, in contrast, there is also research showing that Ca^{2+} flux is not necessary for necroptosis. A study revealed that in L929, NIH 3T3, and HT-29 cells, TNFα, smac and zVAD treatment induced two distinct events. One was an early Ca^{2+} flux, which was not required for necroptosis. The other was a late formation of 4 nm in diameter pores in the cell membrane that were concomitant with cell death. This study identified that the late membrane pore formation was a core event in necroptosis execution (Ros, Pena-Blanco et al. 2017).

1.5 RIPK1 and acute pancreatitis

RIPK1 is an upstream and pleiotropic node within cell survival and cell death making it a crucial but controversial research area. An interactions network for AP associated protein kinases (based on Gene Ontology Annotations through protein kinase database and PubMed) showed that 28 kinases play a role in AP including RIPK1 (Li, Ma et al. 2013). The study showed that the level of intact RIPK1 directly correlated with necrosis in CER-AP. Degradation of RIPK1 in CER-AP was inhibited by caspase inhibitors, and caspase induced with caerulein triggered RIPK1 cleavage (Mareninova, Sung et al. 2006).

A recent study showed that deletion of X-linked inhibitor of apoptosis protein (xIAP) increased caspase activities and RIPK1 degradation, leading to enhanced apoptosis and reduced necrosis in PACs, which resulted in the reduction of amylase activity, NF-κB activation, TNFα and IL-6 levels, and ameliorated the severity of AP (Liu, Chen et al. 2017). Furthermore, Nec-1 combined with zVAD-fmk reduced acinar cell injury and cell death in both CER-AP and TLCS-AP models (Louhimo, Steer et al. 2016). A new RIPK1 inhibitor, 1-(2,4-dichlorobenzyl)- 3-nitro-1*H*-pyrazole, and Nec-1 both showed good protective effects in L-arginine-induced pancreatitis (Zou, Xiong et al. 2016).

Other studies, however, have shown that Nec-1 administration alone did not have a protective effect in CER-AP nor did make AP worse. Nec-1 combined with zVAD even increased the pancreatic damage (Linkermann, Brasen et al. 2012). Another group also showed that Nec-1 did not protect against necrosis in CER-AP mice and CCK-stimulated PAC cell death. In this study knockdown

of intact RIPK1 with siRNA inhibited NF-κB activation and increased isolated PAC necrosis (Wu, Mulatibieke et al. 2017). Gene modification studies also showed that $Ripk1^{KD/KD\ D138N}$ mutant mice did not show improved CER-AP pancreas morphology and serum amylase (Newton, Dugger et al. 2016). Furthermore, RIPK1 P-loop deficiency $Rip1^{\Delta/\Delta}$ mice also did not ameliorate caerulein-induced pancreatitis (Liu, Fan et al. 2017). Table 1.5 contains a summary of experimental details from the relevant studies.

The variability in outcomes from multiple studies may be due to: 1) RIPK1 dependent necroptosis being dependent on the toxin applied (see chapter 1 section 1.4.3 for further details), and the different causes of AP may contribute to the differences, 2) the half-life of Nec-1 is short (Teng, Degterev et al. 2005) and Nec-1 delivered by i.p. injections may affect its potency, 3) different doses of Nec-1 used in these studies may affect the results (Takahashi, Duprez et al. 2012). The experiments which showed that Nec-1 was effective in AP used a relatively high dose of Nec-1, 4) different treatment times of Nec-1 and the sample collection times; for example, in CER-AP, inflammation and PAC necrosis were prominent at 6 h but only reached to maximum after 12 h (Wu, Mulatibieke et al. 2017), 5) Differences in sex and age of the animals used. For example, a study showed that gender-specific differences were noted with a more rapid Nec-1s clearance in females (Teng, Degterev et al. 2005). This may be due to gender-specific differences in compound metabolism (Mugford and Kedderis 1998).

Table 1.5 The effects of RIPK1 on experimental acute pancreatitis

	AP	Animal	AP induction	Inhibitors/ genotype	Results	Publications
Not Improved	CER	6-8 weeks female C57BL/6	i.p. 50μg Cer/kg once every h for 10 h	i.p. 1.65 mg /kg Nec-1 10 min before AP. Every 2 h for 10h 1/5 of 1.65 mg/kg Nec-1 was applied	Nec-1 did not ameliorate CER-AP	(Linkermann, Brasen et al. 2012)
	CER	11~13 weeks female C57BL/6	i.p. 50μg Cer/kg once every h for 7 h	*Ripk1*$^{KD/KD}$ mice expressing catalytically inactive RIPK1 mutant D138N	Pancreas morphology and serum amylase levels did not improve	(Newton, Dugger et al. 2016)
	CER	8 weeks, male, C57BL/6	i.p. 50μg Cer/kg once every h for 12 h	RIP1$^{\Delta}$, was with two amino acids $G_{26}F_{27}$ in the P-loop of RIP1 deleted	RIP1$^{\Delta}$ did not ameliorate CER-AP	(Liu, Fan et al. 2017)
	CER	7~8 weeks C57BL/6 and SD rats	i.p. 50 μg Cer/kg once every h for 7 h or 10h	i.p. 0.5 mg/kg and 1 mg/kg; 2 mg/kg Nec-1.	Nec-1 did not protect against necrosis	(Wu, Mulatibieke et al. 2017)
Improved	CER	20~30 g non–sex selected, C57BL/6	i.p. 50 μg Cer/kg once every h for 12 h	i.p. 6 mg/kg Nec-1 and 11.7 mg/kg zVAD. 30 min before AP induction	Nec-1 prevented acinar cell injury/death	(Louhimo, Steer et al. 2016)
	TLCS	20~30 g non-sex selected, C57BL/6	50 μL 10 mmol/L TLCS	i.p. 6 mg/kg Nec-1 and 11.7 mg/kg zVAD. 30 min before AP induction or 2h 4h and 6h after induction	Nec-1 prevented acinar cell death in 30min pretreat,2h and 4h treatment	(Louhimo, Steer et al. 2016)
	L-arginine	20~24 g male C57BL/6	i.p. 8% L-arginine twice in an hour	i.p. RIPK1 inhibitor 4b and Nec-1 ,10 mg/kg/day for 5 days.	Nec-1 and 4b showed protective effect on pancreas	(Zou, Xiong et al. 2016)

1.6 RIPK1 kinase gene modification mice

The gene modification of RIPK1 kinase activity is considered to be the most accurate way to research the involvement of this multi-function protein. Firstly, a RIPK1 deficient mouse strain was generated through knockout the RIPK1 gene. However, these mice failed to gain weight and displayed perinatal lethality accompanied by gross immune system abnormalities (Kelliher, Grimm et al. 1998). The mechanism responsible for the developmental failure of RIPK1 deficient mice remains unresolved. However, it seems that the scaffolding function of RIPK1 affects cell survival pathways.

Therefore, instead of knockout of the intact RIPK1, a selective knockout and knockin modification of RIPK1 was applied. For example, a phenotype of RIPK1 knockin, kinase-dead ($Rip1^{KD/KD}$) mice expressing an ATP binding site (K45A) mutant in the catalytic triad residues named as $Ripk1^{K45A}$ was generated. This strain is fertile and also showed the ability to reverse inflammatory disease (Kaiser, Daley-Bauer et al. 2014). The research showed that TNFα-induced apoptosis and the NF-κB pathway were unaffected in $Ripk1^{K45A}$. In addition, $Ripk1^{K45A}$ macrophages displayed poor trimerization of MLKL in response to TNFα/zVAD, and after treatment with LPS/zVAD for 6 h, the expression of IL-1α, TNFα and IL-10, but not IL-6 was reduced (Berger, Kasparcova et al. 2014, Kaiser, Daley-Bauer et al. 2014). Also, after injected with B16-F10 cells, tumor nodules in the lung of $Ripk1^{K45A}$ mice were decreased by 38.3%(±8.5%) compared to Wt mice (Hanggi, Vasilikos et al. 2017).

Another kinase dead mouse strain RIPK1$^{D138N/D138N}$, involving a mutation in the catalytic activation loop, was also fertile and expressed normal amounts of RIPK3 and MLKL (Newton, Dugger et al. 2014). *In vivo* experiments in the RIPK1$^{D138N/D138N}$ strain showed that it was protected against TNFα-induced shock (Polykratis, Hermance et al. 2014). More recently, a novel RIPK1 kinase-dead mutant was generated by altering the P-loop in KD. Consistent with previous studies on other kinase-dead strains, this RIP1$^{\Delta}$ exhibited TNFα-induced necroptosis similar to Ripk1^{K45A} or RIPK1$^{D138N/D138N}$ (Liu, Fan et al. 2017). However, there were different impacts of kinase mutations. For example, with respect to the embryonic development of Fadd$^{-/-}$ mice, RIP1$^{\Delta}$ rescued Fadd$^{-/-}$ mouse lethality but Ripk1^{K45A} did not (Liu, Fan et al. 2017).

There are also conditional knockout mice related to RIPK1. For example, mice lacking RIPK1 in intestinal epithelial cells (IEC) spontaneously developed severe intestinal inflammation associated with IEC apoptosis, villus atrophy, loss of goblet and Paneth cells which led to early death (Dannappel, Vlantis et al. 2014, Takahashi, Vereecke et al. 2014) . RIPK1^{E-KO} mice, which were generated from a conditional deletion of the RIPK1 in skin epithelial cells, progressively developed severe inflammatory skin lesions (Dannappel, Vlantis et al. 2014). Ripk1^{LPC-KO} mice, which were generated from conditional knockout of RIPK1 in liver parenchymal cells, exhibited elevated apoptosis induced by both Concanavalin A and TNFα , and showed improvement of severe hepatitis (Filliol, Piquet-Pellorce et al. 2016).

A few studies have also combined RIPK1 knockout with other gene knockouts to evaluate the possible relationship between these proteins. For example, while Ripk1$^{-/-}$ mice displayed perinatal lethality, Ripk1$^{-/-}$Ripk3$^{-/-}$Casp8$^{-/-}$ and Ripk1$^{-/-}$Ripk3$^{-/-}$Fadd$^{-/-}$ mice gained weight over time and appeared similar to their littermates for several months (Dillon, Weinlich et al. 2014, Kaiser, Daley-Bauer et al. 2014).

Furthermore, Fadd$^{-/-}$Ripk1$^{-/-}$ double-knockout T cells were resistant to death induced by Fas or TNFα (Zhang, Zhou et al. 2011) but Fadd$^{-/-}$Ripk1$^{-/-}$ mice did not survive the first day of postnatal life (Dillon, Weinlich et al. 2014), suggesting that the *in vitro* RIPK1 knockout may not be representive of *in vivo* experimental changes.

1.7 Pharmacological inhibitors of RIPK1

Necrostatins were identified in a cell based screen for TNFα/zVAD-induced necroptosis in the human U937 cell line. Necrostatin family members, including Nec-1, Nec-3, Nec-4, Nec-7 and Nec-1 stable (Nec-1s), all showed good inhibition of RIPK1 kinase activity and lacked activity against RIPK2 and RIPK3 (Degterev, Hitomi et al. 2008, Christofferson, Li et al. 2012). Besides the necrostatin family, other types of RIPK1 inhibitors such as GSK 963', cpd27, pazopanib, PN10, GSK2606414, GSK2656157 and GSK2982772 were developed (Figure 1.7).

1.7.1 Necrostatin-1

Nec-1 is the first and most popular inhibitor of RIPK1 for necroptosis experimental studies. It has been shown that Nec-1 affected RIPK1 kinase activity by stabilising the RIPK1 activation loop and the surrounding structural elements (Xie, Peng et al. 2013), and binding to Ser161 inhibited RIPK1 phosphorylation (Degterev, Hitomi et al. 2008, McQuade, Cho et al. 2013). It also abolished the assembly of RIPK1 and RIPK3 necrosome formation (Xie, Peng et al. 2013) without affecting the RIPK1 mediated NF-κB pathway (Degterev, Huang et al. 2005). Nec-1 failed to block necroptosis in the absence of RIPK1, indicating that its ability to suppress necroptosis was indeed RIPK1 dependent (Kearney, Cullen et al. 2014).

However, the inhibition by Nec-1 of RIPK1 not only affected necroptosis, but also the apoptotic complex formation by a reduced recruitment of RIPK1 and caspase-8 to FADD (Duprez, Bertrand et al. 2012). Nec-1 also inhibited RIPK1 to prevent association of FADD with NEMO (Biton and Ashkenazi 2011). A study showed that ferroptosis is also Nec-1 sensitive under some conditions, and more specific inhibitor Nec-1s did not affect ferroptosis (Friedmann Angeli, Schneider et al. 2014).

Besides such effects relevant to RIPK1, Nec-1 is also a potent inhibitor of the enzyme indoleamine 2,3-dioxygenase (IDO) a constituent of the tryptophan-kynurenine pathway (Takahashi, Duprez et al. 2012, Vandenabeele, Grootjans et al. 2013). The details of IDO inhibition will be discussed in the section 1.8).

Other than binding issues, Nec-1 has a short half-life ($T_{1/2}$<5 min in a mouse microsomal assay) and relatively low solubility (Teng, Degterev et al. 2005). Nec-1 effects are also very dose-dependent. For example, high doses of Nec-1 inhibited T cell receptor activation in L929 cells independently of RIPK1 (Cho, McQuade et al. 2011). In contrast, mice were sensitised to TNF-induced SIRS when 10-fold lower doses of Nec-1 were administered (6mg/kg and 0.6 mg/kg) (Takahashi, Duprez et al. 2012). This may help to explain some controversies among published studies.

Even so, inhibiting RIPK1 through Nec-1 has been extensively used in a wide range of pathological cell death studies and has shown protective effects in diseases such as ischemia-reperfusion injury (Degterev, Huang et al. 2005, Smith, Davidson et al. 2007, Xu, Chua et al. 2010, Northington, Chavez-Valdez et al. 2011, Linkermann, Brasen et al. 2012), neurodegenerative diseases (Li, Yang et al. 2008, Zhu, Zhang et al. 2011), inflammatory diseases (Zitvogel, Kepp et al. 2010, Duprez, Takahashi et al. 2011), hepatitis (Jouan-Lanhouet, Arshad et al. 2012), lethal irradiation (Huang, Epperly et al. 2016), indicating its potential as a therapeutic drug. However, a few studies also showed that Nec-1 did not improve cell death but accelerated it under certain conditions. For example, Nec-1 accelerated time to death and worsened organ damage after TNFα-induced shock in the absence of caspase inhibition (Linkermann, Brasen et al. 2012). Another group also reported that Nec-1 worsened outcome in a peritoneal sepsis model (McNeal, LeGolvan et al. 2011).

The potential of Nec-1 to interfere with other signalling proteins and issues relating to the dosage of complicate the interpretation of studies reporting Nec-1 effects. Therefore, in the present study pharmacological inhibition of RIPK1 kinase was coupled with gene modification to confirm the function of RIPK1.

1.7.2 Other Necrostatins

Nec-3 and Nec-4 have very similar binding compared with Nec-1 which is located in the ATP-binding active centre. Their effect is similar to Nec-1 and these three necrostatins can cross compete, but to varying degrees (Choi, Keys et al. 2012, Maki, Smith et al. 2012). Another necrostatin Nec-7 inhibits necroptosis independently of RIPK1 (Zheng, Degterev et al. 2008). Nec-1s, an Nec-1 analogue, was developed to increase selectivity and potentially avoid target effects other than RIPK1 inhibition. It was found to be more selective for RIPK1 (Christofferson, Li et al. 2012) and was demonstrated to be very effective in reducing brain injury (Degterev, Huang et al. 2005).

Extensive structure-activity analysis of Nec-1 and other necrostatins revealed that small changes of these molecules could lead to the robust loss of activity. Also, necrostatins may have physical limitations on maximal robustness due to the small size of the molecules (Najjar, Suebsuwong et al. 2015). Therefore, based on those shortcomings of necrostatins alternatives for RIPK1 kinase inhibition have been explored.

1.7.3 Other RIPK1 inhibitors

Recently a different group of RIPK1 inhibitors was described, including cpd27 (Harris, Bandyopadhyay et al. 2013). These molecules were selected from *in*

vitro kinase targeted libraries using the recombinant RIPK1 kinase domain. X-ray structure analysis revealed that these RIPK1 inhibitors were overlapping with the necrostatin binding site. The optimised inhibitors in these series displayed low nanomolar potency against RIPK1 *in vitro*, and cpd 27 showed an efficient inhibition of TNFα-induced toxicity at the 20 mg/kg dose *in vivo* (Najjar, Suebsuwong et al. 2015).

Another RIPK1 inhibitor developed by Glaxo Smith Kline (GSK), designated GSK'963, was shown to display low nanomolar activity on necroptosis in various cellular models (Berger, Harris et al. 2015). GSK'963 blocked Yersinia. Pestis-induced cell death and inhibited caspase8 enzyme activity after infection (Weng, Marty-Roix et al. 2014). It also inhibited TNFα/zVAD-induced necroptosis *in vivo* at a 2 mg/kg dose. Although it is an excellent tool to study RIPK1 inhibition in vitro, GSK'963 had minimal oral exposure in rodents limiting further development (Berger, Harris et al. 2015).

Further, GSK identified a novel RIPK1 kinase inhibitor, [1,4] oxazepin-3-yl)-1H-1,2,4-triazole-3-carboxamide 5 (GSK2982772), from a DNA-encoded library with high RIP1 potency and kinase selectivity. It has excellent activity in both RIP1 cellular systems, preventing TNF induced necrotic cell death, and an ulcerative colitis explant assay blocking spontaneous cytokine release. The highly favorable physicochemical and absorption, distribution, metabolism, and excretion-toxicity in pharmacokinetics (ADMET) properties of GSK2982772, combined with high potency, led to a predicted low oral dose in humans (6.3 mg and 60 mg once daily, achieving 50 and 90% RIP1 inhibition over 24 h, respectively) and other species (ranging from 2 to 1000 mg/kg in

both rat and cynomolgus monkey), and became the first-in-class RIP1 inhibitor for clinical trials. It recently completed phase 1 evaluation, and phase 2a clinical trials in psoriasis, rheumatoid arthritis, and ulcerative colitis patients are currently underway. However, worth to mention that, GSK2982772 exhibited equivalent RIP1 potency against human and monkey, but was significantly less potent against nonprimate RIPK1 (Harris, Berger et al. 2017).

A recent screen of the clinical kinase inhibitor library identified a pan-tyrosine kinase inhibitor (TKI) called pazopanib as a suppressor of necroptosis through efficiently inhibiting RIPK1 (Fauster, Rebsamen et al. 2015). Pazopanib was also described as a Type I ATP competitive inhibitor of vascular endothelial growth factor (VEGF) (van Geel, Beijnen et al. 2012). Therefore, in order to improve its activity on RIPK1 kinase inhibition, a group of ponatinib/necrostatin-1 “hybrid” inhibitors which were designated as “PN” were designed. PN10 is one of the most effective members in the PN series, and displayed excellent selectivity for RIPK1 and RIPK1 dependent necroptosis (Najjar, Suebsuwong et al. 2015).

The other new RIPK1 inhibitor, named 1-(2, 4-dichlorobenzyl)-3-nitro-1H-pyrazole, also inhibited RIPK1/RIPK3/MLKL signalling with an EC_{50} value of 0.160 μM in the cell necroptosis inhibitory assay and a Kd (equilibrium dissociation constant) value of 0.078 μM against RIPK1 kinase. It also showed a good protective effect in the L-arginine-induced AP mouse model (Zou, Xiong et al. 2016).

Very recent research has found that protein kinase R (PKR)-like endoplasmic reticulum kinase (PERK) inhibitors were also potent RIPK1 inhibitors. PERK

is an ER-anchored receptor and inhibition of PERK can reduce ER stress through the unfolded protein response (UPR) network. The inhibitors of PERK have become attractive tools for the potential therapeutic manipulation of the UPR in inflammatory conditions. Two commonly used PERK inhibitors, GSK2606414 and GSK2656157, showed complete repression of TNFα-mediated RIPK1 kinase-dependent cell death through direct RIPK1 inhibition, an effect independent of PERK inactivation. *In vivo* studies also showed that GSK2656157 administration protected mice from lethal doses of TNFα independently of PERK inhibition and as efficiently as GSK'963 (Rojas-Rivera, Delvaeye et al. 2017).

Sorafenib is already clinically used to treat hepatocellular carcinoma, renal cell carcinoma, and acute myeloid leukemia. It exerts anti-tumor effects by inhibiting kinases involved in cell proliferation and survival. A recent study demonstrated that this anti-cancer agent also acts an inhibitor of RIPK-dependent cell death at lower concentration. However, Sorafenib is not a specific RIPK1 inhibitor, it can bind either a complex containing RIPK1, RIPK3 and MLKL or to each of these proteins separately (Martens, Jeong et al. 2017). In vivo study showed that Sorafenib protected against TNF-induced SIRS (Duprez, Takahashi et al. 2011), and renal ischemia-reperfusion injury (Linkermann, Stockwell et al. 2014).

Overall, these new RIPK1 inhibitors have broadened the availability for the pharmacological evaluation in necroptosis or other pathways relevant to RIPK1 *in vitro* and *in vivo*. However, it should be borne in mind that the dose

and other effects rather than specific RIPK1 inhibition need to be considered during the planning of studies.

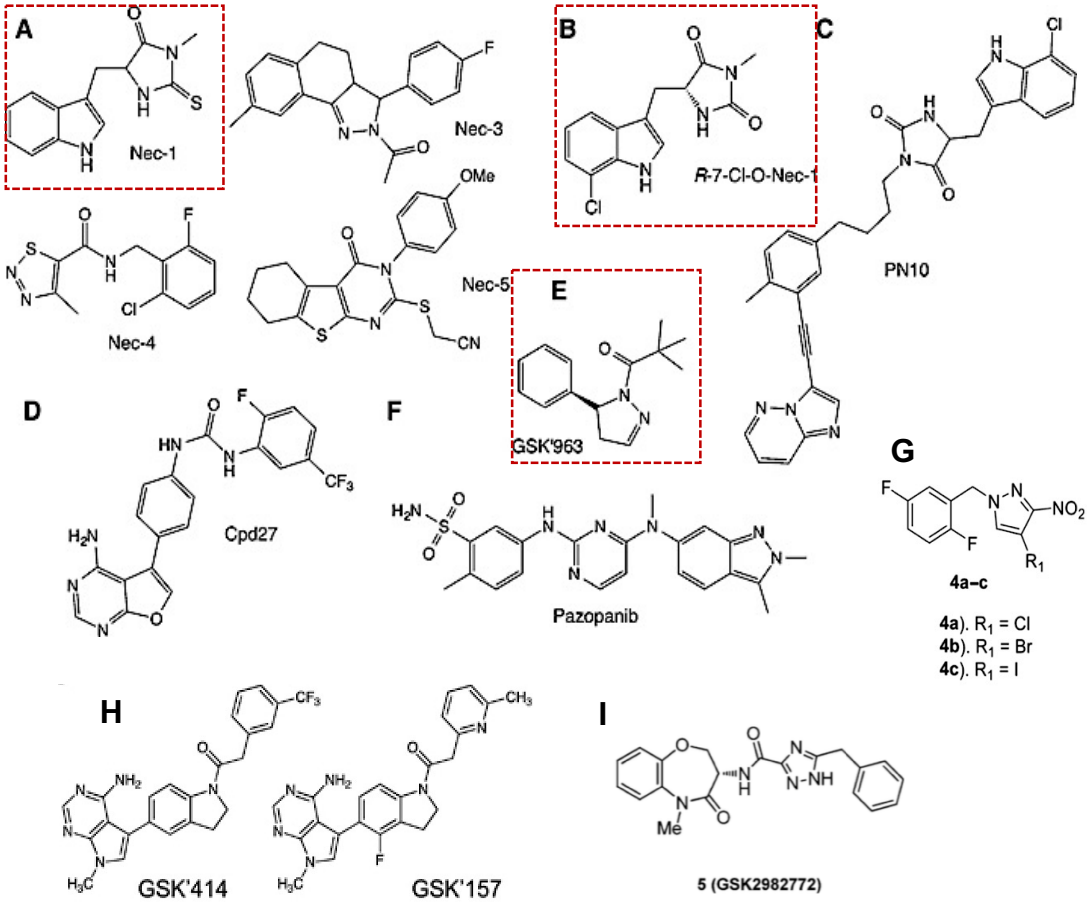

Figure 1.7 Chemical structures of RIPK1 kinase inhibitors. **A)** Necrostatins identified in a cell based screen. **B)** Nec-1s. **C)** PN10. **D)** Cpd27. **E)** GSK'963. **F)** Pazopanib. **G)** 4b. **H)** GSK2606414 and GSK2656157. **I)** GSK2982772. A, B and E were used in this project. Adapted from (Degterev and Linkermann 2016, Zou, Xiong et al. 2016, Rojas-Rivera, Delvaeye et al. 2017).

1.8 Acute pancreatitis and the kynurenine pathway

1.8.1 The Kynurenine pathway

The kynurenine pathway (KP) is the main tryptophan metabolic route (up to 95%). Firstly, tryptophan is catalysed by primary enzymes (indoleamine-2,3-dioxygenase (IDO) and tryptophan 2,3-dioxygenase (TDO)) through a rate-limiting process to generate formylkynurenine. Then, formylkynurenine is converted into L-kynurenine and further converted into downstream intermediates based on different catalytic enzymes, including kynurenic acid, anthranilic acid, 3-hydroxy-L-kynurenine (3-HK), 3-hydroxyanthranilic acid (3-HAA), quinolinic acid (Quin), and finally, production of oxidised nicotinamide adenine dinucleotide oxidised (NAD^+) (Grohmann, Fallarino et al. 2003) (Figure 1.8.1). Changes in the kynurenin/tryptophan ratio have been reported for the pathogenesis of arthritis, HIV/AIDS, neuropsychiatric disorders, cancer and inflammation (Huengsberg, Winer et al. 1998, Stone 2001, Schroecksnadel, Kaser et al. 2003, Suzuki, Suda et al. 2010, Campbell, Charych et al. 2014).

IDO is a family of enzymes (IDO1 and IDO2) that converts tryptophan into kynurenine. Although IDO2 shares 43% sequence identity with IDO1, the two enzymes have a different expression, distribution and activity (Ball, Sanchez-Perez et al. 2007). For example, studies showed that IDO1 was expressed in placenta, lung, spleen, liver, kidney, stomach, intestine and brain. Whereas, IDO2 was expressed at low levels in the liver, testis and thyroid (Lob, Konigsrainer et al. 2009, van Baren and Van den Eynde

2015). IDO1 showed higher enzymatic activity than IDO2 for catalysing tryptophan in humans and other species (Ball, Sanchez-Perez et al. 2007, Yuasa, Ball et al. 2009).

Although both catalyse tryptophan, they exert different functions. For example, IDO2-overexpressing human 293 cells were unresponsive to tryptophan restoration after tryptophan depletion by IDO2 activity, in contrast to IDO1 overexpressing cells, which responded fully (Metz, Duhadaway et al. 2007). IDO1 loss was sufficient to reduce tumour formation (Muller, Sharma et al. 2008), whereas IDO2 loss had no effect on either tumour formation or progression (Metz, Smith et al. 2014). Furthermore, IDO2 was crucial for the development of arthritis whereas IDO1 was completely dispensable, shown by IDO2 inhibitor (D-1MT) treatment which attenuated rheumatoid arthritis (Scott, DuHadaway et al. 2009) . $IDO1^{-/-}$ and $IDO2^{-/-}$ mice both had a reduction in contact stimulation, however, only loss of IDO2 was associated with a reduction in systemic levels of cytokines including IFN-γ, TNFα, and IL-6, suggesting that IDO2 helps regulate adaptive immunity (Jux, Kadow et al. 2009).

IDO1 and IDO2 are also connected with each other, since the deficiency of IDO1 function in $IDO1^{-/-}$ mice also displayed a reduced IDO2 function. IDO1 deficiency abolished responses to D-1MT even though IDO1 was dispensable for rheumatoid arthritis, suggesting an IDO1-IDO2 genetic interaction in immune control (Scott, DuHadaway et al. 2009).

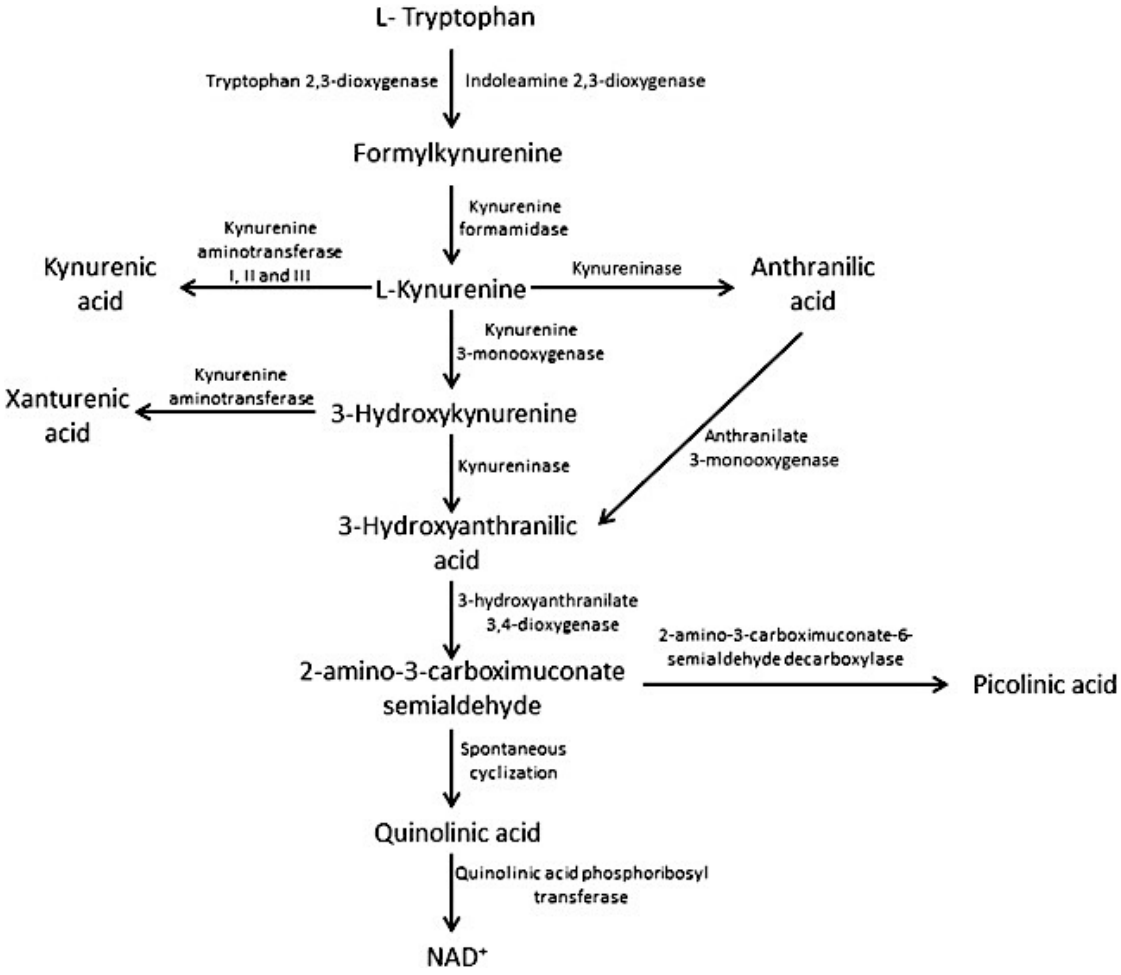

Figure 1.8.1 The essential enzymes and products been involved in kynurenine pathway. Adapted from (Gonzalez Esquivel, Ramirez-Ortega et al. 2017).

1.8.2 Pharmacological inhibitors of IDO

1-methyl-D/L-tryptophan (1-MT) and methyl thiohydantoin-DL-tryptophan (MTH-trp) are two important tryptophan analogues which have been used as IDO inhibitors.

1-MT inhibits both IDO1 and IDO2. It exists as two stereoisomers, 1-D-MT and 1-L-MT. Most preclinical studies have used the racemic mixture of 1-D/L-MT to inhibit IDO and have shown promising results. For example, 1-MT reduced the tumour volume of mice preimmunized with a tumour antigen (Uyttenhove, Pilotte et al. 2003), while 1-MT in combination with chemotherapeutic agents induced regression of established murine breast cancers (Muller, DuHadaway et al. 2005). Instead of mixed effects of those two stereoisomers together, studies showed that IDO1 was the preferred target of 1-L-MT, while 1-D-MT preferentially inhibited IDO2 (Metz, Duhadaway et al. 2007, Lob, Konigsrainer et al. 2008, Lob, Konigsrainer et al. 2009, Opitz, Litzenburger et al. 2009). However, L-1-MT was much more effective than 1-D-MT in inhibition of the kynurenine pathway. The binding affinity for 1-MT was 34 mM and the EC_{50} for IDO inhibition was 266.9 (Koblish, Hansbury et al. 2010).

MTH-trp is also called Nec-1. Both 1-MT and MTH-trp suppressed IFN-γ induced IDO mRNA and protein levels in CMT-93 cells (Okamoto, Tone et al. 2007), and blocked IDO activity induced by LPS/IFN-γ in dendric cells (Jurgens, Hainz et al. 2009, Pfeifer, Schreder et al. 2012). Although the binding affinity for MTH-Trp is 11.6 μM, and EC_{50} against IDO is 12.85 which is less than 1-MT (Koblish, Hansbury et al. 2010), in a cell-based assay, MTH-Trp showed ~20-fold more potency than 1-MT (Muller, DuHadaway et al.

2005). Like 1-MT, MTH-trp retarded tumour outgrowth but did not promote regression. Also, MTH-trp produced no evidence of gross toxicity in the mice during treatment or at necropsy (Muller, DuHadaway et al. 2005, Hou, Muller et al. 2007).

Although 1-MT and Nec-1/MTH-Trp share a common indole moiety, studies demonstrated that 1-MT neither affected human nor mouse cell necroptosis (Takahashi, Duprez et al. 2012, Degterev, Maki et al. 2013) (Vandenabeele, Grootjans et al. 2013). The extent to which the effects of Nec-1/MTH-Trp may be attributed to inhibition of RIPK1 or IDO in disease models are difficult to address.

Based on their structures, a few drugs have been developed and been taken through to clinical trials as potential therapeutic candidates. For example, 1-D-MT is currently used as Indoximod (NLG-8189) to inhibit IDO2 in phase 2 clinical trials as an adjunct to chemotherapy and reverses IDO-mediated immune suppression. Another drug Epacadostat (INCB024360) is a potent and selective IDO1 inhibitor with an IC_{50} of 10 nM and displays high selectivity over other related enzymes such as IDO2 and TDO (Sheridan 2015).

1.8.3 The Kynurenine pathway and AP

In AP patients, it was observed that organ dysfunction was associated in real time with increased plasma kynurenine, and that kynurenine levels were higher in patients who required mechanical ventilation or haemodialysis than in those who did not (Mole, McFerran et al. 2008). This research also showed that kynurenine catabolites of tryptophan including 3-hydroxykynurenine were transported in mesenteric lymph and contributed to pancreatitis-associated organ failure in rats and humans. Further research showed that inhibition of kynurenine monooxygenase (KMO), which is a flavin adenine dinucleotide (FAD) dependent monooxygenase located on the outer mitochondrial membrane, resulted in reduced levels of 3-hydroxykynurenine and quinolinic acid beneficial to the treatment. Also, a KMO deficient mouse was protected against extra-pancreatic tissue injury to the lung, kidney and liver in experimental AP multiple organ dysfunction syndromes (Abdel-Magid 2015).

A potent and specific inhibitor of KMO, GSK180, resulted in rapid changes of the kynurenine pathway metabolites *in vivo* against multiple organ dysfunctions in a rat bile acid infusion and CER-AP model (Mole, Webster et al. 2016). Furthermore, a clinical cohort study found a strong correlation between 3-hydroxykynurenine concentration and the systemic inflammatory burden measured by C-reactive protein levels. This cohort also showed that TNFα and IL-6 correlated strongly with the 3-hydroxykynurenine concentration (Skouras, Zheng et al. 2016).

Based on the clinical and basic research in AP and KMO, a series of potent, competitive and highly selective KMO inhibitors have been discovered which

demonstrated good cellular potency and clear pharmacodynamic activity *in vivo* (Skouras, Zheng et al. 2016, Walker, Ancellin et al. 2017). Compound 28 showed protective effects against extra-pancreatic tissue injury including kidney and lung during experimental AP in rats, and will now progress toward clinical evaluation for the treatment of AP (Liddle, Beaufils et al. 2017). However, besides these studies, no other research has been directed towards the relevance of IDO to the pathophysiology AP.

1.9 Aims and objectives

AP is a severe and potentially fatal human disease characterised by parenchymal necrosis with associated inflammation. Necroptosis is currently the best characterised form of regulated necrosis and is mediated through RIPK1, RIPK3 and the downstream protein MLKL. Accumulating studies demonstrated that necroptosis plays a crucial role in the pathogenesis of AP related to RIPK3 and MLKL. However, the functions of RIPK1 in the pancreas have remained unclear. The aim of this project was to elucidate the role of RIPK1 in AP through investigation of:

1. Whether pancreatitis relevant toxins induce RIPK1 kinase dependent cell death in PACs.
2. Whether alterations of Ca^{2+} and ROS contribute to RIPK1 kinase dependent cell death in PACs.
3. The potential role of RIPK1 kinase activity in experimental AP models.
4. Whether RIPK1 could be a potential target for AP treatment.

Chapter 2: Material and Methods

2.1 Animals and genotyping

2.1.1 Animals

C57BL/6J: male C57BL/6J mice (20~25 g) were from Charles River UK Ltd (Margate, UK). The mice were housed at room temperature (22~25 °C) under a 12-hour light/dark cycle with free access to standard laboratory chow and water.

Ripk1^{K45A} mice: The kinase-dead knock-in (Ripk1^{K45A}) mouse was generated by GSK. Ripk1^{K45A} mouse with a point mutation in the catalytic lysine (K45A) in exon 3 of the RIPK1 gene constructed from C57BL/6J mouse DNA (Figure 2.1.1)(Berger, Kasparcova et al. 2014). Ripk1^{K45A} mice were born at the expected Mendelian ratios from the interbreeding of heterozygous mice. The colony was also housed at room temperature (22~25 °C) under a 12-hour light/dark cycle with free access to standard laboratory chow and water. This strain will express the normal level of RIPK1, however the kinase activity was muted (Kaiser, Daley-Bauer et al. 2014).

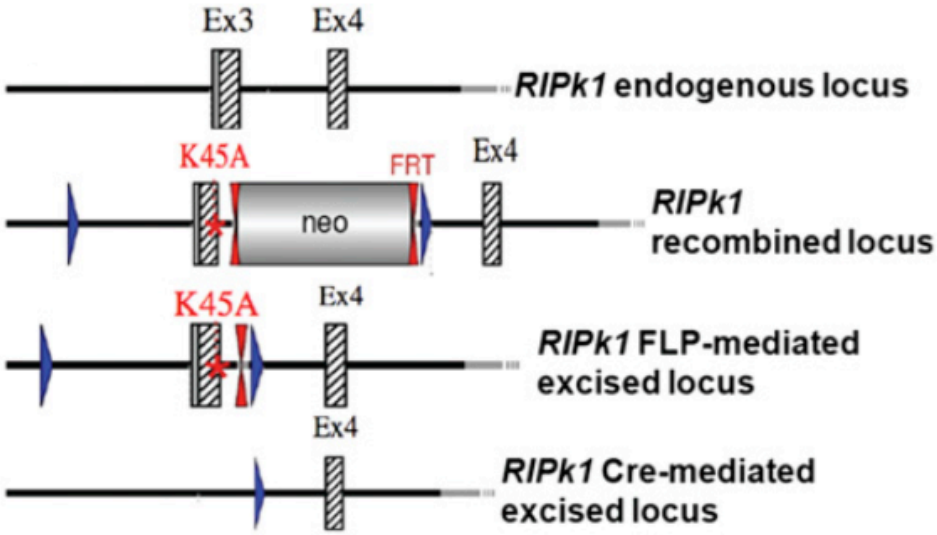

Figure 2.1.1 Ripk1^{K45A} gene modification. RIPK1 gene-targeting vector was constructed from C57BL/6J mouse DNA by inserting the K45A point mutation into Ripk*1* exon3 and also inserting a Neo cassette in intron 3 flanked by FRT sites for Flp-mediated excision. Exon 3 was flanked by loxP sites, enabling access to its deletion through Cre action. Adapted from (Berger, Kasparcova et al. 2014).

2.1.2 Ripk1^{K45A} mice genotyping

DNA extraction

Ear notches from subject mice were used for DNA extraction according to the supplier's instruction (DNeasy Blood & Tissue Kits Cat No./ID: 69504, Qiagen, CA). Ear notches were placed in 1.5 ml micro centrifuge tubes with 180 µl Buffer ATL and 20 µl Proteinase K. This mixing was vortexed and incubated at 56°C overnight until completely lysed. Fur was removed and the lysate were centrifuged at 16,000 g. 200 µl Buffer AL was added next and vortexed, followed by adding 200 µl ethanol (96~100%). The mixture was pipetted into a DNeasy mini spin column with a 2ml collection tube and was centrifuged at 6000 g for 1 min. Flow-through was discarded and the spin column was added to a new 2 ml collection tube. 500 µl Buffer AW1 was added and centrifuged for 1 min at 6000 g. Flow-through was discard and spin column was placed in a new 2 ml collection tube. 500 µl Buffer AW2 was added and centrifuged for 3 min at 20,000 g. Flow through was discarded and the spin column was transferred to a new 2 ml micro centrifuge tube. Then 200 µl Buffer AE was added for elution and incubated for 1 min at room temperature then centrifuged for 1 min at 6000 g. The final steps can be repeated to achieve higher DNA concentration. The DNA concentration was determined by spectrophotometric absorption at 230, 260, and 280 nm and the quality was calculated as the A_{260}/A_{230} and A_{260}/A_{280} ratios.

Standard PCR

All Ripk1^{K45A} animals used for breeding were tested using standard PCR to DNA then make sure each mouse was homozygous. The following

genotyping primers offered by GSK and were used in the PCR (generated by Eurofins Genomics, UK):

69277 flp-JEM 2, 5'-CTCTGATTGCTTTATAGGACACAGCACTAAGC-3'; (32)

69278 flp-JEM 2, 5'-GTCTTCAGTGATGTCTTCCTCGTATATTTCTCAAG-3'; (35)

575 bp for the Ripk1^{K45A} allele and 473 bp for the Wt allele (length of DNA).

50 μl reaction system was mixed on ice for further PCR steps (Table 2.1.2 A). PCR tubes were transferred from ice to the PCR machine with the block preheated to 95°C before thermos-cycling (Table 2.1.2 B). PCR reaction products were used immediately or stored in -20°C for further use.

Table 2.1.2 A: Reaction buffer recipe for 50 μl reaction system

Component	50 μl reaction (μl)
AmpliTaq Gold® Buffer	5
25 mM $MgCl_2$	4
10 mM dNTP mix	1
AmpliTaq Gold® DNA polymerise (5 U/ μl)	0.25
Template DNA	5
Forward primer	2.5
Reverse primer	2.5
Autoclaved distil water	29.75

Table 2.1.2 B Thermo-cycling conditions for a routine PCR

Step	Temperature	Time
Initial denaturation	95°C	12 min
45 cycles	95°C 60°C 72°C	50 s 45 s 1 min
Final extension	72°C	10 min
Hold	10°C	/

Agarose gel electrophoresis

50 μl of PCR reaction mixture and 5 μl DNA ladder (QIAGEN) were loaded onto a 1% TBE agarose gel containing GelRed Nucleic Acid Stain (Biobium). Electrophoresis was performed at 80 V for 2 hours. After electrophoresis, DNA fragments in the agarose gels were imaged under UV light.

2.2 *In vitro* experiments

2.2.1 Preparation of isolated pancreatic acinar cells

Freshly isolated PACs were obtained from the pancreas of adult C57BL/6J or Ripk1^{K45A} mice using a standard collagenase digestion procedure. 1ml of warm collagenase (220 units/ml, Worthington Biochemical Corporation, Lakewood, NJ) was injected into the pancreas. The pancreas was incubated at 37 °C for 18 min in collagenase. After collagenase incubation, the pancreas was placed in a polycarbonate tube and the pancreatic tissue was dissociated by micropipette tips in NaHEPES buffered salt solution. The extracellular NaHEPES buffered salt solution contained: 140 NaCl, 4.7 KCl, 1.13 MgCl2, 1 CaCl2, 10 D-glucose, and 10 HEPES (mM). The final pH of the solution was

adjusted to pH 7.35. A cloudy supernatant then went through the 100 μm cell filter. This process was continued until cloudy solution was no longer obtained. The tube contained go through solution with cells was then centrifuged at 800 g for 2 minute to form a pellet which will be re-suspended in NaHEPES buffered salt solution for further use. All experiments on isolated PACs were performed at room temperature (23~25 °C) and the cells were used within 5 h after isolation if not otherwise stated.

2.2.2 Confocal fluorescence microscopy

Cell death assays

PACs isolated from mouse were treated with either Nec-1 or toxins (TLCS (500 μM); POAEE (100 μM)) at room temperature for 30 min. Then cells were centrifuged (800 g for 2 min) and resuspended in 1ml NaHepes buffered salt solution with PI (PI, 10 μg/ml; excitation 488 nm, emission 630-693 nm; Sigma) and Hoechst 33342 (10 μg/mL; excitation 364 nm, emission 405-450 nm; Molecular Probes). TLCS and POAEE stimulated cells were distributed into 96-well glass bottom plates (150 μl/well) and imaged using LSM710 systems. The total number of cells was indicated by Hoechst, and necrosis cells were indicated by PI uptake. The total number of cells displaying PI uptake was counted in more than 3 wells and more than 12 random fields of each differently treated group of each isolate to give a percentage, averaged across fields as mean ± SEM from at least 3 mice.

Immunofluorescence experiments

Cells were isolated and mixed with toxin or drug before being seeded onto the Poly-L-lysine coated 35mm glass bottom dishes. After being seeded, the cells were allowed to adhere for 30 min at room temperature. Cells were washed 3 times with PBS and then fixed in 4% paraformaldehyde for 20 min. Once fixed, cells were washed in PBS three times (each 3 min), and permeabilized with PBS containing 0.2% Triton X-100 for 5 min. After permeabilized, non-specific bindings were blocked with 10% goat serum and 1% bovine serum albumen in PBS for 1 hour. The cells were then incubated with blocking solution containing monoclonal primary antibodies against RIPK1 (1:200), RIPK3 (1:100). Cells were washed three times in PBS before incubation with corresponding secondary antibody(s). The cells were incubated with 594 (1:500), 647 (1:500) conjugated secondary antibodies for 30 min at room temperature in the dark. Cells were washed 3 times in PBS and preserved in 0.02% Azide PBS at 4 °C prior to imaging using laser scanning microscopes (LSM) 710 systems.

Calcium signals

Cells isolated from mouse were loaded with 1 μM Fura-2-AM (Sigma) and incubated for 40 min at room temperature (23~25°C) with permanent agitation, followed by washing and centrifugation at 800 g for 2 minutes. During experiments, the cells were placed and attached to the cover slip that had been coated with poly-L-lysine (0.01%), which was attached to an open perfusion chamber (allow cells to settle onto the coverslip for 10s). Once the cells were settled, initiated superfusion of NaHepes buffered salt solution for a stable baseline (180-200s). A flow rate of ~ 3 ml/min was sufficient to allow

rapid buffer exchange without disturbing cells that had attached to the cover slip. After the stable baseline continuously perfused with NaHepes buffered salt solution or the solution with toxins or drugs. For experiments using Fura2, the background subtraction was carried out independently at each of the two wavelengths and ratios (340 nm/380 nm), which were proportional to cytosolic calcium ($[Ca^{2+}]_c$), were calculated for each image. Exposure time at 500ms and the cycle at 10s were used in the experiments.

2.2.3 Plate reader assays

Necrosis measurement

Since CCK (10nM) did not have sufficient PAC necrosis on the confocal assay, a plate reader overnight protocol was used as a replacement to measure the necrosis in isolated PACs. CCK (10 nM) with or without Nec-1 treatments were distributed into 96-well plate (400 μl/well) with PI (PI, 10 μg/ml; excitation 488 nm, emission 630~693 nm; Sigma) and measured in a plate reader (excitation filter 485 nm; emission filter 530 nm) (BMG Labtech, UK) at 37°C for 8 hours.

Apoptosis measurement

Freshly isolated murine PACs were incubated with Caspase3/7 green with or without Nec-1 at 37°C for 30 minutes, then stimulated with toxins to induce apoptosis measured by Caspase3/7 green (excitation filter 540 nm; emission filter 590 nm) in a plate reader (BMG Labtech, UK) at 37°C for 8 hours.

ROS measurement

Freshly isolated murine PACs were incubated with 5 μM chloromethyl-2,7-dichlorodihydrofluorescein diacetate acetyl (CM-H_2DCFDA) and Nec-1 or 1-MT (Sigma) at 37°C for 30 min. After cells were washed and centrifuged (800 g for 2 min), cells were re-suspended in NaHepes buffered salt solution with the same drug concentration and distributed into the 96 wells plate. ROS production in PACs were measured at excitation 488 nm and emission 505~550 nm after stimulation with toxins in plate reader (BMG Labtech, UK) at 37°C for 5 hours.

2.2.4 Western blot experiments

Isolated PACs were unstimulated or treated with different toxins (TLCS for 0 h, 2 h and 4 h) at 37°C. The protein was extracted by radioimmunoprecipitation assay (RIPA) buffer (Sigma) contains protease inhibitor cocktail (Thermo Scientific), phosphatase cocktail 2 (Sigma) and phosphatase cocktail 3 (Sigma) 1:100 rotated for 30 min at 4 °C, and centrifuged at 16,000 g for 15 min at 4 °C. The supernatant was collected and stored at -80 °C for further use. Protein concentration was determined by the BCA assay kit (Thermo Scientific). Proteins were separated by SDS-PAGE using a NuPAGE™ 4%-12% Bis-Tris Protein Gels (ThermoFisher scientific) and transferred onto nitrocellulose membranes. Non-specific bindings were blocked by 3% (w/v) non-fat milk in PBS for 1 hour. Blots were then incubated at 4 °C overnight with primary antibody to RIPK1 (Mouse Anti-RIP from BD Transduction Lab: BD610458; 1:500); RIPK3 (Rabbit Anti-RIP3 from Abcam: ab152130; 1:500), cytochrome C (purified Mouse Anti-Cytochrome C antibody from BD Pharmingen™: 556433, 1:500) and calnexin (Rabbit Anti-Calnexin antibody

from Sigma: c4731, 1:2000) in 3% (w/v) nonfat milk in PBS. After the first antibody, the membranes were washed once with 0.05%-tween in PBS and 3 times with PBS (5 min/each). Then incubated for 1 h with the peroxidase-labelled secondary antibody (Anti-Mouse IgG from Sigma: A5278, 1:1000 and Anti-Rabbit IgG from Sigma: A0545, 1:1000) in 3% (w/v) nonfat milk in PBS. Blots were developed for visualisation using an enhanced chemiluminescence (ECL) detection kit (Thermo Scientific) through Bio-Rad ChemiDoc^{TM} XRS+ System. Images were processed through Bio-Rad Image Lab ^{TM} software.

2.3 *In vivo* experiments

2.3.1 Experimental acute pancreatitis models

TLCS-induced bile acid AP (TLCS-AP)

Bile acid saline solution preparation: A fresh stock solution of bile acid on the day of surgery was prepared by dissolving TLCS (Sigma) with saline for a final concentration of 20 mM and then adjusted to 3 mM.

Methyl blue solution preparation: A stock solution by dissolving methyl blue in saline was prepared to obtain a final concentration of 100 mg/ml. This stock solution can be stored at 4 °C for ~1 month. 0.5 μl of 100 mg/ml methyl blue was added into 1ml of TLCS solution to make it being visible just before the surgery.

Surgical procedures: AP was induced by retrograde infusion of 3 mM TLCS into pancreatic duct by an infusion pump at the speed of 5 μl/min for 10 minutes. Anaesthesia was achieved by consistently providing isoflurane and

O_2 gas. Analgesia was achieved by s.c. injection of 1 mg/kg buprenorphine hydrochloride (Vetergesic, 0.3mg/ml solution) before the surgery. During the surgery, a midline laparotomy was performed and the first loop of the duodenum was identified under a dissecting microscope. That loop was rotated to expose the pancreas and posterior surface of the duodenum. A traction suture was used to immobilize the surface of the duodenum and the papilla of Vater at the duodenum-pancreatic junction was identified on the posterior surface of the duodenum. A 30G blunt-tipped catheter that attached to infusion tube connected to an infusion pump was inserted into the common bile duct via the papilla of Vater in the surface of the duodenum. Then, the infusion catheter was placed 1 mm into the bile duct, well before the entry of the pancreatic duct. A neuro-bulldog clamp was used to clamp the pancreatic duct at the liver hilum. Afterwards, 3 mM TLCS solution was infused into the bile-pancreatic duct for 10 minute by the infusion pump. After infusion, the catheter as well as the securing ligature and the neuro-bulldog clamp were removed. Finally, the laparotomy was closed in two layers (Figure 2.3.1 A). The sham group mice were received same operation. After 24 hours which is severe AP time point (Wen, Voronina et al. 2015), the pancreas head was collected and fixed with 10% formalin overnight before being subjected to H&E staining; the pancreas body was collected for MPO. The right lung was collected for MPO and formalin was injected into the left lung and kept for H&E. Whole blood was taken and serum was collected by 1,500 g × 10 min centrifugation for amylase and IL-6 assay.

Fatty acid ethyl ester AP (FAEE-AP)

The combination of ethanol (1.35 g/kg) and POA (800 mM) at 50 μl/kg/25 g mice body weight was injected through i.p. at one hour interval. To avoid the local damage at the injection site, 200 μl saline was pre-injected before POA and ethanol. Analgesia was achieved through s.c. injection of 1 mg/kg buprenorphine hydrochloride. After 24 hours, the samples were collected which is the t severe AP model (Figure 2.3.1 B) (Wen, Voronina et al. 2015). The sham group mice were received two hourly intraperitoneal injections of the same volume of saline. The pancreas head was collected and fixed with 10% formalin before subjected to H&E staining; the pancreas body was collected for trypsin; the pancreas tail was collected for MPO. The right lung was collected for MPO and formalin was injected into the left lung and kept for H&E. Whole blood was taken, and serum was collected by 1,500 g × 10 min centrifugation for amylase and IL-6 assay.

Caerulein acute pancreatitis (CER-AP)

Caerulein pancreatitis was induced by 7 hourly i.p. injections of 50 μg/kg caerulein, with controls receiving saline. Mice were sacrificed and samples were collected 12 h after the first injection which is the most severe time point of CER-AP (Figure 2.3.1 C)(Wen, Voronina et al. 2015) (Wu, Mulatibieke et al. 2017). The control mice were received seven hourly intraperitoneal injections at the same volume of saline. The pancreas head was collected and fixed by 10% formalin before subjected to H&E staining; the pancreas body was collected for trypsin; the pancreas tail was collected for MPO. The right lung was collected for MPO and formalin was injected into the left lung

and kept for H&E. Whole blood was taken and serum was collected by 1,500 g × 10 min centrifugation for amylase and IL-6 assay.

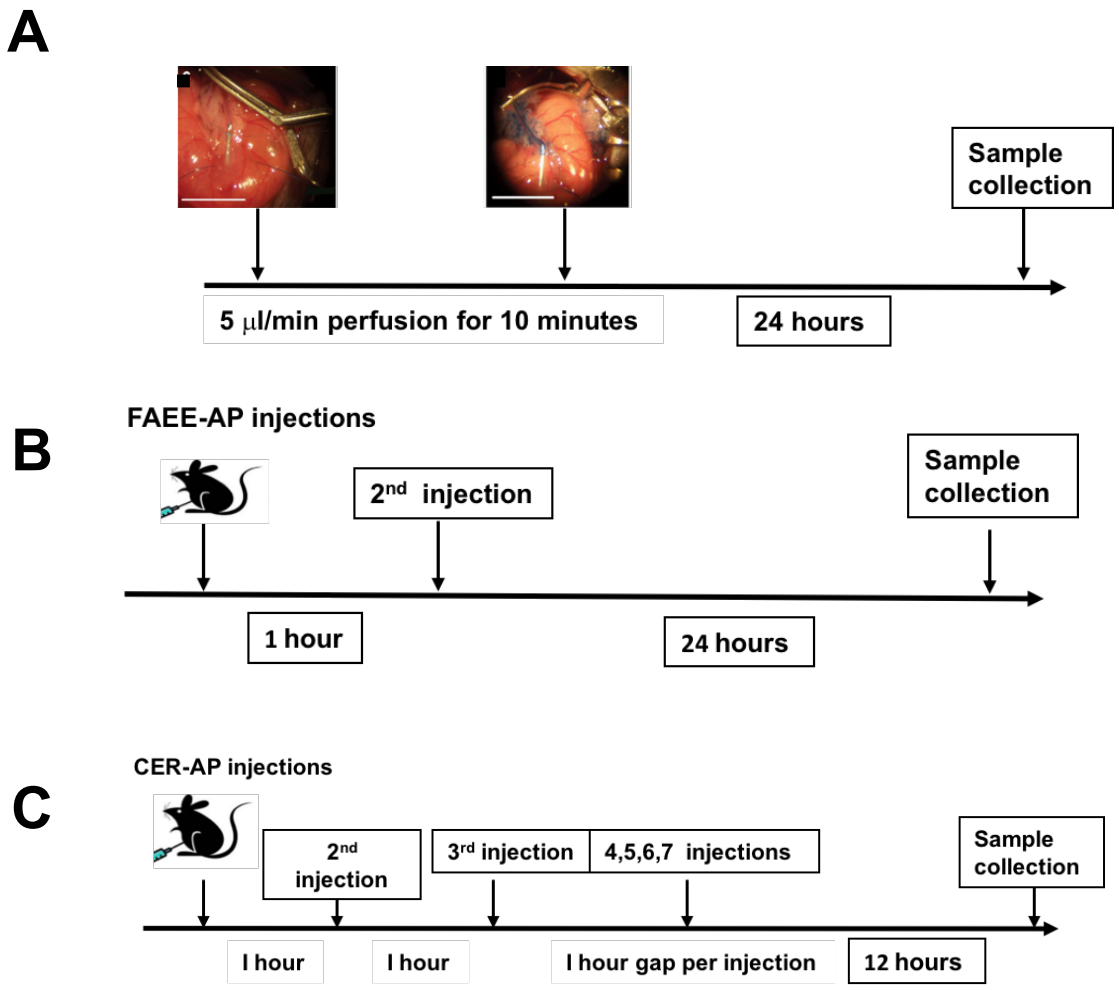

Figure 2.3.1 A) The flow chart of TLCS-AP procedure. The volume of TLCS (5 µl/min,3mM), infusion time (10 min) and modelling time (24h) were indicated in the chart (Images adapted from (Perides, van Acker et al. 2010)). **B) The flow chart of FAEE-AP procedure.** The injection time points of FAEE-AP (2 injections,1 h gap) and the modelling time (24 h) were indicated in the chart. **C) The flow chart of CER-AP procedure.** The injection time points of CER-AP (7 injections,1 h gap each) and the modelling time (12h) were indicated in the chart.

2.3.2 Drug concentrations and preparation for mini-pump

Osmotic Mini Pump

ALZET osmotic pumps are miniature and implantable method for drug delivery at constant and controlled rates for durations ranging from one day to several weeks, without external connections of other devices or frequent animal handling. The principle of mini pump operation is through an osmotic pressure difference between a compartment within the pump, which is a salt sleeve, and the tissue environment. The high osmolality of the salt sleeve causes water flux into the pump through a semi-permeable membrane which forms the outer surface of the pump. When the water enters the salt sleeve, it compresses the flexible reservoir, displacing the drug from the pump into the outside environment at a controlled, predetermined rate (Theeuwes and Yum 1976) (Figure 2.3.2 A).

Necrostatin-1

Necrostatin-1 (5-(1H-indol-3-ylmethyl)-2-thiohydantoins) is an inhibitor of RIPK1 in the necroptosis pathway (Figure 2.3.2 B). Its molecular weight is 259.33 and the solubility in DMSO is ~25 mg/ml, in EtOH is ~6 mg/ml. Clearance rate is 61 ml/min/kg. EC_{50} of Nec-1 determined for inhibition of necroptosis in FADD deficient Jurkat T cells treated with TNFα is 0.49 μM (Teng, Degterev et al. 2005). The concentration delivery by mini pump was calculated based on EC_{50} and clearance rate.

Infusion rate =steady state concentration*clearance rate

Calculation example:

1 mouse =25 g;

25g mouse clearance rate =61 ml/min/kg * 0.025 kg=1.525 ml/min

Steady state concentration (based on the EC_{50}):

0.49 μM * 259.33/1 ml=0.127 μg/ml

Infusion rate=1.525 ml/min*0.127 μg/ml=0.1937 μg/min

24 hours' total drug=0.1937 μg/min*60 min*24 hours=278.892 μg

200 μl pump drug concentration=278.892 μg / (8 μl*24 hours)

=1.4526 mg/ml

5 times: 5*EC_{50}=1.05 μM; 1.4526*5=7.2628 mg/ml

The concentration of Nec-1 applied in the *in vivo* experiments was 5 times the EC_{50} which is 7.26 mg/ml (56 mg/kg/24hours). Nec-1 was dissolved in 10% DMSO mixed with 90% poly ethylene glycol (PEG) Mn 400 at 37º C.

Epacadostat

Epacadostat (INCB24360) is a potent and selective IDO 1 inhibitor in Phase 2 clinical trials as cancer therapy (Figure 2.3.2 C). Its molecular weight is 438.23 and its solubility is 87 mg/ml in DMSO, and 53 mg/ml in warm EtOH or <1 mg/ml in water. Its IC_{50} is 10 nM. For *in vivo* experiments the solubility of Epacadostat is 30 mg/ml in 10% DMSO and 90% PEG 400. It can be given orally twice a day at the dose of ~100 mg/kg, or given through s.c. pump at the dose of 50 mg/kg (Koblish, Hansbury et al. 2010).

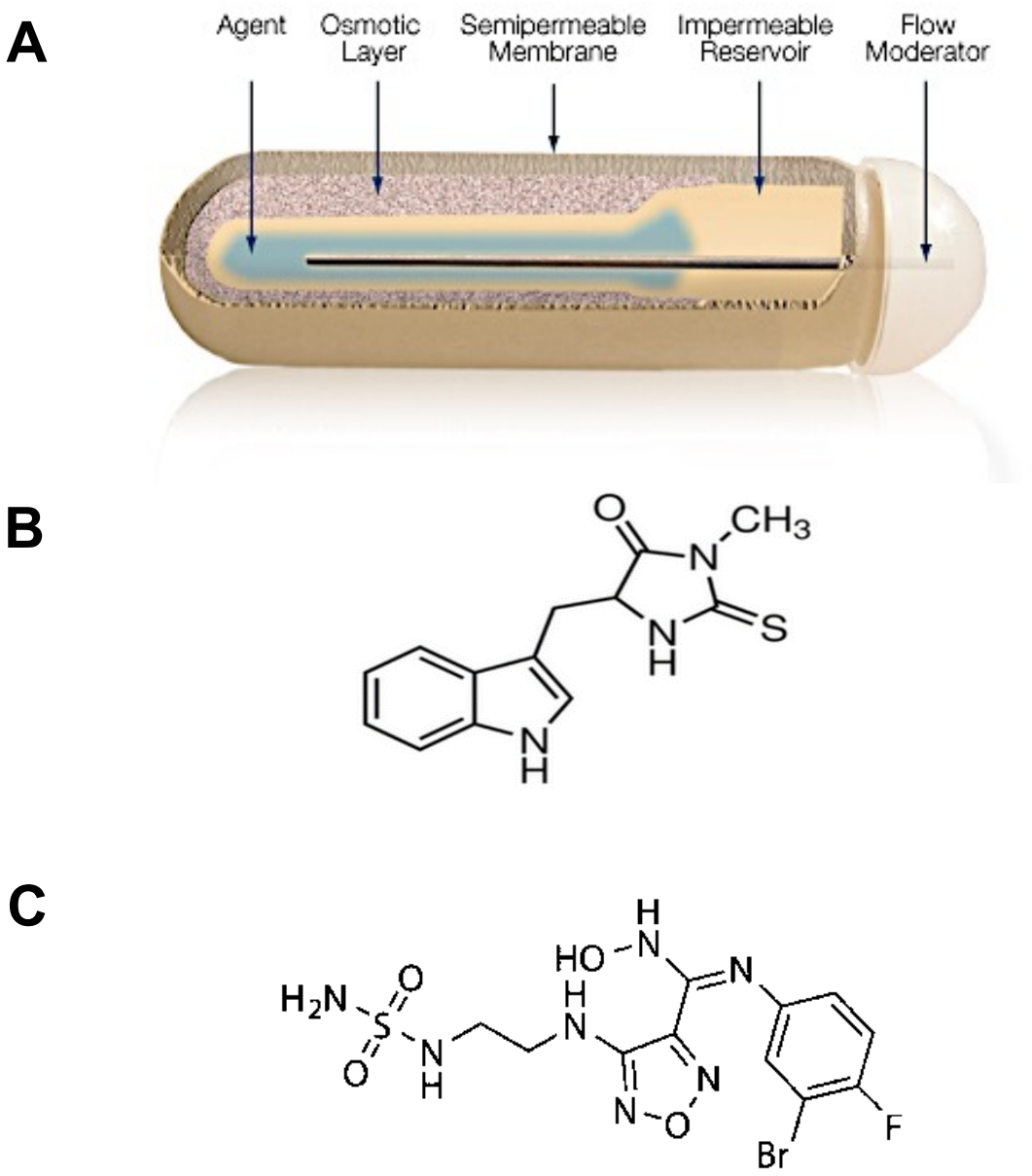

Figure 2.1.4 A) An illustration of a mini pump structure. Tested agent in a compatible solvent was loaded into the impermeable reservoir. The semipermeable membrane allows water influx into the pump. The osmotic layer in the salt sleeve compresses the flexible reservoir, pumping the tested solution at controlled rate through the flow moderator (Figure adapted from ALZET osmotic pumps official website). **B) Molecular structural formula of Necrostatin-1. C) Molecular structural formula of Epacadostat.**

2.3.3 ALZET® Osmotic Pump procedures

ALZET® Mini-osmotic pumps (pump type: 2001D) were used for experiments. The pumping rate for 2001D is 8.0 µl/hour, and reservoir volume is 200 µl. It delivers solution continuously for 24 hours.

The preparations of pumps are as follows: empty pump and its flow moderator was weighed together. The pumps were then filled with drug solution using a syringe. Plunger of the syringe was pushed at upright position to avoid air bubbles. The syringe was carefully removed when the solution was spilling out. Pumps were weighed and filled with the flow moderator again. The filled volume should be more than 90% of the reservoir volume. Finally, incubated the pumps with prepared drug in Eppendorfs filled with saline at 37º C for 3 h. The pump would start working immediately once the pump was inserted into the mice. **Pump insertion**: once the mouse was anesthetized, the implantation site was shaved, an adjacent incision was made at the back of the neck. A haemostat was inserted into the incision to create a pocket for the pump. A filled pump was insert into the pocket. Made sure the pump location would not affect the eating and drinking of the mouse. Wound was closed with sutures. After insertion, mice were kept in the warm-box and allowed to be awakened. Mini pumps contained drug were inserted into the mice at 0.5 h after TLCS-AP induction, 1 h after 2nd injection of FAEE-AP and 3rd injection of CER-AP. The times of pump insertion and sample collection in three AP-models are shown in the flow chart below, respectively (Figure 2.3.3 A, B, C).

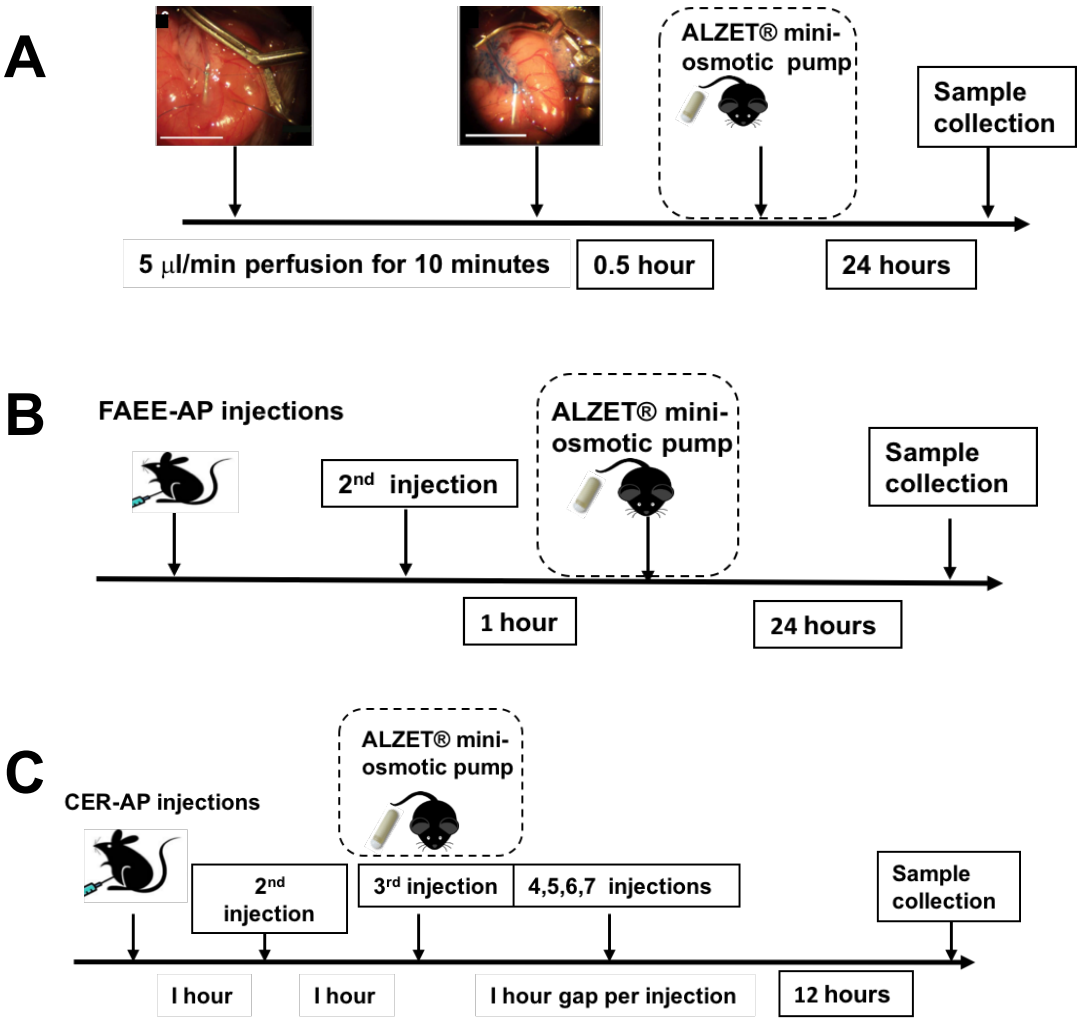

Figure 2.3.3. A) The flow chart of mini pump and TLCS-AP procedures. The concentration of TLCS (5 μl/min), infusion time (10 min), pump insertion time point (0.5 h after infusion) and modelling time (24h) were indicated in the chart. Images were adapted from (Perides, van Acker et al. 2010). **B) The flow chart of mini pump and FAEE-AP procedures.** The injection time points of FAEE-AP (2 injections, 1 h gap), pump insertion time point (1 hour after 2nd injection) and the modelling time (24 h) were indicated in the chart. **C) The flow chart of mini pump and CER-AP procedures**. The injection time points of CER-AP (7 injections,1 h gap each), pump insertion time point (between 3rd injection and 4th injection) and the modelling time (12 h) were indicated in the chart.

2.3.4 Evaluation of experimental AP severity

The severity of AP was evaluated by pancreatic histology of oedema, inflammation, necrosis, local biochemical parameters of amylase, trypsin and pancreatic MPO activity, systemic pancreatitis-associated biochemical parameters of IL-6, lung MPO activity and TNFα.

Histology Analysis

Pancreatic tissues were collected and fixed in 10% formalin, embedded in paraffin and stained through H&E. Scorings were performed on 10 random fields (x200) by 2 blinded independent investigators. Grading (scale, 0~3) of oedema, inflammatory cell infiltration and PAC necrosis were made and calculated as the means ± SEM (>=5 mice/group) (Wildi, Kleeff et al. 2007).

Bio-parameter processing

Pancreatic trypsin activity: pancreatic tissue was homogenized in 5 mM 4-morpholinepropane sulfonic acid (MOPS) buffer (containing 250 mM sucrose and 1 mM magnesium sulphate, pH 6.5) followed by centrifugation at 1,500 g for 5 min at 4°C. The supernatant was added to 96-well plate containing pre-warmed pH 8.0 assay buffer (50 mM Tris, 150 mM NaCl, 1 mM $CaCl_2$, 1% (w/v) bovine serum albumin and trypsin peptide Boc-Gln-Ala-Arg-MCA substrate). Fluorescence was measured by an established protocol from POLARstar Omega Microplate Reader instructions on a fluorescent plate reader (BMG Labtech, UK) (excitation, 380 nm; emission, 440 nm). Pancreatic trypsin activity was calculated as the difference of fluorescence intensity between 0 min and 5 min. **Myeloperoxidase (MPO)**: Pancreatic and lung

tissue were homogenized in a 100 mM phosphate buffer (pH 7.4) with protease inhibitors followed by centrifugation at 16000 g for 15 minutes at 4°C (twice for pancreas and three times for lung). The pellet was re-suspended in 100 mM pH 5.4 phosphate buffer (containing 0.5% hexadecyltrimethyl ammonium bromide, 10 mM EDTA and protease inhibitors), then underwent freeze-thawed three times, sonicated for 30 seconds and centrifuged at 16,000 g for 15 minutes at 4°C. MPO activity was measured in the supernatant mixed with 3,3,5,5-tetramethylbenzidine with freshly added 0.01% H_2O_2. Absorbance was measured at 655 nm in the plate reader (BMG Labtech, UK) and MPO activity was calculated as the difference between 0 and 3 min (Dawra, Ku et al. 2008). After blood was collected and centrifuged at 1,500 g for 10 minutes. **Serum amylase** was determined by a Roche Analyser (Roche) tested in Clinical Biochemistry Department of Royal Liverpool University Hospital using a kinetic method; **Serum interleukin (IL)-6** and **serum TNFα** were determined by enzyme-linked Quantikine ELISA assay (R&D Systems).

2.4 Statistical analysis

Results were presented as mean ± SEM obtained from three or more independent experiments. Prism 5.0 software (GraphPad Software Inc., La Jolla, CA) was used to perform statistical analyses. All data were analysed using ANOVA (more than two groups), T-test (two groups) for parametric data or two-way ANOVA when there is interaction between the two independent variables on the dependent variable. P values of <0.05 were considered to indicate significant differences.

2.5 Study Approval

Animal studies were ethically reviewed and conducted according to UK Animals Act of 1986 (Scientific Procedures), approved by the UK Home Office (PPL 70/8109).

Chapter 3 Results: The expression and distribution of RIPK1 and RIPK3 in PAC from Ripk1^{K45A} and Wt mice

3.1 Introduction

Studies showed that RIPK1 kinase-dead knock-in ($Ripk1^{K45A}$) mice have normal litter sizes, the same phenotype and fertility compared with strain matched wild type animals (C57BL/6J) (Berger, Kasparcova et al. 2014, Kaiser, Daley-Bauer et al. 2014, Shutinoski, Alturki et al. 2016) (see Chapter 1 for further details). For the RIPK1 and RIPK3 protein expression, the Human Protein Atlas database showed that the human pancreas has a medium protein level of RIPK1 and RIPK3 (Uhlen, Oksvold et al. 2010). The protein expression of RIPK1 and its necroptosis inducing partner RIPK3 were expressed in multiple tissues and cell types, including the spleen, thymus, lymph nodes, macrophages and MEFs in $Ripk1^{K45A}$ mice compared with Wt (Berger, Kasparcova et al. 2014, Kaiser, Daley-Bauer et al. 2014).

For the RIPK1 and RIPK3 distribution, the Human Protein Atlas database showed that RIPK1 and RIPK3 were mainly localized to the plasma membrane and cytosol (Uhlen, Oksvold et al. 2010). Murine immunofluorescence experiments in rat osteocytes (Cui, Zhu et al. 2016), rat oligodendrocyte progenitor cells (Qu, Tang et al. 2017), and mice cortical neurones (Chen, Yu et al. 2012) also showed that RIPK1 and RIPK3 were expressed in the cytoplasm and were up-regulated or co-localized with each other when necroptosis was stimulated (Cui, Zhu et al. 2016, Zhang, Li et al. 2016, Qu, Tang et al. 2017). However, less information was available about RIPK1 protein expression and distribution in mouse PAC in $Ripk1^{K45A}$ or C57BL/6J. The aim of this chapter was to set up a stable $Ripk1^{K45A}$ homozygous colony for further experiments and, further, to confirm the protein expression and

distribution of RIPK1 and RIPK3 from both Ripk1^{K45A} and Wt isolated PACs by western blot and immunofluorescence.

3.2 Results

3.2.1 Ripk1^{K45A} genotyping and breeding

After testing the genotype of each mouse, the male/female homozygous mice were then kept for further breeding (Figure 3.2.1). However, it is worth mentioning that the Ripk1^{K45A} homozygous colony encountered breeding difficulties after 2 years of a stable birth rate. All of the homozygous breeding pairs of Ripk1^{K45A} stopped giving birth to new litters for 4 months, for a reason that is not yet clear. Because of the high cost and low productivity, we subsequently stopped breeding this colony.

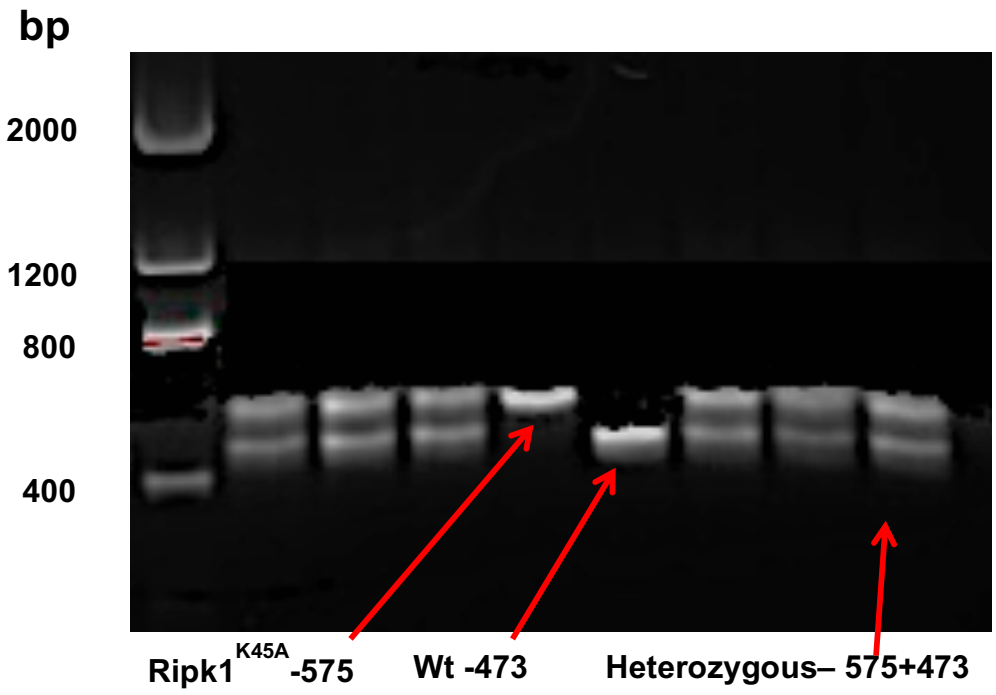

Figure 3.2.1 Representative image of PCR experiment distinguishing Wt, heterozygous and homozygous Ripk1^{K45A}. Each lane represents a mouse. The band that only appeared at 473 represented Wt, the band that only appeared at 575 represented Ripk1^{K45A} homozygous, and the two bands that appeared at both 473 and 575 represented Ripk1^{K45A} heterozygous.

3.2.2 The protein expression and distribution of RIPK1 and RIPK3

The results showed that RIPK1 and RIPK3 were expressed in both Ripk1^{K45A} and Wt mouse pancreas. Calnexin was used as an internal control (Figure 3.3.2). GAPDH and β-actin produced the same results as calnexin (data not shown), although calnexin had the strongest intensity of the three. The results indicated that no differences in RIPK1 and RIPK3 expression existed between PAC from Ripk1^{K45A} and Wt mice (Figure 3.2.2.A) (Need to mention that the bands were from same membrane but different lanes which were not closed to each other. In order to see the comparison clearly, the bands were cut and put together in Figure 3.2.2 B). Immunofluorescence experiments showed a diffuse cytosolic distribution with some punctate dots in the PAC for RIPK1 (green) and RIPK3 (magenta). The combination of RIPK1 and RIPK3 panels (green and magenta) showed no coloclisation in both PAC from Ripk1^{K45A} and Wt. The distribution of RIPK1 and RIPK3 in isolated PAC from Ripk1^{K45A} showed a similar pattern compared with Wt, and no apparent differences were observed (Figure 3.2.2.B).

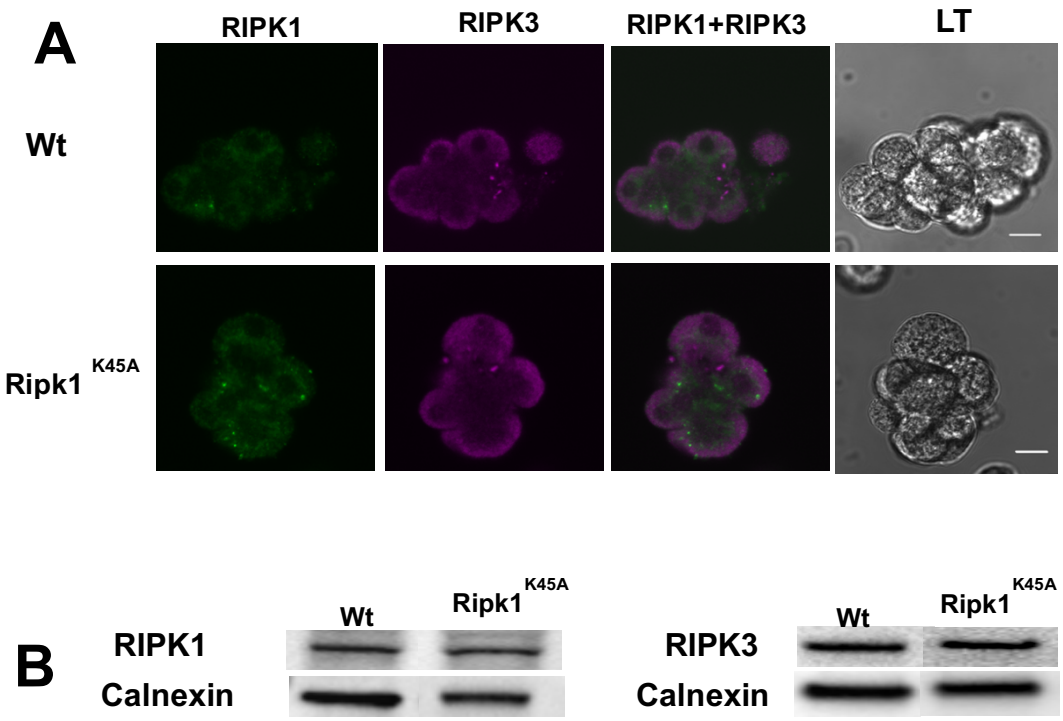

Figure 3.3.2.A) Western blot of RIPK1 and RIPK3 expressions in isolated PAC from Wt and Ripk1^{K45A} mice. RIPK1 and RIPK3 appeared at 60KD and 57KD, respectively, in both Ripk1^{K45A} and Wt. Calnexin is shown as a loading control. Data are representative at least for 3 Wt and Ripk1^{K45A} mice. **B) Representative images of RIPK1 and RIPK3 distribution in isolated PACs from Ripk1^{K45A} and strain matched Wt.** Fluorescence microscopy images show the cellular distribution of RIPK1 (green) and RIPK3 (magenta) in both Ripk1^{K45A} and Wt PACs. The transparent light (LT) images show the structure of the cells (scale bar: 10 μm). Data are representative of at least 3 mice per group.

3.3 Discussion

The results described in this chapter demonstrated that Ripk1^{K45A} homozygous mice have a similar phenotype and body weight compared with strain matched Wt (body weight 20~25 g at the age range of 8-10 week), suggesting that Ripk1^{K45} kinase activity modification did not affect RIPK1 expression at normal conditions. However, the reason why infertility occurred after two years of stable breeding is unclear. Also, Ripk1^{K45A} kinase activity modification did not affect RIPK1 and RIPK3 protein expression and distribution under normal conditions.

The variation in fertility between the Wt mice and the transgenic mice from the same background strain could be a consequence of the transgene insertion, resulting in the disruption of a gene (or genes), or the knockout of a function that could be linked to gametogenesis, resulting in abnormal sperm production, oocyte genesis or other fertility regulators (Vasudevan, Raber et al. 2010). Even the genes which are not directly involved in reproduction may show a pleiotropic phenotype with decreased sperm production (Toshimori, Ito et al. 2004) and reduced fertility (Baker, Bronner et al. 1995). The underlying mechanisms of changes observed in the Ripk1^{K45A} mice strain warrant further investigation.

Chapter 4 Results: The effects of Ripk1^{K45A} on toxin-induced PAC cell death

4.1 Introduction

Pancreatic necrosis is a major determinant of severity in AP patients and experimental AP (Kaiser, Grady et al. 1995, Petrov, Shanbhag et al. 2010). However, PAC apoptosis may be protective during the pathogenesis of AP by avoiding the necrotic cell death pathway (Bhatia 2004, Criddle, Gerasimenko et al. 2007). Therefore, control of the balance between cell death may have therapeutic value. RIPK1 has emerged as an important determinant of cell death including apoptosis, necrosis and necroptosis in response to cellular stress, and its kinase activity may affect the cell death balance (see Chapter 1 for further details). Studies on Ripk1^{K45A} mice showed that TNFα induced necroptosis but did not affect apoptosis and NF-κB in macrophages (Berger, Kasparcova et al. 2014, Kaiser, Daley-Bauer et al. 2014). However, other research using Ripk1^{K45A} mice showed that RIPK1 kinase activity promoted hepatocyte necroptosis induced by concanavalin A but also protected hepatocytes from massive apoptosis (Filliol, Piquet-Pellorce et al. 2016). The causes of different outcomes in apoptosis from Ripk1^{K45A} are not clear but may vary according to different cell type and toxins.

The aim of this chapter was to test the possible effects of RIPK1 kinase modification (Ripk1^{K45A}) on PAC necrosis and apoptosis in response to AP relevant toxins TLCS, POAEE and CCK.

4.2 Results

4.2.1 The effects of Ripk1^{K45A} on TLCS-induced PAC necrosis and apoptosis

The effects of Ripk1^{K45A} modification on necrosis and apoptosis compared to Wt were evaluated in response to TLCS (500 μM). Previous experiments by our group using confocal microscopy showed that TLCS induced significant PAC necrosis (Booth, Murphy et al. 2011, Wen, Voronina et al. 2015). The current experiments using a confocal microscope approach showed that Ripk1^{K45A} PACs exhibited the same basal necrosis as Wt PACs. TLCS elevated necrosis in both Ripk1^{K45A} and Wt PACs. However, the level was significantly reduced by Ripk1^{K45A} modification (by 51.76%) (Figure 4.2.1 A). Ripk1^{K45A} PACs showed the same basal apoptosis compared with Wt. TLCS increased apoptosis in both strains. However, the Ripk1^{K45A} modification significantly elevated TLCS induced PAC apoptosis compared to Wt (increased by 97.06%) (Figure 4.2.1 B). Meanwhile, Ripk1^{K45A} accelerated the appearance of cytosolic cytochrome C, measured with Western blot, induced by 500 μM TLCS from 4 hours to 2 hours compared with Wt, which confirmed the stimulation of apoptosis in the genetically modified cells (Figure 4.2.1 C). (The percentage was calculated by (Ripk1^{K45A} stimulation group-Ripk1^{K45A} control)/ (toxin group- Wt control)).

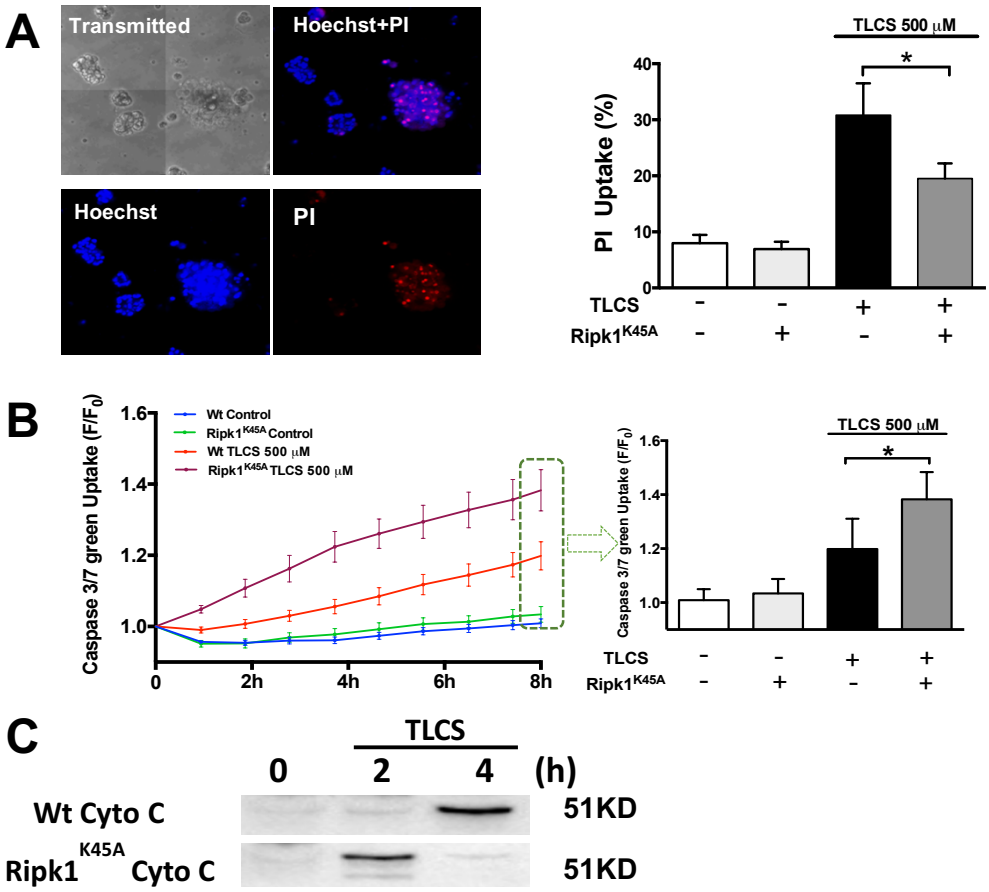

Figure 4.2.1 Comparative effects of TLCS on PAC necrosis and apoptosis from Ripk1^{K45A} and Wt mice. A) Typical confocal images of isolated murine PAC necrosis stimulated by TLCS (Blue: Hoechst indicated total cell number; Red: Propidium Iodide (PI) indicated necrotic cell number). The bar graph (right) shows the effects of Ripk1^{K45A} on TLCS (500 μM) induced necrosis compared with Wt. **B)** The line graph shows the effects of Ripk1^{K45A} on TLCS (500 μM) induced apoptosis compared with Wt. Bar chart (right) shows the value of apoptosis at the 8h time point. The data were normalised to F/F_0. **C)** Representative western blot images show cytochrome C (55 KD) in Ripk1^{K45A} and Wt with or without TLCS (500 μM). Images are representative at least 3 mice per group. Significant differences between Ripk1^{K45A} and Wt groups were analysed (*$p<0.05$). All data showed in A and B are the mean ± SEM of at least 3 mice per group.

4.2.2 The effects of Ripk1^{K45A} on POAEE-induced PAC necrosis and apoptosis

POAEE (100 μM) was applied to evaluate the effects of Ripk1^{K45A} on PAC necrosis and apoptosis compared to Wt. Previous experiments by our group using confocal microscopy showed that POAEE induced significant PAC necrosis (Huang, Booth et al. 2014). Consistent with this, our current results showed that 100 μM POAEE elevated necrosis in Wt mice. This increase in necrosis was significantly reduced by Ripk1^{K45A} modification (by 97.95%) (Figure 4.2.2 A). However, 100 μM POAEE did not induce distinguishable apoptosis in this plate reader assay (Figure 4.2.2 B). A higher concentration of POAEE at 500 μM was also tested; however, the results were as the same as POAEE at 100 μM with no apoptosis detected (data not shown). (The percentage was calculated by (Ripk1^{K45A} stimulation group- Ripk1^{K45A} control)/ (toxin group- Wt control)).

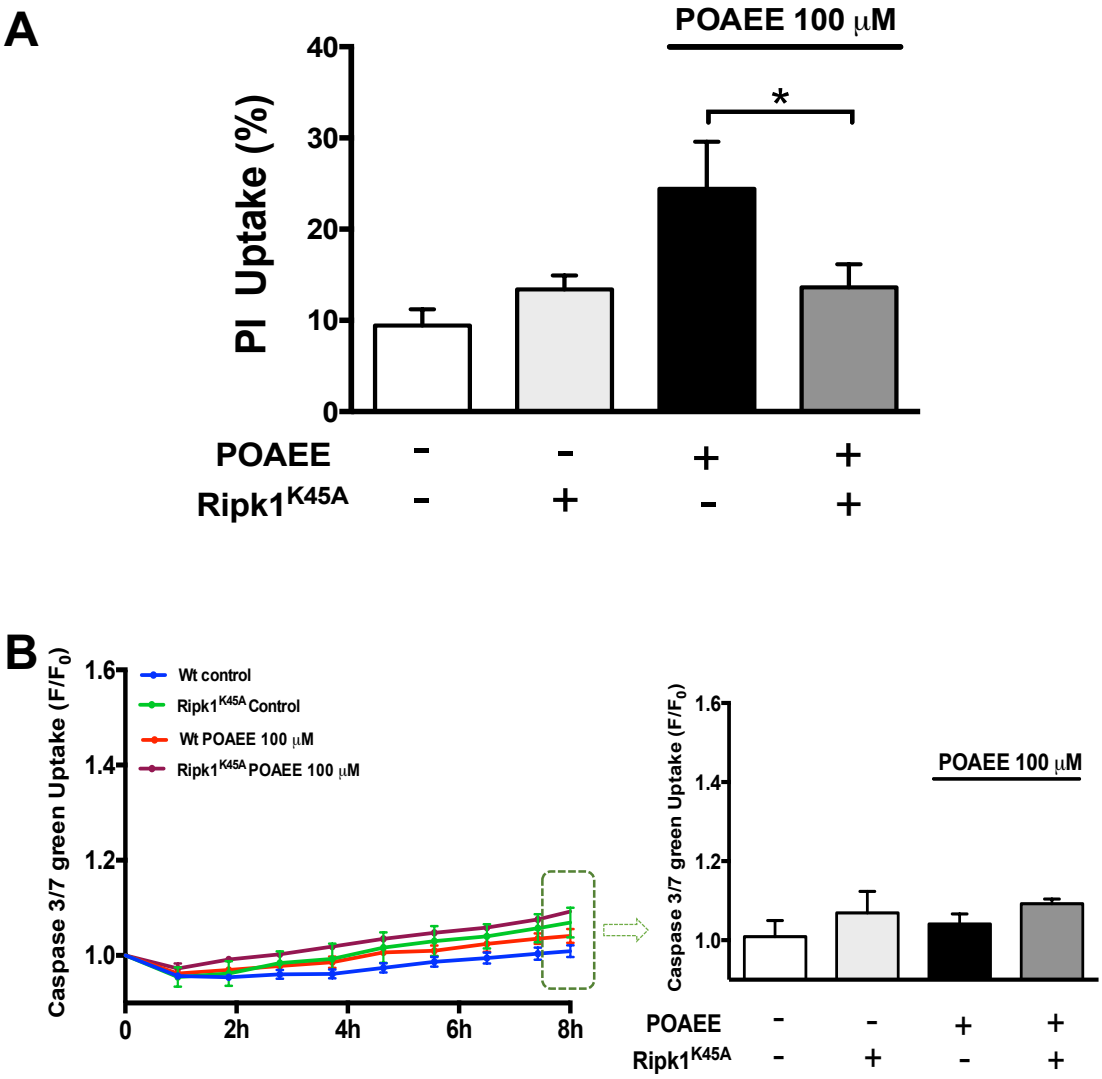

Figure 4.2.2 Comparative effects of POAEE on PAC necrosis and apoptosis from Ripk1^{K45A} and Wt mice. A) The bar graph shows the effects of Ripk1^{K45A} on POAEE (100 μM) induced necrosis compared with Wt. **B)** The line graph shows the effects of POAEE (100 μM) on Ripk1^{K45A} and Wt PAC apoptosis. Bar chart (right) shows the value of apoptosis at the 8 h time point. The data were normalised to F/F_0. Significant differences between Ripk1^{K45A} and Wt were analysed (*$p<0.05$). All data showed in A and B are the mean ± SEM of at least 3 mice per group.

4.2.3 The effects of Ripk1^{K45A} on CCK-induced PAC necrosis and apoptosis

CCK (10 nM) was applied to evaluate the effects of Ripk1^{K45A} modification on PAC necrosis and apoptosis compared to Wt. Results showed that CCK elevated necrosis in both Ripk1^{K45A} and Wt PACs. No significant differences were observed between Ripk1^{K45A} and Wt PAC necrosis induced by CCK (Figure 4.2.3 A). However, 10 nM CCK did not induce sufficient apoptosis in both strains (Figure 4.2.3 B). A higher concentration of CCK at 100 nM was also tested, however, the results were as the same as CCK at 10 nM with no apoptosis detected (data not shown). (The percentage was calculated by (Ripk1^{K45A} stimulation group- Ripk1^{K45A} control)/ (toxin group- Wt control)).

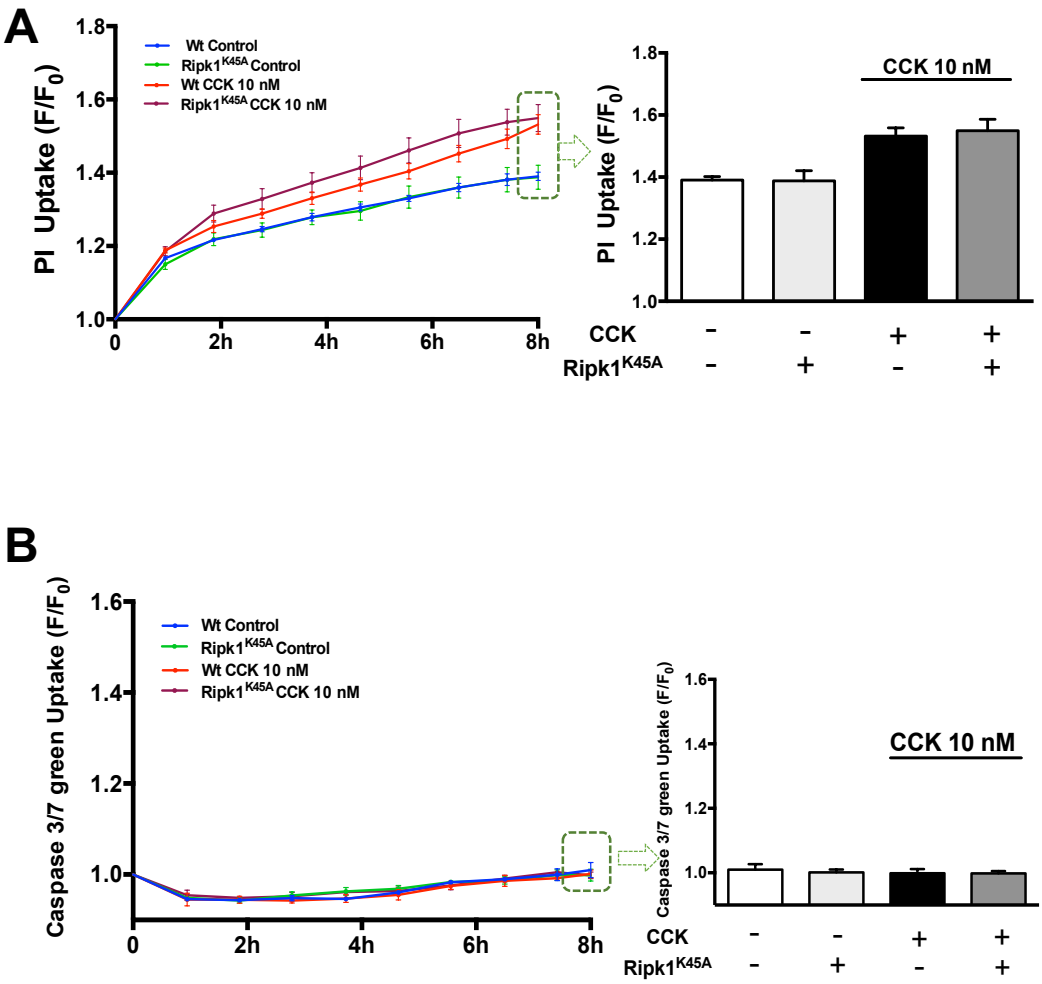

Figure 4.2.3 Comparative effects of CCK on PAC necrosis and apoptosis from Ripk1^{K45A} and Wt mice. A) The line graph (left) shows CCK (10 nM) induced necrosis in Ripk1^{K45A} and Wt. Bar chart (right) shows the value of necrosis at the 8h time point. **B)** The line graph (left) shows the effect of CCK (10 nM) on apoptosis in Ripk1^{K45A} and Wt. Bar chart (right) shows the value of apoptosis at the 8h time point. The data were normalised to F/F_0. Significant differences of Ripk1^{K45A} and Wt group were analysed (*$p<0.05$). All data showed in A and B are the mean ± SEM of at least 3 mice per group.

4.3 Discussion

The balance between necrosis and apoptosis in AP is critical to the disease outcome (Kloppel and Maillet 1993, Criddle, Gerasimenko et al. 2007). Previous studies showed that RIPK1 related cell death is cell type and toxin dependent (see Chapter 1 for further details). Since there is no established means of detecting necroptosis directly (He, Huang et al. 2016), we measured total necrosis, which has the same endpoint as necroptosis, and determined RIPK1 dependent necroptosis based on RIPK1 kinase activity modification.

The results in this chapter demonstrate that TLCS (500 μM), POAEE (100 μM) and CCK (10 nM) all induced a large amount of PAC necrosis. $Ripk1^{K45A}$ kinase activity modification significantly reduced the necrotic cell number in mouse PACs exposed to TLCS (reduced by 51.76%) and almost back to control in POAEE treatment (reduced by 97.95%), but did not affect CCK-induced cell death, suggesting TLCS, POAEE and CCK induced cell death through different mechanisms. TLCS and POAEE induced necrosis was reduced by RIPK1 modification suggesting these two toxins could induce RIPK1 dependent necroptosis in PACs. However, CCK induced cell death was not affected by RIPK1 kinase modification suggesting necroptosis is not the main type of cell death induced by CCK in PACs which correlated with the study which showed that that RIPK1/RIPK3 complex was not observed in CCK-induced PAC necrosis (Wu, Mulatibieke et al. 2017).

These findings of necroptosis induced by TLCS are consistent with published data which showed that TLCS increased both PI uptake and LDH leakage in PACs, and 250 μM TLCS led to formation of a detergent-insoluble pellet that

contained both RIPK1 and RIPK3 at 2 hours (Louhimo, Steer et al. 2016). However, how much Ripk1^{K45A} affects TLCS induced PAC necroptosis is not certain since a study showed that Ripk1^{K45A} macrophages were completely protected from TNFα/zVAD induced necroptosis (Berger, Kasparcova et al. 2014). However, another study showed that Ripk1^{K45A} cells were significantly, but not completely, resistant to mouse dermal fibroblast (MDF) necroptosis stimulation by TNF/Smac/ZVAD (Liu, Fan et al. 2017).

The results from this chapter showed that TLCS (500 μM) also induced significant apoptosis. However, CCK (10 nM and 100 nM) and POAEE (100 μM and 500 μM) did not induce PAC apoptosis in this assay. The findings are therefore in agreement with studies which showed that application of TLCS to PACs caused caspase activation, consistent with induction of the apoptosis (Criddle, Gillies et al. 2006), and in hepatocytes, TLCS activated caspases 8, 9 and 3 via NADPH oxidase-mediated ROS production (Reinehr, Becker et al. 2005). However, studies on hyperstimulation with CCK in isolated PACs from rats showed that CCK (>0.1 nM) stimulated apoptosis accompanied by caspase activation, cytochrome C release, and mitochondrial depolarization. The apoptosis was measured by nuclei containing condensed and/or fragmented chromatin marked by Hoechst 33258 under a confocal microscope (Gukovskaya, Gukovsky et al. 2002). Application of POAEE has also been shown to induce apoptosis in mice isolated PACs, albeit much less than necrotic cell death; 200 µM POAEE increased apoptosis from 0.4% to 10.8% detected via rhodamine 110-aspartic acid amide in a confocal cell death assay (Huang, Booth et al. 2014). The differences may be a result of the

different detection methods and reagents used, suggesting that confocal microscopy evaluation of single cells may be a more sensitive approach. In addition, the use of caspase 3/7 green may not be sensitive enough for measuring apoptosis induced by CCK and POAEE, and further optimization or other methods such as TUNNEL may be warranted in future studies. Thus, from the present data there can be no definitive conclusions regarding any potential effect of Ripk1^{K45A} on CCK or POAEE on apoptosis, although this pathway is minor compared to the primary driver of cell death induced by these toxins.

The effects of Ripk1^{K45A} on apoptosis are controversial (Berger, Kasparcova et al. 2014, Kaiser, Daley-Bauer et al. 2014, Filliol, Piquet-Pellorce et al. 2016). The data from this chapter demonstrates that Ripk1^{K45A} modification did not significantly potentiate TLCS induced apoptosis. However, there was a trend towards increased apoptosis which correlated with prior research showing that RIPK1 repression sensitized L929 cell switching from necroptosis to apoptosis in response to TNFα stimulation (Vanlangenakker, Bertrand et al. 2011, Remijsen, Goossens et al. 2014), that RIPK1 kinase activity protected hepatocytes from concanavalin A induced apoptosis (Filliol, Piquet-Pellorce et al. 2016), and studies showing that when necroptosis is blocked, cells developed apoptosis based on the presence of caspase 8 and cFLIPL (Melo-Lima, Celeste Lopes et al. 2014). These studies suggest that Ripk1^{K45A} may divert cell death to apoptosis when kinase activity is inhibited. However, the current results in PACs suggest that apoptosis was not affected by Ripk1^{K45A} modification, as previously reported in mice macrophages (Berger, Kasparcova et al. 2014, Kaiser, Daley-Bauer et al. 2014), and are in

agreement with evidence showing that RIPK1 mediated ER stress-induced apoptosis independently of its kinase activity in MEFs (Estornes, Aguileta et al. 2014).

Cytochrome C is a multi-functional enzyme, and its release is a central event in apoptosis in AP; the earlier it occurs, the sooner apoptosis is initiated (Odinokova, Sung et al. 2008, Odinokova, Sung et al. 2009). Under normal conditions, cytochrome C resides in the mitochondria and its exodus into the cytoplasm induces apoptosis. The data from this chapter demonstrate that Ripk1^{K45A} modification increased TLCS induced cytochrome C release from mitochondria to the cytoplasm in PACs, which would be in accord with any potentiating effects on TLCS-induced apoptosis.

Collectively, based on the responses of RIPK1 kinase activity, we concluded that TLCS (500 μM) and POAEE (100 μM) induced RIPK1-dependent necroptosis, with RIPK1 dependent necroptosis playing more important role in POAEE-induced PAC cell death. However, CCK (10 nM) induced PAC death was independent of RIPK1 kinase activity. These investigations may shed some light as to why necroptosis research has shown different results in previous AP studies (See Table 1.5 in Chapter 1, Section 1.5 for further details). Therefore, based on the cell death assays from our study any potential manipulation of RIPK1 as a therapeutic target may need to carefully consider the different AP aetiologies. Results from *in vitro* assays suggest RIPK1 kinase activity inhibition might be a useful target in treating alcohol-related AP.

Chapter 5 Results: Effects of RIPK1 inhibitors on toxin-induced PAC cell death

5.1 Introduction

Nec-1 has been shown to inhibit RIPK1 kinase activity and reduce necroptosis via stabilising RIPK1 and the surrounding structural elements (Xie, Peng et al. 2013), inhibiting RIPK1 phosphorylation (Degterev, Hitomi et al. 2008, McQuade, Cho et al. 2013) and abolishing necrosome formation (Xie, Peng et al. 2013).

The aim of this chapter was to test the effects of RIPK1 inhibitors on AP relevant toxin-induced cell death. The selectivity of Nec-1 has been questioned with another target previously identified (Takahashi, Duprez et al. 2012); therefore more selective RIPK1 inhibitors, Nec-1s and a novel compound GSK 963' were also tested to confirm the involvement of the RIPK1-dependent necroptosis in PACs (Takahashi, Duprez et al. 2012, Berger, Harris et al. 2015). In addition, the effects of gene modification shown in Chapter 4 were compared with the effects of pharmacological inhibition of PAC cell death.

5.2 Results

5.2.1 Effects of Nec-1, Nec-1s and GSK'963 on TLCS-induced PAC necrosis and apoptosis

Our results showed that the elevated necrosis in PACs induced by TLCS (500 μM) was significantly reduced by Nec-1 in a concentration-dependent manner (3 μM,10 μM and 30 μM), and by Nec-1s (10 μM) and GSK'963 (1μM) treatment. Nec-1 at 10 μM showed the greatest reduction of necrosis (by

84.68%) compared with 3 μM (by 55.79%), 30 μM (by 48.97%), Nec-1s 10 μM (by 51.38%) and GSK'963 1 μM (by 51.96%) (Figure 5.2.1 A and B). 500 μM TLCS elevated PAC apoptosis and the increased level was significantly reduced by Nec-1 (10 μM) treatment (by 88.45%) (Figure 5.2.1 C) (The percentage was calculated by (treatment group-control)/ (toxin group-control)).

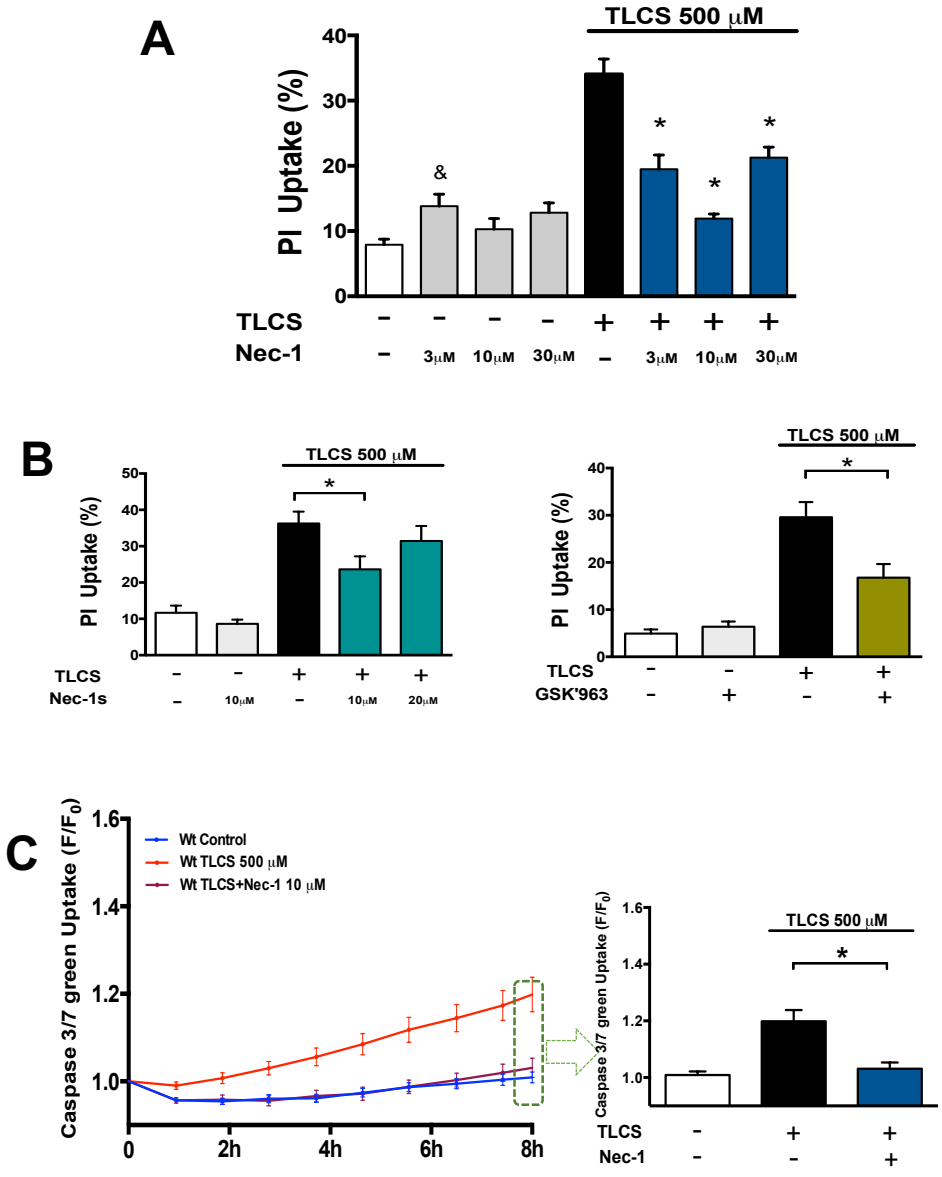

Figure 5.2.1 Effects of Nec-1, Nec-1s and GSK'963 on TLCS-induced PAC cell death. **A)** The bar graph shows the effects of Nec-1 at 3,10,30 μM (blue) on TLCS (500 μM) induced necrosis. **B)** Bar graphs show the effects of Nec-1s (left) at 10 and 20 μM (green) and GSK'963 (right) at 1 μM (yellow) on TLCS (500 μM) necrosis. **C)** The line graph (left) shows the effects of Nec-1 at 10 μM (purple) on TLCS (500 μM) induced apoptosis. Bar chart (right) shows the value of apoptosis at the 8 h time point. The data were normalised to F/F_0. Significant differences between Nec-1 only and control were analysed (&p<0.05), and comparison between Nec-1 treatment and non-treated groups were analysed (*p<0.05). All data showed in A, B and C is the mean ± SEM and representative of at least 3 mice per group.

5.2.2 Effects of Nec-1 and GSK'963 on POAEE-induced PAC necrosis and apoptosis

The results showed that 100 μM POAEE elevated necrosis in PACs and that this increase was significantly reduced by Nec-1(10 μM) (by 82.61%) (Figure 5.2.2 A) and GSK'963 (10 μM) (by 95.42%) (Figure 5.2.2 B) treatment. As in the previous chapter 100 μM POAEE did not significantly increase apoptosis *per se*, and Nec-1 with POAEE did not alter apoptosis significantly (Figure 5.2.2 C) (The percentage was calculated by (treatment group-control)/(toxin group-control group)).

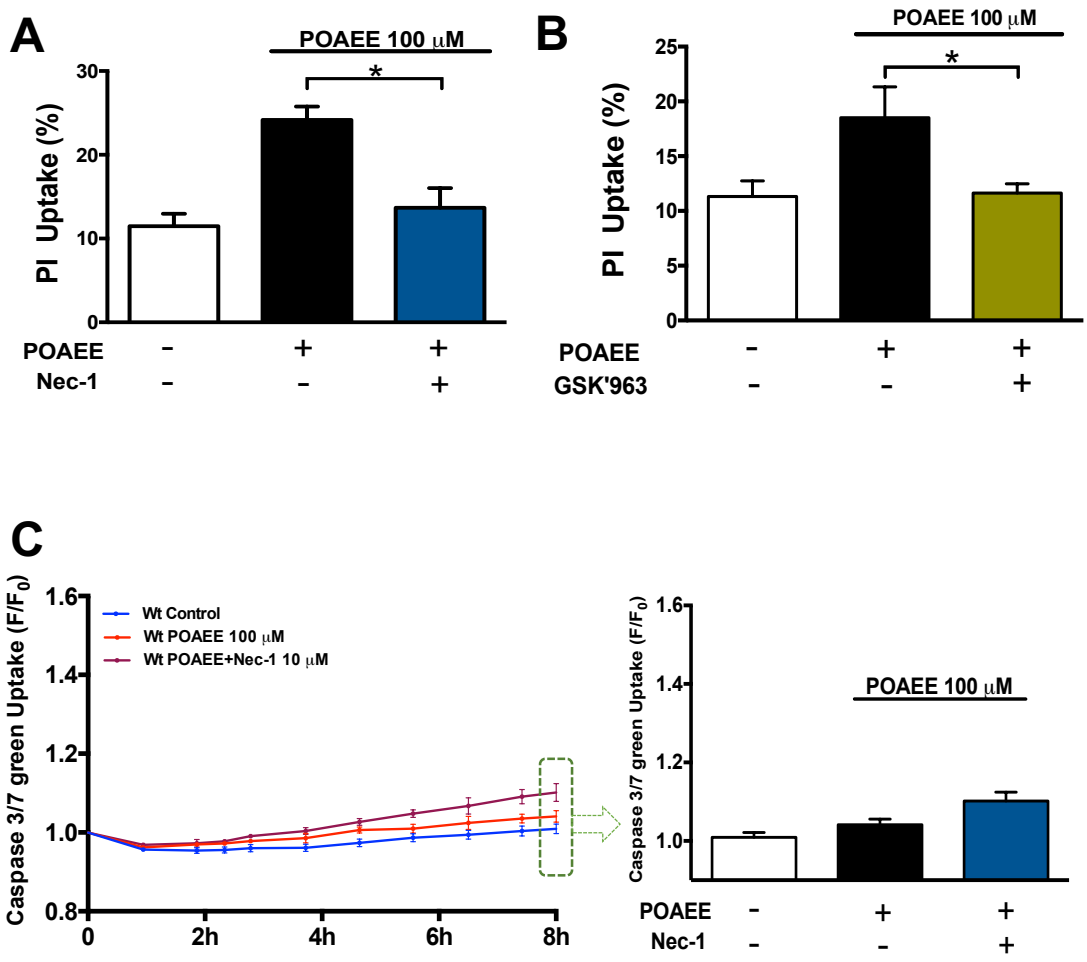

Figure 5.2.2 Effects of Nec-1 and GSK'963 on POAEE-induced PAC cell death. A) The bar graph shows the effect of Nec-1 at 10 μM (blue) on POAEE (100 μM) induced necrosis. **B)** The bar graph shows the effect of GSK'963 at 10 μM (yellow) on POAEE (100 μM) induced necrosis. **C)** The line graph (left) shows the effects of Nec-1 at 10 μM (purple) and POAEE (100 μM) on PAC apoptosis. The bar chart (right) shows the level of apoptosis at the 8h time point. The data were normalised to F/F_0. Significant differences between Nec-1 or GSK 963' treatment and POAEE groups were analysed (*$p<0.05$). All data showed in A, B and C are the mean ± SEM and representative of at least 3 mice per group.

5.2.3 Effects of Nec-1 on CCK-induced PAC necrosis and apoptosis

The results showed that Nec-1 at 10 μM did not affect apoptosis or necrosis *per se* compared with control. Necrosis was significantly elevated by CCK from 3 h to 8 h and this increase was significantly reduced by Nec-1 (by 85.09%) (Figure 5.2.3 A). However, as previously shown 10 nM CCK did not significantly increase apoptosis *per se*, and Nec-1 with CCK did not affect apoptosis significantly (Figure 5.2.3 B) (Figure 5.2.2 C) (The percentage was calculated by (treatment group-control)/ (toxin group-control group)).

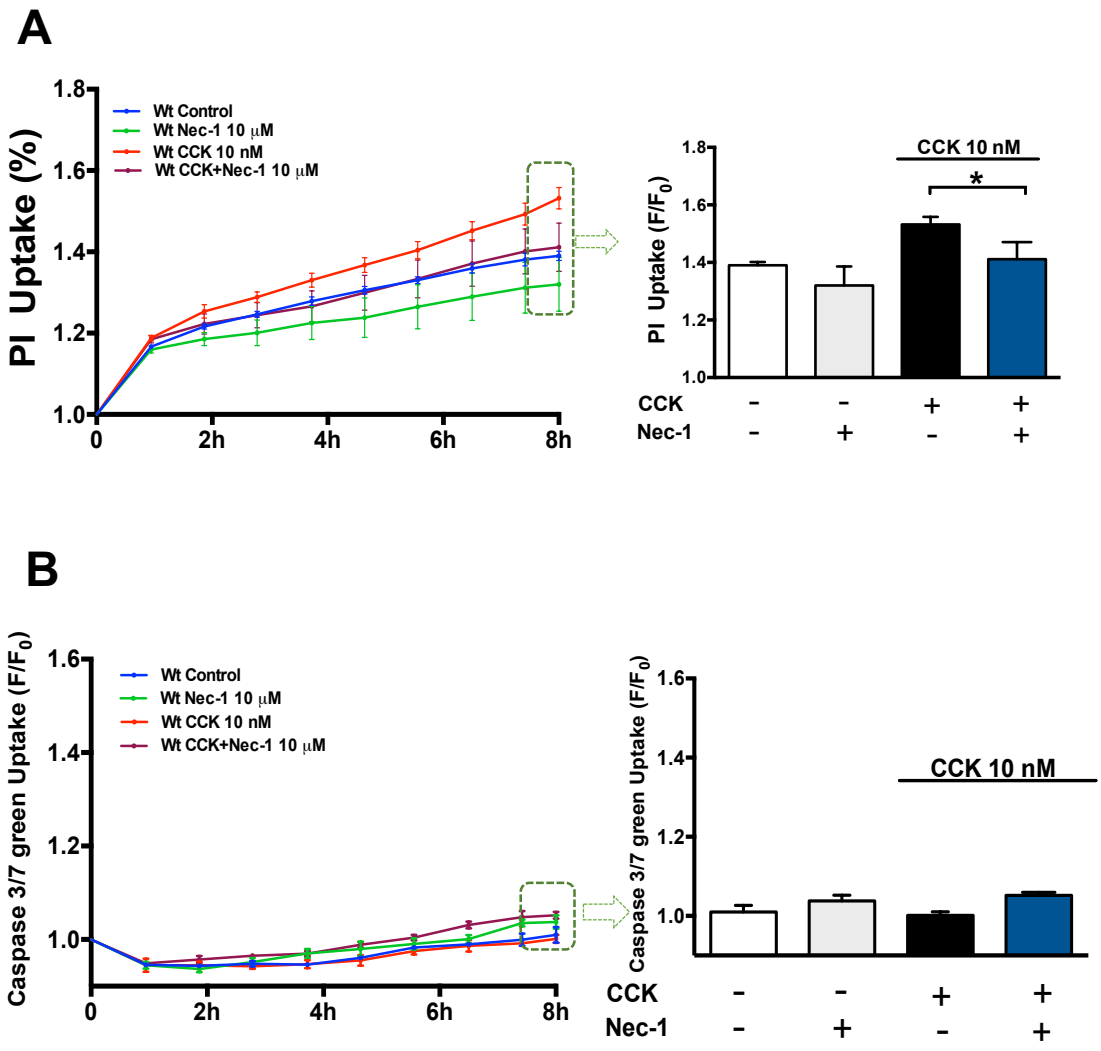

Figure 5.2.3 Effects of Nec-1 on CCK-induced PAC cell death. A) The line graph (left) shows the effect of Nec-1(10 μM) on CCK (10 nM) induced necrosis. The bar chart (right) shows the value of necrosis at the 8h time point. **B)** The line graph (left) shows the effects of Nec-1 and CCK (10 nM) on apoptosis. The bar chart represented 8h time point. Bar chart shows the value of necrosis at the 8h time point. The data were normalised to F/F_0. Significant differences between Nec-1 treatment and non-treated groups were analysed (*$p<0.05$). All data showed in A and B are the mean ± SEM of at least 3 mice per group.

5.3 Discussion

The data reported in this chapter show that Nec-1 (10 μM) and GSK'963 (10 μM) significantly reduced necrosis in mouse PACs exposed to POAEE (100 μM) by 82.61% and 95.41%, respectively. GSK'963 is a more potent RIPK1 kinase inhibitor compared to Nec-1 and its inhibition correlated to the effect of $Ripk1^{K45A}$ in POAEE induced cell death (reduced by 97.95%), suggesting that RIPK1 dependent necroptosis is relevant to POAEE-induced necrosis and may be inhibited by RIPK1 kinase inhibition.

Our results with different concentrations of Nec-1 showed that Nec-1 has a bell-shaped effect on TLCS-induced necrosis. Therefore, a lower dose of 3 μM showed slight toxicity compared with control, and at 10 μM there was a maximal inhibition of RIPK1 kinase dependent necroptosis. These data are consistent with a study which showed that low doses of Nec-1 indicated toxicity which sensitized mice to TNF-induced mortality (Takahashi, Duprez et al. 2012). Interestingly, application of Nec-1 (10 μM) induced greater reductions of TLCS (by 84.68%) and CCK (by 85.09%) induced necrosis compared to $Ripk1^{K45A}$ modification on TLCS (by 51.75%) and CCK (no effect), suggesting effects of Nec-1 other than purely necroptosis inhibition. A study showed that co-treatment of Nec-1 at 10,30 and 60 μM did not reverse ATP depletion induced by CCK or L-Arginine (Wu, Mulatibieke et al. 2017) and the reasons underlying such differences warrant further investigation.

In order to substantiate the possible additional effects of Nec-1, more specific RIPK1 kinase inhibitors Nec-1s and GSK'963 were tested. Nec-1s and

GSK'963 maximally reduced TLCS induced necrosis by 51.38% and 51.96%, respectively, compared with the reduction induced by Ripk1^{K45A} modification (by 51.76%). These inhibitors did not only confirm that the inhibition of RIPK1 kinase activity halved the TLCS (500 μM)-induced necrosis but also indicated that the Nec-1 has other effects besides the inhibition of RIPK1-dependent necroptosis.

The results from this chapter also show that Nec-1 significantly reduced apoptosis in mouse PACs exposed to TLCS (by 88%), whereas Ripk1^{K45A} did not significantly alter TLCS-induced apoptosis. This further indicates that there are additional effects of Nec-1 other than RIPK1 kinase inhibition that contribute to its pharmacological actions. As discussed in Chapter 4, the mechanism of RIPK1 kinase activity in apoptosis is poorly understood, with some reports showing that RIPK1 inhibition sensitised cells to apoptosis (Vanlangenakker, Bertrand et al. 2011, Remijsen, Goossens et al. 2014), and other results showing that RIPK1 inhibition did not affect apoptosis (Berger, Kasparcova et al. 2014, Kaiser, Daley-Bauer et al. 2014). Moreover, the effects of Nec-1 are highly controversial. Studies showed that Nec-1 significantly induced apoptosis in neutrophils (Jie, He et al. 2016), yet reduced the ovary cell apoptosis caused by ovary transplantation (Lee, Youm et al. 2014). Knockdown of RIPK1 significantly decreased BV6/IFNα-mediated apoptosis, whereas Nec-1 provided no protection (Reiter, Eckhardt et al. 2016).

Collectively, these investigations of RIPK1 kinase inhibitors on PAC cell death correlated with Ripk1^{K45A} results, and confirmed that in PACs, RIPK1

dependent necroptosis may account for approximately half of the TLCS-induced necrosis and for more than 90% of POAEE-induced necrosis. Furthermore, comparisons made between Ripk1^{K45A}, Nec-1, Nec-1s and GSK'963 show that besides RIPK1-dependent necroptosis inhibition, Nec-1 is likely to possess other effects. These findings suggest that Nec-1 might be more effective in ameliorating TLCS-AP and CER-AP compared with Ripk1^{K45A}.

Chapter 6 Results: Effects of Ripk1^{K45A} and Nec-1 on ROS production in isolated PACs

6.1 Introduction

An imbalance of ROS production and antioxidant status leads to oxidative stress and is associated with diseases including the pathogenesis of AP (Booth, Murphy et al. 2011, Werner, Hartwig et al. 2012, Armstrong, Cash et al. 2013). ROS production by bile acid contributed to the balance of cell death modalities which may play an important critical role in the outcome of the disease (Booth, Murphy et al. 2011).

Given the differences between the effects of Ripk1^{K45A} and pharmacological inhibitors on cell death modalities in the previous chapters, possible mechanisms underlying cellular actions were evaluated. ROS has been proposed to exert an important role in the execution of necroptosis dependent on cell type and toxins and there is inconsistency in the literature. For example, although necroptosis in HT-29 and Jurkat T cells was not inhibited by ROS scavengers (He, Wang et al. 2009), H_2O_2 induced necrosis was dependent on RIPK1 in MEFs (Shen, Lin et al. 2004).

The aim of this chapter was to evaluate whether ROS may contribute to the effects induced by Ripk1^{K45A} modification and Nec-1 against TLCS, POAEE and CCK induced cell death. In addition another target of Nec-1, the enzyme IDO (Vandenabeele, Grootjans et al. 2013), was inhibited using 1-MT (Takahashi, Duprez et al. 2012, Degterev, Maki et al. 2013) to investigate whether it contributed to TLCS-induced ROS production, and therefore might contribute to Nec-1's actions.

6.2 Results

6.2.1 Effects of Ripk1^{K45A} and Nec-1 on TLCS-induced ROS production

The results showed that Ripk1^{K45A} modification did not affect PAC basal ROS production compared with Wt. As previously demonstrated in isolated PACs using confocal microscopy (Booth, Murphy et al. 2011), TLCS (500 μM) induced a sustained elevation of ROS compared with control in both Ripk1^{K45A} and Wt PACs. TLCS induced ROS was not significantly different between Ripk1^{K45A} and Wt, although there was a trend towards an increase (Figure 6.2.1 A). In contrast, Nec-1 (30 μM) which did not affect basal ROS generation *per se*, significantly decreased TLCS-induced ROS production from 1 hour onwards (Figure 6.2.1 B).

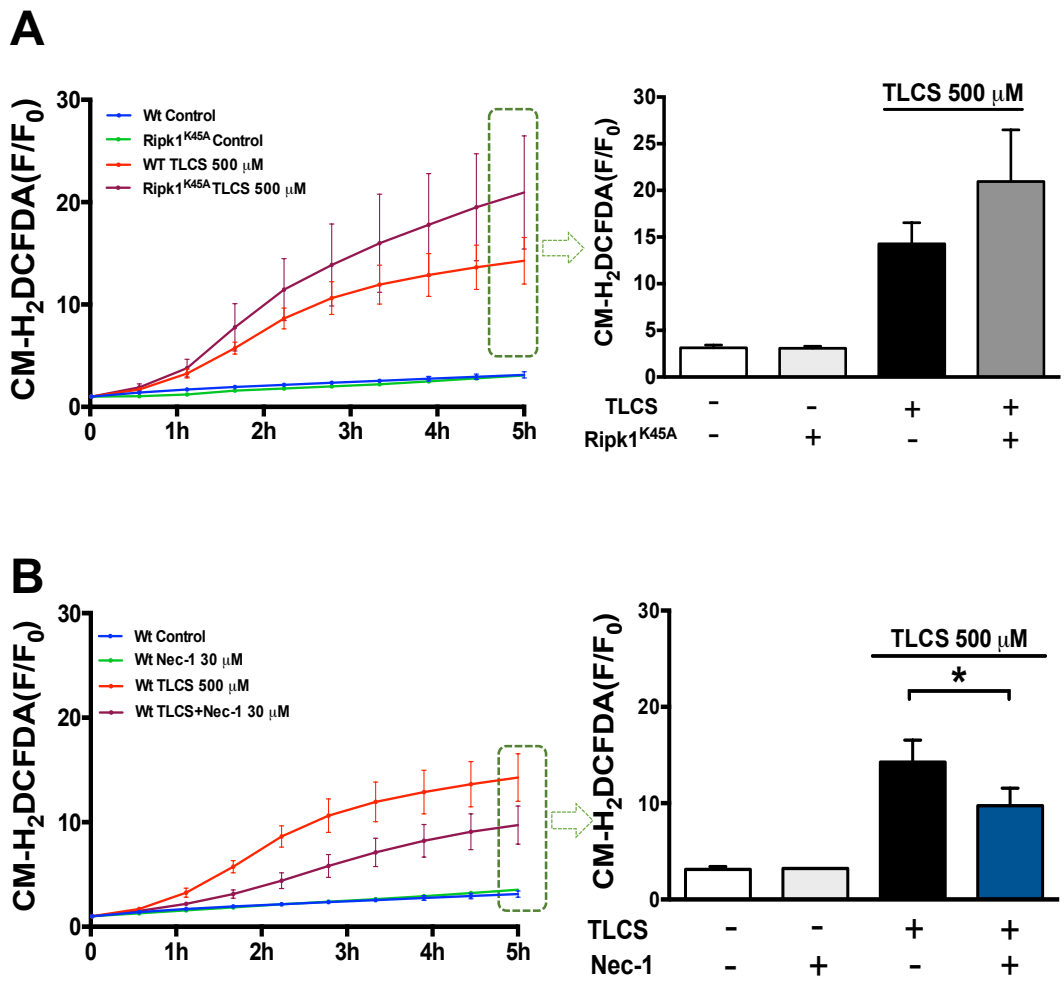

Figure 6.2.1 Effects of Ripk1^{K45A} and Nec-1 on TLCS induced PAC ROS production. Mean data from experiments on murine PAC shows that **A**) the effects of Ripk1^{K45A} on TLCS (500 μM) induced intracellular ROS production. Bar chart (right) shows the value of ROS level at the 5 h time point. **B)** the effects of Nec-1 (30 μM) on TLCS (500 μM) induced intracellular ROS production. Bar chart (right) shows the value of ROS level at the 5 h time point. Data are shown as normalised changes from basal fluorescence levels (F/F_0). Significant differences between Ripk1^{K45A} or Nec-1 and stimulated control were analysed (*$p<0.05$). All values are the means ± SEM of at least 3 mice per group.

6.2.2 Effects of Ripk1^{K45A} and Nec-1 on POAEE-induced ROS production

The results showed that application of POAEE (100 μM) did not increase ROS production (Figure 6.2.2). Neither did POAEE at 500 μM (data not shown). Application of POAEE (100 μM) to Ripk1^{K45A} PACs did not affect ROS production either (Figure 6.2.2 A). Nec-1 at 30 μM showed no effect on ROS production with or without POAEE (100 μM) (Figure 6.2.2 B).

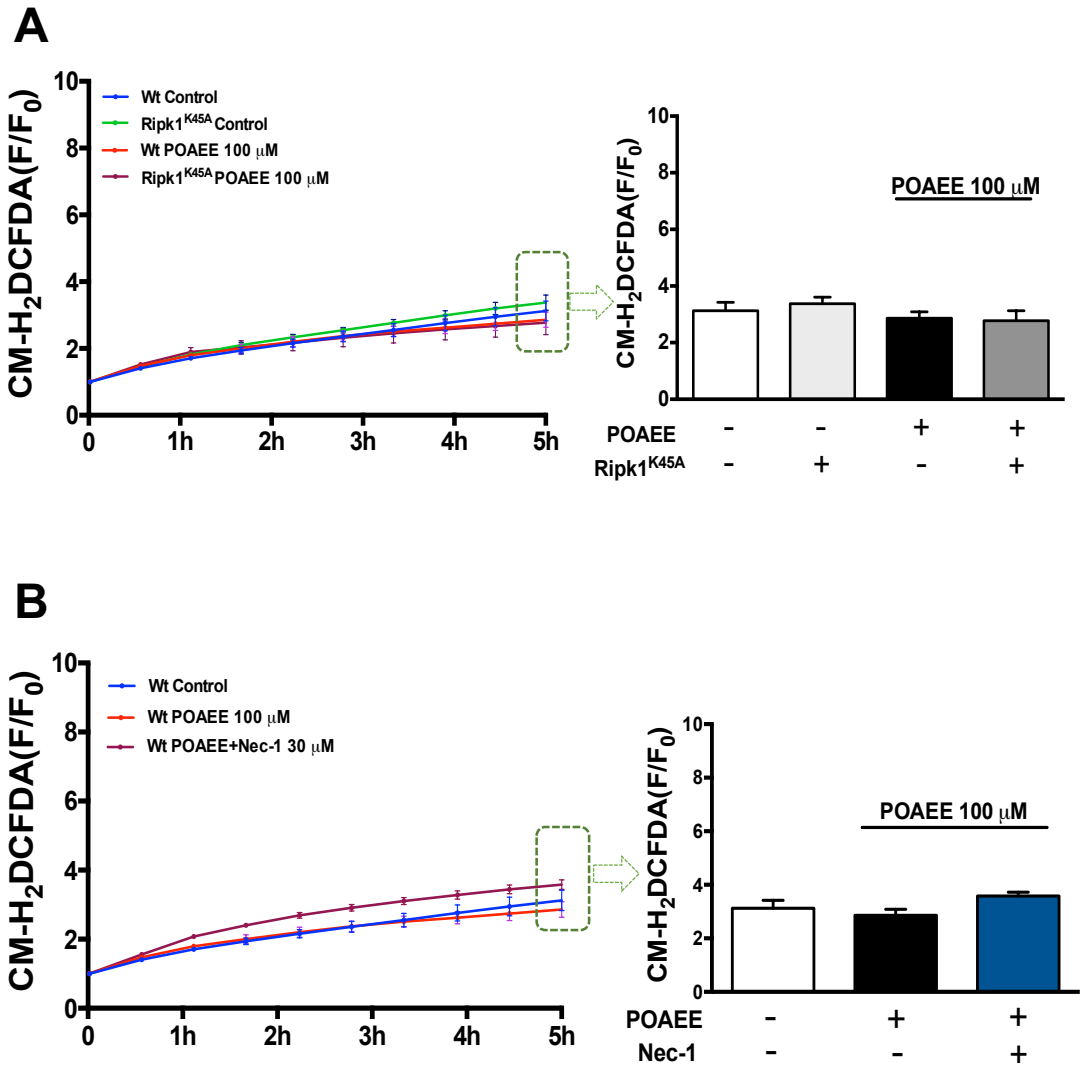

Figure 6.2.2 Effects of Ripk1^{K45A} and Nec-1 with POAEE on PAC ROS production. Mean data from experiments on murine PACs shows that **A)** the effects of Ripk1^{K45A} and POAEE (100 μM) on intracellular ROS production. The bar chart (right) shows the value of ROS level at the 5 h time point. **B)** the effects of Nec-1 and POAEE (100 μM) on intracellular ROS production. The bar chart (right) shows the value of ROS level at the 5 h time point. Data are shown as normalised changes from basal fluorescence levels (F/F_0). Significant differences between Ripk1^{K45A} or Nec-1 and Wt were analysed (*$p<0.05$). All values are the means ± SEM of at least 3 mice per group.

6.2.3 Effects of Ripk1^{K45A} and Nec-1 on CCK-induced ROS production

The results showed that application of CCK (10 nM) did not cause significant ROS production (Figure 6.2.3). Application of CCK to Ripk1^{K45A} PACs also did induce any ROS production (Figure 6.2.3 A). Nec-1 at 30 μM showed no effect on ROS production with or without CCK (10 nM) (Figure 6.2.3 B).

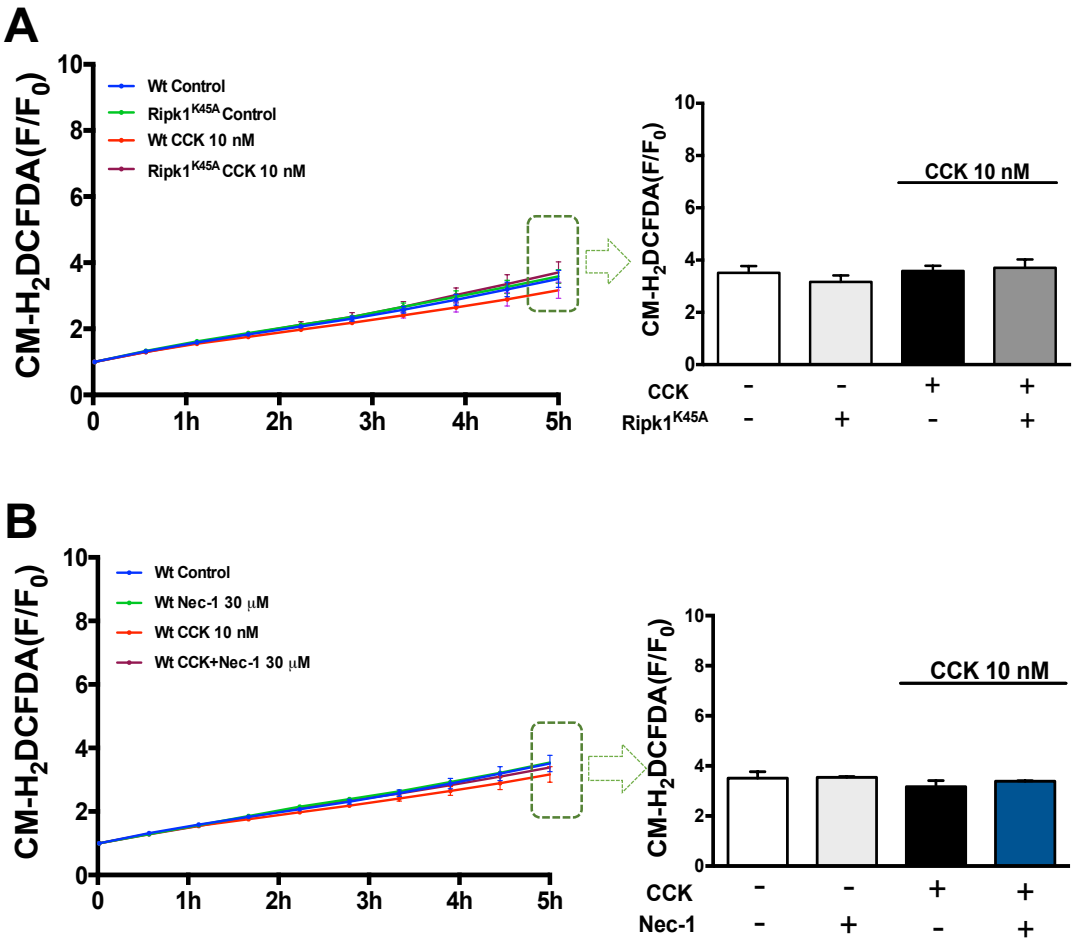

Figure 6.2.3 Effects of Ripk1^{K45A} and Nec-1 with CCK on PAC ROS production. Mean data from experiments on murine PACs shows that **A)** the effects of CCK (10 nM) on Ripk1^{K45A} intracellular ROS production. The bar chart (right) shows the value of ROS level at the 5 h time point. **B)** the effects of Nec-1 and CCK (10 nM) on intracellular ROS production. The bar chart (right) shows the value of ROS level at the 5 h time point. Data are shown as normalised changes from basal fluorescence levels (F/F_0). The differences were analysed between Ripk1^{K45A} or Nec-1 to stimulated control (*$p<0.05$). All values are the means ± SEM of at least 3 mice per group.

6.2.4 Effects of Nec-1 on TLCS-induced ROS production in Ripk1^{K45A}, and 1-MT on TLCS-induced ROS production

Nec-1 was applied to PACs isolated from Ripk1^{K45A} mice to evaluate any potential additional effects. The results showed that TLCS (500 μM) induced ROS production in Ripk1^{K45A} from 30 min onwards, and that Nec-1 (30 μM) significantly decreased the ROS production generated by 500 μM TLCS in Ripk1^{K45A} PACs (Figure 6.2.4 A). 1-MT was also applied separately to see whether inhibition of IDO might affect TLCS-induced ROS production. The results showed that 1-MT (30 μM) did not significantly change basal ROS generation, although there was a trend toward a decreased response from 1 hour onwards (Figure 6.2.4 B).

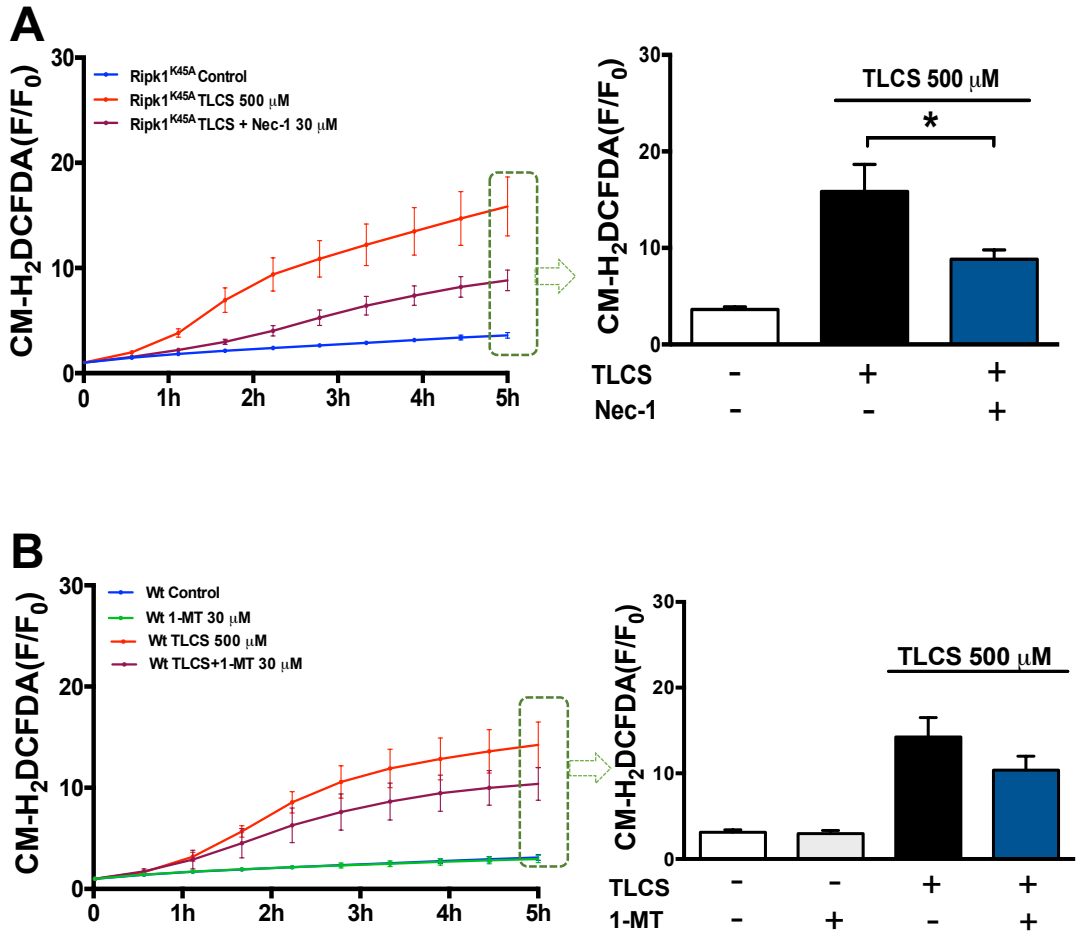

Figure 6.2.4 Effects of Nec-1 on TLCS-induced ROS production in Ripk1^{K45A} PACs, and 1-MT on TLCS-induced ROS production. Mean data from experiments shows that **A)** the effects of Nec-1 (30 μM) on TLCS (500 μM) induced ROS production in Ripk1^{K45A}. The bar chart (right) shows the value of ROS production at the 8 h time point. **B)** The effects of 1-MT (30 μM) on TLCS (500 μM) induced ROS production. The bar chart (right) shows the value of ROS production at the 8 h time point. Data are shown as normalised changes from basal fluorescence levels (F/F_0). The differences were analysed between Nec-1 or 1-MT treatment to stimulated control (*$p<0.05$). All values are the means ± SEM of at least 3 mice per group.

6.3 Discussion

The work described in this chapter shows that TLCS (500 μM) induced ROS production significantly, however, POAEE (100 μM) and CCK (10 nM) did not induce significant ROS changes in this plate reader assay. The current data are consistent with our previous study which showed that the ROS probe H_2CMDCFDA successfully detected ROS responses in single isolated cells induced by TLCS (Booth, Murphy et al. 2011). However, H_2CMDCFDA was not sensitive enough to detect the ROS changes upon application of CCK (10 nM) (Chvanov, Huang et al. 2015). A new lipophilic ROS indicator, H_2RB-$C_{18,}$ which preferentially reports ROS at plasma membrane regions showed better sensitivity to ROS than cytosolic ROS indicator H_2CMDCFDA, in response to 10 nM CCK and 20 μM POAEE (Chvanov, Huang et al. 2015) potentially because this approach avoids effects of endogenous cytosolic antioxidants. Also, previous work with H_2CMDCFDA in isolated PACs, measured with confocal microscopy, demonstrated that POAEE did not induce significant elevations of ROS (Booth, PhD Thesis University of Liverpool 2010). These results suggest that ROS production induced by CCK and POAEE is not a major contributor to their cellular actions and that RIPK1 kinase activity would not be affected to any extent.

Furthermore, Ripk1^{K45A} modification did not significantly affect TLCS-induced ROS production, although there was a slight trend to an increased level. This result is contrary to a previous study which showed that Ripk1^{K45A} modification reduced salmonella typhimurium infection-induced necrosis associated with a reduction of ROS in macrophages (Shutinoski,

Alturki et al. 2016). However, Nec-1 significantly decreased TLCS-induced ROS production in PACs, consistent with studies showing that the RIPK1$^{-/-}$ and Nec-1 efficiently reduced ROS accumulation and necroptosis induced by different toxins in diverse cell types (Lin, Choksi et al. 2004, Shen, Lin et al. 2004, Shindo, Kakehashi et al. 2013, Desai, Kumar et al. 2016). TNFα-induced necroptosis and ROS elevation in L929 cells was shown to be generated via the mitochondrial Complex I but not by NADPH oxidase components (Vanlangenakker et al., 2011). NADPH oxidase is not present in primary PACs and much of the increase in intracellular ROS in response to bile acid and menadione occurred within mitochondria (Gukovskaya, Gukovsky et al. 2002, Criddle, Gillies et al. 2006, Booth, Murphy et al. 2011). The present data suggest that reduction of Nec-1 on TLCS-induced ROS may mediated via a reduction of mitochondrial ROS production through mechanisms as yet undefined.

In accord the pivotal role of ROS in promoting PAC apoptosis, Nec-1 also reduced apoptosis induced by TLCS. ROS-induced cytochrome C release, leading to ATP-dependent caspase activation and apoptosis, occurs in many cell types including acinar cells (Yerushalmi, Dahl et al. 2001, Orrenius, Gogvadze et al. 2007). The effects of Nec-1 on TLCS-induced ROS production correlated to the effects of Nec-1 on TLCS-induced apoptosis, suggesting that Nec-1 inhibition of TLCS-induced ROS production might also be relevant to modulation of apoptosis.

There is also possible that Nec-1 inhibits RIPK1 in a kinase-independent manner and also that RIPK1 might exert its effect on ROS in a kinase-

independent manner. Since study showed that the Nec-1 can affect Ser161 so that mediated kinase inhibition (Xie, Peng et al. 2013). However, the necroptosis inhibition caused by Ser161 was not fully (Degterev, Hitomi et al. 2008). The mechanism of it need further elucidation and this can be achieved by gene deletion. If RIPK1 is increasing ROS in a kinase-dependent manner then one would expect this to be lost in RIPK1 $^{-/-}$.

Tryptophan loading induces oxidative stress in healthy humans, and this oxidative stress was considered as a result of QUIN, 3-HK and 3-HANA generation and their pro-oxidant activity (Feksa, Latini et al. 2006). IDO activation and L-Trp metabolism within the kynurenine pathway protected against the oxidative process (Takahashi, Duprez et al. 2012, Yeung, Terentis et al. 2015). Evaluation of whether Nec-1 has additional effects other than RIPK1 inhibition, such as IDO inhibition, showed that TLCS induced ROS production was inhibited by Nec-1 (by 41%) in PACs isolated from Ripk1^{K45A}, however, the IDO inhibitor 1-MT did not significantly decrease TLCS-induced ROS production. These results suggest that the inhibitory effects of Nec-1 on TLCS-induced ROS production are independent of IDO inhibition.

Collectively, Nec-1 inhibits Ripk1^{K45A} induced ROS independently of its kinase activity. And the kynurenine pathway was not involved in the reduction of TLCS-induced ROS production.

Chapter 7 Results: Effects of Ripk1^{K45A} and Nec-1 on Ca^{2+} signals in isolated PACs

7.1 Introduction

Application of physiological concentrations of CCK (1~50 pM) resulted in the initiation of Ca^{2+} oscillations in PACs. These oscillations are characterised by repetitive, regular cycles of elevated and subsequently decreasing Ca^{2+} levels (Iwatsuki and Petersen 1977), and the second messengers (Thorn and Petersen 1993), cADPR (Thorn, Gerasimenko et al. 1994, Cancela, Gerasimenko et al. 2000) and NAADP are required for CCK to be able to elicit repetitive Ca^{2+} spikes through IP3Rs and RyRs receptor stimulation (Cancela, Gerasimenko et al. 2000, Cancela, Van Coppenolle et al. 2002).

Disruption of normal Ca^{2+} signals was demonstrated to be a trigger for the development of AP. Hyperstimulation of PACs with CCK, bile salts and non-oxidative ethanol metabolites induced sustained cytosolic Ca^{2+} elevations linked to intracellular digestive enzyme activation and necrosis (Raraty, Ward et al. 2000, Kim, Kim et al. 2002, Voronina, Longbottom et al. 2002) (Criddle, Raraty et al. 2004, Criddle, Murphy et al. 2006, Petersen 2009). Subsequent cellular injury was reduced either by the removal of Ca^{2+} from external solution or by blockade of SOCE channels on the plasma membrane (Petersen, Sutton et al. 2006, Gerasimenko, Gryshchenko et al. 2013, Lankisch, Apte et al. 2015). ORAI1 is the principal component of the SOCE channel in the PACs, which associates with stromal interaction molecule (STIM)-1 on store depletion, and its inhibitor GSK-7975A inhibited SOCE induced by thapsigargin in isolated murine PACs reducing necrosis induced by toxins that cause AP (Gerasimenko, Gryshchenko et al. 2013, Wen, Voronina et al. 2015).

Whether Ca^{2+} signals are vital in RIPK1 dependent necroptosis is uncertain. Studies showed that thapsigargin induced Ca^{2+} elevations which triggered RIPK1 mediated necroptosis in different cell types, and both $RIP1^{-/-}$ and calcium chelation decreased this Ca^{2+} dependent necroptosis (Jiang, Mao et al. 2009, Luan, Jin et al. 2015). In addition, in PACs, preloading cells with Ca^{2+} chelator reduced caerulein or TLCS induced ATP depletion, necrosome formation and PAC injury, and by adding Nec-1 to the caerulein or TLCS treated cells did not change TLCS or caerulein induced ATP depletion proved that necrosome formation, and PAC death occurred downstream of a pathologic cytoplasmic calcium elevation (Louhimo, Steer et al. 2016).

However, studies also showed that necroptosis induced by TLR3/4 did not trigger an early Ca^{2+} flux, and the early increase in cytosolic Ca^{2+} observed in TNFα-induced necroptosis was related to a TNF/RIP1/TAK1 survival pathway that was dispensable for necroptosis (Ros, Pena-Blanco et al. 2017).

To date no study has been done specifically addressing the possible effects of RIPK1 kinase activity on AP relevant Ca^{2+} signals. The aim of this chapter was to use real-time confocal microscopy of freshly isolated PACs to distinguish whether $Ripk1^{K45A}$ modification affected TLCS and CCK induced physiological and/or pathological cytosolic Ca^{2+} elevations. For the comparison, pharmacological inhibition of RIPK1 with Nec-1 was used on TLCS and CCK-induced Ca^{2+} signals.

7.2 Results

7.2.1 Effects of Ripk1^{K45A} and Nec-1 on CCK-induced Ca^{2+} oscillation

The results showed that Ca^{2+} oscillations were induced by CCK (20 pM) in PACs isolated from Ripk1^{K45A} and Wt mice maintained in 1 mM external Ca^{2+} (Figure 7.2.1). The characteristics of the Ca^{2+} oscillations were not different between Ripk1^{K45A} and Wt PACs, evaluated as the area under the curve (Figure 7.2.1.A,B&C). Nec-1 (30 μM) did not affect CCK-induced Ca^{2+} oscillations when applied after CCK stimulation nor did it inhibit the CCK response when applied ahead of CCK stimulation (Figure 7.2.1 D&E).

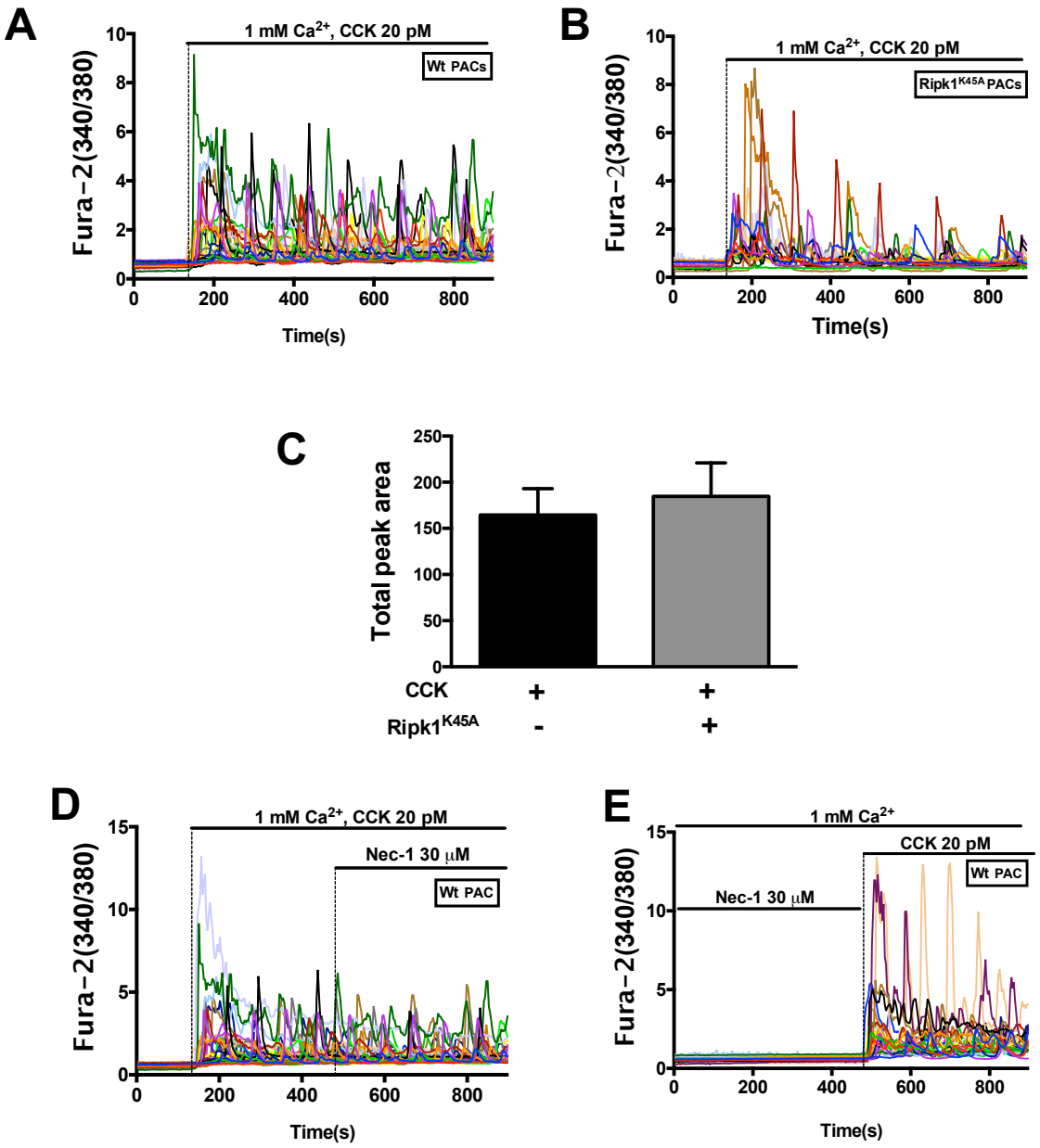

Figure 7.2.1 Effects of Ripk1^{K45A} and Nec-1 on CCK evoked Ca^{2+} oscillations in PAC. **A)** The effects of CCK (20 pM) in Wt PACs (n=28). **B)** The effects of CCK (20 pM) in Ripk1^{K45A} PACs (n=20). C) The mean value of area under the curve from each single cell comparison between A) & B). (*p<0.05). **D&E)** The effects of Nec-1 (30 μM) on CCK evoked Ca^{2+} oscillations (n=28). No difference was observed compared with A) and B) Each curve represented a single cell. The data are presented as originally 340nm/380nm. The experiments have been repeated on 3 mice.

7.2.2 Effects of Ripk1^{K45A} and Nec-1 on TLCS-induced sustained Ca^{2+} elevation

Isolated PACs were maintained in 5 mM external Ca^{2+} and perfused with TLCS (500 μM) to induce a stable sustained elevation of $[Ca^{2+}]_c$ (Figure 7.2.2). The results showed that TLCS induced sustained elevations of $[Ca^{2+}]_c$ in isolated PACs from both Ripk1^{K45A} and Wt mice (Figure 7.2.2). Interestingly, the Ripk1^{K45A} modification in mice PACs significantly increased the TLCS-induced Ca^{2+} elevation (by 62.65%) (Comparison was made at the peak time and an end point between Ripk1^{K45A} and Wt groups (Figure 7.2.2 A).

Application of Nec-1 did not cause a major alteration of the bile acid-induced plateau. However, it is difficult to conclude whether the small but significant difference between Nec-1 and control from 600s to 1000s was attributable to an effect of Nec-1 since differences in the Ca^{2+} plateau between control and test happened before the application of Nec-1 (normalisation was also performed at 600s when Nec-1s was applied but did not help interpretation of the data) (Figure 7.2.2 B). However, application of Nec-1s did not affect the TLCS-induced Ca^{2+} elevation (also confirmed by the normalisation at 600s (F/F_{600}) when Nec-1s was applied) (Figure 7.2.2.C). A slight increase of the Ca^{2+} signal which happened at 600s may have been caused by the changing of perfusion syringes and not represent a real response.

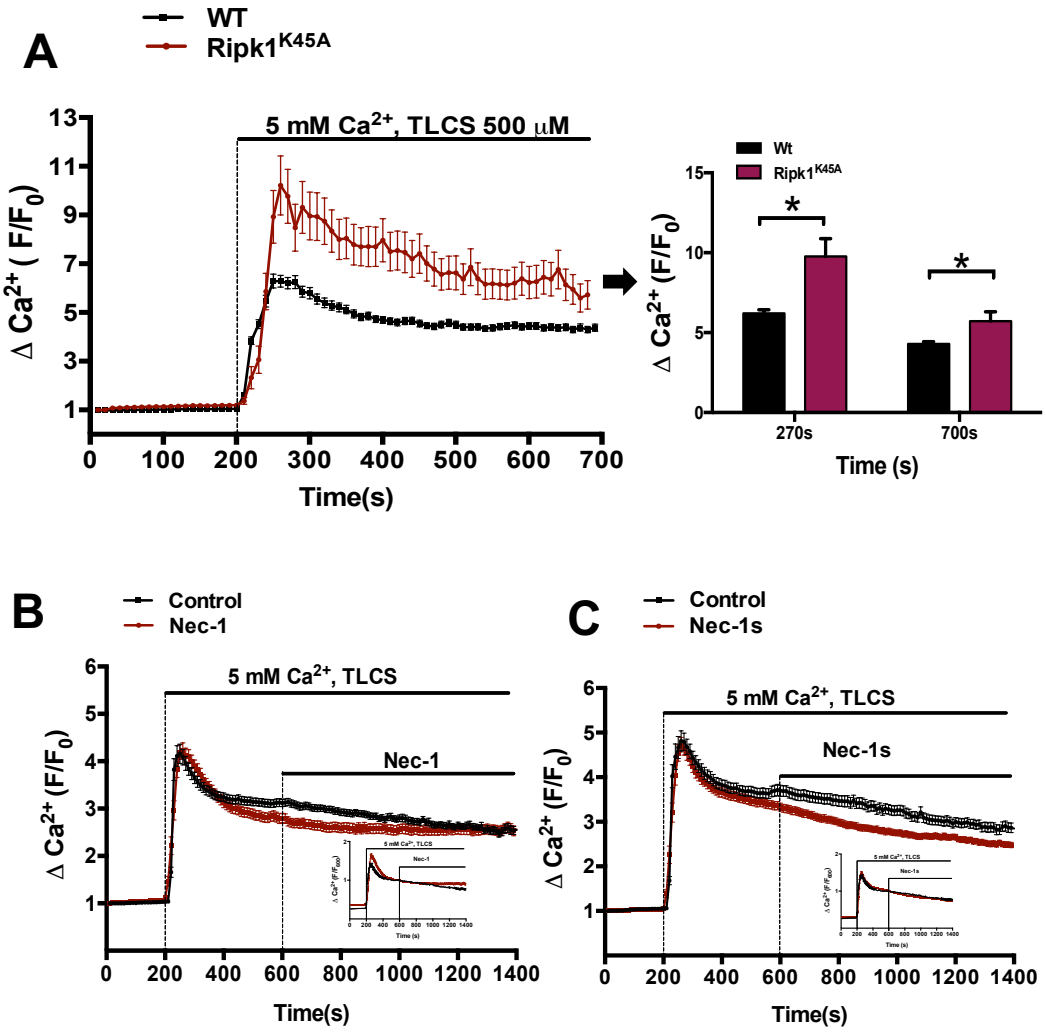

Figure 7.2.2 Effects of Ripk1^{K45A} modification and Nec-1 on TLCS-induced Ca^{2+} elevation in PACs. The Isolated PACs were maintained in 5 mM external Ca^{2+} and **A)** TLCS (500 μM) was applied at 200s in both Ripk1^{K45A} (red) (n=30) and Wt (black) (n=20). The bar chart (right) shows the value of F/F_0 in Wt (black) and Ripk1^{K45A} (red) at 270s and 700s (*p<0.05). **B)** TLCS (500 μM) was applied at 200s. Nec-1 (30 μM) (red) was applied at 600s (n=50) compared with control (black) (n=80). And the normalised data (F/F_{600}) were shown. **C)** TLCS (500 μM) was applied at 200s. Nec-1s (30 μM) (red) was applied at 600s (n=76) compared with control (black) (n=81). And the normalised data (F/F_{600}) were shown. All values are means ± SEM from at least 3 mice per group.

7.2.3 Effects of Ripk1^{K45A} and Nec-1/1s on CCK-induced sustained Ca^{2+} elevation

Isolated PACs were maintained in 5 mM external Ca^{2+} and perfused with supramaximal CCK (1 nM) to induce sustained elevations of $[Ca^{2+}]_c$ in Ripk1^{K45A} and Wt PACs (Figure 7.2.3). The results showed that CCK (1 nM) induced sustained elevation of $[Ca^{2+}]_c$ in PACs from both Ripk1^{K45A} and Wt mice (Figure 7.2.3 A & B). As with TLCS previously, Ripk1^{K45A} modification elevated the CCK induced Ca^{2+} peak compared with control (by 41.72%) (A comparison was made at the peak time and an end point between Ripk1^{K45A} and Wt) (Figure 7.2.3 A). The results showed that the application of Nec-1 at 0.5 and 3 μM did not affect the CCK-induced sustained Ca^{2+} plateau, however, Nec-1 at 10 and 50 μM significantly inhibited this sustained Ca^{2+} elevation by 41.31% and 44.14%, respectively (a comparison was made at 1400s between Nec-1 and the control) (Figure 7.2.3 B). To assess whether the effects of Nec-1 on Ca^{2+} was mediated through RIPK1 kinase activity, Nec-1s was applied at 10 and 50 μM. The data showed that Nec-1s at 10 and 50 μM significantly reduced the CCK-induced sustained Ca^{2+} elevation by 39.41% and 29.57%, respectively (comparison was made at the 1400s between Nec-1s and control) (Figure 7.2.3 C).

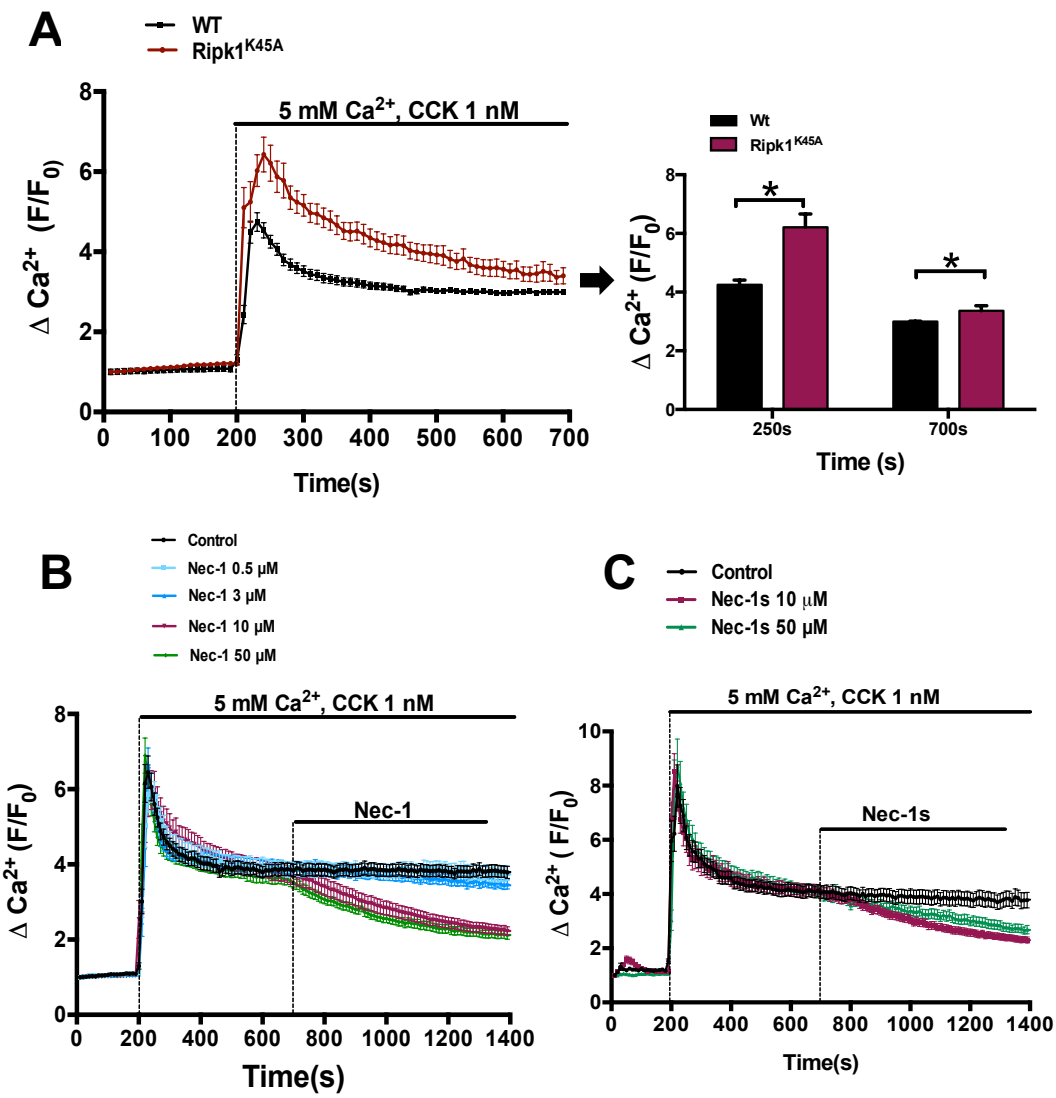

Figure 7.2.3 Effects of Ripk1^{K45A} modification and Nec-1/1s on CCK-induced sustained Ca^{2+} elevation in PACs. The isolated PACs were maintained in 5 mM external Ca^{2+} and **A)** CCK (1 nM) was applied at 200s in both Ripk1^{K45A} (red) (n=20) and Wt (black) (n=30). The bar chart (right) shows the value of F/F_0 in Wt (black) and Ripk1^{K45A} (red) at 250s and 700s (*$p<0.05$). **B)** after a stable plateau was formed, Nec-1 (0.5,3,10,50 μM) were applied at 700 s. **C)** after a stable plateau was formed, Nec-1s (10,50 μM) were applied at 700 s. Data are shown as normalised changes from basal fluorescence levels (F/F_0). All values are the means ± SEM from at least 3 mice per group.

7.2.4 Effects of Nec-1 on store-operated Ca^{2+} entry

Thapsigargin was used in zero external Ca^{2+} to stimulate Ca^{2+} store depletion, through its inhibition of SERCA, in order to assess whether Nec-1 inhibition of the cytosolic Ca^{2+} elevation was via mediated through a reduction of SOCE. Application of this protocol showed that Nec-1 only minimally decreased the Ca^{2+} signal compared to GSK-7975A which greatly inhibited the thapsigargin-induced store-operated Ca^{2+} influx (Figure 7.2.4).

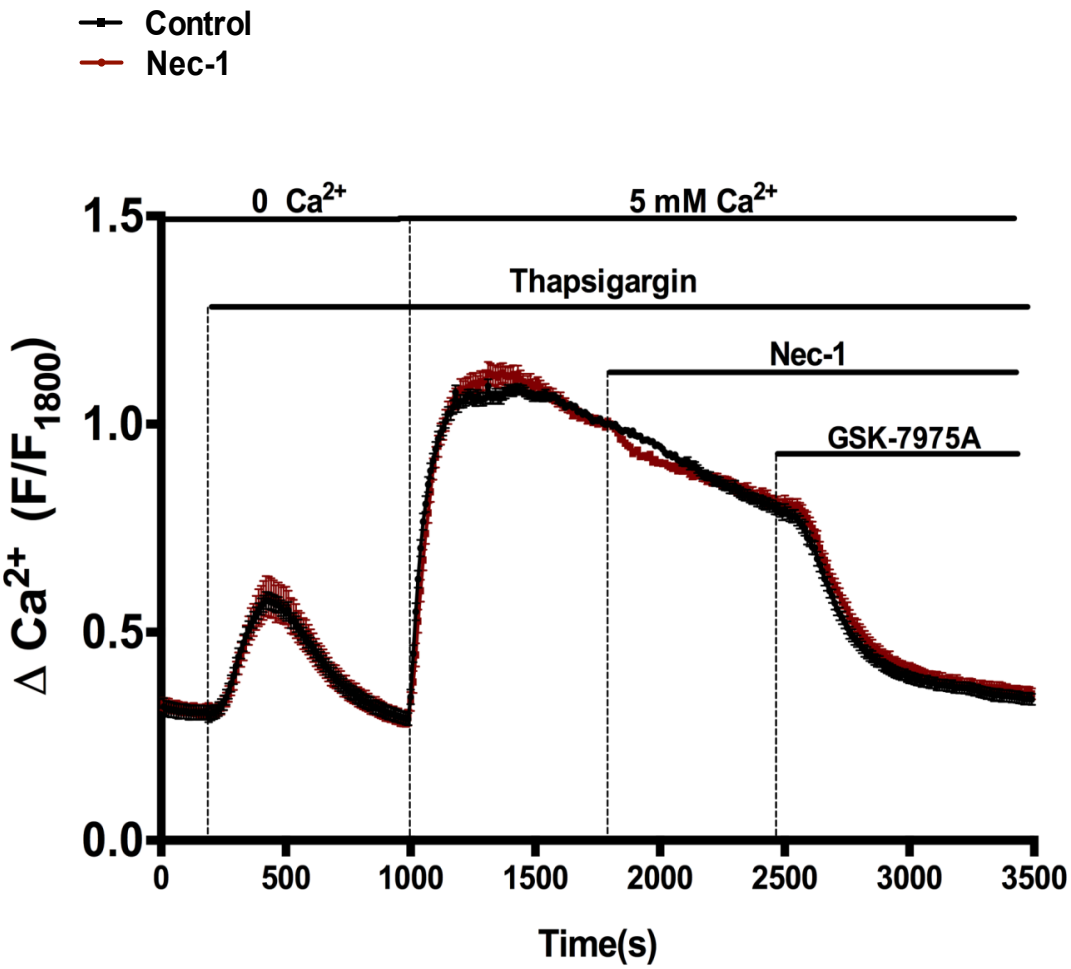

Figure 7.2.4 Effects of Nec-1 on the store-operated Ca^{2+} entry in PACs. Thapsigargin induced PAC store depletion in a 0 Ca^{2+} environment and shown as a transient Ca^{2+} raise. 5 mM Ca^{2+} applied from 1000s induced Ca^{2+} entry through SOCE and a $[Ca^{2+}]_c$ increase. Nec-1 was applied from 1800s to 2500s (red) compared with control (black). GSK-7975A (10 μM) as a positive control was applied at 2500s and inhibited Ca^{2+} influx. Data are shown as normalised changes from fluorescence levels at 1800s (F/F_{1800}). All values are the means ± SEM from at least 3 mice per group.

7.3 Discussion

The work described in this chapter shows that Ripk1^{K45A} and Nec-1 did not affect physiological CCK (20 pM) induced Ca^{2+} oscillations in isolated murine PACs. Such cytosolic Ca^{2+} spikes are primarily due to the release of Ca^{2+} from intracellular stores which is dependent on both IP_3Rs and RyRs. The cytosolic Ca^{2+} rise is brought back to basal levels through the actions of the SERCA pump, which refills the ER, and the PMCA pump which extrudes Ca^{2+} out of the cell (Petersen and Tepikin 2008). The results suggest that none of these processes were affected by Ripk1^{K45A} and Nec-1 under physiological conditions.

Bile acids have been shown to cause sustained elevations of $[Ca^{2+}]_c$ in PACs (Kim, Kim et al. 2002, Voronina, Longbottom et al. 2002). In PACs, evidence suggests that the G protein-coupled bile acid receptor 1 (Gpbar1) which is located in the apical region is relevant to the sustained elevations of $[Ca^{2+}]_c$. A previous study has shown that 500 μM TLCS elicited pathological Ca^{2+} elevations in PACs, and that this effect was mostly absent in PACs from Gpbar1 knockout mice (Perides, Laukkarinen et al. 2010). Multiple studies showed that bile acids induce Ca^{2+} release from the ER store and stimulate the acidic store in the apical ZG area through the activation of IP_3R and RyRs (Gerasimenko, Flowerdew et al. 2006, Fischer, Gukovskaya et al. 2007). Furthermore, they have been shown to cause the inhibition of the SERCA pump and activation of SOCE (Kim, Kim et al. 2002), mitochondrial membrane depolarization (Voronina, Barrow et al. 2004) and depletion of both cytosolic

and mitochondrial adenosine triphosphate (ATP) leading to cellular injury (Voronina, Barrow et al. 2010).

Bile-induced formation of global calcium signals occurred similarly as for endogenous hormones and neurotransmitters. The signals originated in the apical part of the cell and then spread as a wave into the basolateral region. The similarity of the signalling patterns and sensitivity to pharmacological inhibition suggests that second messengers (IP_3, cADP-ribose, NAADP) also mediate the response to bile acids (Voronina, Longbottom et al. 2002).

In the present study $Ripk1^{K45A}$ modification significantly potentiated both pathological TLCS (500 μM) and CCK (1 nM) hyperstimulation induced Ca^{2+} elevations. The initial rise of Ca^{2+} affected by $Ripk1^{K45A}$ modification, which is resultant at least in part from a Ca^{2+} release of internal Ca^{2+} stores, may suggest an action of RIPK1 on ER store Ca^{2+} content or alternatively a promotion of Ca^{2+} entry on store depletion. However, physiological Ca^{2+} signals induced by pM CCK were not affected by $Ripk1^{K45A}$ modification and would suggest that internal Ca^{2+} stores are not affected by RIPK1. Although there is scant information in the literature about possible links of RIPK1 to calcium handling, a previous study showed that an early increase in cytosolic Ca^{2+} in TNFα-induced necroptosis was related to the TNF/RIP1/TAK1 survival pathway. This did not require the activation of the necrosome and was dispensable for necroptosis (Ros, Pena-Blanco et al. 2017), suggesting the $Ripk1^{K45A}$ modification induced potentiation of Ca^{2+} elevation in the present results are likely to be independent of necroptosis.

In contrast to $Ripk1^{K45A}$ modification, Nec-1/1s significantly inhibited CCK-

induced sustained Ca^{2+} elevations in mouse PACs suggesting a reduction of Ca^{2+} influx into the cell via SOCE or a more efficient clearance of Ca^{2+} from the cytosol via ATP-dependent pumps. However, Nec-1 did not reduce SOCE in the standard protocol using thapsigargin, compared to the large effect of GSK-7975A, suggesting that inhibition of Nec-1/1s on CCK-induced Ca^{2+}elevation was not induced by SOCE inhibition and may point to actions on SERCA or PMCA that improve clearance. However, Nec-1/1s did not affect the TLCS-induced sustained Ca^{2+} elevation, suggesting SERCA/PMCA were not affected under these conditions. In addition, a potential direct inhibition of CCK receptors may be ruled out as only Ca^{2+} plateaux caused by hyperstimulation were affected by Nec-1/1s whereas oscillatory Ca^{2+} signals in response to pM CCK were unchanged. The underling mechanism of Nec-1 on Ca^{2+} signalling is therefore intriguing and undoubtedly complex, something which warrants further study.

Collectively, any effects that elicit Ca^{2+} extrusion via plasma PMCA, inhibit Ca^{2+} entry via SOCE, inhibit Ca^{2+} release from intracellular stores or promote Ca^{2+} uptake into the ER through SERCA are considered to be beneficial for AP by reducing cytosolic Ca^{2+} overload (Petersen and Sutton 2006)(Criddle review 2016). The work in this chapter demonstrated that the $Ripk1^{K45A}$ modification did not affect physiological Ca^{2+} but potentiated pathological Ca^{2+} increases by an unknown mechanism. Similarly, the effects of Nec-1/1s to reduce CCK-induced sustained Ca^{2+} elevations are currently unclear, but the reduction of such sustained Ca^{2+} elevations might be beneficial for AP.

Chapter 8 Results: Effects of Ripk1^{K45A} in experimental AP models

8.1 Introduction

Studies have demonstrated that Ripk1^{K45A} modification protected against necroptosis in macrophages (Berger, Kasparcova et al. 2014), improved TNFα+zVAD induced lethal shock (Shutinoski, Alturki et al. 2016), concanavalin A-induced liver injury (Filliol, Piquet-Pellorce et al. 2016), and reduced tumor nodules in the lung by 38% (Hanggi, Vasilikos et al. 2017). In addition, results from Chapter 4 showed that Ripk1^{K45A} protected against TLCS- and POAEE-induced PAC necrosis indicating the potential value of RIPK1 as a target for AP treatment. However, the area is controversial and previous experiments in kinase modified mice strains Ripk1$^{KD/KD\ D138N}$ and Rip1$^{\Delta/\Delta}$ showed that there was no improvement in CER-AP (Newton, Dugger et al. 2016, Liu, Fan et al. 2017).

The different modifications of RIPK1 kinase activity may have different outcomes, an aspect that was discussed in Chapters 1, 4 and 5 which showed that toxins acted differently on PAC cell death pathways. The data indicated that RIPK1 kinase inhibition may contribute differently to different types of AP, and no study so far has evaluated RIPK1 kinase activity in the newer model of alcoholic pancreatitis, FAEE-AP.

The experiments in this chapter were designed to test whether RIPK1 kinase inhibition through Ripk1^{K45A} modification would affect the outcome of different experimental AP models.

8.2 Results

8.2.1 Effects of Ripk1^{K45A} in TLCS-AP

H&E staining showed that there was no difference in histological pancreatic appearances of Ripk1^{K45A} compared to Wt mice between sham in both strains, and there showed less necrosis in Ripk1^{K45A} AP groups (Figure 8.2.1.A). Histopathological scoring divided into oedema, inflammation, necrosis and the total score showed no significant differences between Ripk1^{K45A} and Wt sham or between Ripk1^{K45A} and Wt TLCS-AP except necrosis which showed improvement in Ripk1^{K45A} mice (Figure 8.2.1.B). Pancreatic MPO and IL-6 were decreased in Ripk1^{K45A} AP compared with Wt AP, however, no improvement was observed in other biochemical parameters (Figure 8.2.1 C).

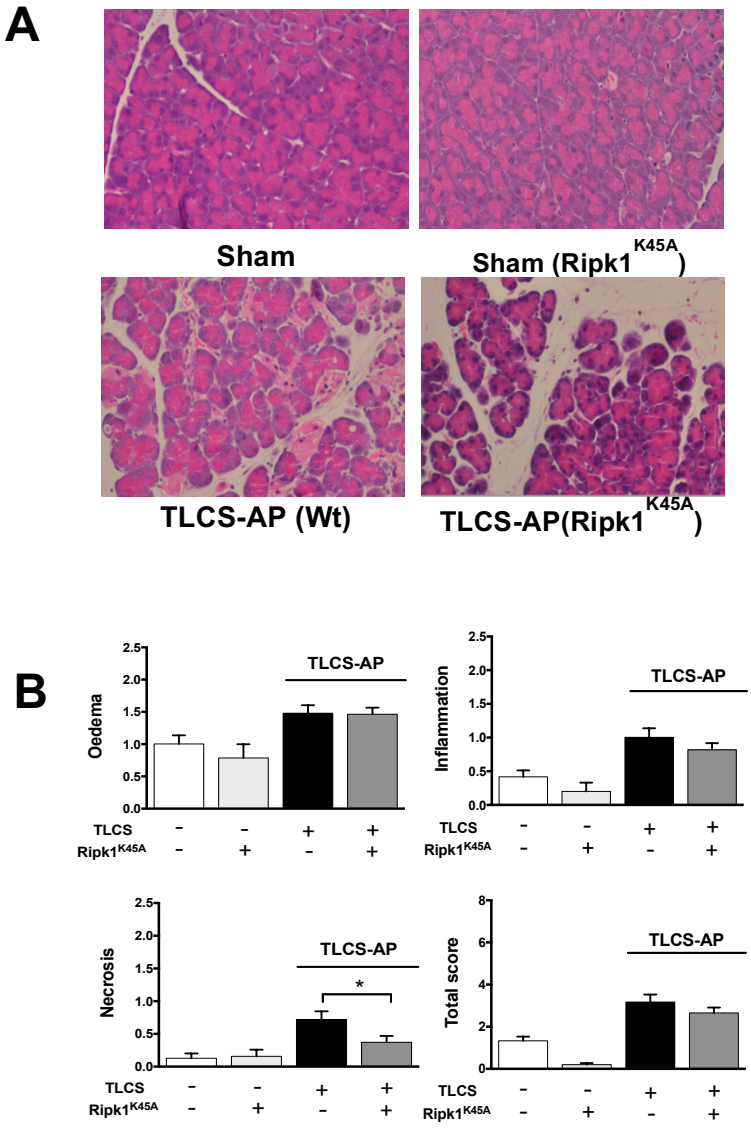

Figure 8.2.1.A) Representative histopathology images for Ripk1^{K45A} and Wt mice following the induction of TLCS-AP. H&E staining (x200). No differences in histopathological appearances were observed between sham Ripk1^{K45A} and Wt. TLCS-AP induced histopathological oedema, infiltration and necrosis in both Ripk1^{K45A} and Wt. Images are representative of at least 5 mice per group. **B) Histopathology scores for Ripk1^{K45A} and Wt mice following the induction of TLCS-AP.** Bar graphs show histopathology scores of oedema, inflammation, necrosis and total score in Ripk1^{K45A} and Wt mice. Significant differences between Ripk1^{K45A} AP and Wt AP were analysed (*$p<0.05$). All values are the means ± SEM from at least 5 mice per group.

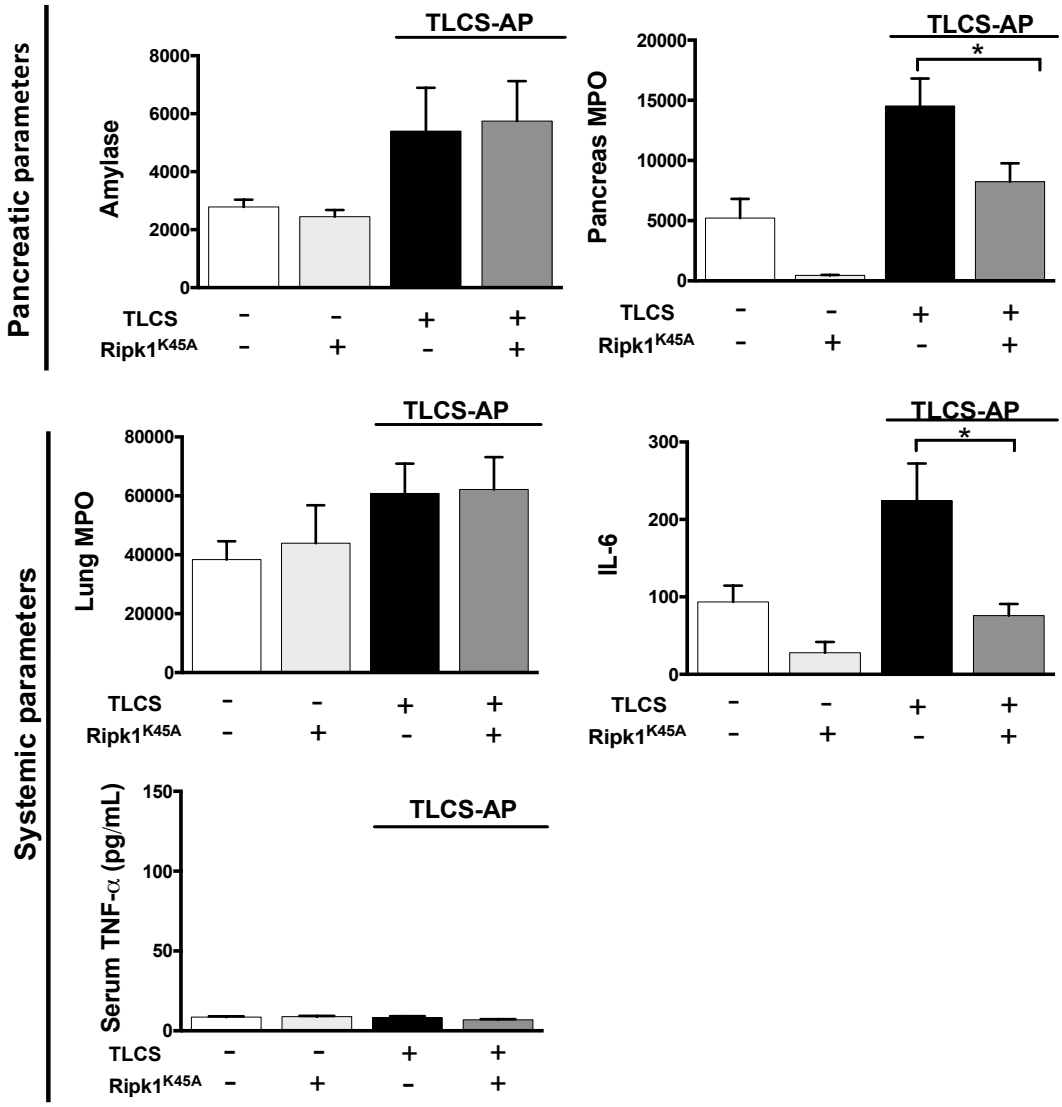

Figure 8.2.1.C Effects of Ripk1^{K45A} on pancreatic and systemic biochemical parameters following the induction of TLCS-AP. Bar graphs show pancreatic parameters of amylase, pancreas MPO and systemic parameters of lung MPO, serum IL-6 and TNFα in Ripk1^{K45A} and Wt. Significant differences between Ripk1^{K45A} AP and Wt AP were analysed (*p<0.05). All values are the means ± SEM from at least 5 mice per group.

8.2.2 Effects of Ripk1^{K45A} in FAEE-AP

H&E staining showed that there was no obvious difference in histological pancreatic appearances of Ripk1^{K45A} compared to Wt between sham and control AP (Figure 8.2.2.A). Pancreatic histopathological scores of oedema was improved in Ripk1^{K45A} mice, however, inflammation, necrosis and total score showed no differences between Ripk1^{K45A} and Wt FAEE-AP groups, (Figure 8.2.2.B). However, the value of amylase was halved, trypsin was decreased as same as control, and TNFα was decreased in Ripk1^{K45A} FAEE-AP compared to Wt FAEE-AP (Figure 8.2.2.C). However, pancreatic MPO, lung MPO and serum IL-6 showed no improvement.

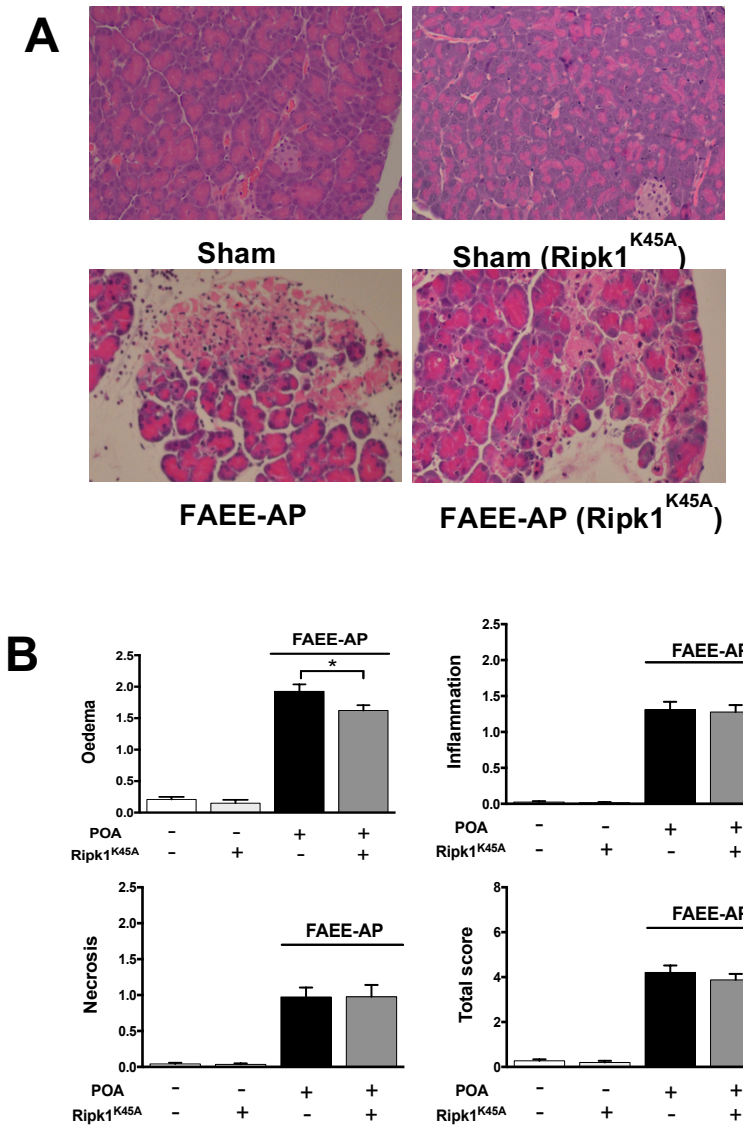

Figure 8.2.2.A) Representative histopathology images for Ripk1^{K45A} and Wt mice following the induction of FAEE-AP. H&E staining (x200). No differences in histopathological were observed between sham Ripk1^{K45A} mice and sham Wt. FAEE-AP induced oedema, inflammation and necrosis in both Ripk1^{K45A} and Wt. Images are representative of at least 5 mice per group. **B) Histopathology pancreatitis scores for Ripk1^{K45A} and Wt mice following the induction of FAEE-AP.** Bar graphs show pancreatitis histopathology score of oedema, inflammation, necrosis and total score in Ripk1^{K45A} and Wt. Significant differences between Ripk1^{K45A} AP and Wt AP were analysed (*$p<0.05$). All values are the means ± SEM of at least 5 mice per group

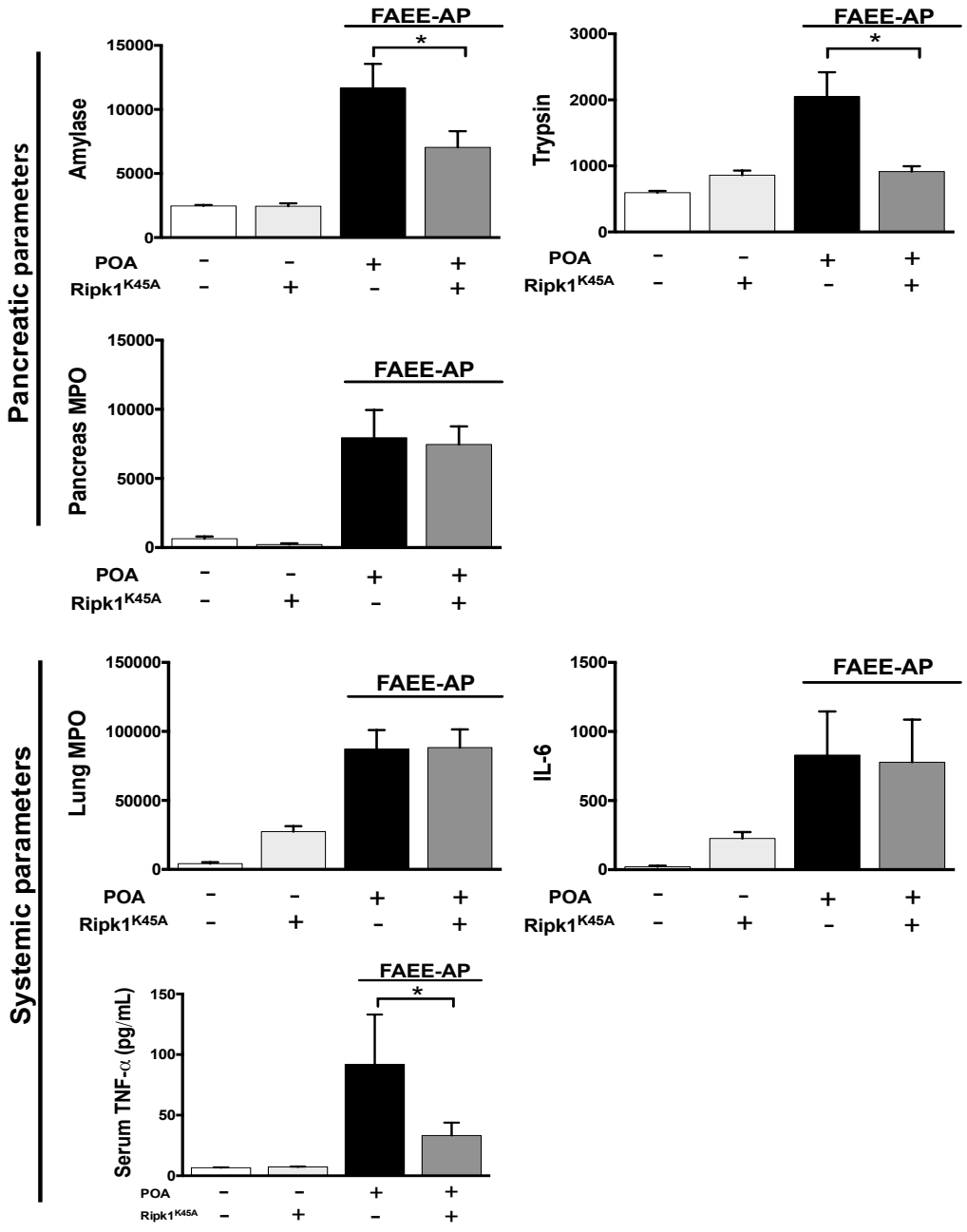

Figure 8.2.2.C Effects of Ripk1^{K45A} on pancreatic and systemic biochemical parameters following the induction of FAEE-AP. Bar graphs show the value of pancreatic parameters of serum amylase, trypsin, pancreas MPO, and systemic parameters of lung MPO, serum IL-6 and TNFα in Ripk1^{K45A} and Wt mice. Significant differences between Ripk1^{K45A} AP and Wt AP were analysed (*$p<0.05$). All values are the means ± SEM of at least 5 mice per group.

8.2.3 Effects of Ripk1^{K45A} in CER-AP

H&E staining showed that there was no difference in histological pancreatic appearances in Ripk1^{K45A} sham compared to Wt sham. Ripk1^{K45A} CER-AP displayed an improvement in pancreatic architecture compared to Wt CER-AP (Figure 8.2.3.A). CER-AP was improved when AP was performed in Ripk1^{K45A} evaluated by histopathological score divided into oedema, infiltration and necrosis (Figure 8.2.3.B). Pancreatic MPO was decreased in Ripk1^{K45A} which correlated with an improvement of local pancreatic injury. However, amylase, trypsin, lung MPO, and IL-6 showed no differences between Ripk1^{K45A} and Wt CER-AP (Figure 8.2.3.C).

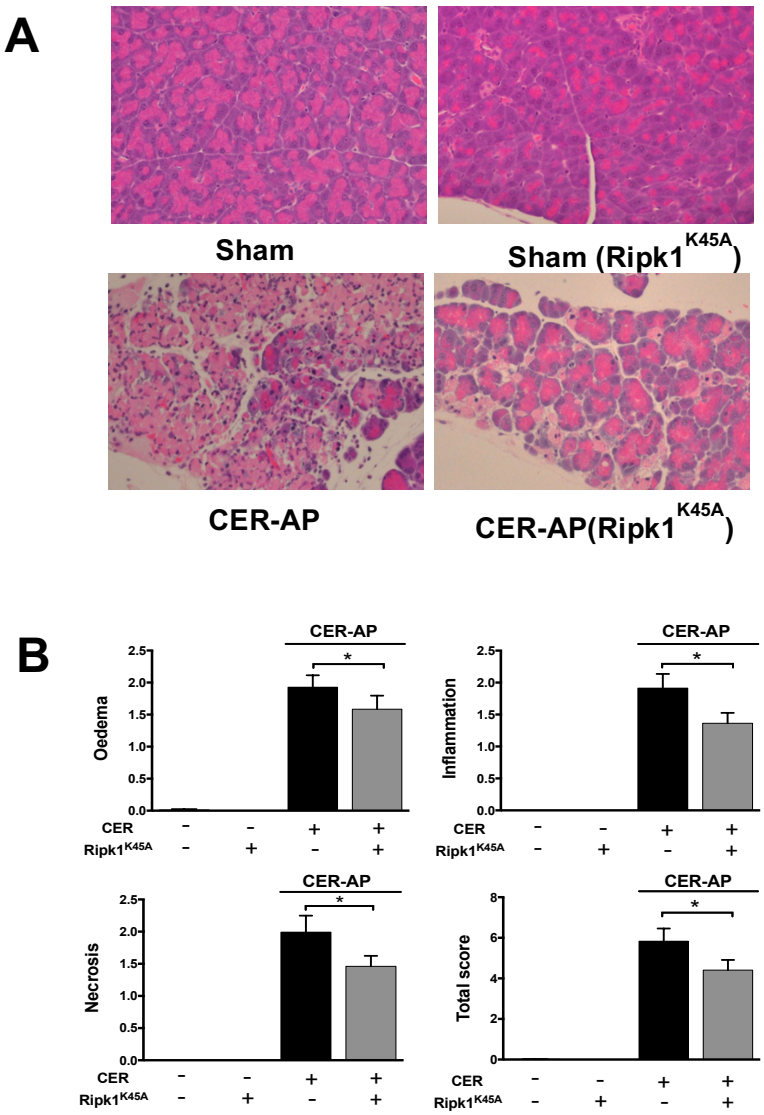

Figure 8.2.3.A) Representative histopathology images for Ripk1^{K45A} and Wt mice following the induction of CER-AP. H&E (x 200). No differences in histopathological appearances were observed between sham Ripk1^{K45A} and sham Wt mice. CER-AP induced oedema, infiltration and necrosis of AP on both strains, which were improved when the model was performed in Ripk1^{K45A} mice. Images are representative of at least 5 mice per group. B) **Histopathology pancreatitis scores for Ripk1^{K45A} and Wt mice following the induction of CER-AP.** Bar graphs show separated pancreatitis histopathology score of oedema, inflammation, necrosis and total score in Ripk1^{K45A} and Wt mice. Significant differences between Ripk1^{K45A} AP and Wt AP were analysed (*$p<0.05$). All values are the means ± SEM of at least 5 mice per group.

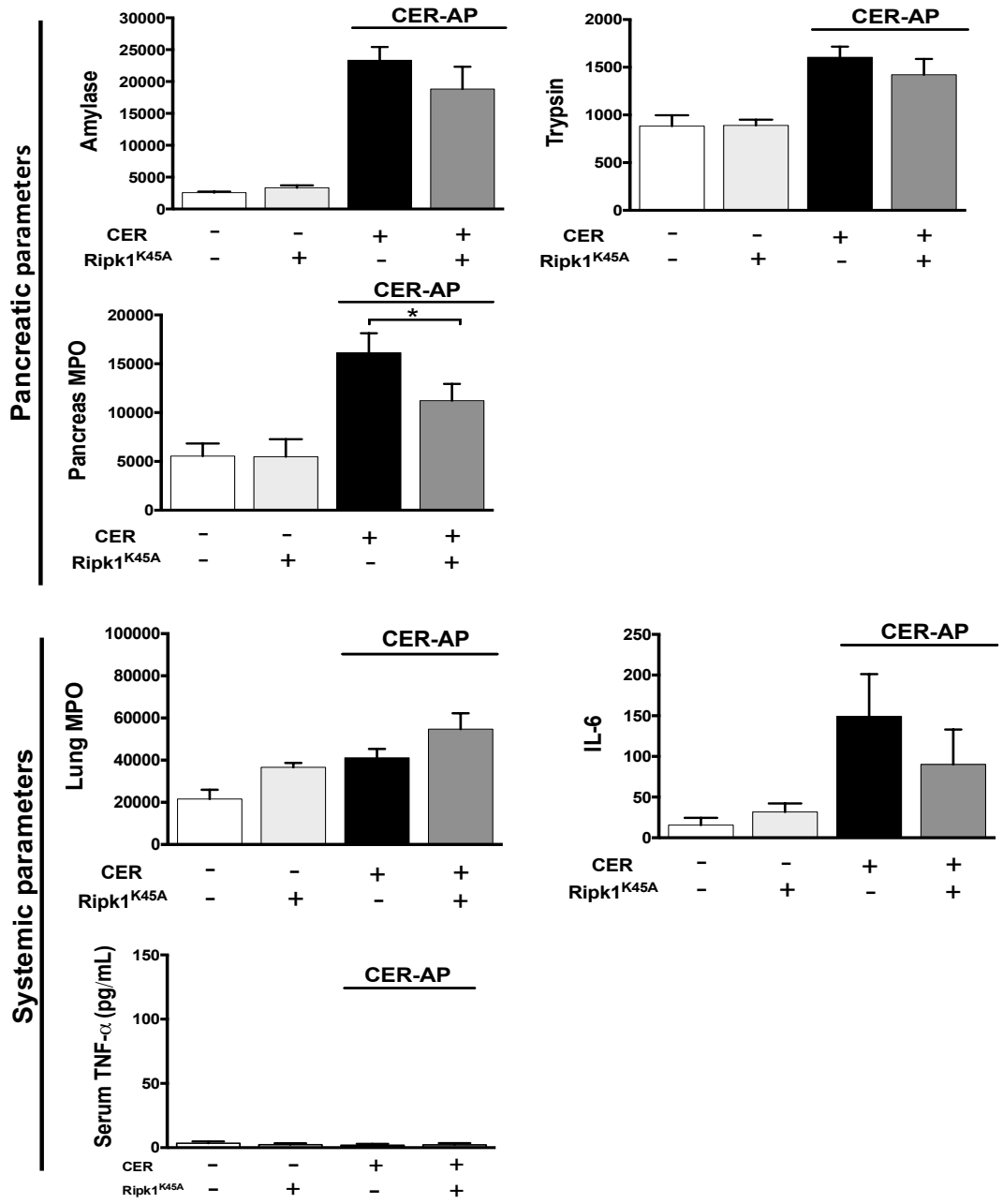

Figure 8.2.3.C Effects of Ripk1^{K45A} on pancreatic and systemic biochemical parameters following the induction CER-AP. Bar graphs show the value of pancreatic parameters of serum amylase, trypsin, pancreas MPO, and systemic parameters including lung MPO, serum IL-6 and TNFα in Ripk1^{K45A} and Wt mice. Significant differences between Ripk1^{K45A} AP and Wt AP were analysed (*$p<0.05$). All values are the means ± SEM of at least 5 mice per group.

8.3 Discussion

The work described in this chapter shows that Ripk1^{K45A} kinase activity modification only partially protected against TLCS-, FAEE- and CER-AP in certain parameters. Ripk1^{K45A} showed better pancreatic injury improvement in the CER-AP histopathology score and pancreatic MPO, and it showed better improvement on parameters in TLCS-AP (Pancreatic MPO, IL6) and FAEE-AP (amylase, trypsin, and TNFα). The different improvements in three models suggests that Ripk1^{K45A} kinase acted differently in these models. It also suggests that the pathogenesis mechanisms of these models are therefore different. Ripk1^{K45A} modification reduced RIPK1 dependent necroptosis under the stimulation of TLCS and POAEE in isolated PACs, and this action may contribute to the partial improvements observed in TLCS and FAEE-AP. Furthermore, Ripk1^{K45A} showed no effects on CCK-induced cell death but improved CER-AP suggesting that there may be additional protective mechanisms rather than RIPK1 dependent cell death in CER-AP. However, clearly the necrosis in histopathology scoring from 3 models did not correlate with *in vitro* cell death experiments described in Chapter 4.

In addition, unlike Ripk1$^{KD/KDD138N}$ and Rip1$^{\Delta/\Delta}$ kinase dead mice strains which showed no improvement on CER-AP (Newton, Dugger et al. 2016, Liu, Fan et al. 2017), Ripk1^{K45A} showed partial beneficial effects on CER-AP local injury. These three genotype mouse strains are all kinase activity knockouts but modified differently in the RIPK1 kinase domain (Kaiser, Daley-Bauer et al. 2014, Zhang, Su et al. 2017). Though studies showed that all three strains developed normally and resisted necroptotic stimuli *in vitro* and *in vivo*, the

comparisons made between Ripk1^{K45A} and Rip1$^{\Delta/\Delta}$ showed that Rip1$^{\Delta/\Delta}$ was a more effective kinase-dead mutation in blocking necroptosis signalling. Also, Ripk1^{K45A} showed no effect on Fadd$^{-/-}$ embryonic lethality but Rip1$^{\Delta/\Delta}$ improved the survival rate (Berger, Kasparcova et al. 2014, Newton, Dugger et al. 2014, Liu, Fan et al. 2017). These data suggest that the different results may cause by different mutations.

Collectively, it can be concluded that *in vitro* studies may lead to results that do not fully correspond to the circumstances occurring around a living organism. The partial effect of Ripk1^{K45A} modification on TLCS-, FAEE- and CER-AP showed that RIPK1 kinase activity through the K45A mutation plays a minimal role in AP, and therefore it is not sufficient to be considered a target for the treatment of AP.

Chapter 9 Results: Effects of Nec-1 in experimental AP models

9.1 Introduction

Nec-1 has been used extensively to investigate a wide range of pathological cell death events mediated through inhibition of RIPK1 kinase activity and has been to show improve multiple diseases including CER-AP, TLCS-AP (Louhimo, Steer et al. 2016) and L-arginine-induced AP (Zou, Xiong et al. 2016). The results from Chapters 5 and 6 demonstrated that Nec-1 protected against TLCS-, CCK- and POAEE-induced necrosis, reduced TLCS induced apoptosis, ROS production and CCK-induced Ca^{2+} elevation, suggesting its potential treatment value in AP. However, there is variability in publications with results showing that there was no improvement of Nec-1 in CER-AP (Linkermann, Brasen et al. 2012, Wu, Mulatibieke et al. 2017). Part of the variability may relate to the pharmacokinetic properties of Nec-1; for example, Nec-1 is a small molecule which has a short half-life, relatively low solubility, and delivery of Nec-1 by injection may affect its potency (Teng, Degterev et al. 2005).

Based on the *in vitro* findings of Nec-1 preserving PAC viability and controversy relating to *in vivo* studies, experiments in this chapter were designed using a novel mini pump approach for Nec-1 delivery to overcome the instability caused by injection. The effects of Nec-1 in different AP models were evaluated as a potential treatment (rather than as a pretreatment before AP induction), and compared with $Ripk1^{K45A}$ modification results.

9.2 Results

9.2.1 Effects of Nec-1 in TLCS-AP

H&E staining showed that Nec-1 administered via mini pump improved pancreatic architecture in experimental AP (Figure 9.2.1.A). Thus, Nec-1 treatment significantly improved oedema, inflammation, necrosis and total histopathology scoring back to control (Figure 9.2.1 B). Pancreatic parameters of amylase and pancreatic MPO were greatly improved after Nec-1 treatment. Systemic parameters such as lung MPO and IL-6 were significantly decreased to the same level of sham control by Nec-1 treatment compared with non-treated AP. The value of serum TNFα in TLCS-AP was too low in all groups for an appropriate comparison to be made (Figure 9.2.1 C).

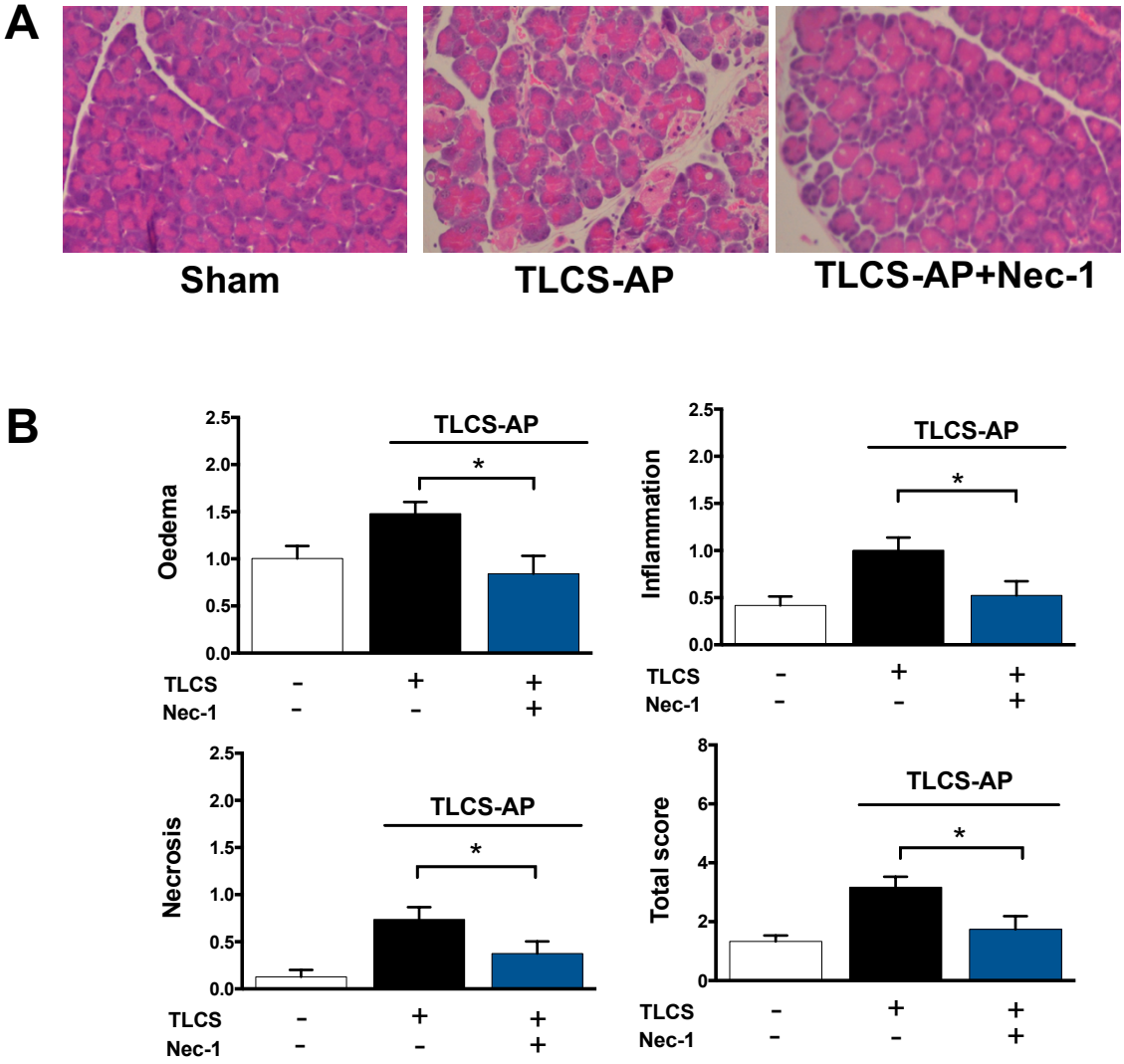

Figure 9.2.1.A) Representative histopathology images for Nec-1 treatment following the induction of TLCS-AP. H&E (x 200) of pancreatic sections. TLCS-AP induced histopathological oedema, neutrophil infiltration and necrosis of AP, which were improved after Nec-1 treatment. Images are representative of at least 5 mice per group. **B) Histopathology pancreatitis scores for Nec-1 treatment following the induction of TLCS-AP.** Bar graphs show separated pancreatitis histopathology scores of oedema, inflammation, necrosis and total score with or without Nec-1 treatment. Significant differences between Nec-1 treatment and non-treated AP were analysed (*$p<0.05$). All values are the means ± SEM from at least 5 mice per group.

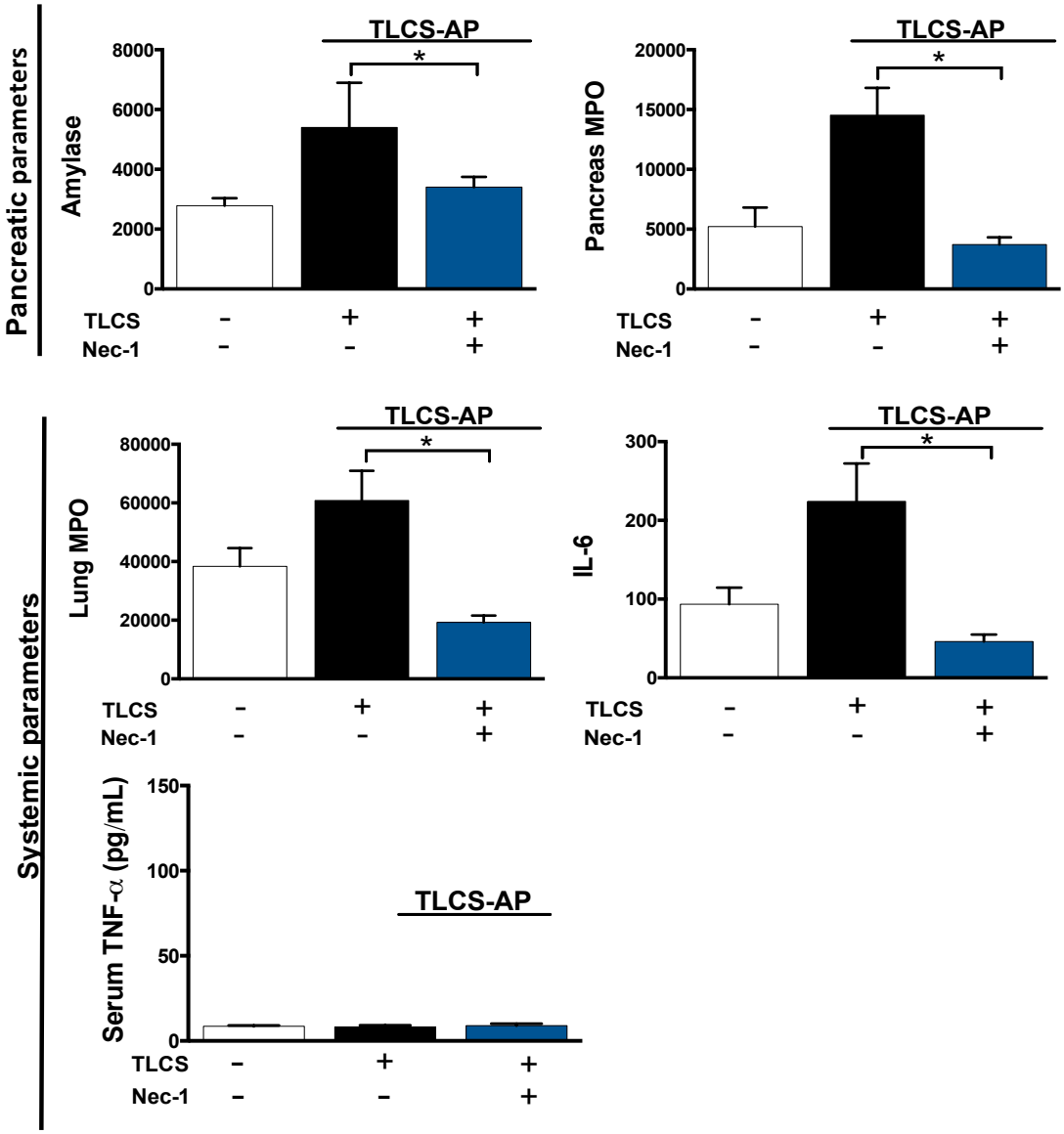

Figure 9.2.1.C Effects of Nec-1 on pancreatic and systemic biochemical parameters following the induction of TLCS-AP. Bar graphs show pancreatic parameters including amylase, pancreas MPO, and systemic parameters including lung MPO, serum IL-6 and TNFα with or without Nec-1 treatment. Significant differences between Nec-1 treatment and non-treated AP were analysed (*p<0.05). All values are the means ± SEM from at least 5 mice per group.

9.2.2 Effects of Nec-1 in FAEE-AP

H&E staining showed that Nec-1 administration via mini pump improved the pancreatic architecture in experimental AP (Figure 9.2.2.A). Thus, Nec-1 treatment significantly halved the value of oedema, inflammation, necrosis and total histopathology scoring compared with FAEE-AP group (Figure 9.2.2 B). Pancreatic parameters including amylase, trypsin and pancreas MPO were significantly improved after Nec-1 treatment. Systemic parameters such as lung MPO, IL-6 and TNFα were all significantly decreased by Nec-1 treatment compared with non-treated AP (Figure 9.2.2 C).

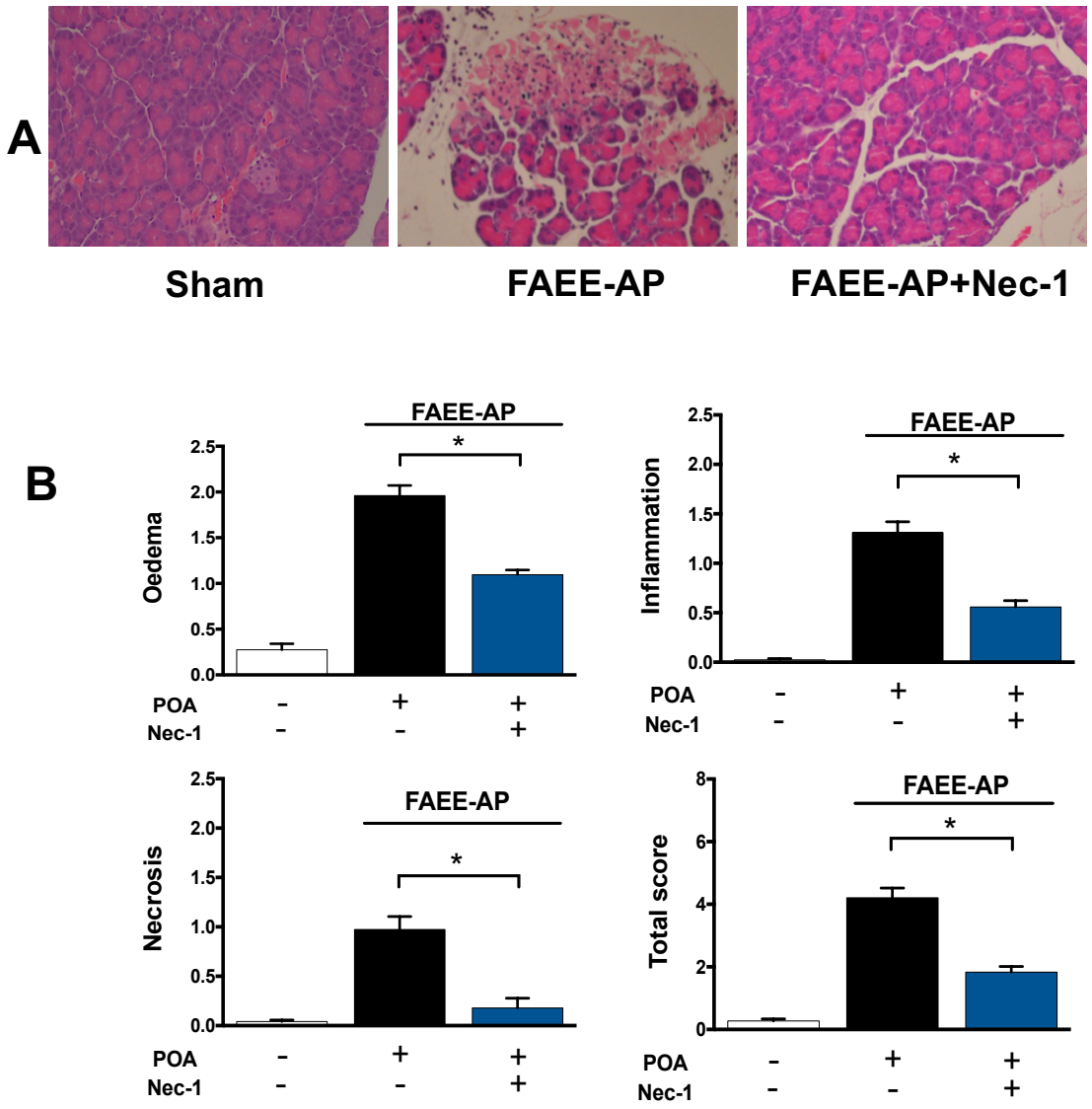

Figure 9.2.2. A) Representative histopathology images for Nec-1 treatment following the induction of FAEE-AP. H&E (x 200) of pancreatic sections. FAEE-AP induced histopathological oedema, neutrophil infiltration and necrosis of AP, which were improved after Nec-1 treatment. Images are representative of at least 5 mice per group. **B) Histopathology pancreatitis scores for Nec-1 treatment following the induction of FAEE-AP.** Bar graphs show separated pancreatitis histopathology scores of oedema, inflammation, necrosis and total score with or without Nec-1 treatment. Significant differences between Nec-1 treatment and non-treated AP were analysed (*$p<0.05$). All values are the means ± SEM from at least 5 mice per group.

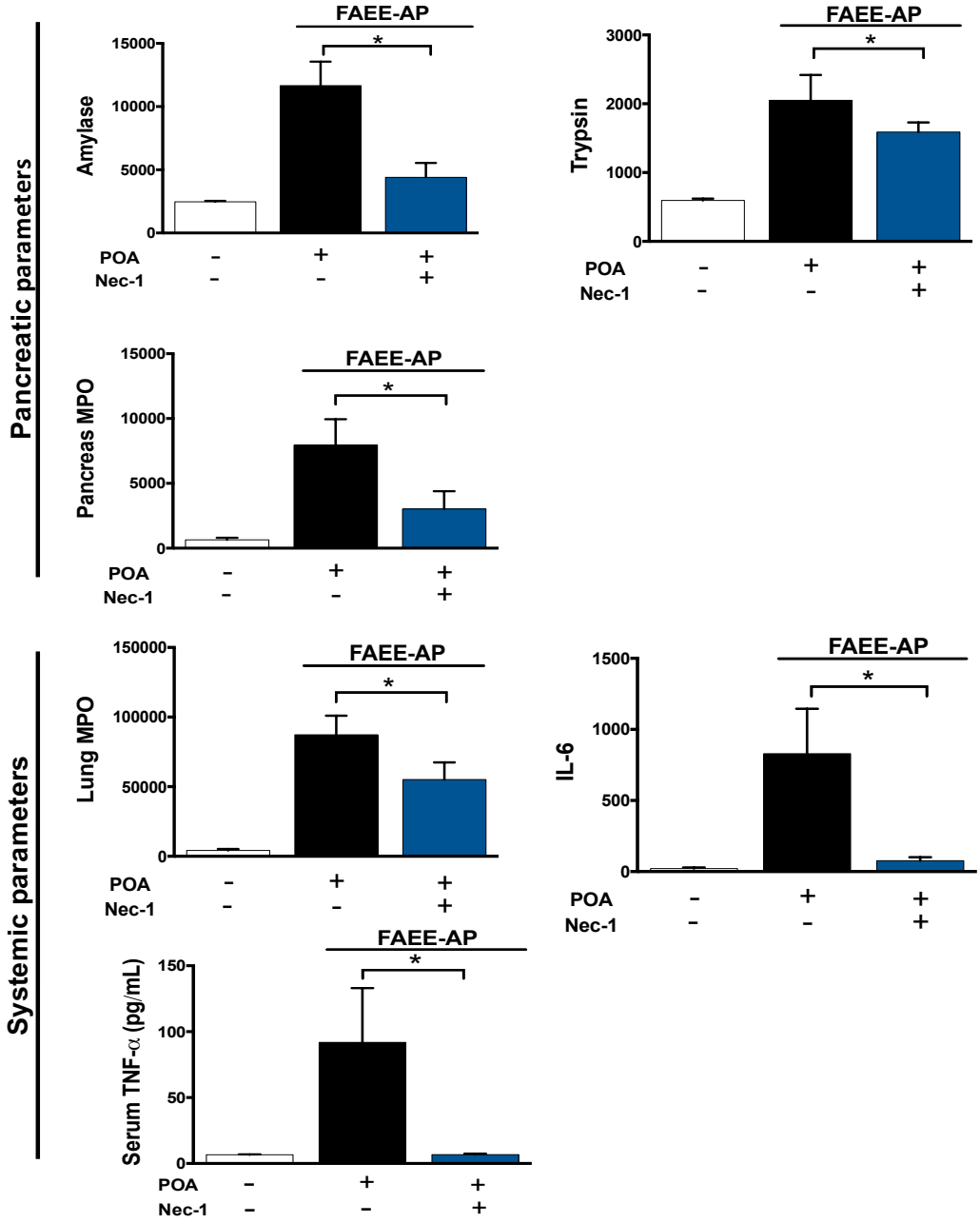

Figure 9.2.2.C Effects of Nec-1 on pancreatic and systemic biochemical parameters following the induction of FAEE-AP. Bar graphs show pancreatic parameters of amylase, trypsin, pancreas MPO and systemic parameters of lung MPO, serum IL-6 and TNFα with or without Nec-1 treatment. Significant differences between Nec-1 treatment and non-treated AP were analysed (*p<0.05). All values are the means ± SEM from at least 5 mice per group.

9.2.3 Effects of Nec-1 in CER-AP

H&E staining showed that Nec-1 administered via mini pump improved pancreatic architecture in experimental AP (Figure 9.2.3.A). Thus, Nec-1 treatment significantly improved oedema, inflammation, necrosis and total histopathology scoring (Figure 9.2.3 B). Pancreatic parameters including amylase, trypsin and pancreas MPO were significantly improved after Nec-1 treatment. Lung MPO was improved after Nec-1 treatment. However, IL-6 was not affected. The value of serum TNFα in CER-AP was too low in all groups for an appropriate comparison to be made (Figure 9.2.3 C).

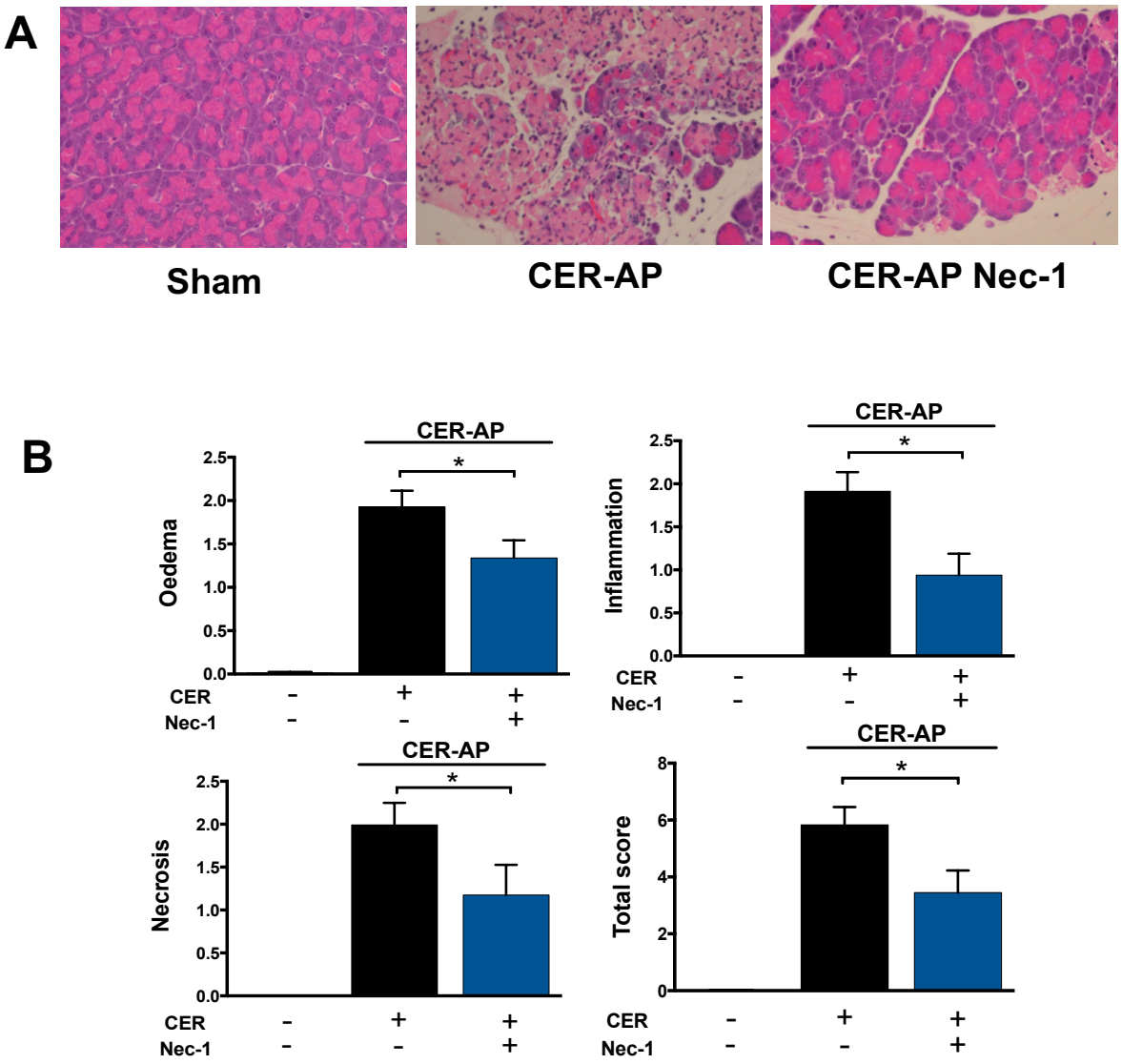

Figure 9.2.3.A) Representative histopathology images for Nec-1 treatment following the induction of CER-AP. H&E (x 200) of pancreatic sections. CER-AP induced histopathological oedema, neutrophil infiltration and necrosis of AP, which were improved after Nec-1 treatment. Images are representative of at least 5 mice per group. **B) Histopathology pancreatitis scores for Nec-1 treatment following the induction of CER-AP.** Bar graphs show separated pancreatitis histopathology scores of oedema, inflammation, necrosis and total score with or without Nec-1 treatment. Significant differences between Nec-1 treatment and non-treated AP were analysed (*$p<0.05$). All values are the means ± SEM from at least 5 mice per group.

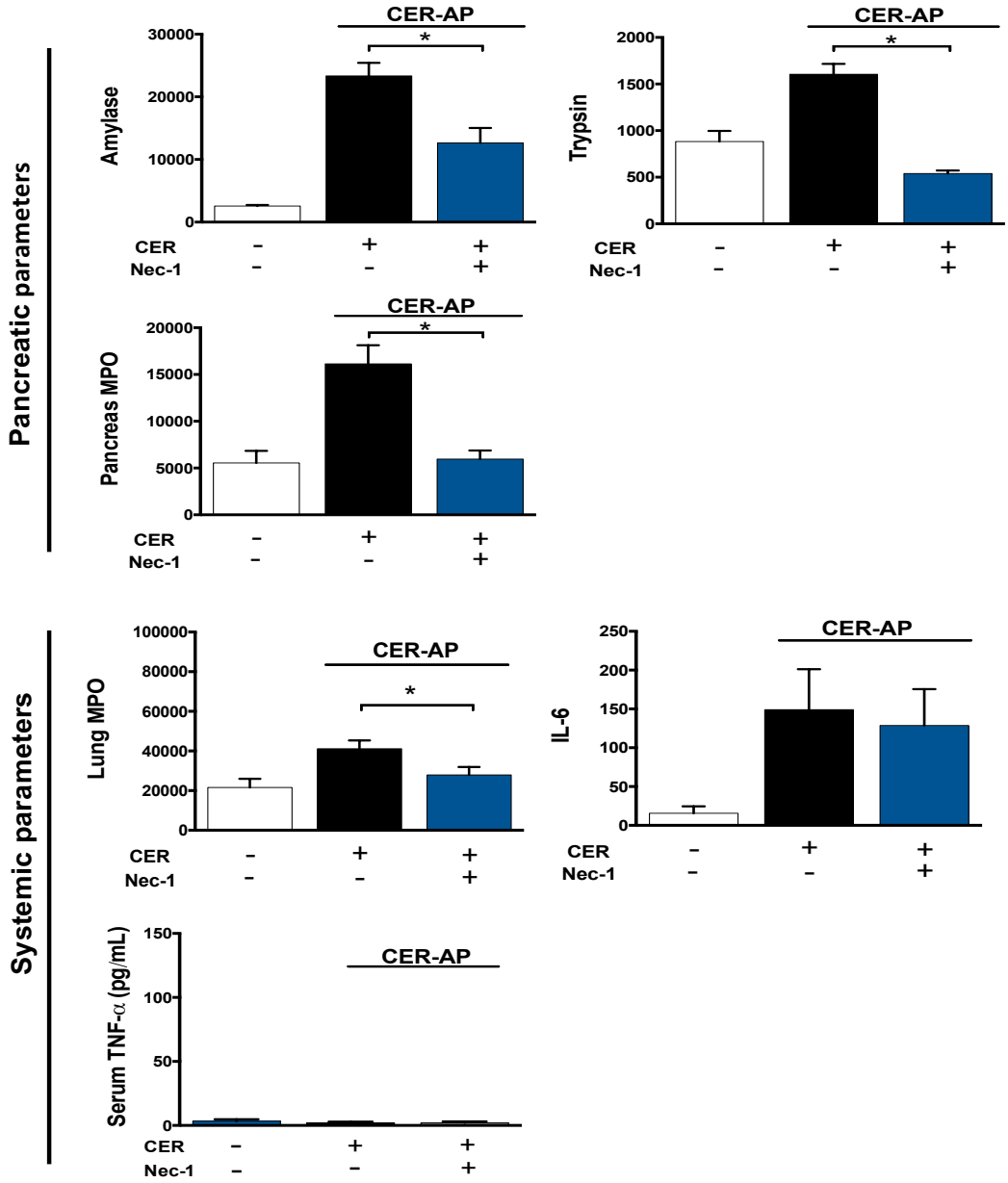

Figure 9.2.3.C Effects of Nec-1 on pancreatic and systemic biochemical parameters following the induction of CER-AP. Bar graphs show pancreatic parameters of amylase, trypsin, pancreas MPO and systemic parameters of lung MPO, serum IL-6 and TNFα with or without Nec-1. Significant differences between Nec-1 treatment and non-treated AP were analysed (*p<0.05). All values are the means ± SEM from at least 5 mice per group.

9.3 Discussion

The work in this chapter shows that mini pump administration of Nec-1 markedly improved local and systemic damage in all three experimental TLCS-, FAEE- and CER-AP models. Consistent findings were seen across all parameters, except in FAEE-AP lung MPO which only showed a trend towards significance. The improvement of Nec-1 on CER-AP and TLCS-AP correlated with the prior studies which demonstrated the protective effects of Nec-1 in experimental AP (Louhimo, Steer et al. 2016). However, our results are contrary to other studies which showed that Nec-1 did not improve CER-AP (Linkermann, Brasen et al. 2012, Wu, Mulatibieke et al. 2017).

The controversial results of Nec-1 on AP may due to (1) different toxins (2) short half-life (3) insufficient dose (4) treatment time. For toxins, our results from Chapter 4 and 5 showed that TLCS, POAEE, and CCK induced different PAC cell death profiles, suggesting that the effect of Nec-1 on different AP models might be different.

For the short half-life and insufficient dose, the half-life ($T_{1/2}$) of Nec-1 in the mouse microsomal assay is <5 min and delivery of Nec-1 by i.p. injections may therefore have reduced its potency and efficacy (Teng, Degterev et al. 2005). The use of the mini pump in our study ensured a constant and effective delivery of Nec-1. The dose of Nec-1 used may also have contributed to the outcome, since a 10-fold lower dose of Nec-1 has been shown to sensitise TNF-induced SIRS (Takahashi, Duprez et al. 2012). In accord, the studies which showed that Nec-1 improved AP used relatively higher doses. Furthermore, Nec-1 at 10 μM in our study showed a better reduction of TLCS-

induced cell death and CCK-induced Ca^{2+} elevation compared with a lower concentration. The dose used in this chapter is 56 mg/kg in total for 12/24 hours compared with the other AP experiments which were less than 6 mg/kg (See Chapter 1, Section 1.5 for further details), suggesting that the higher dose of Nec-1 is necessary for a better improvement of AP. However, higher doses of Nec-1 might be less effective since 30 μM Nec-1 were less effective than 10 μM in inhibiting cell death in isolated PACs. In addition, it is likely that a high dose of Nec-1 will promote interaction with other targets. However, a study has shown that high doses of Nec-1 inhibit T cell receptor activation in L929 cells independently of RIPK1 (Cho, McQuade et al. 2011), and the situation is likely to be complex. However, our data clearly showed that all parameters were reduced in all AP models.

With respect to the treatment time, some studies applied Nec-1 as a pre-treatment and the results were variable (Linkermann, Brasen et al. 2012) (Louhimo, Steer et al. 2016). Other studies used it as a treatment also results with different outcomes (Wu, Mulatibieke et al. 2017) (Zou, Xiong et al. 2016), suggesting that the pre-treatment or treatment of Nec-1 is not the pivotal determining factor, and may be less important than the dose applied in each study. However, the treatment time is crucial and may need to be early, for example in TLCS-AP, administration of Nec-1 2 and 4 hours after TLCS infusion completely halted the progression of PAC cell death but application of Nec-1 at 6 h failed to improve the extent of the cell death (Louhimo, Steer et al. 2016).

The magnitude of improvements from Nec-1 treatment were much greater compared to those obtained from the Ripk1^{K45A} mice in all three models, which correlated with superior reduction by Nec-1 of TLCS and CCK induced necrosis compared to Ripk1^{K45A}. Though similar reductions of POAEE induced necrosis in vitro were shown by Nec-1 and Ripk1^{K45A}, Nec-1 still demonstrated a better improvement in FAEE-AP. This may due to the multiple targets of Nec-1 including the IDO kynurenine pathway (Vandenabeele, Grootjans et al. 2013). However, whether such IDO inhibition by Nec-1/MTH-Trp contributes to the improvement of AP is unclear.

Collectively, all the problems mentioned above have made study design for Nec-1 a complicated area and there is a need to consider drug administration carefully (Takahashi, Duprez et al. 2012, Vandenabeele, Grootjans et al. 2013). The beneficial effects of Nec-1 at 56 mg/kg is likely not only to involve RIPK1 dependent cell death but also other targets. Therefore, the next experiments were designed to test whether the IDO kynurenine pathway was involved in experimental AP.

Chapter 10 Results: Effects of IDO inhibition in experimental AP

10.1 Introduction

In vivo experiments improved by Nec-1 have usually been interpreted as the involvement of necroptosis. However, Nec-1 is also called MTH-Trp which has been described as an inhibitor of IDO (Vandenabeele, Grootjans et al. 2013), which catabolizes tryptophan into kynurenine. Studies showed that both necroptosis and kynurenine pathways contribute to AP severity and play important roles in pathogenesis of AP (Abdel-Magid 2015) (see Chapter 1 for further details). The potential importance of the kynurenine pathway in AP was shown by inhibition of KMO which is the other important enzyme in the kynurenine pathway (Mole, Webster et al. 2016). However, the possible involvement of IDO in the beneficial effects of Nec-1 in AP was not been shown, and therefore the experiments described in this chapter were designed to assess whether inhibition of IDO through Epacadostat affects TLCS-AP and whether the effects were comparable with those of Nec-1.

10.2 Results

H&E staining showed that Epacadostat administered significantly improved pancreatic architecture in experimental AP (Figure 10.2.A). Histopathological scores showed that Epacadostat significantly improved oedema, inflammation and necrosis (Figure 10.2.B), reducing these parameters to control levels, and which correlated with decreased of pancreatic MPO. However, amylase, lung MPO and IL-6 did not show significant differences between treated and non-treated groups (Figure 10.2.C).

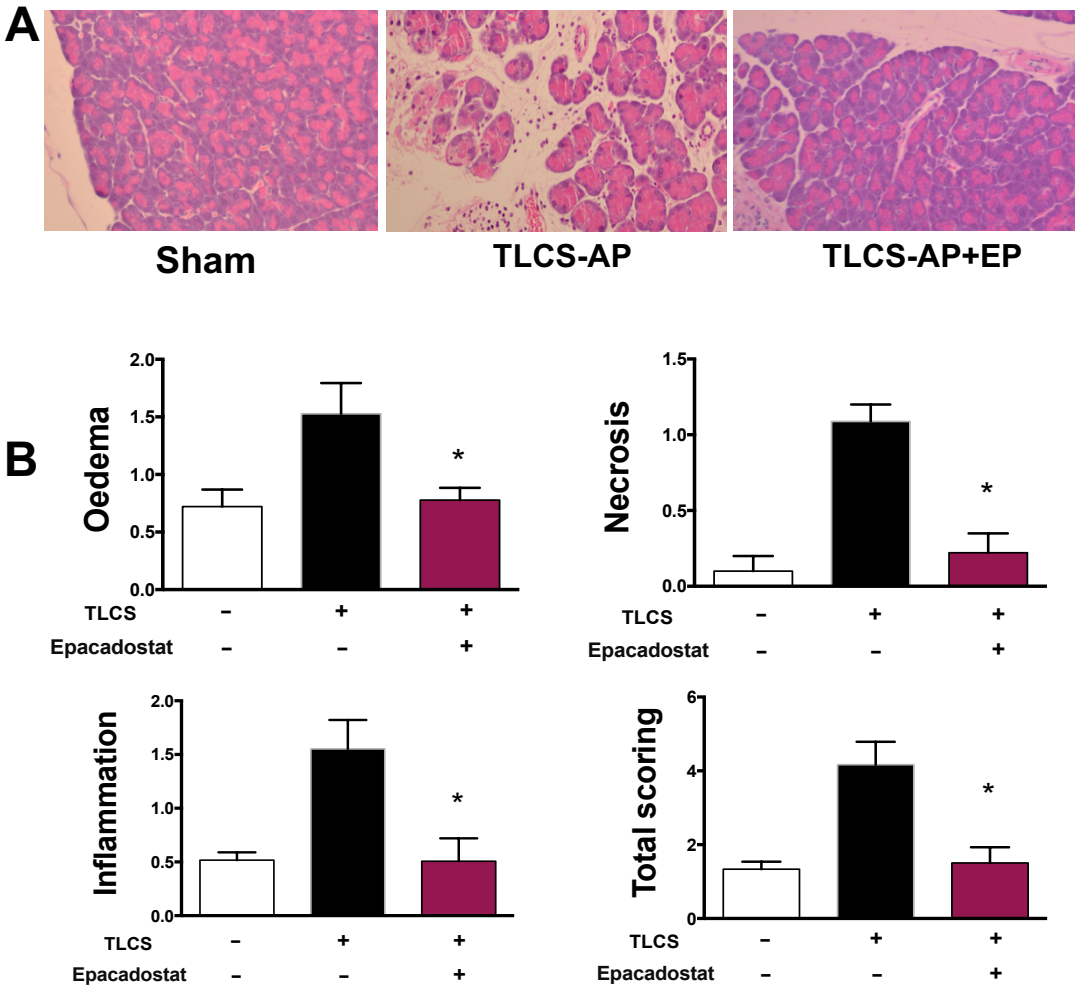

Figure 10.2. A) Representative histopathology images for Epacadostat treatment following the induction of TLCS-AP. H&E staining images (x200) of pancreatic sections. TLCS-AP induced histopathological oedema, neutrophil infiltration and necrosis of AP, which were improved after Epacadostat treatment. Images are representative of at least 5 mice per group. **B) Histopathology pancreatitis scores for Epacadostat treatment following the induction of TLCS-AP.** Bar graphs show separated pancreatitis histopathology scores of oedema, inflammation, necrosis and total score with or without Epacadostat treatment. Significant differences between Epacadostat treatment and non-treated AP were analysed (*$p<0.05$). All values are the means ± SEM from at least 5 mice per group.

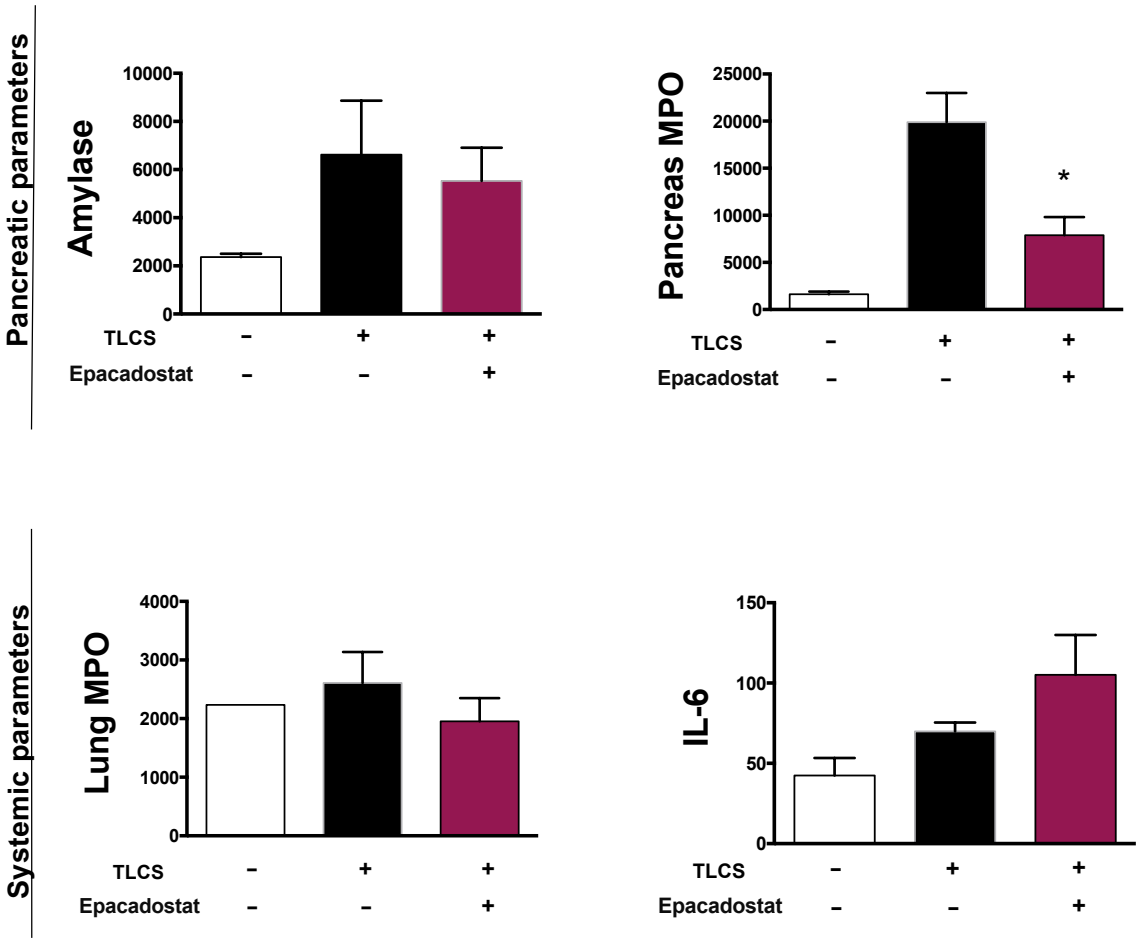

Figure 10.2.C Effects of Epacadostat on pancreatic and systemic biochemical parameters following the induction of TLCS-AP. Bar graphs show pancreatic parameters of amylase, pancreas MPO, and systemic parameters of lung MPO, serum IL-6 with or without Epacadostat. Significant differences between Epacadostat treatment and non-treated AP were analysed (*$p<0.05$). All values are the means ± SEM from at least 5 mice per group.

10.3 Discussion

The work in this chapter shows that Epacadostat significantly reduced the histopathology score and pancreatic MPO in TLCS-AP, suggesting that the IDO/kynurenine pathway contributed to the pathophysiology of TLCS-AP, and that the inhibition of IDO by Nec-1 may contribute to its beneficial effects in experimental AP.

However, it is apparent that Nec-1 exhibited better effects than Epacadostat in ameliorating TLCS-AP, suggesting that the improvements seen with Nec-1 may involve both RIPK1 dependent cell death and IDO inhibition and possibly other targets. As an IDO inhibitor, the specificity of Nec-1/MTH-Trp is unclear, and it may affect both IDO1 and IDO2. Although in murine species IDO1 showed much greater activity than IDO2 and mediates most of catalysis function in the first step of the kynurenine pathway, the possible effect on IDO2 may still contribute to Nec-1's actions especially on immune system. For example, $Ido1^{-/-}$ and $Ido2^{-/-}$ mice both showed a reduction in contact hypersensitivity. However, only loss of IDO2 was associated with a reduction in systemic levels of cytokines including IFN-γ, TNFα, and IL-6 (Jux, Kadow et al. 2009), which correlates with our results showing that Nec-1 had better beneficial effects than Epacadostat especially on the reduction of systemic inflammation in TLCS-AP.

It is worthy of note that The Expression Altas Database and the Human Protein Atlas database show that both mouse and human pancreas have a low expression of IDO1/2 in PACs (Uhlen, Oksvold et al. 2010), casting some doubt on whether inhibition of IDO might explain the improvement on

pancreatic local injury caused by Epacadostat. However, the expression of IDO1/2 in epithelial cells in general is high (Uhlen, Oksvold et al. 2010) and the effects of IDO inhibition in normal primary pancreatic duct cells is unknown. Studies in cancer research showed that IDO1 and IDO2 are overexpressed in pancreatic ductal adenocarcinomas (Witkiewicz, Williams et al. 2008, Witkiewicz, Costantino et al. 2009). Since the procedure of TLCS-AP involves cannulation of pancreatic duct, potential actions at ductal cells may contribute to the observed beneficial effects of Epacadostat and further investigation is warranted.

Collectively, IDO inhibition partially improved TLCS-AP likely through inhibition of the kynurenine pathway, and such an action may at least partially account for the improvement of Nec-1/MTH-Trp on TLCS-AP.

Chapter 11 Overview and conclusions

11.1 RIPK1-dependent PAC cell death induced by TLCS, POAEE and CCK

Severe AP is usually accompanied by a large amount of PAC necrosis (Kaiser, Saluja et al. 1995, Petrov, Shanbhag et al. 2010, Wang, Han et al. 2013). This PAC necrosis is largely uncontrolled and can be initiated by a variety of toxins, including bile salts, POAEE and CCK (Booth, Murphy et al. 2011, Huang, Booth et al. 2014, Wen, Voronina et al. 2015), which induce cytosolic Ca^{2+} overload, ROS generation, mitochondrial dysfunction and failure of ATP production (Kruger, Albrecht et al. 2000, Gerasimenko, Gerasimenko et al. 2002, Kim, Kim et al. 2002, Criddle, Murphy et al. 2006, Voronina, Barrow et al. 2010, Booth, Murphy et al. 2011). Because of its unregulated characteristics, direct manipulation of PAC necrosis to treat AP was unlikely until programmed necrosis was discovered. Necroptosis is precisely controlled through RIPK1, RIPK3 and MLKL, however, RIPK1 activation may not constitute an absolute requirement for necroptosis induction. For example, murine cytomegalovirus infection induced RIPK3-dependent but RIPK1-independent necroptosis (Upton, Kaiser et al. 2010), RIPK1 deficient hematopoietic cells still underwent RIPK3-mediated necroptosis (Roderick, Hermance et al. 2014), TNFα activated RIPK3 in the absence of RIPK1 induced cell death (Moujalled, Cook et al. 2013), and RIPK1/RIPK3 complex was not observed and RIPK3-dependent cell death play an important role in CCK-induced PAC necrosis (Wu, Mulatibieke et al. 2017).

Our data suggest that PACs can undergo RIPK1 dependent cell death, although this only partially contributes to necrotic cell death. TLCS at 500 μM

and POAEE at 100 μM could induce RIPK1 dependent necroptosis, whereas RIPK1 dependent necroptosis contributed less to CCK induced cell death.

11.2 RIPK1-dependent necroptosis as an AP treatment

Accumulating studies have shown that necroptosis contributes to various pathophysiological conditions, and RIPK1 inhibition is partially or completely crucial in necroptosis associated disease involving tissue damage, myocardial infarction, stroke, neurodegeneration and ischemia-reperfusion injury (McCully, Wakiyama et al. 2004, Zhang, Chen et al. 2005, Liu, Bao et al. 2015, Su, Yang et al. 2015). RIPK1 dependent necroptosis appears to contribute differently under various types of pathological stimulation. The mechanisms underlying the AP models used are likely to be different, which may also affect the outcome of RIPK1 kinase inhibition. The comparison of TLCS-, FAEE- and CER-AP showed that FAEE-AP caused more systemic inflammation, however, TLCS and CER induced comparatively more pancreatic local injury (Figure 11.2), suggesting that reducing inflammation as a therapeutic strategy may be more effective in the FAEE-AP model, and reducing local injury may be more effective in TLCS and CER-AP models.

Our data suggested that inhibition of RIPK1 kinase activity showed only partial beneficial effects on TLCS-, FAEE- and CER-AP, suggesting that RIPK1 kinase activity would not be an appropriate target for therapeutic intervention in TLCS, FAEE and CER-AP. In addition, the partial effects were different among three models, with $Ripk1^{K45A}$ presenting best improvement in FAEE-

AP, indicating a complex involvement of RIPK1 in cell death processes.

It is important to mention that this project focused on the RIPK1 kinase-dependent necroptosis in AP, however, the RIPK1-independent necroptosis may also contribute to the improvement of AP. For example, one study showed that the RIPK1/RIPK3 complex was not observed in CCK-induced PAC necrosis, and that the knockdown of RIPK1 enhanced RIPK3 expression, suggesting that RIPK3-dependent, but not RIPK1-dependent, necroptosis may contribute to pancreatic damage in experimental CER-AP. Meanwhile, this study also suggested that the protective effects of RIPK1 may have occurred through inhibition of RIPK3-mediated necroptosis in experimental pancreatitis (Wu, Mulatibieke et al. 2017). In addition, RIPK3 and MLKL studies have been more consistent and showed improvement in both CER- and TLCS-AP (He, Wang et al. 2009, Wu, Huang et al. 2013, Louhimo, Steer et al. 2016, Liu, Fan et al. 2017), however, a study also showed that RIPK3 deficiency did not protect against CER-AP (Newton, Dugger et al. 2016).

The discrepancy between the Nec-1 results and RIPK3-deficiency is confusing, and the underlying mechanism of RIPK1-independent cell death warrants further research.

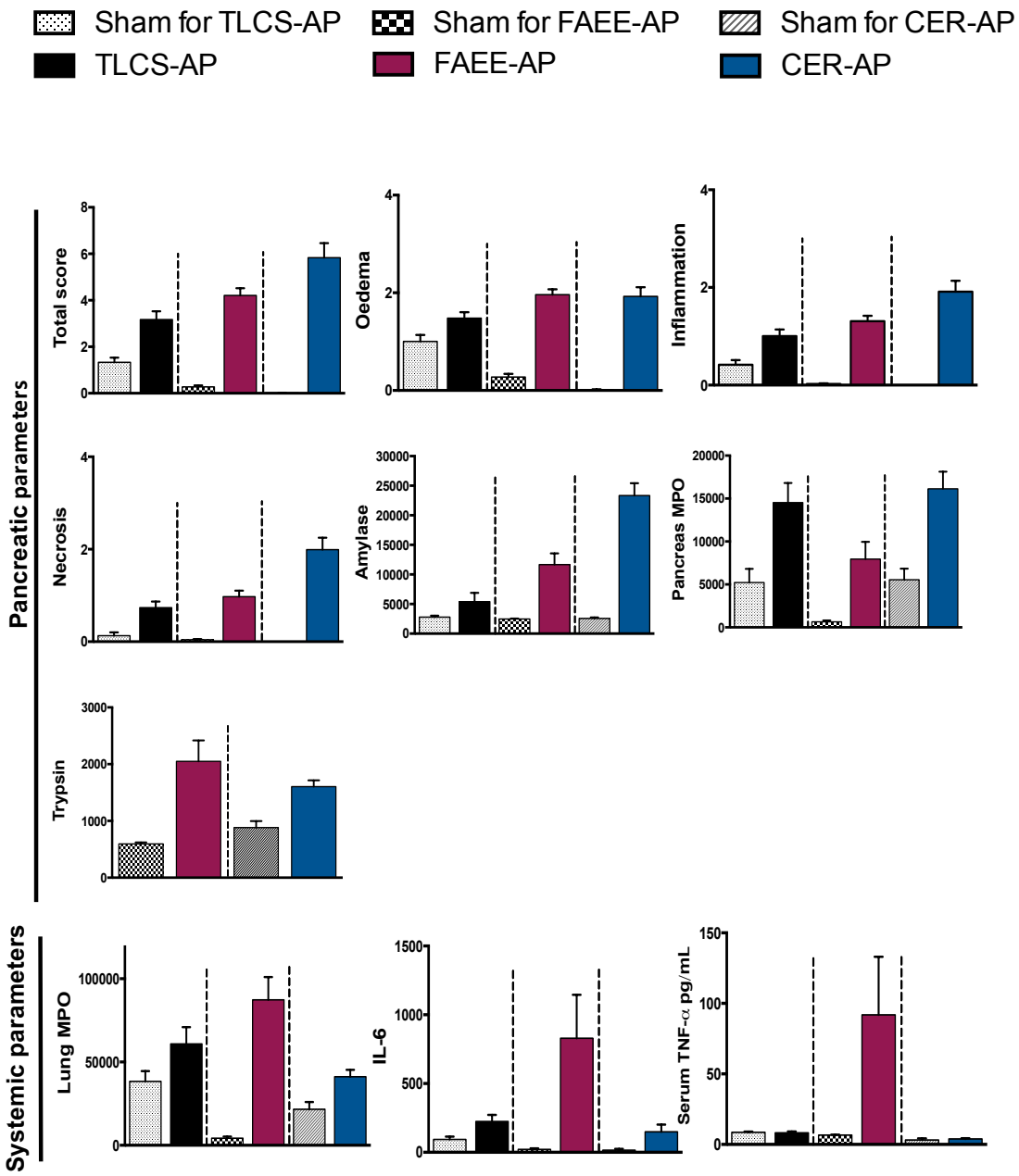

Figure 11.2 The pancreatitis parameters of TLCS, FAEE, and CER-AP. Bar graphs shows pancreatic parameters including oedema, inflammation, necrosis, total score, amylase, pancreas MPO, and trypsin, and systemic parameters including Lung MPO, IL-6 and TNFα in TLCS- (black), FAEE- (red) and CER- (blue) AP. All values are the means ± SEM from at least 5 mice per group.

11.3 Different mechanisms of Ripk1^{K45A} and Nec-1

Nec-1 was extensively used in evaluations of a wide range of diseases as a potential treatment drug, including ischemia-reperfusion injury (Degterev, Huang et al. 2005, Smith, Davidson et al. 2007, Xu, Chua et al. 2010, Northington, Chavez-Valdez et al. 2011, Linkermann, Brasen et al. 2012), neurodegenerative diseases (Li, Yang et al. 2008, Zhu, Zhang et al. 2011), inflammatory diseases (Zitvogel, Kepp et al. 2010, Duprez, Takahashi et al. 2011), hepatitis (Jouan-Lanhouet, Arshad et al. 2012), and lethal irradiation (Huang, Epperly et al. 2016). Although Nec-1 has multiple targets, the effect of Nec-1 is generally always explained in the literature as acting via the inhibition of RIPK1. However, clearly our results show that evaluation of RIPK1 kinase activity through Nec-1 cannot reflect the pure effect of RIPK1 kinase dependent cell death on the disease because of its multi-target effects. A few studies have emphasised that Nec-1 has multiple targets and have suggested that combination methods, including gene modification, and more specific inhibitors are required to evaluate the relevance of RIPK1 kinase activity in necroptosis investigations (Takahashi, Duprez et al. 2012, Vandenabeele, Grootjans et al. 2013).

In AP studies, Nec-1 has been tested on CER-, TLCS - and L-arginine AP. Some studies showed that Nec-1 improved CER-AP, TLCS-AP (Louhimo, Steer et al. 2016) and L-arginine-induced AP (Zou, Xiong et al. 2016). Others showed that Nec-1 did not improve CER-AP (Linkermann, Brasen et al. 2012) (Wu, Mulatibieke et al. 2017).

Our data using gene modification and more specific inhibitors suggest that the effects of Ripk1^{K45A} and Nec-1 are different. Under the stimulation of TLCS (500 μM), Ripk1^{K45A} reduced the RIPK1 dependent necroptosis but did not affect apoptosis. Nec-1 exerted with a similar action to Ripk1^{K45A} to reduce the RIPK1 dependent necroptosis, although its effects were more pronounced. In addition, Nec-1 reduced PAC apoptosis, an action linked to its ability to reduce ROS production, and which was independent of IDO inhibition. Under the stimulation of CCK (10 nM), Ripk1^{K45A} modification did not show any protective effects, and it actually increased the pathological CCK-induced Ca^{2+} elevation. However, in contrast Nec-1 showed protective effects which are likely to be through reduction of the RIPK1 dependent necroptosis and the inhibition of CCK-induced Ca^{2+} elevation. Under the stimulation of POAEE (100μM), both Ripk1^{K45A} and Nec-1 reduced the RIPK1 dependent necroptosis and effects on other pathways warrant further research.

11.4 Future work

Several avenues of research explored in this project could be developed further. Firstly, there was not sufficient time to test specific RIPK1 kinase inhibitors (e.g. Nec-1s) on CCK-induced cell death to confirm the effect of RIPK1 kinase activity. Secondly, the CCK and POAEE induced apoptosis and ROS production assays need to be optimized. Depending on the outcome, further studies on whether RIPK1 kinase activity affects CCK and POAEE induced apoptosis and ROS production could be carried out. Thirdly, the expression of RIPK3 and MLKL in pancreas from Nec-1 treated AP and Ripk1^{K45A} is worth testing, since the results may be different. Finally, the effect

of IDO in PACs is unclear. Therefore certain experiments can be performed; 1) Western blot or immunohistochemical experiments can be done to confirm the expression of IDO1/2 in PACs or pancreatic duct cells, 2) CER-AP or FAEE-AP evaluation of Epacadostat can be done for comparison and to eliminate possible effects due to any direct damage induced by ductal infusion in TLCS-AP, 3) whether IDO inhibition could affect cell death pathways in isolated PACs warrant further research, and 4) The possible effects of IDO2 can be addressed through a specific IDO2 inhibitor (Indoximod) in the future.

11.5 Concluding remarks

In this present study, the effects of RIPK1 kinase activity through Ripk1^{K45A} modification and pharmacological inhibitors were investigated on the pathogenesis of AP *in vitro* and *in vivo*. Briefly, we found that over 90% of POAEE (100 μM) and 50% of TLCS (500 μM) induced PAC necrosis was RIPK1 kinase dependent necroptosis, however, CCK (10 nM) induced PAC necrosis was RIPK1 kinase independent, proved by both Ripk1^{K45A} modification and specific RIPK1 kinase inhibitors (Nec-1s and GSK'963). RIPK1 kinase inhibitor Nec-1 showed additional effects other than inhibiting RIPK1 kinase activity on TLCS and CCK induced necrosis. This additional effect was also presented in the *in vivo* studies which showed that Nec-1 markedly improved local and systemic damage in TLCS-, FAEE- and CER-AP models; however, Ripk1^{K45A} just showed partial effects on three models. It is likely that IDO inhibition as the other target of Nec-1/MTH-Trp played a partial role in Nec-1's improvement of TLCS-AP.

We also demonstrated that Ripk1^{K45A} and Nec-1 acted differently on TLCS-

induced ROS production. Furthermore, the Ripk1^{K45A} modification did not affect physiological Ca^{2+} signals but potentiated pathological Ca^{2+} elevations via an undefined mechanism. Similarly, Nec-1/1s reduced CCK hyperstimulation induced sustained Ca^{2+} elevations, although the underlying mechanism is unclear.

These investigations have underlined the complexity of the field of RIPK1 and necroptosis, consistent with the great variability between published studies in the area of cell death in general and specifically in AP research. Clearly the RIPK1 is not appropriate as a potential therapeutic target for AP. However, Nec-1 exerted significant beneficial effects in multiple models of AP, through multiple pathways, suggesting that further elucidation of its protective effects might assist development of future therapies.

Chapter 12 Bibliography

(1985). "Memoir on the pancreas and on the role of pancreatic juice in digestive processes, particularly in the digestion of neutral fat. By Claude Bernard. 1856. Translated by John Henderson." Monogr Physiol Soc **42**: 1-131.
Abdel-Magid, A. F. (2015). "Kynurenine Monooxygenase (KMO) Inhibitors for the Treatment of Acute Pancreatitis and Neurodegenerative Disorders." ACS Med Chem Lett **6**(9): 954-955.
Acosta, J. M. and C. L. Ledesma (1974). "Gallstone migration as a cause of acute pancreatitis." N Engl J Med **290**(9): 484-487.
Ahmad, M., S. M. Srinivasula, L. Wang, R. V. Talanian, G. Litwack, T. Fernandes-Alnemri and E. S. Alnemri (1997). "CRADD, a novel human apoptotic adaptor molecule for caspase-2, and FasL/tumor necrosis factor receptor-interacting protein RIP." Cancer Res **57**(4): 615-619.
Aho, H. J., S. M. Koskensalo and T. J. Nevalainen (1980). "Experimental pancreatitis in the rat. Sodium taurocholate-induced acute haemorrhagic pancreatitis." Scand J Gastroenterol **15**(4): 411-416.
Aho, H. J., T. J. Nevalainen, V. T. Havia, R. J. Heinonen and A. J. Aho (1982). "Human acute pancreatitis: a light and electron microscopic study." Acta Pathol Microbiol Immunol Scand A **90**(5): 367-373.
Aho, H. J., T. J. Nevalainen, R. L. Lindberg and A. J. Aho (1980). "Experimental pancreatitis in the rat. The role of phospholipase A in sodium taurocholate-induced acute haemorrhagic pancreatitis." Scand J Gastroenterol **15**(8): 1027-1031.
Andrzejewska, A., J. W. Dlugosz and G. Jurkowska (1998). "The effect of antecedent acute ethanol ingestion on the pancreas ultrastructure in taurocholate pancreatitis in rats." Exp Mol Pathol **65**(2): 64-77.
Armstrong, J. A., N. Cash, P. M. Soares, M. H. Souza, R. Sutton and D. N. Criddle (2013). "Oxidative stress in acute pancreatitis: lost in translation?" Free Radic Res **47**(11): 917-933.
Ashby, M. C. and A. V. Tepikin (2001). "ER calcium and the functions of intracellular organelles." Semin Cell Dev Biol **12**(1): 11-17.
Baker, S. M., C. E. Bronner, L. Zhang, A. W. Plug, M. Robatzek, G. Warren, E. A. Elliott, J. Yu, T. Ashley, N. Arnheim, R. A. Flavell and R. M. Liskay (1995). "Male mice defective in the DNA mismatch repair gene PMS2 exhibit abnormal chromosome synapsis in meiosis." Cell **82**(2): 309-319.
Ball, H. J., A. Sanchez-Perez, S. Weiser, C. J. Austin, F. Astelbauer, J. Miu, J. A. McQuillan, R. Stocker, L. S. Jermiin and N. H. Hunt (2007). "Characterization of an indoleamine 2,3-dioxygenase-like protein found in humans and mice." Gene **396**(1): 203-213.
Barcia, R. N., N. S. Valle and J. D. McLeod (2003). "Caspase involvement in RIP-associated CD95-induced T cell apoptosis." Cell Immunol **226**(2): 78-85.
Basit, F., L. M. van Oppen, L. Schockel, H. M. Bossenbroek, S. E. van Emst-de Vries, J. C. Hermeling, S. Grefte, C. Kopitz, M. Heroult, P. Hgm Willems and W. J. Koopman (2017). "Mitochondrial complex I inhibition triggers a mitophagy-dependent ROS increase leading to necroptosis and ferroptosis in melanoma cells." Cell Death Dis **8**(3): e2716.
Baumgartner, H. K., J. V. Gerasimenko, C. Thorne, L. H. Ashurst, S. L. Barrow, M. A. Chvanov, S. Gillies, D. N. Criddle, A. V. Tepikin, O. H. Petersen, R. Sutton, A. J. Watson and O. V. Gerasimenko (2007). "Caspase-8-mediated apoptosis induced by oxidative stress is independent of the intrinsic pathway and dependent on cathepsins." Am J Physiol Gastrointest Liver Physiol **293**(1): G296-307.

Bawnik, J. B., R. Orda and T. Wiznitzer (1974). "Acute necrotizing pancreatitis. An experimental model." Am J Dig Dis **19**(12): 1143-1147.
Berger, S. B., P. Harris, R. Nagilla, V. Kasparcova, S. Hoffman, B. Swift, L. Dare, M. Schaeffer, C. Capriotti, M. Ouellette, B. W. King, D. Wisnoski, J. Cox, M. Reilly, R. W. Marquis, J. Bertin and P. J. Gough (2015). "Characterization of GSK'963: a structurally distinct, potent and selective inhibitor of RIP1 kinase." Cell Death Discov **1**: 15009.
Berger, S. B., V. Kasparcova, S. Hoffman, B. Swift, L. Dare, M. Schaeffer, C. Capriotti, M. Cook, J. Finger, A. Hughes-Earle, P. A. Harris, W. J. Kaiser, E. S. Mocarski, J. Bertin and P. J. Gough (2014). "Cutting Edge: RIP1 kinase activity is dispensable for normal development but is a key regulator of inflammation in SHARPIN-deficient mice." J Immunol **192**(12): 5476-5480.
Berridge, M. J., P. Lipp and M. D. Bootman (2000). "The versatility and universality of calcium signalling." Nat Rev Mol Cell Biol **1**(1): 11-21.
Bertrand, M. J., S. Milutinovic, K. M. Dickson, W. C. Ho, A. Boudreault, J. Durkin, J. W. Gillard, J. B. Jaquith, S. J. Morris and P. A. Barker (2008). "cIAP1 and cIAP2 facilitate cancer cell survival by functioning as E3 ligases that promote RIP1 ubiquitination." Mol Cell **30**(6): 689-700.
Bhatia, M. (2004). "Apoptosis of pancreatic acinar cells in acute pancreatitis: is it good or bad?" J Cell Mol Med **8**(3): 402-409.
Bhatia, M., M. A. Wallig, B. Hofbauer, H. S. Lee, J. L. Frossard, M. L. Steer and A. K. Saluja (1998). "Induction of apoptosis in pancreatic acinar cells reduces the severity of acute pancreatitis." Biochem Biophys Res Commun **246**(2): 476-483.
Bianchi, L., B. Gerstbrein, C. Frokjaer-Jensen, D. C. Royal, G. Mukherjee, M. A. Royal, J. Xue, W. R. Schafer and M. Driscoll (2004). "The neurotoxic MEC-4(d) DEG/ENaC sodium channel conducts calcium: implications for necrosis initiation." Nat Neurosci **7**(12): 1337-1344.
Biczo, G., P. Hegyi, S. Dosa, N. Shalbuyeva, S. Berczi, R. Sinervirta, Z. Hracsko, A. Siska, Z. Kukor, K. Jarmay, V. Venglovecz, I. S. Varga, B. Ivanyi, L. Alhonen, T. Wittmann, A. Gukovskaya, T. Takacs and Z. Rakonczay, Jr. (2011). "The crucial role of early mitochondrial injury in L-lysine-induced acute pancreatitis." Antioxid Redox Signal **15**(10): 2669-2681.
Biton, S. and A. Ashkenazi (2011). "NEMO and RIP1 control cell fate in response to extensive DNA damage via TNF-alpha feedforward signaling." Cell **145**(1): 92-103.
Booth, D. M., J. A. Murphy, R. Mukherjee, M. Awais, J. P. Neoptolemos, O. V. Gerasimenko, A. V. Tepikin, O. H. Petersen, R. Sutton and D. N. Criddle (2011). "Reactive oxygen species induced by bile acid induce apoptosis and protect against necrosis in pancreatic acinar cells." Gastroenterology **140**(7): 2116-2125.
Brackett, K. A., A. Crocket and S. N. Joffe (1983). "Ultrastructure of early development of acute pancreatitis in the rat." Dig Dis Sci **28**(1): 74-84.
Bruce, J. I. E. (2017). "Metabolic regulation of the PMCA: Role in cell death and survival." Cell Calcium.
Bugiantella, W., F. Rondelli, M. Boni, P. Stella, A. Polistena, A. Sanguinetti and N. Avenia (2016). "Necrotizing pancreatitis: A review of the interventions." Int J Surg **28 Suppl 1**: S163-171.
Cai, Z., S. Jitkaew, J. Zhao, H. C. Chiang, S. Choksi, J. Liu, Y. Ward, L. G. Wu and Z. G. Liu (2014). "Plasma membrane translocation of trimerized MLKL protein is required for TNF-induced necroptosis." Nat Cell Biol **16**(1): 55-65.
Campbell, B. M., E. Charych, A. W. Lee and T. Moller (2014). "Kynurenines in CNS disease: regulation by inflammatory cytokines." Front Neurosci **8**: 12.

Cancela, J. M., O. V. Gerasimenko, J. V. Gerasimenko, A. V. Tepikin and O. H. Petersen (2000). "Two different but converging messenger pathways to intracellular Ca(2+) release: the roles of nicotinic acid adenine dinucleotide phosphate, cyclic ADP-ribose and inositol trisphosphate." EMBO J **19**(11): 2549-2557.
Cancela, J. M., F. Van Coppenolle, A. Galione, A. V. Tepikin and O. H. Petersen (2002). "Transformation of local Ca2+ spikes to global Ca2+ transients: the combinatorial roles of multiple Ca2+ releasing messengers." EMBO J **21**(5): 909-919.
Chan, F. K., J. Shisler, J. G. Bixby, M. Felices, L. Zheng, M. Appel, J. Orenstein, B. Moss and M. J. Lenardo (2003). "A role for tumor necrosis factor receptor-2 and receptor-interacting protein in programmed necrosis and antiviral responses." J Biol Chem **278**(51): 51613-51621.
Chen, W. W., H. Yu, H. B. Fan, C. C. Zhang, M. Zhang, C. Zhang, Y. Cheng, J. Kong, C. F. Liu, D. Geng and X. Xu (2012). "RIP1 mediates the protection of geldanamycin on neuronal injury induced by oxygen-glucose deprivation combined with zVAD in primary cortical neurons." J Neurochem **120**(1): 70-77.
Chetty, U., H. M. Gilmour and T. V. Taylor (1980). "Experimental acute pancreatitis in the rat--a new model." Gut **21**(2): 115-117.
Chiu, L. Y., F. M. Ho, S. G. Shiah, Y. Chang and W. W. Lin (2011). "Oxidative stress initiates DNA damager MNNG-induced poly(ADP-ribose)polymerase-1-dependent parthanatos cell death." Biochem Pharmacol **81**(3): 459-470.
Cho, Y., T. McQuade, H. Zhang, J. Zhang and F. K. Chan (2011). "RIP1-dependent and independent effects of necrostatin-1 in necrosis and T cell activation." PLoS One **6**(8): e23209.
Cho, Y. S., S. Challa, D. Moquin, R. Genga, T. D. Ray, M. Guildford and F. K. Chan (2009). "Phosphorylation-driven assembly of the RIP1-RIP3 complex regulates programmed necrosis and virus-induced inflammation." Cell **137**(6): 1112-1123.
Choi, S., H. Keys, R. J. Staples, J. Yuan, A. Degterev and G. D. Cuny (2012). "Optimization of tricyclic Nec-3 necroptosis inhibitors for in vitro liver microsomal stability." Bioorg Med Chem Lett **22**(17): 5685-5688.
Christofferson, D. E., Y. Li, J. Hitomi, W. Zhou, C. Upperman, H. Zhu, S. A. Gerber, S. Gygi and J. Yuan (2012). "A novel role for RIP1 kinase in mediating TNFalpha production." Cell Death Dis **3**: e320.
Chvanov, M., W. Huang, T. Jin, L. Wen, J. Armstrong, V. Elliot, B. Alston, A. Burdyga, D. N. Criddle, R. Sutton and A. V. Tepikin (2015). "Novel lipophilic probe for detecting near-membrane reactive oxygen species responses and its application for studies of pancreatic acinar cells: effects of pyocyanin and L-ornithine." Antioxid Redox Signal **22**(6): 451-464.
Committee, A. S. o. P., M. A. Anderson, L. Fisher, R. Jain, J. A. Evans, V. Appalaneni, T. Ben-Menachem, B. D. Cash, G. A. Decker, D. S. Early, R. D. Fanelli, D. A. Fisher, N. Fukami, J. H. Hwang, S. O. Ikenberry, T. L. Jue, K. M. Khan, M. L. Krinsky, P. M. Malpas, J. T. Maple, R. N. Sharaf, A. K. Shergill and J. A. Dominitz (2012). "Complications of ERCP." Gastrointest Endosc **75**(3): 467-473.
Criddle, D. N. (2016). "Reactive oxygen species, Ca(2+) stores and acute pancreatitis; a step closer to therapy?" Cell Calcium **60**(3): 180-189.
Criddle, D. N., J. V. Gerasimenko, H. K. Baumgartner, M. Jaffar, S. Voronina, R. Sutton, O. H. Petersen and O. V. Gerasimenko (2007). "Calcium signalling and pancreatic cell death: apoptosis or necrosis?" Cell Death Differ **14**(7): 1285-1294.
Criddle, D. N., S. Gillies, H. K. Baumgartner-Wilson, M. Jaffar, E. C. Chinje, S. Passmore, M. Chvanov, S. Barrow, O. V. Gerasimenko, A. V. Tepikin, R. Sutton and O. H. Petersen (2006). "Menadione-induced reactive oxygen species generation via

redox cycling promotes apoptosis of murine pancreatic acinar cells." J Biol Chem **281**(52): 40485-40492.
Criddle, D. N., J. Murphy, G. Fistetto, S. Barrow, A. V. Tepikin, J. P. Neoptolemos, R. Sutton and O. H. Petersen (2006). "Fatty acid ethyl esters cause pancreatic calcium toxicity via inositol trisphosphate receptors and loss of ATP synthesis." Gastroenterology **130**(3): 781-793.
Criddle, D. N., M. G. Raraty, J. P. Neoptolemos, A. V. Tepikin, O. H. Petersen and R. Sutton (2004). "Ethanol toxicity in pancreatic acinar cells: mediation by nonoxidative fatty acid metabolites." Proc Natl Acad Sci U S A **101**(29): 10738-10743.
Criddle, D. N., R. Sutton and O. H. Petersen (2006). "Role of Ca2+ in pancreatic cell death induced by alcohol metabolites." J Gastroenterol Hepatol **21 Suppl 3**: S14-17.
Cristofanon, S., B. A. Abhari, M. Krueger, A. Tchoghandjian, S. Momma, C. Calaminus, D. Vucic, B. J. Pichler and S. Fulda (2015). "Identification of RIP1 as a critical mediator of Smac mimetic-mediated sensitization of glioblastoma cells for Drozitumab-induced apoptosis." Cell Death Dis **6**: e1724.
Croall, D. E. and K. Ersfeld (2007). "The calpains: modular designs and functional diversity." Genome Biol **8**(6): 218.
Cui, H., Y. Zhu and D. Jiang (2016). "The RIP1-RIP3 Complex Mediates Osteocyte Necroptosis after Ovariectomy in Rats." PLoS One **11**(3): e0150805.
Cullen, S. P., C. M. Henry, C. J. Kearney, S. E. Logue, M. Feoktistova, G. A. Tynan, E. C. Lavelle, M. Leverkus and S. J. Martin (2013). "Fas/CD95-induced chemokines can serve as "find-me" signals for apoptotic cells." Mol Cell **49**(6): 1034-1048.
Dannappel, M., K. Vlantis, S. Kumari, A. Polykratis, C. Kim, L. Wachsmuth, C. Eftychi, J. Lin, T. Corona, N. Hermance, M. Zelic, P. Kirsch, M. Basic, A. Bleich, M. Kelliher and M. Pasparakis (2014). "RIPK1 maintains epithelial homeostasis by inhibiting apoptosis and necroptosis." Nature **513**(7516): 90-94.
Dasgupta, M., M. K. Agarwal, P. Varley, T. Lu, G. R. Stark and E. S. Kandel (2008). "Transposon-based mutagenesis identifies short RIP1 as an activator of NFkappaB." Cell Cycle **7**(14): 2249-2256.
Davidson, S. M. (2010). "Endothelial mitochondria and heart disease." Cardiovasc Res **88**(1): 58-66.
Dawra, R., Y. S. Ku, R. Sharif, D. Dhaulakhandi, P. Phillips, V. Dudeja and A. K. Saluja (2008). "An improved method for extracting myeloperoxidase and determining its activity in the pancreas and lungs during pancreatitis." Pancreas **37**(1): 62-68.
Dazai, Y., I. Katoh, Y. Hara, R. Yoshida and K. Kurihara (1991). "Two cases of adult T-cell leukemia associated with acute pancreatitis due to hypercalcemia." Am J Med **90**(2): 251-254.
Degterev, A., J. Hitomi, M. Germscheid, I. L. Ch'en, O. Korkina, X. Teng, D. Abbott, G. D. Cuny, C. Yuan, G. Wagner, S. M. Hedrick, S. A. Gerber, A. Lugovskoy and J. Yuan (2008). "Identification of RIP1 kinase as a specific cellular target of necrostatins." Nat Chem Biol **4**(5): 313-321.
Degterev, A., Z. Huang, M. Boyce, Y. Li, P. Jagtap, N. Mizushima, G. D. Cuny, T. J. Mitchison, M. A. Moskowitz and J. Yuan (2005). "Chemical inhibitor of nonapoptotic cell death with therapeutic potential for ischemic brain injury." Nat Chem Biol **1**(2): 112-119.
Degterev, A. and A. Linkermann (2016). "Generation of small molecules to interfere with regulated necrosis." Cell Mol Life Sci **73**(11-12): 2251-2267.
Degterev, A., J. L. Maki and J. Yuan (2013). "Activity and specificity of necrostatin-1, small-molecule inhibitor of RIP1 kinase." Cell Death Differ **20**(2): 366.

Dellinger, E. P., C. E. Forsmark, P. Layer, P. Levy, E. Maravi-Poma, M. S. Petrov, T. Shimosegawa, A. K. Siriwardena, G. Uomo, D. C. Whitcomb, J. A. Windsor, R. Pancreatitis Across Nations Clinical and A. Education (2012). "Determinant-based classification of acute pancreatitis severity: an international multidisciplinary consultation." Ann Surg **256**(6): 875-880.
Desai, J., S. V. Kumar, S. R. Mulay, L. Konrad, S. Romoli, C. Schauer, M. Herrmann, R. Bilyy, S. Muller, B. Popper, D. Nakazawa, M. Weidenbusch, D. Thomasova, S. Krautwald, A. Linkermann and H. J. Anders (2016). "PMA and crystal-induced neutrophil extracellular trap formation involves RIPK1-RIPK3-MLKL signaling." Eur J Immunol **46**(1): 223-229.
Devin, A., Y. Lin and Z. G. Liu (2003). "The role of the death-domain kinase RIP in tumour-necrosis-factor-induced activation of mitogen-activated protein kinases." EMBO Rep **4**(6): 623-627.
Devin, A., Y. Lin, S. Yamaoka, Z. Li, M. Karin and Z. Liu (2001). "The alpha and beta subunits of IkappaB kinase (IKK) mediate TRAF2-dependent IKK recruitment to tumor necrosis factor (TNF) receptor 1 in response to TNF." Mol Cell Biol **21**(12): 3986-3994.
Dillon, C. P. and S. Balachandran (2016). "StIKKing it to a death kinase: IKKs prevent TNF-alpha-induced cell death by phosphorylating RIPK1." Cytokine **78**: 47-50.
Dillon, C. P., R. Weinlich, D. A. Rodriguez, J. G. Cripps, G. Quarato, P. Gurung, K. C. Verbist, T. L. Brewer, F. Llambi, Y. N. Gong, L. J. Janke, M. A. Kelliher, T. D. Kanneganti and D. R. Green (2014). "RIPK1 blocks early postnatal lethality mediated by caspase-8 and RIPK3." Cell **157**(5): 1189-1202.
Dohrman, A., T. Kataoka, S. Cuenin, J. Q. Russell, J. Tschopp and R. C. Budd (2005). "Cellular FLIP (long form) regulates CD8+ T cell activation through caspase-8-dependent NF-kappa B activation." J Immunol **174**(9): 5270-5278.
Dondelinger, Y., M. A. Aguileta, V. Goossens, C. Dubuisson, S. Grootjans, E. Dejardin, P. Vandenabeele and M. J. Bertrand (2013). "RIPK3 contributes to TNFR1-mediated RIPK1 kinase-dependent apoptosis in conditions of cIAP1/2 depletion or TAK1 kinase inhibition." Cell Death Differ **20**(10): 1381-1392.
Dondelinger, Y., S. Jouan-Lanhouet, T. Divert, E. Theatre, J. Bertin, P. J. Gough, P. Giansanti, A. J. Heck, E. Dejardin, P. Vandenabeele and M. J. Bertrand (2015). "NF-kappaB-Independent Role of IKKalpha/IKKbeta in Preventing RIPK1 Kinase-Dependent Apoptotic and Necroptotic Cell Death during TNF Signaling." Mol Cell **60**(1): 63-76.
Duprez, L., M. J. Bertrand, T. Vanden Berghe, Y. Dondelinger, N. Festjens and P. Vandenabeele (2012). "Intermediate domain of receptor-interacting protein kinase 1 (RIPK1) determines switch between necroptosis and RIPK1 kinase-dependent apoptosis." J Biol Chem **287**(18): 14863-14872.
Duprez, L., N. Takahashi, F. Van Hauwermeiren, B. Vandendriessche, V. Goossens, T. Vanden Berghe, W. Declercq, C. Libert, A. Cauwels and P. Vandenabeele (2011). "RIP kinase-dependent necrosis drives lethal systemic inflammatory response syndrome." Immunity **35**(6): 908-918.
Dusetti, N. J., Y. Jiang, M. I. Vaccaro, R. Tomasini, A. Azizi Samir, E. L. Calvo, A. Ropolo, F. Fiedler, G. V. Mallo, J. C. Dagorn and J. L. Iovanna (2002). "Cloning and expression of the rat vacuole membrane protein 1 (VMP1), a new gene activated in pancreas with acute pancreatitis, which promotes vacuole formation." Biochem Biophys Res Commun **290**(2): 641-649.
Dynek, J. N., T. Goncharov, E. C. Dueber, A. V. Fedorova, A. Izrael-Tomasevic, L. Phu, E. Helgason, W. J. Fairbrother, K. Deshayes, D. S. Kirkpatrick and D. Vucic

(2010). "c-IAP1 and UbcH5 promote K11-linked polyubiquitination of RIP1 in TNF signalling." EMBO J **29**(24): 4198-4209.
Emmerich, C. H., A. C. Schmukle and H. Walczak (2011). "The emerging role of linear ubiquitination in cell signaling." Sci Signal **4**(204): re5.
Estornes, Y., M. A. Aguileta, C. Dubuisson, J. De Keyser, V. Goossens, K. Kersse, A. Samali, P. Vandenabeele and M. J. Bertrand (2014). "RIPK1 promotes death receptor-independent caspase-8-mediated apoptosis under unresolved ER stress conditions." Cell Death Dis **5**: e1555.
Fauster, A., M. Rebsamen, K. V. Huber, J. W. Bigenzahn, A. Stukalov, C. H. Lardeau, S. Scorzoni, M. Bruckner, M. Gridling, K. Parapatics, J. Colinge, K. L. Bennett, S. Kubicek, S. Krautwald, A. Linkermann and G. Superti-Furga (2015). "A cellular screen identifies ponatinib and pazopanib as inhibitors of necroptosis." Cell Death Dis **6**: e1767.
Feddersen, C. O., S. Willemer, W. Karges, A. Puchner, G. Adler and P. V. Wichert (1991). "Lung injury in acute experimental pancreatitis in rats. II. Functional studies." Int J Pancreatol **8**(4): 323-331.
Feksa, L. R., A. Latini, V. C. Rech, M. Wajner, C. S. Dutra-Filho, A. T. de Souza Wyse and C. M. Wannmacher (2006). "Promotion of oxidative stress by L-tryptophan in cerebral cortex of rats." Neurochem Int **49**(1): 87-93.
Filliol, A., C. Piquet-Pellorce, J. Le Seyec, M. Farooq, V. Genet, C. Lucas-Clerc, J. Bertin, P. J. Gough, M. T. Dimanche-Boitrel, P. Vandenabeele, M. J. Bertrand and M. Samson (2016). "RIPK1 protects from TNF-alpha-mediated liver damage during hepatitis." Cell Death Dis **7**(11): e2462.
Fischer, L., A. S. Gukovskaya, J. M. Penninger, O. A. Mareninova, H. Friess, I. Gukovsky and S. J. Pandol (2007). "Phosphatidylinositol 3-kinase facilitates bile acid-induced Ca(2+) responses in pancreatic acinar cells." Am J Physiol Gastrointest Liver Physiol **292**(3): G875-886.
Foitzik, T., C. Fernandez-del Castillo, M. J. Ferraro, K. Mithofer, D. W. Rattner and A. L. Warshaw (1995). "Pathogenesis and prevention of early pancreatic infection in experimental acute necrotizing pancreatitis." Ann Surg **222**(2): 179-185.
Forkink, M., J. A. Smeitink, R. Brock, P. H. Willems and W. J. Koopman (2010). "Detection and manipulation of mitochondrial reactive oxygen species in mammalian cells." Biochim Biophys Acta **1797**(6-7): 1034-1044.
Fortes, G. B., L. S. Alves, R. de Oliveira, F. F. Dutra, D. Rodrigues, P. L. Fernandez, T. Souto-Padron, M. J. De Rosa, M. Kelliher, D. Golenbock, F. K. Chan and M. T. Bozza (2012). "Heme induces programmed necrosis on macrophages through autocrine TNF and ROS production." Blood **119**(10): 2368-2375.
Fortunato, F., H. Burgers, F. Bergmann, P. Rieger, M. W. Buchler, G. Kroemer and J. Werner (2009). "Impaired autolysosome formation correlates with Lamp-2 depletion: role of apoptosis, autophagy, and necrosis in pancreatitis." Gastroenterology **137**(1): 350-360, 360 e351-355.
Freeman, M. L. and N. M. Guda (2004). "Prevention of post-ERCP pancreatitis: a comprehensive review." Gastrointest Endosc **59**(7): 845-864.
Friedman, H. S., R. Lowery, E. Shaughnessy and J. Scorza (1983). "The effects of ethanol on pancreatic blood flow in awake and anesthetized dogs." Proc Soc Exp Biol Med **174**(3): 377-382.
Friedmann Angeli, J. P., M. Schneider, B. Proneth, Y. Y. Tyurina, V. A. Tyurin, V. J. Hammond, N. Herbach, M. Aichler, A. Walch, E. Eggenhofer, D. Basavarajappa, O. Radmark, S. Kobayashi, T. Seibt, H. Beck, F. Neff, I. Esposito, R. Wanke, H. Forster, O. Yefremova, M. Heinrichmeyer, G. W. Bornkamm, E. K. Geissler, S. B. Thomas,

B. R. Stockwell, V. B. O'Donnell, V. E. Kagan, J. A. Schick and M. Conrad (2014). "Inactivation of the ferroptosis regulator Gpx4 triggers acute renal failure in mice." Nat Cell Biol **16**(12): 1180-1191.
Frossard, J. L., M. L. Steer and C. M. Pastor (2008). "Acute pancreatitis." Lancet **371**(9607): 143-152.
Georgiadis, V. and R. A. Knight (2012). "Necroptosis: STAT3 kills?" JAKSTAT **1**(3): 200-202.
Gerasimenko, J. V., S. E. Flowerdew, S. G. Voronina, T. K. Sukhomlin, A. V. Tepikin, O. H. Petersen and O. V. Gerasimenko (2006). "Bile acids induce Ca2+ release from both the endoplasmic reticulum and acidic intracellular calcium stores through activation of inositol trisphosphate receptors and ryanodine receptors." J Biol Chem **281**(52): 40154-40163.
Gerasimenko, J. V., O. V. Gerasimenko, A. Palejwala, A. V. Tepikin, O. H. Petersen and A. J. Watson (2002). "Menadione-induced apoptosis: roles of cytosolic Ca(2+) elevations and the mitochondrial permeability transition pore." J Cell Sci **115**(Pt 3): 485-497.
Gerasimenko, J. V., O. V. Gerasimenko and O. H. Petersen (2014). "The role of Ca2+ in the pathophysiology of pancreatitis." J Physiol **592**(2): 269-280.
Gerasimenko, J. V., O. Gryshchenko, P. E. Ferdek, E. Stapleton, T. O. Hebert, S. Bychkova, S. Peng, M. Begg, O. V. Gerasimenko and O. H. Petersen (2013). "Ca2+ release-activated Ca2+ channel blockade as a potential tool in antipancreatitis therapy." Proc Natl Acad Sci U S A **110**(32): 13186-13191.
Gerlach, B., S. M. Cordier, A. C. Schmukle, C. H. Emmerich, E. Rieser, T. L. Haas, A. I. Webb, J. A. Rickard, H. Anderton, W. W. Wong, U. Nachbur, L. Gangoda, U. Warnken, A. W. Purcell, J. Silke and H. Walczak (2011). "Linear ubiquitination prevents inflammation and regulates immune signalling." Nature **471**(7340): 591-596.
Glick, D., S. Barth and K. F. Macleod (2010). "Autophagy: cellular and molecular mechanisms." J Pathol **221**(1): 3-12.
Gonzalez Esquivel, D., D. Ramirez-Ortega, B. Pineda, N. Castro, C. Rios and V. Perez de la Cruz (2017). "Kynurenine pathway metabolites and enzymes involved in redox reactions." Neuropharmacology **112**(Pt B): 331-345.
Grimm, S., B. Z. Stanger and P. Leder (1996). "RIP and FADD: two "death domain"-containing proteins can induce apoptosis by convergent, but dissociable, pathways." Proc Natl Acad Sci U S A **93**(20): 10923-10927.
Grohmann, U., F. Fallarino and P. Puccetti (2003). "Tolerance, DCs and tryptophan: much ado about IDO." Trends Immunol **24**(5): 242-248.
Guice, K. S., K. T. Oldham, K. J. Johnson, R. G. Kunkel, M. L. Morganroth and P. A. Ward (1988). "Pancreatitis-induced acute lung injury. An ARDS model." Ann Surg **208**(1): 71-77.
Gukovskaya, A. S. and I. Gukovsky (2012). "Autophagy and pancreatitis." Am J Physiol Gastrointest Liver Physiol **303**(9): G993-G1003.
Gukovskaya, A. S., I. Gukovsky, Y. Jung, M. Mouria and S. J. Pandol (2002). "Cholecystokinin induces caspase activation and mitochondrial dysfunction in pancreatic acinar cells. Roles in cell injury processes of pancreatitis." J Biol Chem **277**(25): 22595-22604.
Gukovskaya, A. S., M. Mouria, I. Gukovsky, C. N. Reyes, V. N. Kasho, L. D. Faller and S. J. Pandol (2002). "Ethanol metabolism and transcription factor activation in pancreatic acinar cells in rats." Gastroenterology **122**(1): 106-118.
Gukovskaya, A. S., E. Vaquero, V. Zaninovic, F. S. Gorelick, A. J. Lusis, M. L. Brennan, S. Holland and S. J. Pandol (2002). "Neutrophils and NADPH oxidase

mediate intrapancreatic trypsin activation in murine experimental acute pancreatitis." Gastroenterology **122**(4): 974-984.
Halestrap, A. P. (2006). "Calcium, mitochondria and reperfusion injury: a pore way to die." Biochem Soc Trans **34**(Pt 2): 232-237.
Hamanaka, R. B. and N. S. Chandel (2010). "Mitochondrial reactive oxygen species regulate cellular signaling and dictate biological outcomes." Trends Biochem Sci **35**(9): 505-513.
Hanggi, K., L. Vasilikos, A. F. Valls, R. Yerbes, J. Knop, L. M. Spilgies, K. Rieck, T. Misra, J. Bertin, P. J. Gough, T. Schmidt, C. R. de Almodovar and W. W. Wong (2017). "RIPK1/RIPK3 promotes vascular permeability to allow tumor cell extravasation independent of its necroptotic function." Cell Death Dis **8**(2): e2588.
Harper, N., S. N. Farrow, A. Kaptein, G. M. Cohen and M. MacFarlane (2001). "Modulation of tumor necrosis factor apoptosis-inducing ligand- induced NF-kappa B activation by inhibition of apical caspases." J Biol Chem **276**(37): 34743-34752.
Harris, P. A., D. Bandyopadhyay, S. B. Berger, N. Campobasso, C. A. Capriotti, J. A. Cox, L. Dare, J. N. Finger, S. J. Hoffman, K. M. Kahler, R. Lehr, J. D. Lich, R. Nagilla, R. T. Nolte, M. T. Ouellette, C. S. Pao, M. C. Schaeffer, A. Smallwood, H. H. Sun, B. A. Swift, R. D. Totoritis, P. Ward, R. W. Marquis, J. Bertin and P. J. Gough (2013). "Discovery of Small Molecule RIP1 Kinase Inhibitors for the Treatment of Pathologies Associated with Necroptosis." ACS Med Chem Lett **4**(12): 1238-1243.
Harris, P. A., S. B. Berger, J. U. Jeong, R. Nagilla, D. Bandyopadhyay, N. Campobasso, C. A. Capriotti, J. A. Cox, L. Dare, X. Dong, P. M. Eidam, J. N. Finger, S. J. Hoffman, J. Kang, V. Kasparcova, B. W. King, R. Lehr, Y. Lan, L. K. Leister, J. D. Lich, T. T. MacDonald, N. A. Miller, M. T. Ouellette, C. S. Pao, A. Rahman, M. A. Reilly, A. R. Rendina, E. J. Rivera, M. C. Schaeffer, C. A. Sehon, R. R. Singhaus, H. H. Sun, B. A. Swift, R. D. Totoritis, A. Vossenkamper, P. Ward, D. D. Wisnoski, D. Zhang, R. W. Marquis, P. J. Gough and J. Bertin (2017). "Discovery of a First-in-Class Receptor Interacting Protein 1 (RIP1) Kinase Specific Clinical Candidate (GSK2982772) for the Treatment of Inflammatory Diseases." J Med Chem **60**(4): 1247-1261.
He, K. L. and A. T. Ting (2002). "A20 inhibits tumor necrosis factor (TNF) alpha-induced apoptosis by disrupting recruitment of TRADD and RIP to the TNF receptor 1 complex in Jurkat T cells." Mol Cell Biol **22**(17): 6034-6045.
He, S., S. Huang and Z. Shen (2016). "Biomarkers for the detection of necroptosis." Cell Mol Life Sci **73**(11-12): 2177-2181.
He, S., L. Wang, L. Miao, T. Wang, F. Du, L. Zhao and X. Wang (2009). "Receptor interacting protein kinase-3 determines cellular necrotic response to TNF-alpha." Cell **137**(6): 1100-1111.
Hegyi, P., Z. Rakonczay, Jr., R. Sari, C. Gog, J. Lonovics, T. Takacs and L. Czako (2004). "L-arginine-induced experimental pancreatitis." World J Gastroenterol **10**(14): 2003-2009.
Hershko, A. and A. Ciechanover (1998). "The ubiquitin system." Annu Rev Biochem **67**: 425-479.
Heyninck, K., D. De Valck, W. Vanden Berghe, W. Van Criekinge, R. Contreras, W. Fiers, G. Haegeman and R. Beyaert (1999). "The zinc finger protein A20 inhibits TNF-induced NF-kappaB-dependent gene expression by interfering with an RIP- or TRAF2-mediated transactivation signal and directly binds to a novel NF-kappaB-inhibiting protein ABIN." J Cell Biol **145**(7): 1471-1482.
Holler, N., R. Zaru, O. Micheau, M. Thome, A. Attinger, S. Valitutti, J. L. Bodmer, P. Schneider, B. Seed and J. Tschopp (2000). "Fas triggers an alternative, caspase-8-

independent cell death pathway using the kinase RIP as effector molecule." Nat Immunol **1**(6): 489-495.
Hong, J. M., S. J. Kim and S. M. Lee (2016). "Role of necroptosis in autophagy signaling during hepatic ischemia and reperfusion." Toxicol Appl Pharmacol **308**: 1-10.
Hou, D. Y., A. J. Muller, M. D. Sharma, J. DuHadaway, T. Banerjee, M. Johnson, A. L. Mellor, G. C. Prendergast and D. H. Munn (2007). "Inhibition of indoleamine 2,3-dioxygenase in dendritic cells by stereoisomers of 1-methyl-tryptophan correlates with antitumor responses." Cancer Res **67**(2): 792-801.
Hou, X., L. Wang, L. Zhang, X. Pan and W. Zhao (2013). "Ubiquitin-specific protease 4 promotes TNF-alpha-induced apoptosis by deubiquitination of RIP1 in head and neck squamous cell carcinoma." FEBS Lett **587**(4): 311-316.
Hsu, H., J. Huang, H. B. Shu, V. Baichwal and D. V. Goeddel (1996). "TNF-dependent recruitment of the protein kinase RIP to the TNF receptor-1 signaling complex." Immunity **4**(4): 387-396.
Huang, W., D. M. Booth, M. C. Cane, M. Chvanov, M. A. Javed, V. L. Elliott, J. A. Armstrong, H. Dingsdale, N. Cash, Y. Li, W. Greenhalf, R. Mukherjee, B. S. Kaphalia, M. Jaffar, O. H. Petersen, A. V. Tepikin, R. Sutton and D. N. Criddle (2014). "Fatty acid ethyl ester synthase inhibition ameliorates ethanol-induced Ca2+-dependent mitochondrial dysfunction and acute pancreatitis." Gut **63**(8): 1313-1324.
Huang, W., M. C. Cane, R. Mukherjee, P. Szatmary, X. Zhang, V. Elliott, Y. Ouyang, M. Chvanov, D. Latawiec, L. Wen, D. M. Booth, A. C. Haynes, O. H. Petersen, A. V. Tepikin, D. N. Criddle and R. Sutton (2017). "Caffeine protects against experimental acute pancreatitis by inhibition of inositol 1,4,5-trisphosphate receptor-mediated Ca2+ release." Gut **66**(2): 301-313.
Huang, W., N. Cash, L. Wen, P. Szatmary, R. Mukherjee, J. Armstrong, M. Chvanov, A. V. Tepikin, M. P. Murphy, R. Sutton and D. N. Criddle (2015). "Effects of the mitochondria-targeted antioxidant mitoquinone in murine acute pancreatitis." Mediators Inflamm **2015**: 901780.
Huang, Z., M. Epperly, S. C. Watkins, J. S. Greenberger, V. E. Kagan and H. Bayir (2016). "Necrostatin-1 rescues mice from lethal irradiation." Biochim Biophys Acta **1862**(4): 850-856.
Huengsberg, M., J. B. Winer, M. Gompels, R. Round, J. Ross and M. Shahmanesh (1998). "Serum kynurenine-to-tryptophan ratio increases with progressive disease in HIV-infected patients." Clin Chem **44**(4): 858-862.
Hur, G. M., J. Lewis, Q. Yang, Y. Lin, H. Nakano, S. Nedospasov and Z. G. Liu (2003). "The death domain kinase RIP has an essential role in DNA damage-induced NF-kappa B activation." Genes Dev **17**(7): 873-882.
Ikeda, F. (2015). "Linear ubiquitination signals in adaptive immune responses." Immunol Rev **266**(1): 222-236.
Inohara, N., T. Koseki, J. Lin, L. del Peso, P. C. Lucas, F. F. Chen, Y. Ogura and G. Nunez (2000). "An induced proximity model for NF-kappa B activation in the Nod1/RICK and RIP signaling pathways." J Biol Chem **275**(36): 27823-27831.
Irving, H. M., A. V. Samokhvalov and J. Rehm (2009). "Alcohol as a risk factor for pancreatitis. A systematic review and meta-analysis." JOP **10**(4): 387-392.
Ishida, Y., Y. Sekine, H. Oguchi, T. Chihara, M. Miura, H. Ichijo and K. Takeda (2012). "Prevention of apoptosis by mitochondrial phosphatase PGAM5 in the mushroom body is crucial for heat shock resistance in Drosophila melanogaster." PLoS One **7**(2): e30265.

Ishizawa, Y. H., K. Tamura, T. Yamaguchi, K. Matsumoto, M. Komiyama, N. Takamatsu, T. Shiba and M. Ito (2006). "Xenopus death-domain-containing proteins FADD and RIP1 synergistically activate JNK and NF-kappaB." Biol Cell **98**(8): 465-478.
Iwatsuki, N. and O. H. Petersen (1977). "Pancreatic acinar cells: localization of acetylcholine receptors and the importance of chloride and calcium for acetylcholine-evoked depolarization." J Physiol **269**(3): 723-733.
Izumi, K. M., E. D. Cahir McFarland, A. T. Ting, E. A. Riley, B. Seed and E. D. Kieff (1999). "The Epstein-Barr virus oncoprotein latent membrane protein 1 engages the tumor necrosis factor receptor-associated proteins TRADD and receptor-interacting protein (RIP) but does not induce apoptosis or require RIP for NF-kappaB activation." Mol Cell Biol **19**(8): 5759-5767.
Jerrells, T. R., N. Chapman and D. L. Clemens (2003). "Animal model of alcoholic pancreatitis: role of viral infections." Pancreas **27**(4): 301-304.
Jia, D., M. Yamamoto and M. Otsuki (2015). "Effect of endogenous cholecystokinin on the course of acute pancreatitis in rats." World J Gastroenterol **21**(25): 7742-7753.
Jiang, C. C., Z. G. Mao, K. A. Avery-Kiejda, M. Wade, P. Hersey and X. D. Zhang (2009). "Glucose-regulated protein 78 antagonizes cisplatin and adriamycin in human melanoma cells." Carcinogenesis **30**(2): 197-204.
Jie, H., Y. He, X. Huang, Q. Zhou, Y. Han, X. Li, Y. Bai and E. Sun (2016). "Necrostatin-1 enhances the resolution of inflammation by specifically inducing neutrophil apoptosis." Oncotarget **7**(15): 19367-19381.
Jin, S., A. I. Orabi, T. Le, T. A. Javed, S. Sah, J. F. Eisses, R. Bottino, J. D. Molkentin and S. Z. Husain (2015). "Exposure to Radiocontrast Agents Induces Pancreatic Inflammation by Activation of Nuclear Factor-kappaB, Calcium Signaling, and Calcineurin." Gastroenterology **149**(3): 753-764 e711.
Johnson, R. H. and J. Doppman (1967). "Duodenal reflux and the etiology of pancreatitis." Surgery **62**(3): 462-467.
Jouan-Lanhouet, S., M. I. Arshad, C. Piquet-Pellorce, C. Martin-Chouly, G. Le Moigne-Muller, F. Van Herreweghe, N. Takahashi, O. Sergent, D. Lagadic-Gossmann, P. Vandenabeele, M. Samson and M. T. Dimanche-Boitrel (2012). "TRAIL induces necroptosis involving RIPK1/RIPK3-dependent PARP-1 activation." Cell Death Differ **19**(12): 2003-2014.
Jurgens, B., U. Hainz, D. Fuchs, T. Felzmann and A. Heitger (2009). "Interferon-gamma-triggered indoleamine 2,3-dioxygenase competence in human monocyte-derived dendritic cells induces regulatory activity in allogeneic T cells." Blood **114**(15): 3235-3243.
Jux, B., S. Kadow and C. Esser (2009). "Langerhans cell maturation and contact hypersensitivity are impaired in aryl hydrocarbon receptor-null mice." J Immunol **182**(11): 6709-6717.
Kaiser, A. M., T. Grady, D. Gerdes, M. Saluja and M. L. Steer (1995). "Intravenous contrast medium does not increase the severity of acute necrotizing pancreatitis in the opossum." Dig Dis Sci **40**(7): 1547-1553.
Kaiser, A. M., A. K. Saluja, L. Lu, K. Yamanaka, Y. Yamaguchi and M. L. Steer (1996). "Effects of cycloheximide on pancreatic endonuclease activity, apoptosis, and severity of acute pancreatitis." Am J Physiol **271**(3 Pt 1): C982-993.
Kaiser, A. M., A. K. Saluja, A. Sengupta, M. Saluja and M. L. Steer (1995). "Relationship between severity, necrosis, and apoptosis in five models of experimental acute pancreatitis." Am J Physiol **269**(5 Pt 1): C1295-1304.

Kaiser, W. J., L. P. Daley-Bauer, R. J. Thapa, P. Mandal, S. B. Berger, C. Huang, A. Sundararajan, H. Guo, L. Roback, S. H. Speck, J. Bertin, P. J. Gough, S. Balachandran and E. S. Mocarski (2014). "RIP1 suppresses innate immune necrotic as well as apoptotic cell death during mammalian parturition." Proc Natl Acad Sci U S A **111**(21): 7753-7758.
Kalai, M., G. Van Loo, T. Vanden Berghe, A. Meeus, W. Burm, X. Saelens and P. Vandenabeele (2002). "Tipping the balance between necrosis and apoptosis in human and murine cells treated with interferon and dsRNA." Cell Death Differ **9**(9): 981-994.
Kataoka, T., R. C. Budd, N. Holler, M. Thome, F. Martinon, M. Irmler, K. Burns, M. Hahne, N. Kennedy, M. Kovacsovics and J. Tschopp (2000). "The caspase-8 inhibitor FLIP promotes activation of NF-kappaB and Erk signaling pathways." Curr Biol **10**(11): 640-648.
Kearney, C. J., S. P. Cullen, D. Clancy and S. J. Martin (2014). "RIPK1 can function as an inhibitor rather than an initiator of RIPK3-dependent necroptosis." FEBS J **281**(21): 4921-4934.
Kelliher, M. A., S. Grimm, Y. Ishida, F. Kuo, B. Z. Stanger and P. Leder (1998). "The death domain kinase RIP mediates the TNF-induced NF-kappaB signal." Immunity **8**(3): 297-303.
Keusekotten, K., P. R. Elliott, L. Glockner, B. K. Fiil, R. B. Damgaard, Y. Kulathu, T. Wauer, M. K. Hospenthal, M. Gyrd-Hansen, D. Krappmann, K. Hofmann and D. Komander (2013). "OTULIN antagonizes LUBAC signaling by specifically hydrolyzing Met1-linked polyubiquitin." Cell **153**(6): 1312-1326.
Khan, M. J., M. Rizwan Alam, M. Waldeck-Weiermair, F. Karsten, L. Groschner, M. Riederer, S. Hallstrom, P. Rockenfeller, V. Konya, A. Heinemann, F. Madeo, W. F. Graier and R. Malli (2012). "Inhibition of autophagy rescues palmitic acid-induced necroptosis of endothelial cells." J Biol Chem **287**(25): 21110-21120.
Kim, J. W., E. J. Choi and C. O. Joe (2000). "Activation of death-inducing signaling complex (DISC) by pro-apoptotic C-terminal fragment of RIP." Oncogene **19**(39): 4491-4499.
Kim, J. Y., K. H. Kim, J. A. Lee, W. Namkung, A. Q. Sun, M. Ananthanarayanan, F. J. Suchy, D. M. Shin, S. Muallem and M. G. Lee (2002). "Transporter-mediated bile acid uptake causes Ca2+-dependent cell death in rat pancreatic acinar cells." Gastroenterology **122**(7): 1941-1953.
Kim, Y. S., M. J. Morgan, S. Choksi and Z. G. Liu (2007). "TNF-induced activation of the Nox1 NADPH oxidase and its role in the induction of necrotic cell death." Mol Cell **26**(5): 675-687.
Kischkel, F. C., D. A. Lawrence, A. Chuntharapai, P. Schow, K. J. Kim and A. Ashkenazi (2000). "Apo2L/TRAIL-dependent recruitment of endogenous FADD and caspase-8 to death receptors 4 and 5." Immunity **12**(6): 611-620.
Kloppel, G. and B. Maillet (1993). "Pathology of acute and chronic pancreatitis." Pancreas **8**(6): 659-670.
Knox, P. G., C. C. Davies, M. Ioannou and A. G. Eliopoulos (2011). "The death domain kinase RIP1 links the immunoregulatory CD40 receptor to apoptotic signaling in carcinomas." J Cell Biol **192**(3): 391-399.
Koblish, H. K., M. J. Hansbury, K. J. Bowman, G. Yang, C. L. Neilan, P. J. Haley, T. C. Burn, P. Waeltz, R. B. Sparks, E. W. Yue, A. P. Combs, P. A. Scherle, K. Vaddi and J. S. Fridman (2010). "Hydroxyamidine inhibitors of indoleamine-2,3-dioxygenase potently suppress systemic tryptophan catabolism and the growth of IDO-expressing tumors." Mol Cancer Ther **9**(2): 489-498.

Kreuz, S., D. Siegmund, J. J. Rumpf, D. Samel, M. Leverkus, O. Janssen, G. Hacker, O. Dittrich-Breiholz, M. Kracht, P. Scheurich and H. Wajant (2004). "NFkappaB activation by Fas is mediated through FADD, caspase-8, and RIP and is inhibited by FLIP." J Cell Biol **166**(3): 369-380.
Kroemer, G., L. Galluzzi and C. Brenner (2007). "Mitochondrial membrane permeabilization in cell death." Physiol Rev **87**(1): 99-163.
Kroemer, G. and L. Zitvogel (2007). "Death, danger, and immunity: an infernal trio." Immunol Rev **220**: 5-7.
Kruger, B., E. Albrecht and M. M. Lerch (2000). "The role of intracellular calcium signaling in premature protease activation and the onset of pancreatitis." Am J Pathol **157**(1): 43-50.
Kurenova, E., L. H. Xu, X. Yang, A. S. Baldwin, Jr., R. J. Craven, S. K. Hanks, Z. G. Liu and W. G. Cance (2004). "Focal adhesion kinase suppresses apoptosis by binding to the death domain of receptor-interacting protein." Mol Cell Biol **24**(10): 4361-4371.
Lampel, M. and H. F. Kern (1977). "Acute interstitial pancreatitis in the rat induced by excessive doses of a pancreatic secretagogue." Virchows Arch A Pathol Anat Histol **373**(2): 97-117.
Lankisch, P. G., M. Apte and P. A. Banks (2015). "Acute pancreatitis." Lancet **386**(9988): 85-96.
Lassus, P., X. Opitz-Araya and Y. Lazebnik (2002). "Requirement for caspase-2 in stress-induced apoptosis before mitochondrial permeabilization." Science **297**(5585): 1352-1354.
Laster, S. M., J. G. Wood and L. R. Gooding (1988). "Tumor necrosis factor can induce both apoptic and necrotic forms of cell lysis." J Immunol **141**(8): 2629-2634.
Laukkarinen, J. M., G. J. Van Acker, E. R. Weiss, M. L. Steer and G. Perides (2007). "A mouse model of acute biliary pancreatitis induced by retrograde pancreatic duct infusion of Na-taurocholate." Gut **56**(11): 1590-1598.
Le, T., J. F. Eisses, K. L. Lemon, J. A. Ozolek, D. A. Pociask, A. I. Orabi and S. Z. Husain (2015). "Intraductal infusion of taurocholate followed by distal common bile duct ligation leads to a severe necrotic model of pancreatitis in mice." Pancreas **44**(3): 493-499.
Lee, J. R., H. W. Youm, S. K. Kim, B. C. Jee, C. S. Suh and S. H. Kim (2014). "Effect of necrostatin on mouse ovarian cryopreservation and transplantation." Eur J Obstet Gynecol Reprod Biol **178**: 16-20.
Lee, T. H., J. Shank, N. Cusson and M. A. Kelliher (2004). "The kinase activity of Rip1 is not required for tumor necrosis factor-alpha-induced IkappaB kinase or p38 MAP kinase activation or for the ubiquitination of Rip1 by Traf2." J Biol Chem **279**(32): 33185-33191.
Lemasters, J. J., T. P. Theruvath, Z. Zhong and A. L. Nieminen (2009). "Mitochondrial calcium and the permeability transition in cell death." Biochim Biophys Acta **1787**(11): 1395-1401.
Li, H., M. Kobayashi, M. Blonska, Y. You and X. Lin (2006). "Ubiquitination of RIP is required for tumor necrosis factor alpha-induced NF-kappaB activation." J Biol Chem **281**(19): 13636-13643.
Li, Y., X. Yang, C. Ma, J. Qiao and C. Zhang (2008). "Necroptosis contributes to the NMDA-induced excitotoxicity in rat's cultured cortical neurons." Neurosci Lett **447**(2-3): 120-123.
Li, Z., B. Ma, M. Lu, X. Qiao, B. Sun, W. Zhang and D. Xue (2013). "Construction of network for protein kinases that play a role in acute pancreatitis." Pancreas **42**(4): 607-613.

Liddle, J., B. Beaufils, M. Binnie, A. Bouillot, A. A. Denis, M. M. Hann, C. P. Haslam, D. S. Holmes, J. P. Hutchinson, M. Kranz, A. McBride, O. Mirguet, D. J. Mole, C. G. Mowat, S. Pal, P. Rowland, L. Trottet, I. J. Uings, A. L. Walker and S. P. Webster (2017). "The discovery of potent and selective kynurenine 3-monooxygenase inhibitors for the treatment of acute pancreatitis." Bioorg Med Chem Lett **27**(9): 2023-2028.
Lin, Y., S. Choksi, H. M. Shen, Q. F. Yang, G. M. Hur, Y. S. Kim, J. H. Tran, S. A. Nedospasov and Z. G. Liu (2004). "Tumor necrosis factor-induced nonapoptotic cell death requires receptor-interacting protein-mediated cellular reactive oxygen species accumulation." J Biol Chem **279**(11): 10822-10828.
Lin, Y., A. Devin, A. Cook, M. M. Keane, M. Kelliher, S. Lipkowitz and Z. G. Liu (2000). "The death domain kinase RIP is essential for TRAIL (Apo2L)-induced activation of IkappaB kinase and c-Jun N-terminal kinase." Mol Cell Biol **20**(18): 6638-6645.
Lin, Y., A. Devin, Y. Rodriguez and Z. G. Liu (1999). "Cleavage of the death domain kinase RIP by caspase-8 prompts TNF-induced apoptosis." Genes Dev **13**(19): 2514-2526.
Linkermann, A., J. H. Brasen, F. De Zen, R. Weinlich, R. A. Schwendener, D. R. Green, U. Kunzendorf and S. Krautwald (2012). "Dichotomy between RIP1- and RIP3-mediated necroptosis in tumor necrosis factor-alpha-induced shock." Mol Med **18**: 577-586.
Linkermann, A., J. H. Brasen, N. Himmerkus, S. Liu, T. B. Huber, U. Kunzendorf and S. Krautwald (2012). "Rip1 (receptor-interacting protein kinase 1) mediates necroptosis and contributes to renal ischemia/reperfusion injury." Kidney Int **81**(8): 751-761.
Linkermann, A. and D. R. Green (2014). "Necroptosis." N Engl J Med **370**(5): 455-465.
Linkermann, A., B. R. Stockwell, S. Krautwald and H. J. Anders (2014). "Regulated cell death and inflammation: an auto-amplification loop causes organ failure." Nat Rev Immunol **14**(11): 759-767.
Liu, T., Y. H. Bao, Y. Wang and J. Y. Jiang (2015). "The role of necroptosis in neurosurgical diseases." Braz J Med Biol Res **48**(4): 292-298.
Liu, W. K., P. F. Yen, C. Y. Chien, M. J. Fann, J. Y. Su and C. K. Chou (2004). "The inhibitor ABIN-2 disrupts the interaction of receptor-interacting protein with the kinase subunit IKKgamma to block activation of the transcription factor NF-kappaB and potentiate apoptosis." Biochem J **378**(Pt 3): 867-876.
Liu, Y., X. D. Chen, J. Yu, J. L. Chi, F. W. Long, H. W. Yang, K. L. Chen, Z. Y. Lv, B. Zhou, Z. H. Peng, X. F. Sun, Y. Li and Z. G. Zhou (2017). "Deletion Of XIAP reduces the severity of acute pancreatitis via regulation of cell death and nuclear factor-kappaB activity." Cell Death Dis **8**(3): e2685.
Liu, Y., C. Fan, Y. Zhang, X. Yu, X. Wu, X. Zhang, Q. Zhao, H. Zhang, Q. Xie, M. Li, X. Li, Q. Ding, H. Ying, D. Li and H. Zhang (2017). "RIP1 kinase activity-dependent roles in embryonic development of Fadd-deficient mice." Cell Death Differ.
Lob, S., A. Konigsrainer, R. Schafer, H. G. Rammensee, G. Opelz and P. Terness (2008). "Levo- but not dextro-1-methyl tryptophan abrogates the IDO activity of human dendritic cells." Blood **111**(4): 2152-2154.
Lob, S., A. Konigsrainer, D. Zieker, B. L. Brucher, H. G. Rammensee, G. Opelz and P. Terness (2009). "IDO1 and IDO2 are expressed in human tumors: levo- but not

dextro-1-methyl tryptophan inhibits tryptophan catabolism." Cancer Immunol Immunother **58**(1): 153-157.
Lombardi, B., L. W. Estes and D. S. Longnecker (1975). "Acute hemorrhagic pancreatitis (massive necrosis) with fat necrosis induced in mice by DL-ethionine fed with a choline-deficient diet." Am J Pathol **79**(3): 465-480.
Louhimo, J., M. L. Steer and G. Perides (2016). "Necroptosis Is an Important Severity Determinant and Potential Therapeutic Target in Experimental Severe Pancreatitis." Cell Mol Gastroenterol Hepatol **2**(4): 519-535.
Luan, Q., L. Jin, C. C. Jiang, K. H. Tay, F. Lai, X. Y. Liu, Y. L. Liu, S. T. Guo, C. Y. Li, X. G. Yan, H. Y. Tseng and X. D. Zhang (2015). "RIPK1 regulates survival of human melanoma cells upon endoplasmic reticulum stress through autophagy." Autophagy **11**(7): 975-994.
Lugea, A., J. Gong, J. Nguyen, J. Nieto, S. W. French and S. J. Pandol (2010). "Cholinergic mediation of alcohol-induced experimental pancreatitis." Alcohol Clin Exp Res **34**(10): 1768-1781.
Ma, B., L. Wu, M. Lu, B. Gao, X. Qiao, B. Sun, D. Xue and W. Zhang (2013). "Differentially expressed kinase genes associated with trypsinogen activation in rat pancreatic acinar cells treated with taurolithocholic acid 3-sulfate." Mol Med Rep **7**(5): 1591-1596.
Mahoney, D. J., H. H. Cheung, R. L. Mrad, S. Plenchette, C. Simard, E. Enwere, V. Arora, T. W. Mak, E. C. Lacasse, J. Waring and R. G. Korneluk (2008). "Both cIAP1 and cIAP2 regulate TNFalpha-mediated NF-kappaB activation." Proc Natl Acad Sci U S A **105**(33): 11778-11783.
Majewski, N., V. Nogueira, P. Bhaskar, P. E. Coy, J. E. Skeen, K. Gottlob, N. S. Chandel, C. B. Thompson, R. B. Robey and N. Hay (2004). "Hexokinase-mitochondria interaction mediated by Akt is required to inhibit apoptosis in the presence or absence of Bax and Bak." Mol Cell **16**(5): 819-830.
Maki, J. L., E. E. Smith, X. Teng, S. S. Ray, G. D. Cuny and A. Degterev (2012). "Fluorescence polarization assay for inhibitors of the kinase domain of receptor interacting protein 1." Anal Biochem **427**(2): 164-174.
Malmstrom, M. L., M. B. Hansen, A. M. Andersen, A. K. Ersboll, O. H. Nielsen, L. N. Jorgensen and S. Novovic (2012). "Cytokines and organ failure in acute pancreatitis: inflammatory response in acute pancreatitis." Pancreas **41**(2): 271-277.
Mareninova, O. A., K. Hermann, S. W. French, M. S. O'Konski, S. J. Pandol, P. Webster, A. H. Erickson, N. Katunuma, F. S. Gorelick, I. Gukovsky and A. S. Gukovskaya (2009). "Impaired autophagic flux mediates acinar cell vacuole formation and trypsinogen activation in rodent models of acute pancreatitis." J Clin Invest **119**(11): 3340-3355.
Mareninova, O. A., K. F. Sung, P. Hong, A. Lugea, S. J. Pandol, I. Gukovsky and A. S. Gukovskaya (2006). "Cell death in pancreatitis: caspases protect from necrotizing pancreatitis." J Biol Chem **281**(6): 3370-3381.
Martens, S., M. Jeong, W. Tonnus, F. Feldmann, S. Hofmans, V. Goossens, N. Takahashi, J. H. Brasen, E. W. Lee, P. Van der Veken, J. Joossens, K. Augustyns, S. Fulda, A. Linkermann, J. Song and P. Vandenabeele (2017). "Sorafenib tosylate inhibits directly necrosome complex formation and protects in mouse models of inflammation and tissue injury." Cell Death Dis **8**(6): e2904.
Martinon, F., N. Holler, C. Richard and J. Tschopp (2000). "Activation of a pro-apoptotic amplification loop through inhibition of NF-kappaB-dependent survival signals by caspase-mediated inactivation of RIP." FEBS Lett **468**(2-3): 134-136.

McConkey, D. J. and S. Orrenius (1996). "The role of calcium in the regulation of apoptosis." J Leukoc Biol **59**(6): 775-783.
McCully, J. D., H. Wakiyama, Y. J. Hsieh, M. Jones and S. Levitsky (2004). "Differential contribution of necrosis and apoptosis in myocardial ischemia-reperfusion injury." Am J Physiol Heart Circ Physiol **286**(5): H1923-1935.
McNamara, C. R., R. Ahuja, A. D. Osafo-Addo, D. Barrows, A. Kettenbach, I. Skidan, X. Teng, G. D. Cuny, S. Gerber and A. Degterev (2013). "Akt Regulates TNFalpha synthesis downstream of RIP1 kinase activation during necroptosis." PLoS One **8**(3): e56576.
McNeal, S. I., M. P. LeGolvan, C. S. Chung and A. Ayala (2011). "The dual functions of receptor interacting protein 1 in fas-induced hepatocyte death during sepsis." Shock **35**(5): 499-505.
McQuade, T., Y. Cho and F. K. Chan (2013). "Positive and negative phosphorylation regulates RIP1- and RIP3-induced programmed necrosis." Biochem J **456**(3): 409-415.
Melino, G., R. A. Knight and P. Nicotera (2005). "How many ways to die? How many different models of cell death?" Cell Death Differ **12 Suppl 2**: 1457-1462.
Melo-Lima, S., M. Celeste Lopes and F. Mollinedo (2014). "Necroptosis is associated with low procaspase-8 and active RIPK1 and -3 in human glioma cells." Oncoscience **1**(10): 649-664.
Metz, R., J. B. Duhadaway, U. Kamasani, L. Laury-Kleintop, A. J. Muller and G. C. Prendergast (2007). "Novel tryptophan catabolic enzyme IDO2 is the preferred biochemical target of the antitumor indoleamine 2,3-dioxygenase inhibitory compound D-1-methyl-tryptophan." Cancer Res **67**(15): 7082-7087.
Metz, R., C. Smith, J. B. DuHadaway, P. Chandler, B. Baban, L. M. Merlo, E. Pigott, M. P. Keough, S. Rust, A. L. Mellor, L. Mandik-Nayak, A. J. Muller and G. C. Prendergast (2014). "IDO2 is critical for IDO1-mediated T-cell regulation and exerts a non-redundant function in inflammation." Int Immunol **26**(7): 357-367.
Micheau, O. and J. Tschopp (2003). "Induction of TNF receptor I-mediated apoptosis via two sequential signaling complexes." Cell **114**(2): 181-190.
Mihaly, S. R., J. Ninomiya-Tsuji and S. Morioka (2014). "TAK1 control of cell death." Cell Death Differ **21**(11): 1667-1676.
Mizushima, N., A. Yamamoto, M. Matsui, T. Yoshimori and Y. Ohsumi (2004). "In vivo analysis of autophagy in response to nutrient starvation using transgenic mice expressing a fluorescent autophagosome marker." Mol Biol Cell **15**(3): 1101-1111.
Mohideen, F., J. A. Paulo, A. Ordureau, S. P. Gygi and J. W. Harper (2017). "Quantitative Phospho-proteomic Analysis of TNFalpha/NFkappaB Signaling Reveals a Role for RIPK1 Phosphorylation in Suppressing Necrotic Cell Death." Mol Cell Proteomics **16**(7): 1200-1216.
Mole, D. J., N. V. McFerran, G. Collett, C. O'Neill, T. Diamond, O. J. Garden, L. Kylanpaa, H. Repo and E. A. Deitch (2008). "Tryptophan catabolites in mesenteric lymph may contribute to pancreatitis-associated organ failure." Br J Surg **95**(7): 855-867.
Mole, D. J., S. P. Webster, I. Uings, X. Zheng, M. Binnie, K. Wilson, J. P. Hutchinson, O. Mirguet, A. Walker, B. Beaufils, N. Ancellin, L. Trottet, V. Beneton, C. G. Mowat, M. Wilkinson, P. Rowland, C. Haslam, A. McBride, N. Z. Homer, J. E. Baily, M. G. Sharp, O. J. Garden, J. Hughes, S. E. Howie, D. S. Holmes, J. Liddle and J. P. Iredale (2016). "Kynurenine-3-monooxygenase inhibition prevents multiple organ failure in rodent models of acute pancreatitis." Nat Med **22**(2): 202-209.

Moquin, D. M., T. McQuade and F. K. Chan (2013). "CYLD deubiquitinates RIP1 in the TNFalpha-induced necrosome to facilitate kinase activation and programmed necrosis." PLoS One **8**(10): e76841.
Moujalled, D. M., W. D. Cook, T. Okamoto, J. Murphy, K. E. Lawlor, J. E. Vince and D. L. Vaux (2013). "TNF can activate RIPK3 and cause programmed necrosis in the absence of RIPK1." Cell Death Dis **4**: e465.
Mounzer, R. and D. C. Whitcomb (2013). "Genetics of acute and chronic pancreatitis." Curr Opin Gastroenterol **29**(5): 544-551.
Mugford, C. A. and G. L. Kedderis (1998). "Sex-dependent metabolism of xenobiotics." Drug Metab Rev **30**(3): 441-498.
Muller, A. J., J. B. DuHadaway, P. S. Donover, E. Sutanto-Ward and G. C. Prendergast (2005). "Inhibition of indoleamine 2,3-dioxygenase, an immunoregulatory target of the cancer suppression gene Bin1, potentiates cancer chemotherapy." Nat Med **11**(3): 312-319.
Muller, A. J., M. D. Sharma, P. R. Chandler, J. B. Duhadaway, M. E. Everhart, B. A. Johnson, 3rd, D. J. Kahler, J. Pihkala, A. P. Soler, D. H. Munn, G. C. Prendergast and A. L. Mellor (2008). "Chronic inflammation that facilitates tumor progression creates local immune suppression by inducing indoleamine 2,3 dioxygenase." Proc Natl Acad Sci U S A **105**(44): 17073-17078.
Murphy, J. A., D. N. Criddle, M. Sherwood, M. Chvanov, R. Mukherjee, E. McLaughlin, D. Booth, J. V. Gerasimenko, M. G. Raraty, P. Ghaneh, J. P. Neoptolemos, O. V. Gerasimenko, A. V. Tepikin, G. M. Green, J. R. Reeve, Jr., O. H. Petersen and R. Sutton (2008). "Direct activation of cytosolic Ca2+ signaling and enzyme secretion by cholecystokinin in human pancreatic acinar cells." Gastroenterology **135**(2): 632-641.
Murphy, J. M., P. E. Czabotar, J. M. Hildebrand, I. S. Lucet, J. G. Zhang, S. Alvarez-Diaz, R. Lewis, N. Lalaoui, D. Metcalf, A. I. Webb, S. N. Young, L. N. Varghese, G. M. Tannahill, E. C. Hatchell, I. J. Majewski, T. Okamoto, R. C. Dobson, D. J. Hilton, J. J. Babon, N. A. Nicola, A. Strasser, J. Silke and W. S. Alexander (2013). "The pseudokinase MLKL mediates necroptosis via a molecular switch mechanism." Immunity **39**(3): 443-453.
Musa, B. E., A. W. Nelson, E. L. Gillette, H. L. Ferguson and W. V. Lumb (1976). "A model to study acute pancreatitis in the dog." J Surg Res **21**(1): 51-56.
Najjar, M., C. Suebsuwong, S. S. Ray, R. J. Thapa, J. L. Maki, S. Nogusa, S. Shah, D. Saleh, P. J. Gough, J. Bertin, J. Yuan, S. Balachandran, G. D. Cuny and A. Degterev (2015). "Structure guided design of potent and selective ponatinib-based hybrid inhibitors for RIPK1." Cell Rep **10**(11): 1850-1860.
Newton, K., D. L. Dugger, A. Maltzman, J. M. Greve, M. Hedehus, B. Martin-McNulty, R. A. Carano, T. C. Cao, N. van Bruggen, L. Bernstein, W. P. Lee, X. Wu, J. DeVoss, J. Zhang, S. Jeet, I. Peng, B. S. McKenzie, M. Roose-Girma, P. Caplazi, L. Diehl, J. D. Webster and D. Vucic (2016). "RIPK3 deficiency or catalytically inactive RIPK1 provides greater benefit than MLKL deficiency in mouse models of inflammation and tissue injury." Cell Death Differ **23**(9): 1565-1576.
Newton, K., D. L. Dugger, K. E. Wickliffe, N. Kapoor, M. C. de Almagro, D. Vucic, L. Komuves, R. E. Ferrando, D. M. French, J. Webster, M. Roose-Girma, S. Warming and V. M. Dixit (2014). "Activity of protein kinase RIPK3 determines whether cells die by necroptosis or apoptosis." Science **343**(6177): 1357-1360.
Niederau, C., L. D. Ferrell and J. H. Grendell (1985). "Caerulein-induced acute necrotizing pancreatitis in mice: protective effects of proglumide, benzotript, and secretin." Gastroenterology **88**(5 Pt 1): 1192-1204.

Niederau, C. and J. H. Grendell (1988). "Intracellular vacuoles in experimental acute pancreatitis in rats and mice are an acidified compartment." J Clin Invest **81**(1): 229-236.
Niederau, C., R. Luthen, M. C. Niederau, J. H. Grendell and L. D. Ferrell (1992). "Acute experimental hemorrhagic-necrotizing pancreatitis induced by feeding a choline-deficient, ethionine-supplemented diet. Methodology and standards." Eur Surg Res **24 Suppl 1**: 40-54.
Nomura, M., A. Ueno, K. Saga, M. Fukuzawa and Y. Kaneda (2014). "Accumulation of cytosolic calcium induces necroptotic cell death in human neuroblastoma." Cancer Res **74**(4): 1056-1066.
Northington, F. J., R. Chavez-Valdez, E. M. Graham, S. Razdan, E. B. Gauda and L. J. Martin (2011). "Necrostatin decreases oxidative damage, inflammation, and injury after neonatal HI." J Cereb Blood Flow Metab **31**(1): 178-189.
O'Donnell, M. A., E. Perez-Jimenez, A. Oberst, A. Ng, R. Massoumi, R. Xavier, D. R. Green and A. T. Ting (2011). "Caspase 8 inhibits programmed necrosis by processing CYLD." Nat Cell Biol **13**(12): 1437-1442.
O'Malley, Y., B. D. Fink, N. C. Ross, T. E. Prisinzano and W. I. Sivitz (2006). "Reactive oxygen and targeted antioxidant administration in endothelial cell mitochondria." J Biol Chem **281**(52): 39766-39775.
Odinokova, I. V., K. F. Sung, O. A. Mareninova, K. Hermann, Y. Evtodienko, A. Andreyev, I. Gukovsky and A. S. Gukovskaya (2009). "Mechanisms regulating cytochrome c release in pancreatic mitochondria." Gut **58**(3): 431-442.
Odinokova, I. V., K. F. Sung, O. A. Mareninova, K. Hermann, I. Gukovsky and A. S. Gukovskaya (2008). "Mitochondrial mechanisms of death responses in pancreatitis." J Gastroenterol Hepatol **23 Suppl 1**: S25-30.
Ohshio, G., A. Saluja and M. L. Steer (1991). "Effects of short-term pancreatic duct obstruction in rats." Gastroenterology **100**(1): 196-202.
Okamoto, T., S. Tone, H. Kanouchi, C. Miyawaki, S. Ono and Y. Minatogawa (2007). "Transcriptional regulation of indoleamine 2,3-dioxygenase (IDO) by tryptophan and its analogue : Down-regulation of the indoleamine 2,3-dioxygenase (IDO) transcription by tryptophan and its analogue." Cytotechnology **54**(2): 107-113.
Onizawa, M., S. Oshima, U. Schulze-Topphoff, J. A. Oses-Prieto, T. Lu, R. Tavares, T. Prodhomme, B. Duong, M. I. Whang, R. Advincula, A. Agelidis, J. Barrera, H. Wu, A. Burlingame, B. A. Malynn, S. S. Zamvil and A. Ma (2015). "The ubiquitin-modifying enzyme A20 restricts ubiquitination of the kinase RIPK3 and protects cells from necroptosis." Nat Immunol **16**(6): 618-627.
Opitz, C. A., U. M. Litzenburger, C. Lutz, T. V. Lanz, I. Tritschler, A. Koppel, E. Tolosa, M. Hoberg, J. Anderl, W. K. Aicher, M. Weller, W. Wick and M. Platten (2009). "Toll-like receptor engagement enhances the immunosuppressive properties of human bone marrow-derived mesenchymal stem cells by inducing indoleamine-2,3-dioxygenase-1 via interferon-beta and protein kinase R." Stem Cells **27**(4): 909-919.
Orabi, A. I., L. Wen, T. A. Javed, T. Le, P. Guo, S. Sanker, D. Ricks, K. Boggs, J. F. Eisses, C. Castro, X. Xiao, K. Prasadan, F. Esni, G. K. Gittes and S. Z. Husain (2017). "Targeted inhibition of pancreatic acinar cell calcineurin is a novel strategy to prevent post-ERCP pancreatitis." Cell Mol Gastroenterol Hepatol **3**(1): 119-128.
Orda, R., N. Hadas, S. Orda and T. Wiznitzer (1980). "Experimental acute pancreatitis. Inducement by taurocholate sodium-trypsin injection into a temporarily closed duodenal loop in the rat." Arch Surg **115**(3): 327-329.

Orrenius, S., V. Gogvadze and B. Zhivotovsky (2007). "Mitochondrial oxidative stress: implications for cell death." Annu Rev Pharmacol Toxicol **47**: 143-183.
Pandol, S. J. (2010). The Exocrine Pancreas. San Rafael (CA).
Pandol, S. J., S. Periskic, I. Gukovsky, V. Zaninovic, Y. Jung, Y. Zong, T. E. Solomon, A. S. Gukovskaya and H. Tsukamoto (1999). "Ethanol diet increases the sensitivity of rats to pancreatitis induced by cholecystokinin octapeptide." Gastroenterology **117**(3): 706-716.
Pandol, S. J., A. K. Saluja, C. W. Imrie and P. A. Banks (2007). "Acute pancreatitis: bench to the bedside." Gastroenterology **132**(3): 1127-1151.
Park, S. M., J. B. Yoon and T. H. Lee (2004). "Receptor interacting protein is ubiquitinated by cellular inhibitor of apoptosis proteins (c-IAP1 and c-IAP2) in vitro." FEBS Lett **566**(1-3): 151-156.
Pasparakis, M. and P. Vandenabeele (2015). "Necroptosis and its role in inflammation." Nature **517**(7534): 311-320.
Perides, G., J. M. Laukkarinen, G. Vassileva and M. L. Steer (2010). "Biliary acute pancreatitis in mice is mediated by the G-protein-coupled cell surface bile acid receptor Gpbar1." Gastroenterology **138**(2): 715-725.
Perides, G., G. J. van Acker, J. M. Laukkarinen and M. L. Steer (2010). "Experimental acute biliary pancreatitis induced by retrograde infusion of bile acids into the mouse pancreatic duct." Nat Protoc **5**(2): 335-341.
Petersen, O. H. (2002). "Calcium signal compartmentalization." Biol Res **35**(2): 177-182.
Petersen, O. H. (2009). "Ca2+ signaling in pancreatic acinar cells: physiology and pathophysiology." Braz J Med Biol Res **42**(1): 9-16.
Petersen, O. H. and R. Sutton (2006). "Ca2+ signalling and pancreatitis: effects of alcohol, bile and coffee." Trends Pharmacol Sci **27**(2): 113-120.
Petersen, O. H., R. Sutton and D. N. Criddle (2006). "Failure of calcium microdomain generation and pathological consequences." Cell Calcium **40**(5-6): 593-600.
Petersen, O. H. and A. V. Tepikin (2008). "Polarized calcium signaling in exocrine gland cells." Annu Rev Physiol **70**: 273-299.
Petrov, M. S., S. Shanbhag, M. Chakraborty, A. R. Phillips and J. A. Windsor (2010). "Organ failure and infection of pancreatic necrosis as determinants of mortality in patients with acute pancreatitis." Gastroenterology **139**(3): 813-820.
Pfeffer, R. B., O. Stasior and J. W. Hinton (1957). "The clinical picture of the sequential development of acute hemorrhagic pancreatitis in the dog." Surg Forum **8**: 248-251.
Pfeifer, S., M. Schreder, A. Bolomsky, S. Graffi, D. Fuchs, S. S. Sahota, H. Ludwig and N. Zojer (2012). "Induction of indoleamine-2,3 dioxygenase in bone marrow stromal cells inhibits myeloma cell growth." J Cancer Res Clin Oncol **138**(11): 1821-1830.
Polykratis, A., N. Hermance, M. Zelic, J. Roderick, C. Kim, T. M. Van, T. H. Lee, F. K. Chan, M. Pasparakis and M. A. Kelliher (2014). "Cutting edge: RIPK1 Kinase inactive mice are viable and protected from TNF-induced necroptosis in vivo." J Immunol **193**(4): 1539-1543.
Popper, H. L., H. Necheles and K. C. Russell (1948). "Transition of pancreatic edema into pancreatic necrosis." Surg Gynecol Obstet **87**(1): 79-82.
Poyet, J. L., S. M. Srinivasula, J. H. Lin, T. Fernandes-Alnemri, S. Yamaoka, P. N. Tsichlis and E. S. Alnemri (2000). "Activation of the Ikappa B kinases by RIP via IKKgamma /NEMO-mediated oligomerization." J Biol Chem **275**(48): 37966-37977.

Qu, Y., J. Tang, H. Wang, S. Li, F. Zhao, L. Zhang, Q. Richard Lu and D. Mu (2017). "RIPK3 interactions with MLKL and CaMKII mediate oligodendrocytes death in the developing brain." Cell Death Dis **8**(2): e2629.
Raraty, M., J. Ward, G. Erdemli, C. Vaillant, J. P. Neoptolemos, R. Sutton and O. H. Petersen (2000). "Calcium-dependent enzyme activation and vacuole formation in the apical granular region of pancreatic acinar cells." Proc Natl Acad Sci U S A **97**(24): 13126-13131.
Rau, B., B. Poch, F. Gansauge, A. Bauer, A. K. Nussler, T. Nevalainen, M. H. Schoenberg and H. G. Beger (2000). "Pathophysiologic role of oxygen free radicals in acute pancreatitis: initiating event or mediator of tissue damage?" Ann Surg **231**(3): 352-360.
Reinehr, R., S. Becker, V. Keitel, A. Eberle, S. Grether-Beck and D. Haussinger (2005). "Bile salt-induced apoptosis involves NADPH oxidase isoform activation." Gastroenterology **129**(6): 2009-2031.
Reiter, M., I. Eckhardt, A. Haferkamp and S. Fulda (2016). "Smac mimetic sensitizes renal cell carcinoma cells to interferon-alpha-induced apoptosis." Cancer Lett **375**(1): 1-8.
Remijsen, Q., V. Goossens, S. Grootjans, C. Van den Haute, N. Vanlangenakker, Y. Dondelinger, R. Roelandt, I. Bruggeman, A. Goncalves, M. J. Bertrand, V. Baekelandt, N. Takahashi, T. V. Berghe and P. Vandenabeele (2014). "Depletion of RIPK3 or MLKL blocks TNF-driven necroptosis and switches towards a delayed RIPK1 kinase-dependent apoptosis." Cell Death Dis **5**: e1004.
Renner, I. G. and J. R. Wisner, Jr. (1986). "Ceruletide-induced acute pancreatitis in the dog and its amelioration by exogenous secretin." Int J Pancreatol **1**(1): 39-49.
Rifai, Y., A. S. Elder, C. J. Carati, D. J. Hussey, X. Li, C. M. Woods, A. C. Schloithe, A. C. Thomas, R. D. Mathison, J. S. Davison, J. Toouli and G. T. Saccone (2008). "The tripeptide analog feG ameliorates severity of acute pancreatitis in a caerulein mouse model." Am J Physiol Gastrointest Liver Physiol **294**(4): G1094-1099.
Roderick, J. E., N. Hermance, M. Zelic, M. J. Simmons, A. Polykratis, M. Pasparakis and M. A. Kelliher (2014). "Hematopoietic RIPK1 deficiency results in bone marrow failure caused by apoptosis and RIPK3-mediated necroptosis." Proc Natl Acad Sci U S A **111**(40): 14436-14441.
Rojas-Rivera, D., T. Delvaeye, R. Roelandt, W. Nerinckx, K. Augustyns, P. Vandenabeele and M. J. M. Bertrand (2017). "When PERK inhibitors turn out to be new potent RIPK1 inhibitors: critical issues on the specificity and use of GSK2606414 and GSK2656157." Cell Death Differ **24**(6): 1100-1110.
Ropolo, A., D. Grasso, R. Pardo, M. L. Sacchetti, C. Archange, A. Lo Re, M. Seux, J. Nowak, C. D. Gonzalez, J. L. Iovanna and M. I. Vaccaro (2007). "The pancreatitis-induced vacuole membrane protein 1 triggers autophagy in mammalian cells." J Biol Chem **282**(51): 37124-37133.
Ros, U., A. Pena-Blanco, K. Hanggi, U. Kunzendorf, S. Krautwald, W. W. Wong and A. J. Garcia-Saez (2017). "Necroptosis Execution Is Mediated by Plasma Membrane Nanopores Independent of Calcium." Cell Rep **19**(1): 175-187.
Saluja, A. K., M. M. Lerch, P. A. Phillips and V. Dudeja (2007). "Why does pancreatic overstimulation cause pancreatitis?" Annu Rev Physiol **69**: 249-269.
Saluja, A. K., L. Lu, Y. Yamaguchi, B. Hofbauer, M. Runzi, R. Dawra, M. Bhatia and M. L. Steer (1997). "A cholecystokinin-releasing factor mediates ethanol-induced stimulation of rat pancreatic secretion." J Clin Invest **99**(3): 506-512.

Sambataro, F. and M. Pennuto (2017). "Post-translational Modifications and Protein Quality Control in Motor Neuron and Polyglutamine Diseases." Front Mol Neurosci **10**: 82.
Sateesh, J., P. Bhardwaj, N. Singh and A. Saraya (2009). "Effect of antioxidant therapy on hospital stay and complications in patients with early acute pancreatitis: a randomised controlled trial." Trop Gastroenterol **30**(4): 201-206.
Schapiro, H., L. G. Britt, C. F. Blackwell and K. J. Gaines (1973). "Acute hemorrhagic pancreatitis in the dog. I. The action of bile." Arch Surg **107**(4): 608-612.
Schroecksnadel, K., S. Kaser, M. Ledochowski, G. Neurauter, E. Mur, M. Herold and D. Fuchs (2003). "Increased degradation of tryptophan in blood of patients with rheumatoid arthritis." J Rheumatol **30**(9): 1935-1939.
Scott, G. N., J. DuHadaway, E. Pigott, N. Ridge, G. C. Prendergast, A. J. Muller and L. Mandik-Nayak (2009). "The immunoregulatory enzyme IDO paradoxically drives B cell-mediated autoimmunity." J Immunol **182**(12): 7509-7517.
Senninger, N., F. G. Moody, J. C. Coelho and D. H. Van Buren (1986). "The role of biliary obstruction in the pathogenesis of acute pancreatitis in the opossum." Surgery **99**(6): 688-693.
Shan, B., F. Ma, M. Wang and X. Xu (2015). "Down-Regulating Receptor Interacting Protein Kinase 1 (RIP1) Promotes Oxaliplatin-Induced Tca8113 Cell Apoptosis." Med Sci Monit **21**: 3089-3094.
Shen, H., C. Liu, D. Zhang, X. Yao, K. Zhang, H. Li and G. Chen (2017). "Role for RIP1 in mediating necroptosis in experimental intracerebral hemorrhage model both in vivo and in vitro." Cell Death Dis **8**(3): e2641.
Shen, H. M., Y. Lin, S. Choksi, J. Tran, T. Jin, L. Chang, M. Karin, J. Zhang and Z. G. Liu (2004). "Essential roles of receptor-interacting protein and TRAF2 in oxidative stress-induced cell death." Mol Cell Biol **24**(13): 5914-5922.
Sheridan, C. (2015). "IDO inhibitors move center stage in immuno-oncology." Nat Biotechnol **33**(4): 321-322.
Shikama, Y., M. Yamada and T. Miyashita (2003). "Caspase-8 and caspase-10 activate NF-kappaB through RIP, NIK and IKKalpha kinases." Eur J Immunol **33**(7): 1998-2006.
Shindo, R., H. Kakehashi, K. Okumura, Y. Kumagai and H. Nakano (2013). "Critical contribution of oxidative stress to TNFalpha-induced necroptosis downstream of RIPK1 activation." Biochem Biophys Res Commun **436**(2): 212-216.
Shutinoski, B., N. A. Alturki, D. Rijal, J. Bertin, P. J. Gough, M. G. Schlossmacher and S. Sad (2016). "K45A mutation of RIPK1 results in poor necroptosis and cytokine signaling in macrophages, which impacts inflammatory responses in vivo." Cell Death Differ **23**(10): 1628-1637.
Siech, M., P. Heinrich and G. Letko (1991). "Development of acute pancreatitis in rats after single ethanol administration and induction of a pancreatic juice edema." Int J Pancreatol **8**(2): 169-175.
Silke, J. and A. Strasser (2013). "The FLIP Side of Life." Sci Signal **6**(258): pe2.
Simpson, C. J., P. G. Toner, K. E. Carr, J. D. Anderson and D. C. Carter (1983). "Effect of bile salt perfusion and intraduct pressure on ionic flux and mucosal ultrastructure in the pancreatic duct of the cat." Virchows Arch B Cell Pathol Incl Mol Pathol **42**(3): 327-342.
Siriwardena, A. K., J. M. Mason, S. Balachandra, A. Bagul, S. Galloway, L. Formela, J. G. Hardman and S. Jamdar (2007). "Randomised, double blind, placebo controlled trial of intravenous antioxidant (n-acetylcysteine, selenium, vitamin C) therapy in severe acute pancreatitis." Gut **56**(10): 1439-1444.

Skouras, C., X. Zheng, M. Binnie, N. Z. Homer, T. B. Murray, D. Robertson, L. Briody, F. Paterson, H. Spence, L. Derr, A. J. Hayes, A. Tsoumanis, D. Lyster, R. W. Parks, O. J. Garden, J. P. Iredale, I. J. Uings, J. Liddle, W. L. Wright, G. Dukes, S. P. Webster and D. J. Mole (2016). "Increased levels of 3-hydroxykynurenine parallel disease severity in human acute pancreatitis." Sci Rep **6**: 33951.
Smith, C. C., S. M. Davidson, S. Y. Lim, J. C. Simpkin, J. S. Hothersall and D. M. Yellon (2007). "Necrostatin: a potentially novel cardioprotective agent?" Cardiovasc Drugs Ther **21**(4): 227-233.
Stanger, B. Z., P. Leder, T. H. Lee, E. Kim and B. Seed (1995). "RIP: a novel protein containing a death domain that interacts with Fas/APO-1 (CD95) in yeast and causes cell death." Cell **81**(4): 513-523.
Stone, T. W. (2001). "Kynurenines in the CNS: from endogenous obscurity to therapeutic importance." Prog Neurobiol **64**(2): 185-218.
Su, Z., Z. Yang, Y. Xu, Y. Chen and Q. Yu (2015). "Apoptosis, autophagy, necroptosis, and cancer metastasis." Mol Cancer **14**: 48.
Suda, J., L. Dara, L. Yang, M. Aghajan, Y. Song, N. Kaplowitz and Z. X. Liu (2016). "Knockdown of RIPK1 Markedly Exacerbates Murine Immune-Mediated Liver Injury through Massive Apoptosis of Hepatocytes, Independent of Necroptosis and Inhibition of NF-kappaB." J Immunol **197**(8): 3120-3129.
Suh, Y. A., R. S. Arnold, B. Lassegue, J. Shi, X. Xu, D. Sorescu, A. B. Chung, K. K. Griendling and J. D. Lambeth (1999). "Cell transformation by the superoxide-generating oxidase Mox1." Nature **401**(6748): 79-82.
Sun, W., X. Wu, H. Gao, J. Yu, W. Zhao, J. J. Lu, J. Wang, G. Du and X. Chen (2017). "Cytosolic calcium mediates RIP1/RIP3 complex-dependent necroptosis through JNK activation and mitochondrial ROS production in human colon cancer cells." Free Radic Biol Med **108**: 433-444.
Sun, X., J. Yin, M. A. Starovasnik, W. J. Fairbrother and V. M. Dixit (2002). "Identification of a novel homotypic interaction motif required for the phosphorylation of receptor-interacting protein (RIP) by RIP3." J Biol Chem **277**(11): 9505-9511.
Sundaresan, M., Z. X. Yu, V. J. Ferrans, K. Irani and T. Finkel (1995). "Requirement for generation of H2O2 for platelet-derived growth factor signal transduction." Science **270**(5234): 296-299.
Suzuki, Y., T. Suda, K. Furuhashi, M. Suzuki, M. Fujie, D. Hahimoto, Y. Nakamura, N. Inui, H. Nakamura and K. Chida (2010). "Increased serum kynurenine/tryptophan ratio correlates with disease progression in lung cancer." Lung Cancer **67**(3): 361-365.
Swaroop, V. S., S. T. Chari and J. E. Clain (2004). "Severe acute pancreatitis." JAMA **291**(23): 2865-2868.
Tait, S. W., A. Oberst, G. Quarato, S. Milasta, M. Haller, R. Wang, M. Karvela, G. Ichim, N. Yatim, M. L. Albert, G. Kidd, R. Wakefield, S. Frase, S. Krautwald, A. Linkermann and D. R. Green (2013). "Widespread mitochondrial depletion via mitophagy does not compromise necroptosis." Cell Rep **5**(4): 878-885.
Takahashi, N., L. Duprez, S. Grootjans, A. Cauwels, W. Nerinckx, J. B. DuHadaway, V. Goossens, R. Roelandt, F. Van Hauwermeiren, C. Libert, W. Declercq, N. Callewaert, G. C. Prendergast, A. Degterev, J. Yuan and P. Vandenabeele (2012). "Necrostatin-1 analogues: critical issues on the specificity, activity and in vivo use in experimental disease models." Cell Death Dis **3**: e437.
Takahashi, N., L. Vereecke, M. J. Bertrand, L. Duprez, S. B. Berger, T. Divert, A. Goncalves, M. Sze, B. Gilbert, S. Kourula, V. Goossens, S. Lefebvre, C. Gunther, C. Becker, J. Bertin, P. J. Gough, W. Declercq, G. van Loo and P. Vandenabeele (2014).

"RIPK1 ensures intestinal homeostasis by protecting the epithelium against apoptosis." Nature **513**(7516): 95-99.
Takemoto, K., E. Hatano, K. Iwaisako, M. Takeiri, N. Noma, S. Ohmae, K. Toriguchi, K. Tanabe, H. Tanaka, S. Seo, K. Taura, K. Machida, N. Takeda, S. Saji, S. Uemoto and M. Asagiri (2014). "Necrostatin-1 protects against reactive oxygen species (ROS)-induced hepatotoxicity in acetaminophen-induced acute liver failure." FEBS Open Bio **4**: 777-787.
Teng, X., A. Degterev, P. Jagtap, X. Xing, S. Choi, R. Denu, J. Yuan and G. D. Cuny (2005). "Structure-activity relationship study of novel necroptosis inhibitors." Bioorg Med Chem Lett **15**(22): 5039-5044.
Testoni, P. A., A. Mariani, A. Giussani, C. Vailati, E. Masci, G. Macarri, L. Ghezzo, L. Familiari, N. Giardullo, M. Mutignani, G. Lombardi, G. Talamini, A. Spadaccini, R. Briglia, L. Piazzi and S. Group (2010). "Risk factors for post-ERCP pancreatitis in high- and low-volume centers and among expert and non-expert operators: a prospective multicenter study." Am J Gastroenterol **105**(8): 1753-1761.
Theeuwes, F. and S. I. Yum (1976). "Principles of the design and operation of generic osmotic pumps for the delivery of semisolid or liquid drug formulations." Ann Biomed Eng **4**(4): 343-353.
Thorn, P., O. Gerasimenko and O. H. Petersen (1994). "Cyclic ADP-ribose regulation of ryanodine receptors involved in agonist evoked cytosolic Ca2+ oscillations in pancreatic acinar cells." EMBO J **13**(9): 2038-2043.
Thorn, P. and O. H. Petersen (1993). "Calcium oscillations in pancreatic acinar cells, evoked by the cholecystokinin analogue JMV-180, depend on functional inositol 1,4,5-trisphosphate receptors." J Biol Chem **268**(31): 23219-23221.
Tinel, H., J. M. Cancela, H. Mogami, J. V. Gerasimenko, O. V. Gerasimenko, A. V. Tepikin and O. H. Petersen (1999). "Active mitochondria surrounding the pancreatic acinar granule region prevent spreading of inositol trisphosphate-evoked local cytosolic Ca(2+) signals." EMBO J **18**(18): 4999-5008.
Ting, A. T., F. X. Pimentel-Muinos and B. Seed (1996). "RIP mediates tumor necrosis factor receptor 1 activation of NF-kappaB but not Fas/APO-1-initiated apoptosis." EMBO J **15**(22): 6189-6196.
Tokunaga, F., S. Sakata, Y. Saeki, Y. Satomi, T. Kirisako, K. Kamei, T. Nakagawa, M. Kato, S. Murata, S. Yamaoka, M. Yamamoto, S. Akira, T. Takao, K. Tanaka and K. Iwai (2009). "Involvement of linear polyubiquitylation of NEMO in NF-kappaB activation." Nat Cell Biol **11**(2): 123-132.
Tonnus, W. and A. Linkermann (2017). "The in vivo evidence for regulated necrosis." Immunol Rev **277**(1): 128-149.
Toshimori, K., C. Ito, M. Maekawa, Y. Toyama, F. Suzuki-Toyota and D. K. Saxena (2004). "Impairment of spermatogenesis leading to infertility." Anat Sci Int **79**(3): 101-111.
Tsai, K., S. S. Wang, T. S. Chen, C. W. Kong, F. Y. Chang, S. D. Lee and F. J. Lu (1998). "Oxidative stress: an important phenomenon with pathogenetic significance in the progression of acute pancreatitis." Gut **42**(6): 850-855.
Tsuji, N., N. Watanabe, T. Okamoto and Y. Niitsu (1994). "Specific interaction of pancreatic elastase and leucocytes to produce oxygen radicals and its implication in pancreatitis." Gut **35**(11): 1659-1664.
Turrens, J. F. (2003). "Mitochondrial formation of reactive oxygen species." J Physiol **552**(Pt 2): 335-344.

Uden, S., D. Bilton, L. Nathan, L. P. Hunt, C. Main and J. M. Braganza (1990). "Antioxidant therapy for recurrent pancreatitis: placebo-controlled trial." Aliment Pharmacol Ther **4**(4): 357-371.
Uhlen, M., P. Oksvold, L. Fagerberg, E. Lundberg, K. Jonasson, M. Forsberg, M. Zwahlen, C. Kampf, K. Wester, S. Hober, H. Wernerus, L. Bjorling and F. Ponten (2010). "Towards a knowledge-based Human Protein Atlas." Nat Biotechnol **28**(12): 1248-1250.
Upton, J. W., W. J. Kaiser and E. S. Mocarski (2010). "Virus inhibition of RIP3-dependent necrosis." Cell Host Microbe **7**(4): 302-313.
Uyttenhove, C., L. Pilotte, I. Theate, V. Stroobant, D. Colau, N. Parmentier, T. Boon and B. J. Van den Eynde (2003). "Evidence for a tumoral immune resistance mechanism based on tryptophan degradation by indoleamine 2,3-dioxygenase." Nat Med **9**(10): 1269-1274.
Vaccaro, M. I., A. Ropolo, D. Grasso and J. L. Iovanna (2008). "A novel mammalian trans-membrane protein reveals an alternative initiation pathway for autophagy." Autophagy **4**(3): 388-390.
van Baren, N. and B. J. Van den Eynde (2015). "Tryptophan-degrading enzymes in tumoral immune resistance." Front Immunol **6**: 34.
van Geel, R. M., J. H. Beijnen and J. H. Schellens (2012). "Concise drug review: pazopanib and axitinib." Oncologist **17**(8): 1081-1089.
Vanden Berghe, T., G. van Loo, X. Saelens, M. Van Gurp, G. Brouckaert, M. Kalai, W. Declercq and P. Vandenabeele (2004). "Differential signaling to apoptotic and necrotic cell death by Fas-associated death domain protein FADD." J Biol Chem **279**(9): 7925-7933.
Vanden Berghe, T., N. Vanlangenakker, E. Parthoens, W. Deckers, M. Devos, N. Festjens, C. J. Guerin, U. T. Brunk, W. Declercq and P. Vandenabeele (2010). "Necroptosis, necrosis and secondary necrosis converge on similar cellular disintegration features." Cell Death Differ **17**(6): 922-930.
Vandenabeele, P., L. Galluzzi, T. Vanden Berghe and G. Kroemer (2010). "Molecular mechanisms of necroptosis: an ordered cellular explosion." Nat Rev Mol Cell Biol **11**(10): 700-714.
Vandenabeele, P., S. Grootjans, N. Callewaert and N. Takahashi (2013). "Necrostatin-1 blocks both RIPK1 and IDO: consequences for the study of cell death in experimental disease models." Cell Death Differ **20**(2): 185-187.
Vanlangenakker, N., M. J. Bertrand, P. Bogaert, P. Vandenabeele and T. Vanden Berghe (2011). "TNF-induced necroptosis in L929 cells is tightly regulated by multiple TNFR1 complex I and II members." Cell Death Dis **2**: e230.
Vanlangenakker, N., T. Vanden Berghe and P. Vandenabeele (2012). "Many stimuli pull the necrotic trigger, an overview." Cell Death Differ **19**(1): 75-86.
Vasilescu, C. and C. Tasca (1991). "Acute experimental pancreatitis--morphological evidence for the development of a multiple organ failure syndrome." Rom J Morphol Embryol **37**(1-2): 25-29.
Vasudevan, K., J. Raber and J. Sztein (2010). "Fertility comparison between wild type and transgenic mice by in vitro fertilization." Transgenic Res **19**(4): 587-594.
Vercammen, D., R. Beyaert, G. Denecker, V. Goossens, G. Van Loo, W. Declercq, J. Grooten, W. Fiers and P. Vandenabeele (1998). "Inhibition of caspases increases the sensitivity of L929 cells to necrosis mediated by tumor necrosis factor." J Exp Med **187**(9): 1477-1485.

Vercammen, D., G. Brouckaert, G. Denecker, M. Van de Craen, W. Declercq, W. Fiers and P. Vandenabeele (1998). "Dual signaling of the Fas receptor: initiation of both apoptotic and necrotic cell death pathways." J Exp Med **188**(5): 919-930.
Virlos, I. T., J. Mason, D. Schofield, R. F. McCloy, J. M. Eddleston and A. K. Siriwardena (2003). "Intravenous n-acetylcysteine, ascorbic acid and selenium-based anti-oxidant therapy in severe acute pancreatitis." Scand J Gastroenterol **38**(12): 1262-1267.
Vivarelli, M. S., D. McDonald, M. Miller, N. Cusson, M. Kelliher and R. S. Geha (2004). "RIP links TLR4 to Akt and is essential for cell survival in response to LPS stimulation." J Exp Med **200**(3): 399-404.
Voronina, S., R. Longbottom, R. Sutton, O. H. Petersen and A. Tepikin (2002). "Bile acids induce calcium signals in mouse pancreatic acinar cells: implications for bile-induced pancreatic pathology." J Physiol **540**(Pt 1): 49-55.
Voronina, S., T. Sukhomlin, P. R. Johnson, G. Erdemli, O. H. Petersen and A. Tepikin (2002). "Correlation of NADH and Ca2+ signals in mouse pancreatic acinar cells." J Physiol **539**(Pt 1): 41-52.
Voronina, S. G., S. L. Barrow, O. V. Gerasimenko, O. H. Petersen and A. V. Tepikin (2004). "Effects of secretagogues and bile acids on mitochondrial membrane potential of pancreatic acinar cells: comparison of different modes of evaluating DeltaPsim." J Biol Chem **279**(26): 27327-27338.
Voronina, S. G., S. L. Barrow, A. W. Simpson, O. V. Gerasimenko, G. da Silva Xavier, G. A. Rutter, O. H. Petersen and A. V. Tepikin (2010). "Dynamic changes in cytosolic and mitochondrial ATP levels in pancreatic acinar cells." Gastroenterology **138**(5): 1976-1987.
Walker, A. L., N. Ancellin, B. Beaufils, M. Bergeal, M. Binnie, D. Clapham, C. P. Haslam, D. S. Holmes, J. P. Hutchinson, J. Liddle, A. McBride, O. Mirguet, C. G. Mowat, P. Rowland, N. Tiberghien, L. Trottet, I. Uings, S. P. Webster, X. Zheng and D. J. Mole (2017). "Development of a Series of Kynurenine 3-Monooxygenase Inhibitors Leading to a Clinical Candidate for the Treatment of Acute Pancreatitis." J Med Chem.
Wallach, D., A. Kovalenko and T. B. Kang (2011). "'Necrosome'-induced inflammation: must cells die for it?" Trends Immunol **32**(11): 505-509.
Wang, G., B. Han, H. Zhou, L. Wu, Y. Wang, G. Jia, J. Lv, Z. Cheng, S. Pan, J. Liu, Y. Zhou and B. Sun (2013). "Inhibition of hydrogen sulfide synthesis provides protection for severe acute pancreatitis rats via apoptosis pathway." Apoptosis **18**(1): 28-42.
Wang, L., F. Du and X. Wang (2008). "TNF-alpha induces two distinct caspase-8 activation pathways." Cell **133**(4): 693-703.
Wang, Q., W. Chen, L. Bai, W. Chen, M. T. Padilla, A. S. Lin, S. Shi, X. Wang and Y. Lin (2014). "Receptor-interacting protein 1 increases chemoresistance by maintaining inhibitor of apoptosis protein levels and reducing reactive oxygen species through a microRNA-146a-mediated catalase pathway." J Biol Chem **289**(9): 5654-5663.
Wang, Y., H. Wang, Y. Tao, S. Zhang, J. Wang and X. Feng (2014). "Necroptosis inhibitor necrostatin-1 promotes cell protection and physiological function in traumatic spinal cord injury." Neuroscience **266**: 91-101.
Wang, Z., H. Jiang, S. Chen, F. Du and X. Wang (2012). "The mitochondrial phosphatase PGAM5 functions at the convergence point of multiple necrotic death pathways." Cell **148**(1-2): 228-243.

Waterworth, M. W., G. O. Barbezat, R. Hickman and J. Terblanche (1974). "Proceedings: Acute pancreatitis in the pig--development of a model and a controlled trial of glucagon treatment." Br J Surg **61**(4): 318.
Weber, H., J. Merkord, L. Jonas, A. Wagner, H. Schroder, U. Kading, A. Werner and W. Dummler (1995). "Oxygen radical generation and acute pancreatitis: effects of dibutyltin dichloride/ethanol and ethanol on rat pancreas." Pancreas **11**(4): 382-388.
Wedgwood, K. R., G. Adler, H. Kern and H. A. Reber (1986). "Effects of oral agents on pancreatic duct permeability. A model of acute alcoholic pancreatitis." Dig Dis Sci **31**(10): 1081-1088.
Wen, L., S. Voronina, M. A. Javed, M. Awais, P. Szatmary, D. Latawiec, M. Chvanov, D. Collier, W. Huang, J. Barrett, M. Begg, K. Stauderman, J. Roos, S. Grigoryev, S. Ramos, E. Rogers, J. Whitten, G. Velicelebi, M. Dunn, A. V. Tepikin, D. N. Criddle and R. Sutton (2015). "Inhibitors of ORAI1 Prevent Cytosolic Calcium-Associated Injury of Human Pancreatic Acinar Cells and Acute Pancreatitis in 3 Mouse Models." Gastroenterology **149**(2): 481-492 e487.
Weng, D., R. Marty-Roix, S. Ganesan, M. K. Proulx, G. I. Vladimer, W. J. Kaiser, E. S. Mocarski, K. Pouliot, F. K. Chan, M. A. Kelliher, P. A. Harris, J. Bertin, P. J. Gough, D. M. Shayakhmetov, J. D. Goguen, K. A. Fitzgerald, N. Silverman and E. Lien (2014). "Caspase-8 and RIP kinases regulate bacteria-induced innate immune responses and cell death." Proc Natl Acad Sci U S A **111**(20): 7391-7396.
Werner, J., W. Hartwig, T. Hackert, H. Kaiser, J. Schmidt, M. M. Gebhard, M. W. Buchler and E. Klar (2012). "Multidrug strategies are effective in the treatment of severe experimental pancreatitis." Surgery **151**(3): 372-381.
Werner, J., M. Laposata, C. Fernandez-del Castillo, M. Saghir, R. V. Iozzo, K. B. Lewandrowski and A. L. Warshaw (1997). "Pancreatic injury in rats induced by fatty acid ethyl ester, a nonoxidative metabolite of alcohol." Gastroenterology **113**(1): 286-294.
Werner, J., M. Saghir, C. Fernandez-del Castillo, A. L. Warshaw and M. Laposata (2001). "Linkage of oxidative and nonoxidative ethanol metabolism in the pancreas and toxicity of nonoxidative ethanol metabolites for pancreatic acinar cells." Surgery **129**(6): 736-744.
Wertz, I. E., K. M. O'Rourke, H. Zhou, M. Eby, L. Aravind, S. Seshagiri, P. Wu, C. Wiesmann, R. Baker, D. L. Boone, A. Ma, E. V. Koonin and V. M. Dixit (2004). "De-ubiquitination and ubiquitin ligase domains of A20 downregulate NF-kappaB signalling." Nature **430**(7000): 694-699.
Whitcomb, D. C. (2001). "Hereditary pancreatitis: a model for understanding the genetic basis of acute and chronic pancreatitis." Pancreatology **1**(6): 565-570.
Wildi, S., J. Kleeff, J. Mayerle, A. Zimmermann, E. P. Bottinger, L. Wakefield, M. W. Buchler, H. Friess and M. Korc (2007). "Suppression of transforming growth factor beta signalling aborts caerulein induced pancreatitis and eliminates restricted stimulation at high caerulein concentrations." Gut **56**(5): 685-692.
Willemer, S., H. P. Elsasser and G. Adler (1992). "Hormone-induced pancreatitis." Eur Surg Res **24 Suppl 1**: 29-39.
Wilson, J. S. and M. V. Apte (2003). "Role of alcohol metabolism in alcoholic pancreatitis." Pancreas **27**(4): 311-315.
Witkiewicz, A., T. K. Williams, J. Cozzitorto, B. Durkan, S. L. Showalter, C. J. Yeo and J. R. Brody (2008). "Expression of indoleamine 2,3-dioxygenase in metastatic pancreatic ductal adenocarcinoma recruits regulatory T cells to avoid immune detection." J Am Coll Surg **206**(5): 849-854; discussion 854-846.

Witkiewicz, A. K., C. L. Costantino, R. Metz, A. J. Muller, G. C. Prendergast, C. J. Yeo and J. R. Brody (2009). "Genotyping and expression analysis of IDO2 in human pancreatic cancer: a novel, active target." J Am Coll Surg **208**(5): 781-787; discussion 787-789.
Wittel, U. A., T. Wiech, S. Chakraborty, B. Boss, R. Lauch, S. K. Batra and U. T. Hopt (2008). "Taurocholate-induced pancreatitis: a model of severe necrotizing pancreatitis in mice." Pancreas **36**(2): e9-21.
Wong, W. W., I. E. Gentle, U. Nachbur, H. Anderton, D. L. Vaux and J. Silke (2010). "RIPK1 is not essential for TNFR1-induced activation of NF-kappaB." Cell Death Differ **17**(3): 482-487.
Wu, J., Z. Huang, J. Ren, Z. Zhang, P. He, Y. Li, J. Ma, W. Chen, Y. Zhang, X. Zhou, Z. Yang, S. Q. Wu, L. Chen and J. Han (2013). "Mlkl knockout mice demonstrate the indispensable role of Mlkl in necroptosis." Cell Res **23**(8): 994-1006.
Wu, J., T. Mulatibieke, J. Ni, X. Han, B. Li, Y. Zeng, R. Wan, X. Wang and G. Hu (2017). "Dichotomy between Receptor-Interacting Protein 1- and Receptor-Interacting Protein 3-Mediated Necroptosis in Experimental Pancreatitis." Am J Pathol.
Wu, J., T. Mulatibieke, J. Ni, X. Han, B. Li, Y. Zeng, R. Wan, X. Wang and G. Hu (2017). "Dichotomy between Receptor-Interacting Protein 1- and Receptor-Interacting Protein 3-Mediated Necroptosis in Experimental Pancreatitis." Am J Pathol **187**(5): 1035-1048.
Xie, T., W. Peng, Y. Liu, C. Yan, J. Maki, A. Degterev, J. Yuan and Y. Shi (2013). "Structural basis of RIP1 inhibition by necrostatins." Structure **21**(3): 493-499.
Xu, G., X. Tan, H. Wang, W. Sun, Y. Shi, S. Burlingame, X. Gu, G. Cao, T. Zhang, J. Qin and J. Yang (2010). "Ubiquitin-specific peptidase 21 inhibits tumor necrosis factor alpha-induced nuclear factor kappaB activation via binding to and deubiquitinating receptor-interacting protein 1." J Biol Chem **285**(2): 969-978.
Xu, X., K. W. Chua, C. C. Chua, C. F. Liu, R. C. Hamdy and B. H. Chua (2010). "Synergistic protective effects of humanin and necrostatin-1 on hypoxia and ischemia/reperfusion injury." Brain Res **1355**: 189-194.
Xu, Y., S. Huang, Z. G. Liu and J. Han (2006). "Poly(ADP-ribose) polymerase-1 signaling to mitochondria in necrotic cell death requires RIP1/TRAF2-mediated JNK1 activation." J Biol Chem **281**(13): 8788-8795.
Yang, W. S., K. J. Kim, M. M. Gaschler, M. Patel, M. S. Shchepinov and B. R. Stockwell (2016). "Peroxidation of polyunsaturated fatty acids by lipoxygenases drives ferroptosis." Proc Natl Acad Sci U S A **113**(34): E4966-4975.
Yerushalmi, B., R. Dahl, M. W. Devereaux, E. Gumpricht and R. J. Sokol (2001). "Bile acid-induced rat hepatocyte apoptosis is inhibited by antioxidants and blockers of the mitochondrial permeability transition." Hepatology **33**(3): 616-626.
Yeung, A. W., A. C. Terentis, N. J. King and S. R. Thomas (2015). "Role of indoleamine 2,3-dioxygenase in health and disease." Clin Sci (Lond) **129**(7): 601-672.
Yu, S., D. Hou, P. Chen, Q. Zhang, B. Lv, Y. Ma, F. Liu, H. Liu, E. J. Song, D. Yang and J. Liu (2015). "Adenosine induces apoptosis through TNFR1/RIPK1/P38 axis in colon cancer cells." Biochem Biophys Res Commun **460**(3): 759-765.
Yu, X., Q. Deng, W. Li, L. Xiao, X. Luo, X. Liu, L. Yang, S. Peng, Z. Ding, T. Feng, J. Zhou, J. Fan, A. M. Bode, Z. Dong, J. Liu and Y. Cao (2015). "Neoalbaconol induces cell death through necroptosis by regulating RIPK-dependent autocrine TNFalpha and ROS production." Oncotarget **6**(4): 1995-2008.
Yuasa, H. J., H. J. Ball, Y. F. Ho, C. J. Austin, C. M. Whittington, K. Belov, G. J. Maghzal, L. S. Jermiin and N. H. Hunt (2009). "Characterization and evolution of

vertebrate indoleamine 2, 3-dioxygenases IDOs from monotremes and marsupials." Comp Biochem Physiol B Biochem Mol Biol **153**(2): 137-144.
Zhang, A., X. Mao, L. Li, Y. Tong, Y. Huang, Y. Lan and H. Jiang (2014). "Necrostatin-1 inhibits Hmgb1-IL-23/IL-17 pathway and attenuates cardiac ischemia reperfusion injury." Transpl Int **27**(10): 1077-1085.
Zhang, D. W., J. Shao, J. Lin, N. Zhang, B. J. Lu, S. C. Lin, M. Q. Dong and J. Han (2009). "RIP3, an energy metabolism regulator that switches TNF-induced cell death from apoptosis to necrosis." Science **325**(5938): 332-336.
Zhang, H., X. Zhou, T. McQuade, J. Li, F. K. Chan and J. Zhang (2011). "Functional complementation between FADD and RIP1 in embryos and lymphocytes." Nature **471**(7338): 373-376.
Zhang, L., K. Blackwell, Z. Shi and H. Habelhah (2010). "The RING domain of TRAF2 plays an essential role in the inhibition of TNFalpha-induced cell death but not in the activation of NF-kappaB." J Mol Biol **396**(3): 528-539.
Zhang, S. Q., A. Kovalenko, G. Cantarella and D. Wallach (2000). "Recruitment of the IKK signalosome to the p55 TNF receptor: RIP and A20 bind to NEMO (IKKgamma) upon receptor stimulation." Immunity **12**(3): 301-311.
Zhang, T., Y. Zhang, M. Cui, L. Jin, Y. Wang, F. Lv, Y. Liu, W. Zheng, H. Shang, J. Zhang, M. Zhang, H. Wu, J. Guo, X. Zhang, X. Hu, C. M. Cao and R. P. Xiao (2016). "CaMKII is a RIP3 substrate mediating ischemia- and oxidative stress-induced myocardial necroptosis." Nat Med **22**(2): 175-182.
Zhang, X., Y. Chen, L. W. Jenkins, P. M. Kochanek and R. S. Clark (2005). "Bench-to-bedside review: Apoptosis/programmed cell death triggered by traumatic brain injury." Crit Care **9**(1): 66-75.
Zhang, Y., S. S. Su, S. Zhao, Z. Yang, C. Q. Zhong, X. Chen, Q. Cai, Z. H. Yang, D. Huang, R. Wu and J. Han (2017). "RIP1 autophosphorylation is promoted by mitochondrial ROS and is essential for RIP3 recruitment into necrosome." Nat Commun **8**: 14329.
Zhang, Z., H. M. Li, C. Zhou, Q. Li, L. Ma, Z. Zhang, Y. Sun, L. Wang, X. Zhang, B. Zhu, Y. S. Hong, C. Z. Wu and H. Liu (2016). "Non-benzoquinone geldanamycin analogs trigger various forms of death in human breast cancer cells." J Exp Clin Cancer Res **35**(1): 149.
Zhao, H., T. Jaffer, S. Eguchi, Z. Wang, A. Linkermann and D. Ma (2015). "Role of necroptosis in the pathogenesis of solid organ injury." Cell Death Dis **6**: e1975.
Zhao, J., S. Jitkaew, Z. Cai, S. Choksi, Q. Li, J. Luo and Z. G. Liu (2012). "Mixed lineage kinase domain-like is a key receptor interacting protein 3 downstream component of TNF-induced necrosis." Proc Natl Acad Sci U S A **109**(14): 5322-5327.
Zheng, W., A. Degterev, E. Hsu, J. Yuan and C. Yuan (2008). "Structure-activity relationship study of a novel necroptosis inhibitor, necrostatin-7." Bioorg Med Chem Lett **18**(18): 4932-4935.
Zhou, X., L. Xie, L. Xia, F. Bergmann, M. W. Buchler, G. Kroemer, T. Hackert and F. Fortunato (2017). "RIP3 attenuates the pancreatic damage induced by deletion of ATG7." Cell Death Dis **8**(7): e2918.
Zhu, S., Y. Zhang, G. Bai and H. Li (2011). "Necrostatin-1 ameliorates symptoms in R6/2 transgenic mouse model of Huntington's disease." Cell Death Dis **2**: e115.
Zitvogel, L., O. Kepp and G. Kroemer (2010). "Decoding cell death signals in inflammation and immunity." Cell **140**(6): 798-804.
Zou, C., Y. Xiong, L. Y. Huang, C. L. Song, X. A. Wu, L. L. Li and S. Y. Yang (2016). "Design, Synthesis, and Biological Evaluation of 1-Benzyl-1H-pyrazole Derivatives

as Receptor Interacting Protein 1 Kinase Inhibitors." Chem Biol Drug Des **87**(4): 569-574.